Copyright 1943, by the American Society of Naval Engineers.

JOURNAL
OF THE
AMERICAN SOCIETY OF NAVAL ENGINEERS

VOL. 55. NOVEMBER 1943 No. 4

The Society as a body is not responsible for statements made by individual members

COUNCIL OF THE SOCIETY
(Under whose supervision this number is published).

Rear Admiral C. L. Brand, U.S.N. — Captain J. N. Heiner, U.S.C.G.
Mr. D. S. Brierley. — Mr. A. F. E. Horn.
Rear Admiral J. J. Broshek, U.S.N. — Rear Admiral Earle W. Mills, U.S.N.
Rear Admiral E. L. Cochrane, U.S.N. — Captain Lisle F. Small, U.S.N.
Captain James E. Hamilton, U.S.N.

SOME EXPERIMENTS IN STRESS-RELIEVING CASTINGS AND WELDED STRUCTURES BY VIBRATION.

By Mr. R. T. McGoldrick * and Captain Harold E. Saunders, U. S. N. †

Introduction.

It has become common practice in industry to stress-relieve castings and welded structures by annealing them in furnaces. If locked-up stresses exist, they relieve themselves by local stretching, upsetting, or distortion of the structure at the elevated temperatures. The equipment required for this operation is often large and expensive.

Certain structures are so large that they cannot be accommodated in annealing furnaces locally available, or perhaps not in

* Senior Physicist, David W. Taylor Model Basin, Washington, D. C.
† Technical Director, David W. Taylor Model Basin, Washington, D. C.

the largest furnace available anywhere. They may be of such form and shape that the orthodox stress-relieving process would cause so much distortion as to render them useless for the purpose intended.

A possible solution of this problem is to permit them to weather or age for an extended period, during which time the natural changes in temperature and the extended "soaking" cause variations and reversals in stress, in the course of which the residual or locked-up stresses are gradually relieved.

This aging process has been extensively applied in the stress-relieving of iron castings, especially where the retention of proper shape after machining is important, as in cast-iron parts for precision instruments and machine tools. It has been more or less taken for granted by those who have used it that this aging process should continue for twelve months or more; manifestly no such delay can be tolerated in the midst of an important or urgent development or production program, and equivalent alternative methods must be sought.

This article describes some experimental methods undertaken by the David W. Taylor Model Basin and one of its contractors * in an attempt to expedite the stress-relieving and stabilizing of welded steel and cast-iron structures by vibration and by a combination of vibration and annealing.

Stress Relieving by Vibration.

Although there has been little opportunity to investigate the theoretical phases of the problem, and it has not been possible to uncover any published literature on this subject, there is some experimental proof that locked-up stresses in a complicated structure can be and are relieved to a considerable extent by the working which the structure receives in service.

There is, for example, the well-known experience with ship structures, immortalized by Kipling, † in which the excess stresses in certain areas are worked out and relieved by the motion of the ship in the seas which she encounters. During this series of loading cycles, in which definite working stresses are developed,

* The Kutztown Foundry and Machine Corporation, Kutztown, Pa.
† "The Ship that Found Herself" from "The Day's Work," by Rudyard Kipling.

these working stresses when combined with the residual stresses reach such high local values that the yield point is exceeded * and plastic flow takes place, reducing the residual stress when the working stress is removed. In the aging process, some action of this kind apparently takes place, but at a much slower rate. Whether it is the combination of the long time of action and the moderate stresses set up by temperature variation, or the slow yielding of the metal through plastic action under the influence of stresses in the elastic range applied for long periods, is not known at present. Possibly it is a combination of both.

In fact, it is considered by many that the operation of riveting in a ship that is partly welded and partly riveted goes far to relieve locked-up stresses in the welded portion of the structure, even before the ship is completed and launched. Working of the ship structure in service undoubtedly does the rest. Recent tests † have proved that in smaller structures stress relief can be accomplished by the steady application of pneumatic riveting hammers to some convenient part of the structure for more or less extended periods.

In the customary annealing process on relatively small units, the residual stresses are largely removed by lowering the yield point temporarily and permitting plastic flow to take place readily under the elevated temperatures. However, there is a reluctance among those who produce fine machinery and precision equipment which must remain stabilized for long periods to accept even the best of annealing processes as the final and complete answer to the problem of internal stabilization in metal parts.

One solution which has been proposed and on which some experiments have been made is a combination of the customary annealing process with vibration of the metal part at a relatively high frequency. If annealing cannot be used, for one reason or another, or if it is considered not adequate by itself, the vibration process is employed as a means of subjecting the part to a great number of working cycles in a short time, in an endeavor to accomplish the same end.

* This action appears to be extremely localized and has no detrimental effect upon the strength or serviceability of the structure as a whole.

† This information has been kindly furnished by Mr. E. H. Ewertz, of the Electric Boat Company at Manitowoc, Wisconsin.

General Considerations.

In the application of these experimental processes, involving a combination of annealing and vibration or of vibration alone, a few simple rules have been followed.

(*a*) The part has been machined or trimmed down as nearly as practicable to its finished size before the stress-relieving process was undertaken.

It was considered that some of the residual stresses, such as those in the skin of a casting, would be removed with the metal, and that the remaining metal would yield more readily to the internal forces. This is the reason for the rather general practice in industry of rough machining castings before annealing.

(*b*) The stresses in the vibrating operation were made as high as possible in an effort to produce the desired effect, but not so high as to damage the part unless a weak spot existed in it.

If a weak spot does exist, the best time to find it is before a great deal of expensive machine or hand-finishing has been done. The localized stresses in the other parts must exceed the yield point, to permit plastic flow to take place.

(*c*) The vibrating operation, and the frequency employed, was selected to suit the particular part or structure.

Setting up resonant vibration in a part will increase the effect for a given excitation, will develop higher stresses than can otherwise be produced, and will decrease the vibration time.

Vibration Experiments to Stabilize Castings.

As an example of the application of these procedures in practice, there will be described the normalizing experiments on two rather different types of iron and semi-steel castings.

The first is the group of chair castings for the support of the heavy rails for the towing carriage tracks at the David W. Taylor Model Basin, developed in 1938 and 1939. A section of one of these castings is shown in Figure 1. Alternate chair castings were 12 feet and 4 feet long. For the main rail these weighed 1695 and 530 pounds respectively; for the steady rail, 770 and 247 pounds each. They were made of high-strength iron castings, with about 30 to 40 per cent of steel scrap. Two of the chain castings installed in the tracks are illustrated in Figure 2.

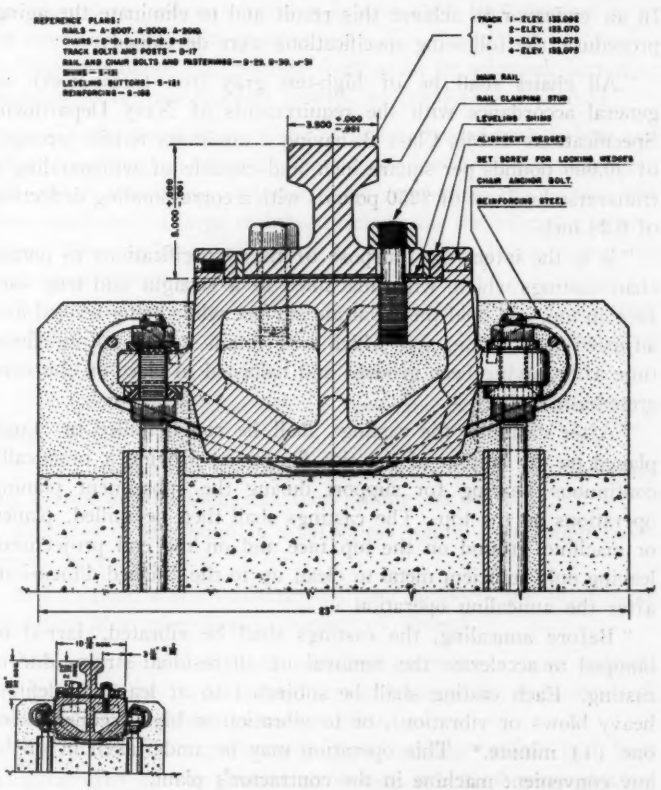

FIGURE 1.—TYPICAL TRACK SECTION THROUGH MAIN RAIL, CHAIR AND FOUNDATION FOR TOWING CARRIAGE TRACKS.

The chair is the box-shaped structure with lugs on the side. Alternate chains were 12 feet long, the remainder were 4 feet long.

The specifications for these chairs called for flat-machined surfaces on the top where the leveling shims under the rails were to bear, accurate to within 0.0015 inch in 6 feet, when measured in any direction. It was imperative that once the chair castings were machined accurately, they remain so for indefinite periods.

In an endeavor to achieve this result and to eliminate the aging procedure, the following specifications were developed:

"All chairs shall be of high-test gray iron (semi-steel), in general accordance with the requirements of Navy Department Specifications 4615b, Class B, having a minimum tensile strength of 30,000 pounds per square inch, and capable of withstanding a transverse load test of 2250 pounds with a corresponding deflection of 0.24 inch.

"It is the intent and purpose of these specifications to obtain chair castings which, when machined to a straight and true surface on top, will hold this accurate surface while being leveled and adjusted to position, and which will retain it for an indefinite time after having been grouted and ballasted in place on the concrete basin walls.

"After cleaning, the castings shall be rough milled or rough planed on the bottom of the side flanges to provide a practically continuous bearing for support during the subsequent planing operations on the top. The castings shall then be milled, planed or machine ground on the top face and on the end projections, leaving only sufficient metal to clean up to the finished dimensions after the annealing operation.

"Before annealing, the castings shall be vibrated, jarred or bumped to accelerate the removal of all residual strains due to casting. Each casting shall be subjected to at least 25 definite heavy blows or vibrations, or to vibration at high frequency for one (1) minute.* This operation may be undertaken in or by any convenient machine in the contractor's plant.

"The chair castings shall be annealed to eliminate stresses in the metal as a result of the casting operation. They shall be loaded on a car or table where they will be adequately and uniformly supported and then be placed in a suitable annealing furnace, which has arrangements for automatic temperature control and recording. The furnace shall be brought to a temperature of from 1000 degrees to 1050 degrees F. and maintained at this temperature for at least six (6) hours. The furnace shall then

* This requirement was admittedly an arbitrary one, arrived at on a basis of production requirements and the experience of a firm which had manufactured cast iron parts successfully for many years.

be allowed to cool at a rate not in excess of 1000 degrees F. in 48 hours, and the castings removed.

"After cooling, the castings shall again be vibrated, jarred or bumped to remove residual strains, as previously described."

It is to be noted that the chairs were vibrated both before and after annealing, and that all these operations took place between the rough machining and the finish machining processes. The contractor used a large molding machine for the vibrating operation. This machine was available and it was large enough to take the whole chair casting.

Before the molding machine was thought of as a vibrating appliance, it was proposed to use one or all of the following vibration treatments on these castings:

1. Suspend them clear of the floor and strike them with a maul, sledge or ram.

2. Roll them along the shop floor by parbuckling, i.e., by winding a rope around them and then pulling on the rope.

3. Carry them around in a springless wagon over rough pavements or roads.

4. Lift them a short distance off their supports and drop them, repeating this operation a number of times.

Although, in the days of vibration generators, these methods all appear rather crude, they are still acceptable substitutes in case a special machine is not available.

Several of the experimental chair castings which had been manufactured by the process previously described were checked carefully at intervals for more than a year, without showing any measureable change in shape. It may of course be argued that this proves nothing, that the chair castings might either have been stabilized without the vibration treatment, or that no stress relief resulting in a change of shape took place within the year in question. It appears at least reasonable in this case, however, to give the combined vibration and annealing operation the benefit of the doubt.

The second example of the application of the vibration-annealing procedure at the Taylor Model Basin was in the manufacture

of a large surface plate and a large layout table in 1942, by the same firm that supplied the rail chairs.

The surface plate is 12 feet 4½ inches long by 3 feet 7½ inches wide by 12 inches deep, and it weighs about 9000 pounds. It is, as shown in Figure 3, a box-shaped iron casting having completely symmetrical upper and lower surfaces and two sets of lightened vertical webs, one longitudinal and the other transverse. It is, by virtue of its designs, well adapted to preserve its shape, apart from any aging or annealing process.*

It was manufactured under specifications almost identical with those for the chair castings, and it was vibrated both before and after annealing in a large molding machine. Its performance since delivery has left nothing to be desired.

In the development of this surface plate, it was at one time hoped to make it of such shape that all the interior as well as the exterior surfaces could be machined. It was believed that still greater stability could be achieved by removing all the skin from the original casting. This design was found not practicable, but an attempt has been made to achieve the same end in the large layout table shown in Figure 4 by the removal of a considerable portion of the casting skin on the interior surfaces in a pickling operation. The holes in the edges were plugged, the casting was stood up on one side, and it was filled with a sulphuric acid solution, which was left there to work for several days.

This large table is in three sections, each 10 feet 8 inches long by 5 feet ¾ inch wide by 9 inches thick. Each section weighed 6150 pounds when finished.

The combined pickling and vibrating operations on these castings have been relatively simple, inexpensive, and easy to combine with the usual machining and annealing operations. Unfortunately, neither the time, the facilities nor the personnel have been available during the war to make precision measurements on these tables over long periods, nor have there been available for comparison any layout tables of exactly the same design which were not subjected to vibration.

* The same remarks apply to the box-shaped chair castings shown in Figures 1 and 2.

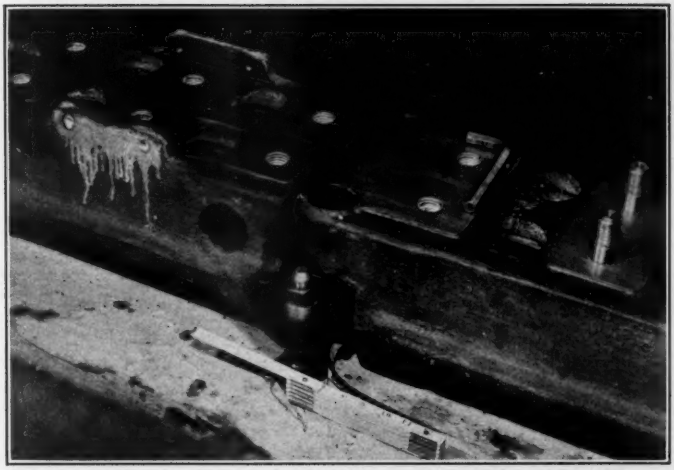

FIGURE 2.—MAIN RAIL CHAIRS FOR CARRIAGE TRACKS.

This is a joint between two of the main rail chairs shown in section in Figure 1. The bosses or "islands" on the top had to be machined accurately and had to remain true to hold the rails in place.

FIGURE 3.—LARGE SURFACE PLATE.

This plate has complete upper and lower surfaces, making it symmetrical about a horizontal plane through the plate at mid-height. It is stiffened internally by a system of longitudinal and transverse lightened webs.

FIGURE 4.—LARGE LAYOUT TABLE, 32 FEET LONG.

This table is in three sections, bolted together. Each section is a symmetrical stiffened casting, with complete upper and lower surfaces, similar to the surface plate shown in Figure 3.

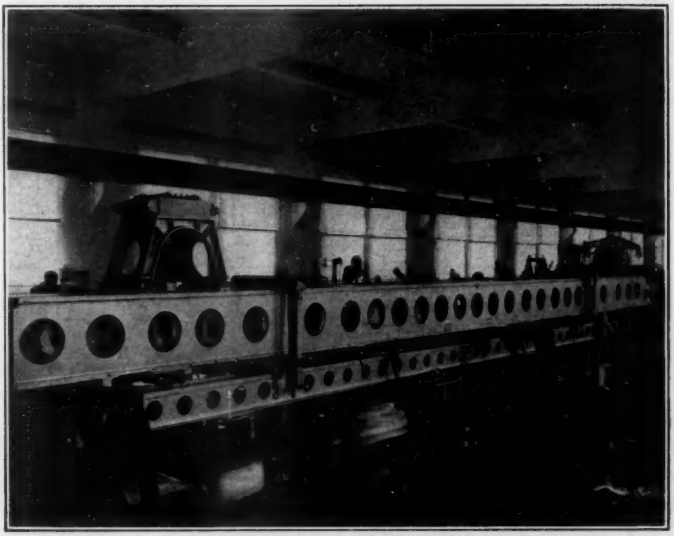

FIGURE 5.—TOWING DYNAMOMETER FOR CARRIAGE I.

The upper girder, built of 1 by 1 by ⅛-inch angles and 0.109-inch sheet steel, forms the fixed foundation structure for all the precision apparatus. The lower beam, built of 1 by 1 by ⅛-inch angles and 0.079-inch sheet steel is the weighing member to which the models are attached.

FIGURE 7.—FIXED DYNAMOMETER GIRDER SETUP FOR STRESS RELIEVING OPERATION.

The clamping arrangement simulates simple support with nodes near the ends. The maximum stress and deflection occur at the center. The vibration generator, shown mounted at the mid-length of the girder, is run at a speed slightly below resonance, which produces a steady forced vibration.

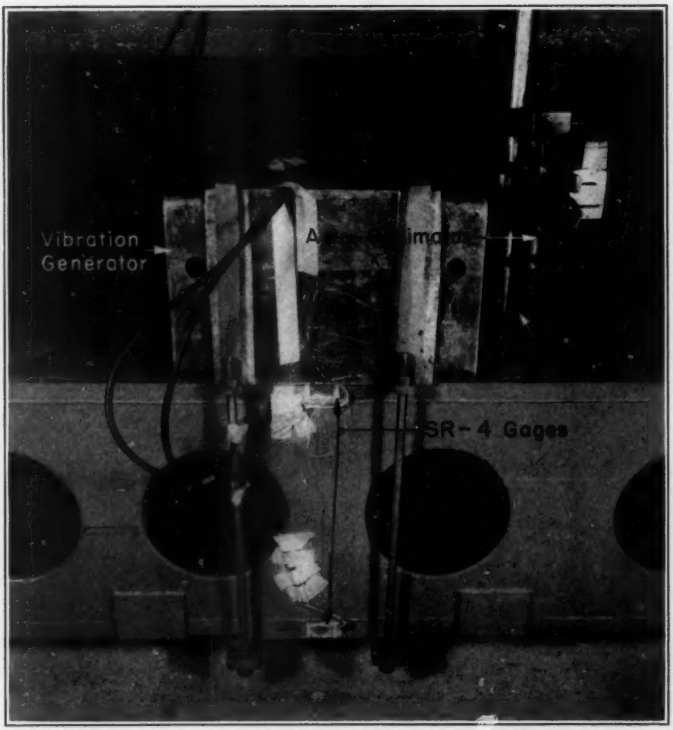

FIGURE 8.—FIXED GIRDER WITH VIBRATION GENERATOR AND DYNAMIC STRAIN GAGES MOUNTED FOR TEST.

The vibration generator is secured to the girder by special U-clamps and tie rods. Metalectric strain pickups were cemented to the girder after the paint had been removed and the surface polished. A Tuckerman optical strain unit was secured to the top of the girder; the fastenings are not shown. The autocollimator with the photographic recording gear was attached to a stand fastened to the foundation. Note the butt weld in the side plate of the girder.

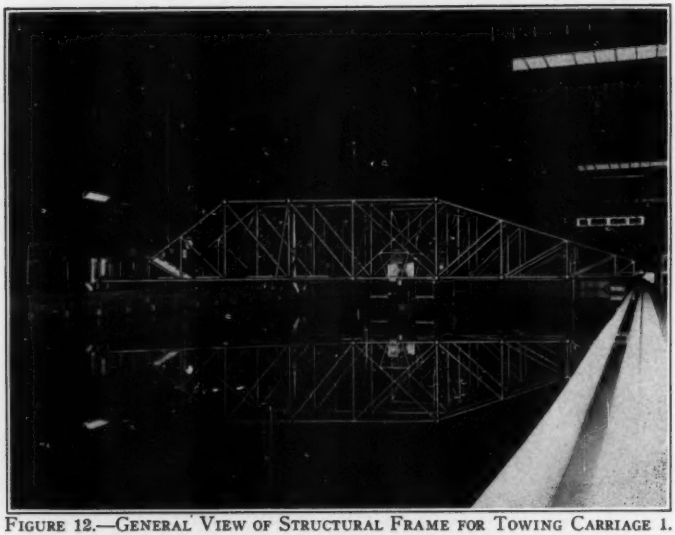

FIGURE 12.—GENERAL VIEW OF STRUCTURAL FRAME FOR TOWING CARRIAGE 1.

The height of each of the four transverse trusses is about 9 feet, and the span between the two rails is 52 feet 8 inches. The frame is of welded seamless steel tubing, with hollow cast steel spheres at the joints. The end of the fixed dynamometer girder can be seen in the center of the frame.

Vibration Experiments on Welded Structures.

The welded tubular structure of the towing carriage designed to run on the Taylor Model Basin carriage tracks previously mentioned was too large for any annealing furnace then available. It was too important a piece of machinery to risk even a minor failure in service, yet such a failure might have been expected in so complex a structure.

This carriage frame was built to carry a large towing dynamometer made up of two large structural parts, a box-shaped foundation girder 15 inches by 16 inches in section and 29 feet 10 inches long, and a floating beam 8 inches by 8 inches by 21 feet 9½ inches long. Both of these parts had to be built with the precision of the chair castings and the surface plates previously described. Like them, they had to remain stable and true for long years of service.

A general view of the two girders assembled in the dyanometer is included in Figure 5. Transverse sections through the girders are shown in Figure 6.

The shorter of the two girders was not too long for the available annealing furnace but there was so little experience with the annealing of a structure having such thin sections, 0.079 inch, that no one was willing to do the pioneer work on this important assembly.

For the stress-relieving operation on these girders, a vibration generator was used which had been developed and built specially for work of this kind. This generator consists essentially of two parallel shafts, motor driven, geared together to run in opposite directions at the same speed and in opposite phase, and carrying eccentric weights on both ends. The small generator used for these experiments was rated at 440 pounds driving force and it had a speed range of from 250 to 3000 Rpm. Both the amplitudes of vibration and the ranges of stress were measured with modern equipment. The process is believed to be of wide general interest and it will therefore be described in some detail.

The girders were supported near the ends on two knife-edges made of structural angles which in turn were bolted down to a special vibration-testing foundation anchored to bed rock. The

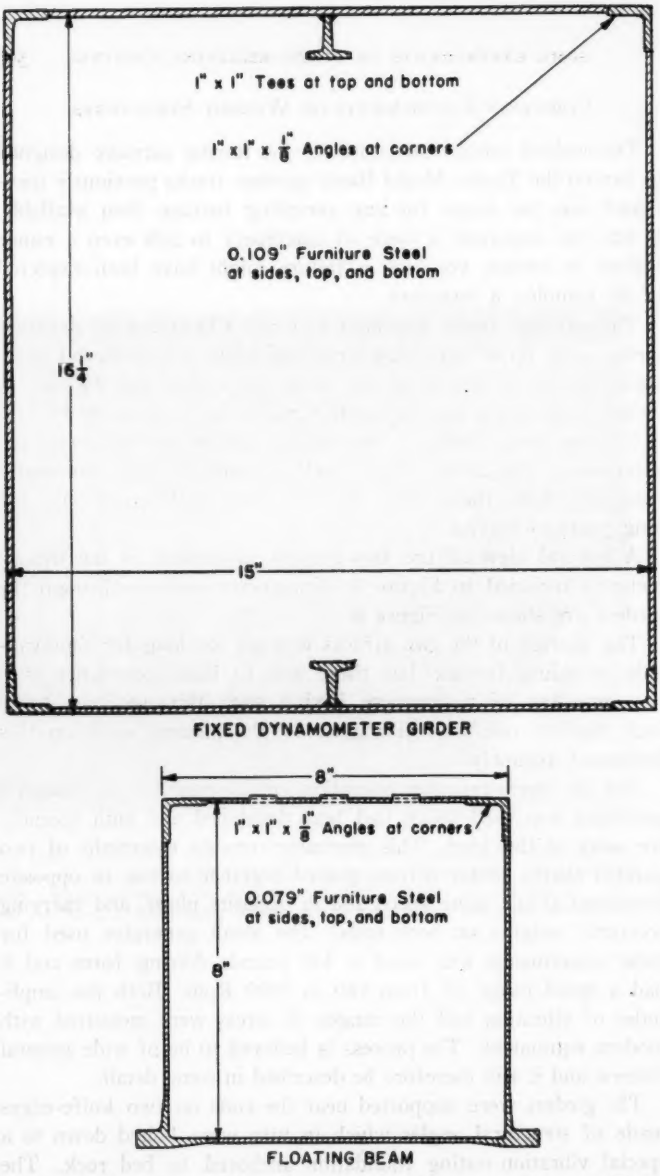

FIGURE 6.—SECTIONS OF FIXED DYNAMOMETER GIRDER AND FLOATING BEAM.

The hollow box-shaped girder structures shown are reinforced at intervals with transverse bulk-heads to hold the sections in shape. The side and top and bottom members are lightened with flanged circular holes as shown in the photographs; the edges of the holes are stiffened by shallow flanges.

girders were held down against the knife-edges by smaller angles and tie rods, as shown in Figure 7. The small vibration generator was clamped on top of the girder at the center as shown in the photograph, Figure 8.

A maximum dynamic stress range* of 15,000 pounds per square inch was adopted, as a satisfactory range for stress relief, and the amplituude required to produce this stress was roughly estimated from the simple beam theory. The natural frequency of the girder in the two-noded flexural mode was also estimated on the assumption of simple support at the knife-edges with the mass of the vibration generator added at the center. An experimental check of the natural frequency was then made by applying an impulse to the girder and tuning a calibrated reed† to the frequency of the resulting vibration. A further check was made of the relation between static stress and deflection by strain gages and dial micrometers.

The vibration generator was then adjusted to an eccentricity sufficient to produce the desired amplitude at a frequency slightly below resonance. On the low side of resonance conditions are stable; that is, the speed fluctuations encountered here for slight changes of voltage are not as wide as those on the high side of the resonance curve. When the amplitude reached the value estimated to give the desired dynamic stress in the girder a check of the stress was made with both metalectric (wire resistance) and optical strain gages set up for dynamic measurements. The vibration generator was then left running at constant speed for a period of 8 hours.‡

Vibration Test Procedure on Welded Box Girders.

The general procedure was as follows:

First, to calculate the elastic constants of the box girders considered as simple beams.

Second, to estimate their natural frequencies when simply supported at the ends with the mass of the vibration generator added at the middle.

* The term "range" as used here covers all values between the specified stress in tension and that stress in compression.

†A Westinghouse reed vibrometer was used.

‡Again this figure was an arbitrary one, arrived at by a consideration of production requirements and some ten years of experience in vibration work.

Third, to estimate the amplitude of vibration required to produce the selected stress range.

Fourth, to check experimentally the static stress produced by a deflection equal to this amplitude.

Fifth, to check experimentally the relation between dynamic stress and amplitude.

Sixth, to determine the form of resonance response of the girder, from which its damping could be estimated.

Seventh, to vibrate the girder for 8 hours or more at the required amplitude and frequency.

The following constants necessary for stress and frequency estimates were first calculated from the dimensions of the girders; see Figure 6.

Constant	*Fixed Girder*	*Floating Beam*
Area of transverse section, square inches	7.33	3.75
Distance from center of gravity of area to bottom, inches	8.0	3.13
Moment of inertia of area with respect to center of gravity axis, inches^4	310.0	38.2
Radius of gyration of area about horizontal axis through center of gravity of section, inches	6.51	3.19
Distance from center of gravity to extreme fiber, inches	8.0	4.99
Section modulus, inches^3	38.7	7.65

The natural frequency of the fixed girder supported on knife-edges over a 28-foot span with the mass of the vibration generator added at the center was estimated by the formula

$$f_1 \cong 21.7 \sqrt{\frac{EI}{\left(W + \frac{17}{35} wl\right) l^3}}$$

where f_1 is the frequency in cycles per second

E is Young's modulus in pounds per square inch

I is the moment of inertia of cross section* in inches^4

W is the weight of the vibration generator in pounds

w is the weight of the girder per unit length in pounds per inch

l is the length of the span in inches.

Substituting numerical values in this formula gives

$$f_1 \cong 21.7^2 \frac{30 \times 10^6 \times 310}{(140 + 339)\,(336)^3}$$

$$f_1 \cong 15.4 \text{ cycles per second} = 924 \text{ cycles per minute}$$

A preliminary estimate was made in the same manner of the amplitude required to produce the desired stress by assuming the girder to deform into a half-sine wave during vibration. On this assumption the maximum stress is given in terms of the deflection at the center by the formula

$$\sigma = \frac{\pi^2 Ec \triangle}{l^2}$$

where E is Young's modulus in pounds per square inch

c is the distance from the neutral axis to the extreme fiber in inches

$\triangle$ is the deflection at the center in inches

l is the length between knife-edges in inches.

Hence to obtain a stress range of 15,000 pounds per square inch or a single stress amplitude of 7500 pounds per square inch the single amplitude required at the center of the girder is

* I is the moment of inertia of the full section, because the lightening holes were near the neutral axis. Because of the stiffening effect of the flanges around them, the presence of the holes was neglected.

$$\triangle = \frac{l^2 \sigma}{Ec\pi^2} = \frac{336 \times 336 \times 7500}{\pi^2 \times 30 \times 10^6 \times 8}$$

or

$$\triangle = 0.36 \text{ inch}$$

The acceleration corresponding to a single amplitude of 0.36 inch at a frequency of 924 cycles per minute is approximately 8½ g. This value was near the upper limit for the vibration generator available but was not too high to be ruled out. Actually when the girder was clamped down with the knife-edges 28 feet apart and the vibration generator was mounted in the center the frequency was found to be 830 cycles per minute. The reduction from the calculated figure of 924 cycles per minute was probably due to one or all three causes, the flexibility of the knife-edges, the effect of the lightening holes, and the incipient instability of the side walls in compression.

When static loads were applied to the fixed girder it was found that a load increment of 554 pounds at the center produced a stress increment of 925 pounds per square inch at a point 11 inches to one side of the center, equivalent to about 990 pounds per square inch in the center, with a deflection of 0.054 inch. These stresses were measured by both Huggenberger extensometers and Tuckerman optical strain gages. If the static stress-deflection ratio held in the dynamic case this would indicate that the single amplitude required for a stress amplitude of 7500 pounds per square inch would have been 0.41 inch. When the girder was set in vibration it was found that a single amplitude of 0.375 inch gave the required stress amplitude. This very closely approximated the value of 0.36 inch estimated for a half-sine wave, which is the theoretical dynamic form where no concentrated mass is added to the beam.

The dynamic stresses were checked both by dynamic Tuckerman gages and SR-4 metalectric strain gages; Figure 8 shows both types of dynamic gages in position on the fixed girder. The Tuckerman gage consists of a strain unit with a rotatable knife-edge prism and an autocollimator for visual reading or photographic recording. The rotatable knife-edge forms an optical lever. The light from an illuminated slit in the focal plane

of the objective of the autocollimator emerges from the objective in the form of parallel rays which are reflected back into the autocollimator by the strain unit, but at an angle which varies with the unit strain. If the strain is dynamic the image of the slit will move back and forth in the focal plane of the objective, where it may be observed with an eyepiece or may be photographed. Both photographic and visual methods were used. A sample photographic record of the dynamic strain due to vibration of the girder is shown in Figure 9.

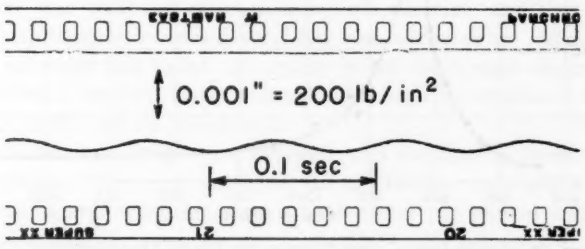

FIGURE 9.—STRAIN RECORD DURING VIBRATION TEST.

This record was taken with a dynamic Tuckerman gage on the fixed dynamometer girder.

The SR-4 gages contain fine wires whose resistance varies with strain. The unit is cemented directly to the stressed member as shown in Figure 8. When current flows through these elements any change in the resistance due to changes in dynamic stress causes a change in the potential at the terminals, which may be amplified and impressed on a cathode-ray beam or measured directly with an electronic voltmeter.

Finally, the eccentricity of the vibration generator was reduced to 10 degrees and the machine was operated through the range of resonance. Amplitudes were observed with a General Radio vibration meter. This is a direct-reading instrument consisting of a piezo crystal pickup unit, an amplifier, a rectifier, and a meter on which amplitudes are given directly. The resonance curve so obtained is shown in Figure 10.

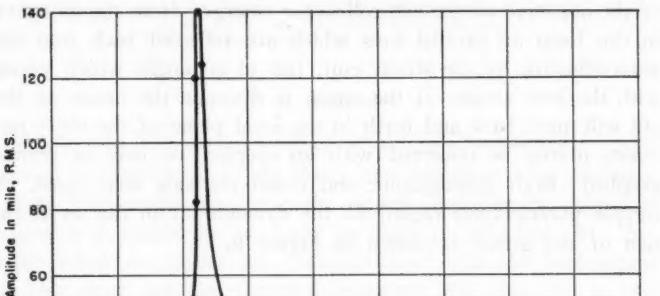

FIGURE 10.—RESONANCE CURVE TAKEN ON FIXED DYNAMOMETER GIRDER.

The amplitudes were measured at the center of the girder. The RMS amplitude $= \frac{\text{(peak single amplitude)}}{\sqrt{2}}$

The damping of a structure can be estimated very simply from the resonance curve obtained with a driving force increasing as the square of the frequency, as in the vibration generator, from the approximate formula

$$\frac{C}{C_c} = \frac{n}{4} \quad \frac{N_2^2 - N_1^2}{N^2_{max}}$$

where C/C_c is the ratio of the actual damping constant to the critical value and n is the ratio of the amplitudes at frequencies N_1 and N_2 to the maximum amplitude occurring at N_{max}. This formula gave a value of 1.6 per cent of critical damping for the fixed girder. An ideal system of one degree of freedom with 1.6 per cent of critical damping has a resonance magnification factor of 31, which means that the single amplitude at resonance will be 31 times the deflection that would exist under the same driving force acting statically. The girder differs from the ideal

system in that its effective dynamic spring constant is not the same as the static constant, because the elastic line has somewhat different forms in the two cases. The driving force of the vibrator at resonance in this instance was 39 pounds and static loading measurements showed that this load would produce a static deflection of 0.00038 inch. The vibration amplitude was 0.14 inch, which indicated a resonance magnification of 37.

The girder was then vibrated for 8 hours at a single amplitude of 0.375 inch and a frequency slightly below resonance. The fact that no change in the natural frequency of the fixed girder was observed after 8 hours of vibration and that the internal damping remained very low was taken as an indication that no welds had failed. No cracks in the welds were observed. How much yielding of the material took place in regions of high stress could not be determined.

A similar procedure was followed with the floating dynamometer beam. This was supported on an 18-foot span. The observed natural frequencies were 1310 cycles per minute without the vibration generator mounted, and 870 cycles per minute with the vibration generator. The machine was run for 8 hours at

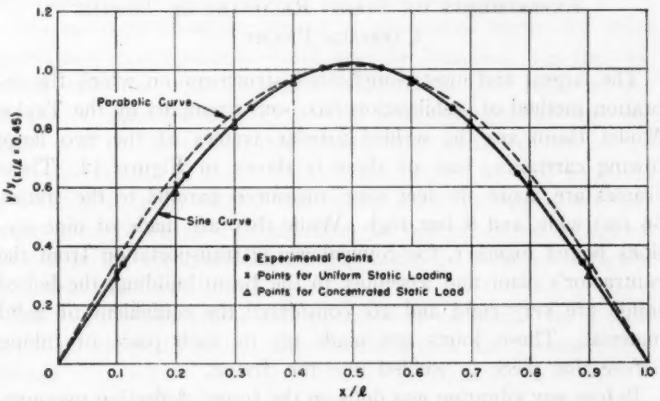

FIGURE 11.—COMPARISON OF VIBRATION PROFILE OF GIRDER WITH THEORETICAL DEFLECTION CURVES OF A SIMPLE BEAM.

The deflection at $x/1 = 0.45$ is set equal to unity in each case.

840 cycles per minute with a maximum dynamic stress range of 15,000 pounds per square inch and a double amplitude of 0.4 inch. The calculated stress for a deflection of 0.4 inch, assuming that the beam deformed into a half-sine wave, is 12,300 pounds per square inch. The amplitude profile of the entire length of beam during resonance was determined experimentally by the use of a small vibrometer. In Figure 11 this form is compared with the deflection curves of a simple beam for the two most common types of static loading, and with the half-sine wave which is the ideal case for free vibration with no added mass. These curves are made to coincide at points 0.05 of the length from the center; these are the points where the deflection was actually measured. The actual deflections fall just about on the half-sine wave, which is midway between the theoretical values for uniform and concentrated static loading, so that any one of these assumptions can be safely used in estimating the relation between stress and amplitude in such a case. As the ratio of the mass of the vibration machine to that of the beam increases, the formula for concentrated load becomes the best approximation.

Experiments on Stress Relieving of Towing Carriage Frame.

The largest and most complicated structures on which the vibration method of stabilization has been attempted by the Taylor Model Basin are the welded tubular frames of the two large towing carriages; one of these is shown in Figure 12. These frames are about 68 feet long, measured parallel to the tracks, 56 feet wide, and 9 feet high. While they are made of nine sections bolted together, for convenience in transportation from the contractor's plant and assembly in the Basin building, the bolted joints are very rigid and are considered the equivalent of solid material. These joints are made up in each piece of tubing *before* that piece is welded into the frame.

Before any vibrating was done on the frame, deflection measurements were taken, first with all the construction supports in place, under the whole frame, and then with the frame supported under the driving wheel and steady wheel locations only, where the

reactions would come in service. The deflection at the center was found to be about 0.1 inch, due to the weight of the structure alone. This result is approximate because it was not certain that in the first condition the frame was uniformly supported all around.

A check was then made to determine how much deflection would be caused by adding a 170-pound dead weight, about equal to the weight of the vibration generator and its clamps, on the member to which the generator was to be attached. The deflection for that load was about 0.0035 inch. On adjacent members the deflection varied from 0.0035 inch to 0.0025 inch, which indicated that the member to which the generator was attached was stiff enough at its joints to transmit most of the vibration to the structure as a whole.

Deflections in the center, in the dynamometer girder position, were measured again when a dead load of 3000 pounds was placed in the dynamometer bay to simulate the weight of the dynamometer and personnel, and of the loads the structure would carry elsewhere when in operation. This deflection at the center of the carriage frame due to increase of load was about 0.1 inch, making a total deflection of about 0.2 inch.

The carriage frame, supported at the points where the drive wheels and steady wheels would later be attached, was then vibrated with the small generator mounted in the center of the frame. A natural frequency of 600 cycles per minute was obtained and the maximum double amplitude at the center of the span was about 0.05 inch. This resulted in an *increase* in stress of about one-eighth of that due to the static load alone, a rather small value to be used in an effort to relieve excess locked-up stresses in the structure but all that could be obtained with the equipment then available.

The vibration generator was operated at resonance for a total period of about 15 hours, with no change in the resonant frequency.

This operation on the first carriage was repeated some three years later on the frame of Towing Carriage 2, built to the same plans. The natural frequency and double amplitude were found to be the same as for the frame of Towing Carriage 1, but be-

cause of other urgent war projects which required the use of the vibrating equipment, the carriage frame was vibrated for a total period of only about 10 hours.

On paper, the low stress range and the relatively short period of vibration, 2 days as compared to an expected life of 50 years, appear quite inadequate. Actually, however, the frame members of Carriage 1 vibrated to a greater amplitude in one cycle of the vibration test than they have been observed to move, at resonant frequency, in more than two years of hard service. There has been not the slightest sign of structural weakness in that time. Again, however, there has been no similar structure, not vibrated, available for comparison.

Discussion.

On the welded structures described, dynamic stress data were taken during the vibrating operation only on the dynamometer fixed girder and on the floating beam. They were taken here merely to furnish a safe guide in applying vibratory loads, and not for the purpose of stress analysis. In general the stresses observed agree with elementary beam theory except as noted previously. However, stresses were measured only on the top and bottom angles, where maximum values are to be expected, and at one point near the center of the beam.

While the damping was very low on the girder and beam at the amplitudes encountered it would not have remained so with increasing amplitude. In view of the high resonance magnification involved, of the order of 30 or more, it might be feared that damage would occur in such a method of stress-relieving owing to accidentally running through resonance. However, there is little danger of this because the damping will increase rapidly as the average stresses approach the elastic limit. If the endurance limit is exceeded there is the possibility of a fatigue failure, but this would occur only after a large number of stress cycles.

It was not practicable in any of the cases described here to measure the amount of stress relief actually obtained. On test specimens used to indicate and measure this stress relief the procedure calls for the more or less destructive process of drilling holes or milling slits in the specimen; this cannot be done in the

testing of parts which are to be used in working structures. Strain gage readings might have been taken at selected stations before and after vibration. This was not done, but observations were made on the general distortion of the structures after the various methods of stress-relieving were carried out.

The shaking and bumping processes described subjected the structures so treated to variations of stress beyond those which would be encountered in subsequent service. It was considered that if the parts or structures showed no large distortion due to this process they would not distort in actual subsequent operation. For instance, the carriage structures were vibrated when loaded to the full service static load and in the fundamental mode of vibration which would occur in actual operation. While the amplitude of the superimposed dynamic stress was only 13 per cent of the static stress it was more than actual operation would put into the structure. Since no observable distortion took place it was assumed that none would take place in actual operation. A similar line of reasoning holds for the dynamometer beams which were dynamically stressed far more drastically than the carriage structure without observable signs of distortion.

Conclusion.

The process of vibrating parts and completed structures may or may not relieve stresses, but it increases confidence in the stability of the shaken part. The evidence of achievement is negative; but the feeling of safety is positive, and this feeling accumulates with compound interest as the years go by and the structures continue to carry their burdens without distress or complaint.

Acknowledgements.

The authors are greatly indebted to Commander J. Ormondroyd, U.S.N.R., of the David Taylor Model Basin Staff, for his valued criticism of and assistance with this paper.

SHIPBOARD POWER CIRCUIT RELAYING.

By Bruce Shipley.

With the increased importance of electrical energy on shipboard, the desirability of improving service continuity cannot be overemphasized. Shore installations for some years have been interconnecting their isolated plants to improve their service continuity, to improve voltage regulations, to reduce power losses, and to gain other advantages beyond the scope of this paper. It is reasonable to believe that shipboard systems will follow the practices of shore installations as it has done in the case of alternating current. Shipboard systems are now being built in such a way that the isolated sources of generation may be interconnected. Interconnections have the disadvantages of placing more exacting requirements on the equipment, and when a fault occurs on the system it is more difficult to isolate the fault properly. Proper isolation of a fault means the prompt removal of only the damaged portion from the electrical power system by automatic relay operation. A good relay system will perform this function regardless of the conditions existing on the power system. Many shipboard relay systems are now so inadequate that this function cannot be performed for all the circuit switching conditions that may be imposed upon them. It is the purpose of this paper to point out the limitations of the available relays for power circuit protection and to discuss a system of relaying that seems to have considerable merit.

The simplest type of relay is the instantaneous over-current relay. This relay may take the form of a simple solenoid which closes its contacts to energize the trip coil of the circuit breaker or it may even be the trip coil itself. In either case it is energized with a current that is proportional to that of the power circuit and when a pre-determined current value is reached the relay opens the breaker without delay. As may be supposed, this

relay can give complete protection only to the simplest power circuits. Figure 1 shows a single line diagram of a power circuit that consists of a generator, a breaker, a power circuit and a load. Ordinarily this circuit may be properly relayed with the simple instantaneous relay. However, if conditions are such that the load current may exceed the short circuit current, the simple relay is not applicable.

Figure 2 shows the simplest circuit that cannot be completely protected by the simple instantaneous relay. In the actual circuit installations there would be loads attached to the buses through breakers. For simplicity these loads are not shown. The breaker "B" could be equipped with the type of relay that has just been discussed. It might appear that a simple instantaneous relay with a higher current setting might also be used on breaker "A". This is not possible because there is no difference in the current magnitudes when a fault occurs on the terminals of breaker "B", regardless of which side of breaker "B" the fault occurs on. Therefore the relay that is applied to breaker "A" must be able to recognize that a fault exists on the load side of breaker "B" but must give breaker "B" time to clear the fault. This clearly indicates a time delay relay. The amount of time delay that breaker "A" must wait depends upon the tripping characteristics of breaker "B". Once the indication to trip is given to the breaker it will trip regardless of whether the indication continues or not. The time it takes the breaker to open after the tripping indication is given is largely a mechanical problem and is caused by the problem of accelerating the mechanical parts. Therefore the time delay relay at breaker "A" is set equal to the tripping time of breaker "B" plus a small margin of time. Now if a fault occurs between breaker "A" and breaker "B", it will not be cleared immediately but must wait for the time delay relay on breaker "A" to function. The time delay relay which is frequently termed inverse time relay is applicable to a number of breakers in series. The breaker that is closest to the generator will require the longest time to trip and the relaying time will be decreased on the other breakers as they approach the last breaker in the series. The disadvantage of this type of relaying is that when there are a large number of breakers in series, the breaker

nearest the generator will allow a fault to persist on the circuit it protects until undue damage or disturbance is caused. Figure 2a shows several breakers in series.

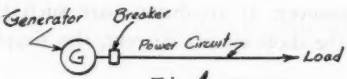

Fig. 1

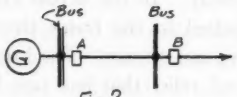

Fig 2

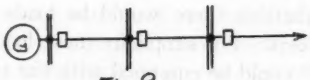

Fig. 2a

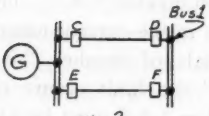

Fig. 3

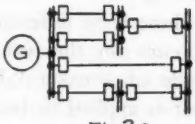

Fig 3a

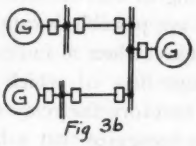

Fig 3b

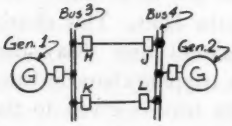

Fig. 4

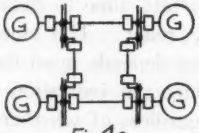

Fig. 4a

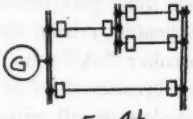

Fig. 4b

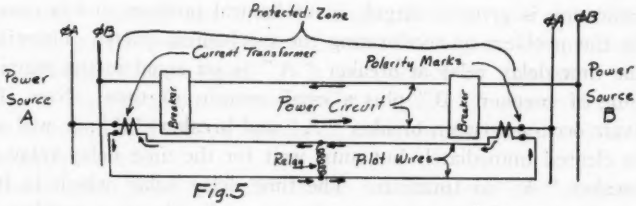

Fig. 5

Figure 3 shows the simplest circuit that cannot be completely protected by time delay current relays. The reason that this configuration cannot be properly protected by time delay relays is as follows: assume a fault between breaker "C" and breaker "D" proper operation would be for breaker "C" and breaker "D" to

trip leaving bus 1 energized through breaker "E" and breaker "F". This could be accomplished by setting breaker "F" on a longer time than breaker "D", and by setting breaker "E" on a longer time than breaker "F". Thus the conditions could be satisfied as long as the faults occurred only between breaker "C" and breaker "D". However, if a fault now occurs between breaker "E" and breaker "F", breaker "D" will open before breaker "F" and then breaker "E" will open to clear the fault. Thus the operation would be incorrect because a fault on the power circuit caused bus 1 to be deenergized. Therefore time delay relays alone cannot be used to relay the circuit configuration as shown in Figure 3. Breaker "F" should never trip for a fault on the circuit between breaker "D" and breaker "C". For a fault in this position the power always flows through breaker "F" in the direction of bus 1. Therefore if a directional relay is applied to breaker "F" it can be connected in such a way that it will close its contacts only when power flows out of bus 1 through breaker "F". The only time this condition exists is when a fault occurs on the power circuit between breaker "F" and breaker "E". This would be correct tripping operation. Now by similar reasoning and from circuit symmetry we may conclude that a directional relay should also be installed on breaker "D" in such a way that it will trip only for power flowing out of bus 1 and toward breaker "C". This will occur only when a fault exists on the power circuit between breaker "D" and breaker "C", which is the only time breaker "D" should trip—so far as power circuit protection is concerned. Now breaker "D" and breaker "F" can trip only for faults on their respective circuits, and the power circuit relaying will be proper when breaker "E" and breaker "C" are fixed so that they can trip only for faults on their respective circuits. With conditions as shown in Figure 3 power can never flow through breaker "E" or breaker "C" toward the generator. Therefore time delay relays may be applied instead of the directional relays on these breakers. Observe the condition that now exists for a fault on the circuit between breaker "D" and breaker "C". All of the power that is flowing into the fault through breaker "D" must also be flowing through breaker "E" and breaker "F". Breaker

"F" has no tendency to trip since the power is flowing through it in the correct direction. Breaker "E" has a tendency to trip since it is carrying fault current. Breaker "E" can have its time delay relay set so that breaker "D" will have time to clear the fault before breaker "E" is tripped. Now by assuming a fault between breaker "E" and breaker "F" the relay on breaker "C" can be set exactly the same as the relay on breaker "E". Thus the two power circuits may be properly protected by the application of directional relays and time delay over-current relays. Directional time delay relays are applicable to circuit configurations that do not have a loop that may be alternately fed from more than one point. However, when the loops contain too many breakers that are in series, the time delay relays may have an objectionably long time setting. Figures 3a and 3b show configurations that may be relayed properly with directional relays.

Figure 4 shows the simplest power circuit configuration that cannot be successfully relayed with time delay, instantaneous or directional relays. Assume that directional time delay relays are applied to breakers "H"-"J"-"K"-"L", and that they are connected in such a way that they will trip only for power flowing toward the lines that they feed. Now assume that generator 2 is not delivering power because its breaker is open. Thus the circuit will be similar to that of Figure 3, and the relay time settings must be similar. That is to say for proper relaying the time settings of the breakers "H"-"K" must be greater than the settings of the relays on breakers "J"-"L". Now the system can be properly relayed. Now assume that generator 1 is out of service and that the system is being supplied from generator 2. Now for proper relaying the time settings for breakers "J"-"L" should be greater than those of breakers "K"-"H". This is not possible since they have been set otherwise to relay properly when the system was fed only from generator 1. Therefore it is not possible to properly relay the circuit configuration of Figure 4 with directional time delay relays. The configurations of Figures 4a and 4b present similar relaying problems and therefore cannot be properly relayed with directional, instantaneous, or time delay relays. Some shipboard power systems can at present be switched into configurations similar to that of Figure 4 and therefore can-

not be properly protected by available relays. Electric Utilities have solved this problem by the application of directional distance relays, carrier current relays, pilot wire relays, or differential relays. Since these relays are extremely delicate, they are not suitable to shipboard use and no more space will be given them. However, for circuits of only a few hundred feet in length, the differential scheme may be applied by using equipment that is now used on shipboard. Since this system seems especially adapted to use on shipboard it will be described in more detail than any of the other relay schemes.

Differential power circuit relaying is based upon the fundamental idea that if the same amount of current comes out of one end of a power circuit that is supplied to the other end of the circuit, no fault exists and therefore no tripping should occur.

In order to compare the two currents at the two ends of the power circuit it is necessary to run pilot wires between the two ends of the power circuit. Figure 5 shows a single phase a. c. circuit with pilot wires and the associated equipment that is necessary to make a current comparison at the two ends of the electrical circuit. For the purpose of explanation assume that a phase to phase fault exists on source "B". This fault will be fed over the protected section and the direction of current flow is shown by the arrows near the power circuit. The currents set up in the pilot wire circuits by the current transformers are shown by the arrows near the pilot wire circuit. The two current transformers are identical and therefore their secondary outputs must be identical if their primary currents are identical. By observing Figure 5 it can be seen that the same current flows through both current transformers, but the current flows through one current transformer in the opposite direction. Therefore, if the current transformer secondaries are connected as shown, the transformer secondaries will feed each other over the pilot wire circuit and no current will flow through the relay coil. This will be the case for all faults that are external to the protected section regardless of the amount of current that flows through the power circuit. Now if the fault is internal to the protected zone, the protected zone will be fed from the two ends and instead of the current circulating between the two current transformer secon-

daries it will add and go through the relay, thus tripping will result. Therefore, the differential relay scheme differentiates between faults that lie within the protected zone and faults that are external. The difficulty with the circuit shown in Figure 5 is that two additional wires would have to be run from the relay to the two trip coils in the two breakers.

Figure 6 shows a method of eliminating the necessity of the extra wires for tripping. This method should work very well if the impedance of the pilot wires is very low as compared to the impedance of the current trip coils. If the ratio of the resistance to the reactance is the same for the pilot wires and the current trip coil, the proportion of the secondary current flowing through the current trip coil will be the ratio of the impedance of one pilot wire to the impedance of one trip coil (for a fault external to the protected zone). Therefore, if the pilot wires have much impedance the circuit could be tripped on heavy external faults. This means that the scheme of Figure 6 could not be set to trip for as little fault current as the scheme shown in Figure 5. However, Figure 6 is complete within itself and no additional tripping power source need be provided, since the tripping power is provided from the fault current that is flowing in the power circuit. Usually, the heavy circuits aboard ship that interconnect two possible sources of generation are already equipped with current transformers, and their breakers usually have current trip coils, and, therefore, the differential circuit as shown in Figure 6 could be installed by merely providing the pilot wire circuit. For this reason the differential protection seems to be especially well adapted to shipboard use. Since the differential scheme shown in Figure 6 is comprised of only the current transformers, the breaker current trip coils, and the pilot circuit, no equipment subject to shock is added.

Figure 7 shows a method of connecting the differential relay scheme so that the impedance of the pilot wire circuit is not so important. This scheme has about the same tripping characteristics as the scheme shown in Figure 5. That is to say that it can be set as sensitively to faults as may be desired. It can be set so sensitive that it will trip for a fault that draws less current than the load, and still there will be no danger of tripping on

heavy faults beyond the protected zone. The disadvantage of this circuit is that it requires three pilot wires instead of two.

So far only the simple ungrounded two-wire circuits have been analyzed. Usually shipboard power is supplied over three-phase

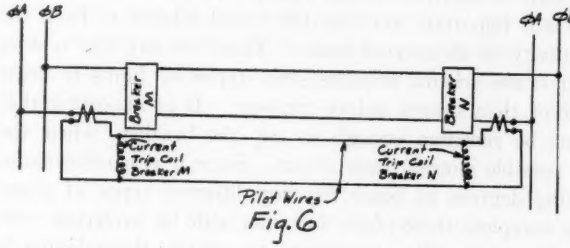

Fig. 6

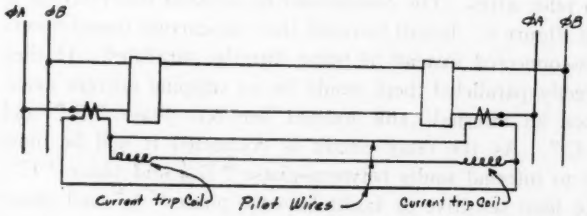

Fig. 7

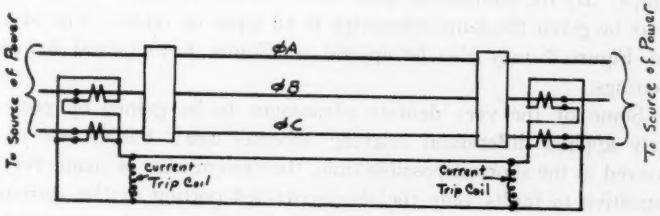

Fig. 8

three-wire ungrounded circuits. From the standpoint of relay protection this is the simplest possible three-phase power circuit. Since at least two phases must be involved to constitute a fault, only two current transformers need be used at each end of the

circuit to provide full protection. The same current transformer requirement is imposed by differential protection. It has been shown that differential relaying removes a fault that lies in its protected zone immediately and is not sensitive to heavy fault currents that flow completely through the protected section. Therefore, it is not important for the differential scheme to have the same sensitivity to all internal faults. That is to say that it does not matter if the scheme requires some types of faults to draw more current than others before tripping. It is important that the scheme be sensitive enough to trip the breakers when the minimum possible internal fault occurs. Since it is permissible to have varying degrees of sensitivity for different types of phase faults, the complete three-phase line may still be protected with only two pilot wires. The connections to perform this relaying is shown in Figure 8. It will be noted that the current transformers are cross-connected instead of being directly paralleled. If they were directly paralleled there would be no tripping current available when an internal fault existed between phase "B" and phase "C". As the relay circuit is connected it will be most sensitive to internal faults between phase "B" and phase "C". It will be least sensitive to faults between phase "A" and phase "B", and phase "A" to phase "C". The sensitivity to three-phase faults will lie between the above sensitivities. These sensitivities are based on each fault drawing the same number of line amps. By the addition of pilot wires the differential relay system may be given the same sensitivity to all types of faults. The idea of Figure 7 may also be applied to Figure 8 to permit lower settings.

Some of the very definite advantages to be gained by properly applied differential relaying schemes are: Faults are removed in the shortest possible time, the system may be made very sensitive to faults, only the short-circuited portion of the system is removed from service and system disturbances are minimized. Since differential relaying works equally well on radial or interconnected systems no constraint need be placed on otherwise desirable power switching arrangements. That is to say that the power system may be operated in any way desired without fear of incorrect circuit relaying if properly protected by differential relaying.

It should be noted that only power circuit protection has been discussed in this paper. No system of relaying is complete until all equipment and buses are properly protected and back-up protection added. It is pointed out that differential protection has long been used on busses and equipment. It is now rapidly gaining popularity in power circuit protection. Differential power circuit protection seems to be the most economical and trouble-free system that can be properly applied on shipboard.

SPEEDING UP THE CHEMICAL ANALYSIS OF MISCELLANEOUS FERROUS ALLOYS BY MEANS OF THE SPECTROGRAPH (1).

By W. H. Hammond (2), and Francis Fong (3).

During the few hours allowed to a ship in drydock, in wartime, the officials in charge of repair and replacement of metal members, be it a hull plate, a gear or a bolt, must have identification of these ferrous alloys at lightning speed.

This identification is the job of the chemist by means of chemical analysis. The most efficient tool which has been developed so far, at the Pearl Harbor Chemical Laboratory to gain the necessary speed is the spectrograph. It is especially adapted to the analysis of steel.

These steels come from various sources. The Laboratory has an assistant at every steel pour at the Foundry, night and day, to take an authentic sample and bring it to the spectrographer for analysis and the report is then phoned back to the Foundry. The welding engineers must have an analysis on a structural ship's plate before prescribing a welding rod to use on that plate. The three quarters to one hour spent in sending a sample to the laboratory, getting a spectrographic analysis and receiving a phoned report, is saved many times over in delays which would be due to ruined work if the analysis were omitted. Of the hundreds of thousands of forging and machine steels in stock at the Supply Department and different shops, it is frequently economical and advisable on account of the crucial service to which some member must be put, to have a complete analysis made before labor time is wasted on forming and heat treating possibly the wrong steel from the right bin. In other cases, even the forty-

---

(1) From a paper read before the spring session of the Hawaiian Academy of Science.
(2) Senior Chemist, U. S. Navy Yard, Pearl Harbor, T. H.
(3) Assistant Chemist (spectrochemist), U. S. Navy Yard, Pearl Harbor.

five minutes which may be consumed for a complete analysis is too slow, and the even quicker techniques of spark and spot testing must be resorted to. Unlike these, the spectrograph gives a complete, quantitative analysis on all common elements in steel except carbon, phosphorus and sulfur. Although not covered specifically in this paper, streamlined methods must also be employed for these three elements.

Obviously, the official methods of the American Society for Testing Materials for steel analysis are too slow for the requirements of a navy yard laboratory in wartime. However, analysis by means of the spectrograph has proven so much of a success at Pearl Harbor that two shifts of eight hours each could work the present spectrograph continuously between seven in the morning and midnight, seven days a week; and the purchase of a second spectrograph, and the training of two more crews of men in the opinion of the authors would be advisable.

This paper represents notes on a study of the criteria, speed, precision and completeness of analysis, which were attained in the comparative analysis of two alloy steels under controlled conditions.

The samples studied were two Bureau of Standards officially analyzed steels, No. 30, a chrome-vanadium alloy and No. 111, a nickel-molybdenum. One group of men who customarily used classical A. S. T. M. methods of analysis and had considerable experience were given the two samples for analysis. Another man who is customarily using the spectrograph but has less general experience, was given the same two samples, included with some routine steels. The relative speed of the two crews on the same samples, one using classical and the other spectrographic techniques was taken from the official and usual labor-time reports of the men.

To control the personal factor due to the fact that competitive human beings made the analyses, the several analysts were not informed that test runs were underway. Red " Urgent " tags were placed upon the samples to insure against avoidable delays. The speed attained in each case were thus not calculated from special runs, but from the usual working speeds for the different techniques.

This general method, which was adhered to, of simulating usual working conditions also affected the degree of control of the other two criteria, precision and completeness of analysis. The precision attained by each analyst was strictly a customary precision, which could be depended on for any routine analysis. The completeness of analysis was faulty in some cases, but the elements looked for were those ordinarily sought by the type of technique.

The spectrograph used was a grating instrument manufactured by the Applied Research Laboratories of Los Angeles, and fully described in a former paper (4). The practical difference between spectrographic and classical metals analysis is that the spectrochemist employs one technique and one operation to analyze all metallic constituents in his sample; the classicist employs a different technique and a separate operation for each element.

The cooperating laboratory in this research was the chemical laboratory at a Mainland Navy Yard. Because this laboratory is faced with approximately the same problems, it was felt that the analysis of the same two steel samples by this staff would have true value as a control operation. The figures given for the work of that laboratory were determined and furnished by the cooperation of the chief chemist. This Yard had no spectrograph at the time, so only classical analysis was employed.

The analysts using classical methods were allowed to employ their own preferred techniques, with the exception that only standard, usually A. S. T. M., or American Society for Testing Materials, techniques are ordinarily employed in navy laboratories. The influence of the red "Urgent" tag was trusted to produce maximum speed obtainable.

The three tables will give the results on the analyses of the two steels. Table No. I gives the results of the comparative analyses of Bureau of Standards chrome-vanadium steel No. 30c (QV).

Three columns are given for the results reported in the Bureau of Standards certificate. The first column gives the minimum result reported as having been secured for each element. The second column gives the maximum result. The third column gives what the Bureau terms the "general average", which is to be accepted presumably as accurate.

(4) See this JOURNAL, Vol. 52, No. 1 (1940); and "Shipbuilding and Shipping Record", Vol. LV, No. 24, P. 611.

The next column gives the results reported by the chemical laboratory of the Mainland Navy Yard. These results were secured by classical methods.

The next column gives the results secured by classical, chemical analysis at Pearl Harbor.

The last column deals with spectrographic results, with comments.

TABLE I.

BUREAU OF STANDARDS SAMPLE No. 30C.

	B. of S. Figures.			*	*P. H.*	*P. H.*	
	Min.	*Max.*	*Aver.*	*Chem.*	*Chem.*	*Spec.*	
Carbon, %	.....	.....	.....	.....	0.48	.....	
Manganese, %	0.700	0.718	0.707	0.71	0.71	0.72	√
Silicon, %	0.230	0.243	0.237	0.25	0.23	0.25	(2)
Chromium, %	0.966	0.990	0.977	0.98	0.98	0.98	√
Nickel, %	0.062	0.100	0.080	0.09	nil	0.08	√
Molybdenum, %	tr.	0.013	0.010	0.02	nil	nil	√
Vanadium, %	0.225	0.240	0.235	0.22	0.23	0.20	(1)
Tungsten, %	.....	.....	.....	.....	.....	nil	(3)
Copper, %	0.086	0.107	0.099	0.09	.....	0.10	√
Aluminum, %	.....	.....	.....	.....	.....	tr.	(3)
Columbium, %	.....	.....	.....	.....	.....	nil	(3)
Tantalum, %	.....	.....	.....	.....	.....	nil	(3)
Titanium, %	.....	.....	.....	.....	.....	nil	(3)
Cobalt, %	.....	.....	.....	.....	.....	nil	(3)

Notes:
"√" means within min. and max. limits of B. of S.
"(1)" means "Too low".
"(2)" means "Too high".
"(3)" means "Positive determinations on elements ignored by other techniques."
"*" means "Mainland Navy Yard".

We will briefly discuss the meaning and basis for the comments. A check mark signifies "within the maximum and minimum limits reported by the Bureau of Standards as having been secured by reputable analysts on the sample." If the result came within the range, when the Bureau of Standards' figures were rounded to two decimals, it was given a check.

We consider, therefore, that a result thus checked as conforming to a reasonable standard of precision. For example, the results for chromium hit 0.98 per cent in each case, coming between 0.966

per cent, the minimum and 0.990 per cent, the maximum. The reasons why the errors in each case have not been calculated statistically and reported are two: (1) results determined under war time conditions of pressure in military laboratories are being compared with results secured presumably under more ideal conditions, and (2) the main purpose of this study was to determine relative speeds for merely acceptable precision.

The figure (1) means "too low" for usual acceptance, as the figure (2) means "too high" an error. The spectrographic aide turned in one low and one high result, (5). In his defense it should be stated that he only graduated from the University of Hawaii in the Class of 1942, has had only about six months' experience on the spectrograph and his work is being compared as far as can be checked, with that of much more experienced men. Also, these two results would still be considered useful in yard practice for purposes of precisely identifying a steel. Speed is the important criterion.

The figure "(3)" points to positive determinations by the spectrograph of elements which are customarily found in certain alloy steels, whose presence affect the physical properties and are thus of engineering importance but whose possible presence was ignored by all chemists but the spectrographer. To the welding engineer, especially, these "nils" are of primary importance.

The reasonable final score for the comparative test on the steel seems to be, that the precision was acceptable under Yard conditions but somewhat less for the spectrographer than obtained by older methods, but the completeness of analysis was much greater. He reported on six alloying elements which were ignored by the others.

Upon the other hand, in defense of classical wet methods, it should be pointed out that the spectrograph at the present time cannot determine carbon, phosphorus and sulfur which are of importance in steel analysis.

Table II gives the results on a comparative study made on Bureau of Standards nickel-molybdenum steel No. 111, identical in nature with the previous study.

(5) His "nil" for molybdenum is considered acceptable for a practical analysis.

TABLE II.

BUREAU OF STANDARDS SAMPLE NO. 111.

	B. of S. Figures.			*	*P. H.*	*P. H.*	
	Min.	*Max.*	*Aver.*	*Chem.*	*Chem.*	*Spec.*	
Carbon, %	.....	.....	.....	.....	0.20	.....	
Manganese, %	0.651	0.670	0.662	0.65	0.65	0.70	(2)
Silicon, %	0.280	0.306	0.292	0.29	0.28	0.29	√
Chromium, %	0.260	0.283	0.272	0.27	0.26	0.25	(1)
Nickel, %	1.73	1.76	1.75	1.77	1.74	1.80	(2)
Molybdenum, %	0.200	0.223	0.215	0.23	0.23	0.22	√
Vanadium, %	0.001	0.005	0.003	tr.	nil	nil	√
Tungsten, %	.....	.....	.....	.....	.....	nil	(3)
Copper, %	0.108	0.133	0.122	0.12	.....	0.12	√
Aluminum, %	.....	.....	.....	.....	.....	nil	(3)
Columbium, %	.....	.....	.....	.....	.....	nil	(3)
Tantalum, %	.....	.....	.....	.....	.....	nil	(3)
Titanium, %	.....	.....	.....	.....	.....	nil	(3)
Cobalt, %	.....	.....	.....	.....	.....	nil	(3)

Notes:
" √ " means within min. and max. limits of B. of S.
" (1) " means " Too low ".
" (2) " means " Too high ".
" (3) " means " Positive determinations on elements ignored by other techniques".
" * " means " Mainland Navy Yard ".

In this case, the spectrographer turned in one low and two high results, (6). In judging this work it should be kept in mind that the yardstick set up has been the purely arbitrary one of the practical conformity with the results of other analysts using other techniques. The precision for the spectrograph is assumed, therefore, to be of somewhat lower value in the study of this sample, but acceptable.

The completeness of analysis is much better for the spectrograph.

It will be observed in Table III that while controlling the conditions of the study as far as could be done without introducing psychologically variant factors, the spectrograph, in the hands of a man who had had the advantage of about six months' training under the supervision of a competent spectrochemist accomplished in one hour what two independent groups of more experienced analysts, using older techniques, accomplished in five and one-half,

(6) His " nil " for Vanadium is considered acceptable.

and in ten hours, respectively. The question of how fast these three sets of analysts could go if warned and trying consciously to make a record has been purposely avoided in this study. The effort was made merely to find what results were actually being obtained under working conditions, on samples which had been marked with the laboratory red "urgent" tags.

TABLE III.

COMPARATIVE SPEED.

(I) Classical Chemical Analysis.

(A) Mainland Navy Yard.
14 determination on 2 steels, analyzed simultaneously.
(Mn, Si, Cu, Ni, Cr, V and Mo) 5½ hrs.

(B) Pearl Harbor.
14 determinations on 2 steels, analyzed simultaneously by two men.
(C, Mn, Si, Ni, Cr, V and Mo) 10 hrs.

(II) Spectrographic Analysis.

(A) Pearl Harbor.
26 determinations on 2 steels, analyzed simultaneously by one man.
(Mn, Si, Ni, Cr, V, Mo, Cu, Al, Cb, Ta, Ti, W, and Co) 1 hr.

The point may be raised that the spectrograph has been proven already to give increased speed of analysis. Why this study?

To a navy man the question has never been settled for the special case of a miscellaneous metal work load to our knowledge. The spectrograph has been proven to increase the speed of analysis and the capacity of a laboratory on a large quantity of the same type of alloys. H. V. and J. R. Churchill, for instance, report that the Aluminum Company of America have fifteen spectrographs employed in its new Kensington laboratory on the analysis of aluminum alloys, and handle 500 samples per day per instrument. (7).

(7) J. O. S. A., XXXI, 10, 611.

Upon the other hand, a Navy Laboratory receives a varying load of many types of which aluminum and steel alloys are merely examples. It is unreasonable to expect the speed per sample from a chemist employing a machine to analyze samples of six different alloys as from a chemist specializing on but one.

The purpose of this study has been to find out definitely and report on the comparative advantage of the spectrograph when applied to one very important type of sample analyzed under the operating conditions of a navy yard laboratory. The results seem to be convincing that the spectrograph gives a satisfactory precision, an improved completeness of analysis and a much improved speed over older techniques under these conditions.

VOLTAGE DROP CALCULATIONS FOR NAVY STANDARD CABLES.

By Herman Schaevitz.

Having had occasion to calculate voltage drops in Navy Standard cables for various currents and power factors, the author felt that charts which would enable the user to determine voltage drops without calculations would be of value.

In working up the various charts and graphs contained in this article, it was thought proper to start at the very beginning with the calculation of the reactance of the cables to be considered since values of reactance for Navy Standard cables are not generally available. In carrying this out, calculations were made, not for three single conductors lying in a conduit, but for an actual three-conductor cable of modern construction.

The input voltage to the cable, and not the load voltage, was used as the base from which the voltage drop was taken. The evaluation of drop factors was made on the basis of a 5 per cent maximum drop instead of the customary 10 per cent. The charts obtained by using drop factors are compared with other charts derived directly from vector diagrams. At the conclusion of this paper it will be shown that the calculated value of percentage voltage drop checks closely with that obtained by using the drop factor-derived charts.

I. Method of Calculating Load Voltage From Given Data.

If the material, area, length and interaxial spacing of the conductors of a cable are known, the resistance and inductance can be calculated. These calculations can be used to determine the voltage at the load end of the cable if the input voltage to the cable, load current, frequency, load power factor, and condition of current balance are known.

The resistance, R_c, of a conductor can be determined from the equation, $R_c = rl/a$, where r is the specific resistance of the material of which the conductor is made, and l and a are the length and cross-sectional area of the conductor, respectively. The direct current resistance resulting from the use of this formula can be corrected to take into account the tendency for the alternating current in a conductor to have a greater density near the outer surface than at the center, i.e., the "skin effect". This crowding of the current into a smaller area is equivalent to current flow in a conductor of higher resistance. At 60 cycles per second the conduuctor cross-section must be very large for the skin effect to be appreciable; a conductor of 300,000 circular mil area has a skin effect ratio of less than 1.01; i.e., less than 1 per cent increase of resistance over the direct current value.

The inductive reactance, X_c, of a two-conductor cable, or a three-conductor cable carrying a balanced three-phase current, can be calculated most exactly by determining the self and mutual geometric mean distances of the conductor strands involved. These calculations will be shown later for Navy Standard cables.

The impedance of the cable, Z_c, is equal to

$$\sqrt{R^2_c + X^2_c}.$$

This impedance is multiplied by the load current to give the actual voltage drop through the cable.

Since it is only in exceptional cases that the actual voltage drop across the cable can be measured, or used, it will be interpreted as a step in the determination of the voltage appearing at the load end of the cable. This value is usually the one desired in cable calculations.

If a vector diagram (Figure I) is drawn showing the magnitude and phase angle, $\phi_1 = \cos^{-1}$ (Load Power Factor), of the load voltage, V_L, the actual voltage drop across the cable, V_c, at its phase angle, $\phi_2 = \cos^{-1}(R_c/Z_c)$, and the voltage at the input end of the cable, V_G, a formula can be derived for the load voltage in terms of V_G, ϕ_1, ϕ_2, and V_c by applying the cosine law:

$$V^2_c + V^2_L - 2V_cV_L\cos(\pi - \phi_1 + \phi_2) = V^2_G$$

$$V_L = V_c\cos(\pi - \phi_1 + \phi_2) \pm \sqrt{V^2_G - V^2_c\sin^2(\pi - \phi_1 + \phi_2)}. \quad (1)$$

The use of this numerical solution for V_L entails quite a bit of calculation if values are to be determined for various combinations of the variables. In this article charts have been developed from which the percentage voltage drop in Navy Standard cables can be taken if the size and length of the cable, and the current and power factor of the load, are known. These charts may be used for commercial, as well as Navy types of cables, if, knowing the X/R ratios for the cables, initial points are found for each cable.

Equation (1) will be used later to derive the final set of per cent voltage drop charts.

II. Derivation of Per Cent Voltage Drop Charts by Graphical Means.

Only a balanced three-phase current flowing in a triple-conductor cable will be considered in this article. Unbalanced currents and unsymmetrical conductor arrangements can be taken into account.

The determination of the value of inductance of current-carrying conductors can best be made using the method of geometric mean distances. This method is fully explained in Woodruff's "Electric Power Transmission and Distribution", second edition, Chapter II.

The 60-cycle reactance of one conductor of the cable under consideration is,

$$X_{60} = 0.0529 \log_{10} \frac{D_m}{D_s} \text{ ohms /1000 feet.} \qquad (2)$$

where D_m, the mutual geometric mean distance, is the distance between conductor centers, and D_s, the self geometric mean distance, is calculated as follows for the various standard Navy conductor strandings:

$$D_s = .0004114 \sqrt{A} \text{ inches (7 strands)} \qquad (3)$$

$$D_s = .0004345 \sqrt{A} \text{ inches (19 strands)} \qquad (4)$$

$$D_s = .0004418 \sqrt{A} \text{ inches (37 strands)} \qquad (5)$$

$$D_s = .0004448 \sqrt{A} \text{ inches (61 strands)} \qquad (6)$$

$$D_s = .0004464 \sqrt{A} \text{ inches (91 strands)} \qquad (7)$$

$$D_s = .0004473 \sqrt{A} \text{ inches (127 strands)} \qquad (8)$$

If A is expressed in circular mils, D_s will be in inches, necessitating that D_m also be expressed in inches in the reactance formula (2).

Tables I and II show the values used in deriving the reactance/resistance ratios for the TLPA- and THFA- types of Navy Standard cables, the calculated reactance/1000 feet of conductor, and the values of X/R (reactance/resistance) used in determining the voltage drop characteristic charts described later in this article.

The distance between conductor centers has been assumed to be the overall diameter of one conductor with its insulation + 10 per cent. To facilitate making voltage drop calculations, a numeric, called the "Drop Factor", can be determined for various X/R ratios of the cable, and various load power factors. "Drop Factor" is defined as the ratio of the cable voltage drop between the input and load ends of the cable to the resistive voltage drop in the cable. This is used in the formula:

$$\text{P.D.} = \frac{\sqrt{3}\,(10.8)\,I_\phi L}{A(450)} \times \text{D.F.} \times 100 \text{ per cent} = \frac{4.15\,I_\phi L}{A} \times \text{D.F., per cent,} \qquad (9)$$

where:

P.D. = Potential drop between input and load ends of a 3-conductor cable carrying a 3-phase balanced current. The impressed voltage is 450 volts line-to-line, and the potential drop is expressed in per cent of 450 volts.

L = Length of one conductor of the cable, in feet.

A = Area of one conductor of the cable, in circular mils.

$I\phi$ = Current in one conductor of the cable, in amperes.

D.F. = Drop factor.

In Figure I is shown the vector relationship between the voltage impressed on a cable, (V_G), the voltage drop in the cable, V_c, and the load voltage, V_L. V_G is largely a function of the generator characteristics, and usually only slightly a function of load. The slope of V_c is equal to the calculated value, X/R, and its length is determined by the load current. V_L is the vector dif-

TABLE I

TLPA-CABLE

Designation	No. of Strands	Area, Circular Mils	d_s Inches	Center Spacing, d_m Inches	Calculated Inductive Reactance ohms/1000'	Specified Resistance 25° C. ohms/1000'	X/R Ratio
TLPA—4	7	4,494	0.0275	0.2288	0.0487	2.49	0.0195
TLPA—9	7	9,030	0.039	0.24	0.042	1.24	0.0335
TLPA—14	7	14,350	0.049	0.271	0.039	0.779	0.0502
TLPA—23	7	22,820	0.062	0.32	0.038	0.492	0.0765
TLPA—30	19	30,780	0.076	0.36	0.036	0.364	0.0987
TPLA—40	19	38,950	0.086	0.39	0.035	0.288	0.121
TLPA—50	19	49,020	0.096	0.43	0.035	0.229	0.151
TLPA—60	37	59,940	0.108	0.46	0.034	0.187	0.1794
TLPA—75	37	75,850	0.122	0.51	0.033	0.148	0.224
TLPA—100	61	98,820	0.140	0.56	0.032	0.113	0.283
TLPA—125	61	125,050	0.157	0.63	0.032	0.090	0.358
TLPA—150	61	157,380	0.176	0.69	0.031	0.072	0.439
TLPA—200	61	198,860	0.198	0.76	0.031	0.056	0.549
TLPA—250	61	250,710	0.223	0.85	0.031	0.045	0.69
TLPA—300	91	296,660	0.243	0.93	0.031	0.038	0.818
TLPA—400	127	414,020	0.288	1.08	0.030	0.027	1.12

TABLE II

TABLE II

THFA-CABLE

Designation	No. of Strands	Area, Circular Mils	d_s Inches	Center Spacing, d_m Inches	Calculated Inductive Reactance ohms/1000'	Specified Resistance 25° C. ohms/1000'	X/R Ratio
THFA—3	7	2,828	0.0219	0.154	0.045	4.05	0.0111
THFA—4	7	4,494	0.0275	0.23	0.049	2.49	0.0198
THFA—9	7	9,030	0.039	0.27	0.044	1.24	0.0356
THFA—14	7	14,350	0.049	0.31	0.043	0.779	0.0548
THFA—23	7	22,820	0.062	0.35	0.040	0.492	0.0811
THFA—30	19	30,780	0.076	0.41	0.039	0.364	0.106
THFA—40	19	38,950	0.086	0.44	0.037	0.288	0.13
THFA—50	19	49,020	0.096	0.47	0.036	0.229	0.159
THFA—60	37	59,940	0.108	0.53	0.037	0.187	0.197
THFA—75	37	75,850	0.121	0.59	0.036	0.148	0.246
THFA—100	61	98,820	0.140	0.65	0.035	0.113	0.312
THFA—125	61	125,050	0.157	0.70	0.034	0.090	0.383
THFA—150	61	157,380	0.176	0.79	0.034	0.072	0.48
THFA—200	61	198,860	0.198	0.85	0.033	0.057	0.593
THFA—250	61	250,710	0.223	0.93	0.033	0.045	0.732
THFA—300	91	296,660	0.243	1.01	0.033	0.038	0.865
THFA—400	127	414,020	0.288	1.13	0.031	0.027	1.16

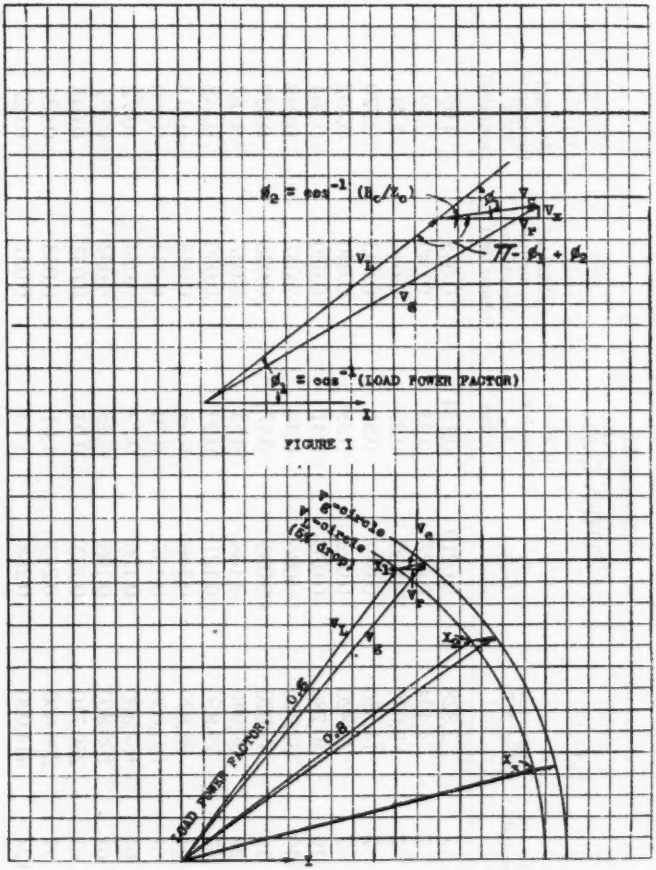
$\phi_2 = \cos^{-1}(R_c/Z_c)$
$\pi - \phi_1 + \phi_2$
$\phi_1 = \cos^{-1}$ (LOAD POWER FACTOR)
I
FIGURE 1
E-circle
I-circle
(IX drop)
LOAD POWER FACTOR
0.6
0.8
1.0

FIGURE 2.

ference between V_G and V_e. The vector triangle is drawn so that V_L makes an angle $\phi_1 = \cos^{-1}$ (load power factor) with the horizontal direction, or the load current, I.

Since $(V_G - V_L) / V_r$, i.e., the drop factor, as defined above, varies with the load on the cable, an assumption of load must be made before proceeding farther. If it is assumed that the cable is used under conditions causing a maximum drop of 5 per cent of the voltage impressed at the generator end of the cable, the resulting drop factors will be theoretically correct only for a 5 per cent voltage drop through the cable. The larger the base—e.g., 10 per cent voltage drop—on which the drop factors are derived, the larger will be the error when calculating small values of percentage voltage drop.

Figure II shows how the vector diagram of Figure I changes for different load power factors on the same cable. A voltage drop of 5 per cent of the impressed voltage, V_G, has been assumed. The slope of V_e is the same for the three cases shown since the same cable is represented.

The points X_1, X_2, and X_3 are the junctions of V_L and V_e. If these points are superimposed, and only the small sections of the V_G — circle adjacent to these points are drawn, the region between the V_G — and V_L — circles can be enlarged. This has been done in Figure III where the lower left-hand corner is the position of X_1, X_2, X_3, etc. The sections of the V_G — circle have been labelled according to their corresponding load power factors.

To use the drop factor chart, the value of X/R is taken from Table I or Table II for the cable being considered, and a line is drawn from the origin (X_1, X_2, X_3, etc.) to the central vertical line at the point designated by the above value of X/R. The slope of this line will then be equal to that of V_e. The horizontal distance between the origin and the intersection of this line with any power factor circle will be the resistive voltage drop in that cable at that load power factor when the total voltage drop is 5 per cent between generator and load over that cable. The ratio of the actual voltage represented by the 5 per cent V_G to the

resistive voltage drop is the drop factor. This ratio is expressed by:

$$\text{D.F.} = \frac{.05V_G}{V_r} \qquad (10)$$

Since the 5 per cent voltage drop is a constant for this chart, the drop factor can be shown as an hyperbolic function of V_r. The hyperbola drawn in Figure III is this function.

To complete the determination of the drop factor, a vertical line is drawn from the intersection of the V_c-line and power factor circle to the hyperbola.

A horizontal line from this point on the hyperbola will intersect the drop factor scale at the correct value of drop factor for the size of cable, and power factor used.

This chart may be used for any impressed voltage if the 5 per cent voltage drop is assumed.

If the values of drop factor taken from Figure III are inserted in equation (9) with constant current and length, curves of percentage voltage, or potential drop as functions of power factor can be drawn as shown in Figure IV for THFA-23 cable at 100 amperes and 100 feet.

It will be noted that the function is shown as a straight line. Since this expresses a direct proportionality between the percentage voltage drop and power factor, charts such as are shown in Figures V, VI, VII, and VIII can be derived. The line of Figure IV now appears as a point on Figure VI. For other cables, the line of Figure IV may not be rectilinear, in which case it will appear as a line in Figures V, VI, VII or VIII.

As an example of the use of these charts (the example is illustrated in Figure V), the per cent voltage drop will be found for the following data: cable, THFA-9; power factor, 0.74; length of single conductor, 154 feet; balanced 3 ϕ current, 24 amperes; applied 3 ϕ voltage, 450 volts.

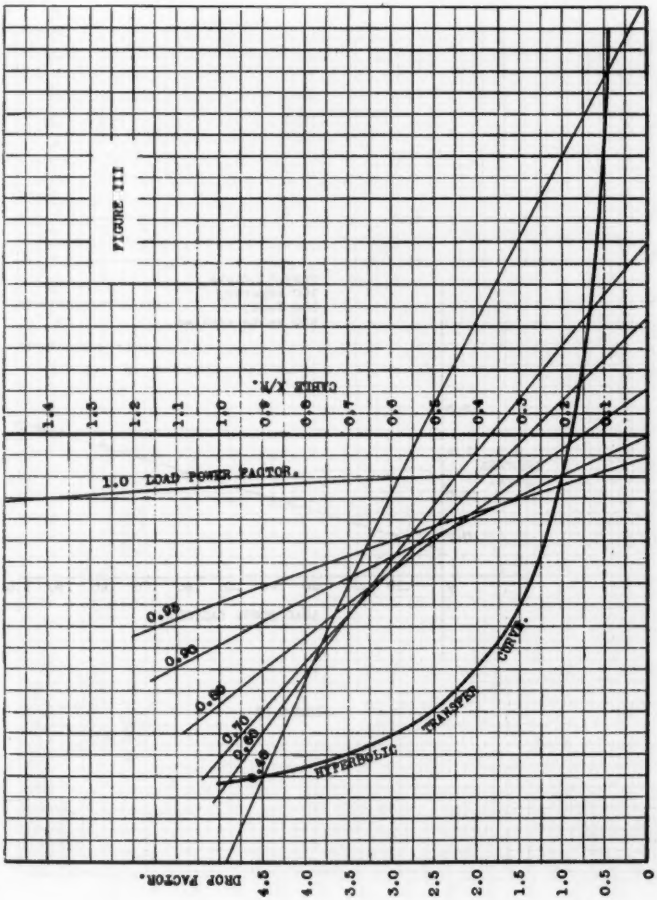
FIGURE III
CHART X/%.
2.4
2.3
2.2
2.1
2.0
0.9
0.8
0.7
0.6
0.5
0.4
0.3
0.2
1.0 LOAD POWER FACTOR.
0.95
0.90
0.85
0.70
0.60
0.40
HYPERBOLIC
TRANSFER
CURVE.
DROP FACTOR.
4.5
4.0
3.5
3.0
2.5
2.0
1.5
1.0
0.5
0

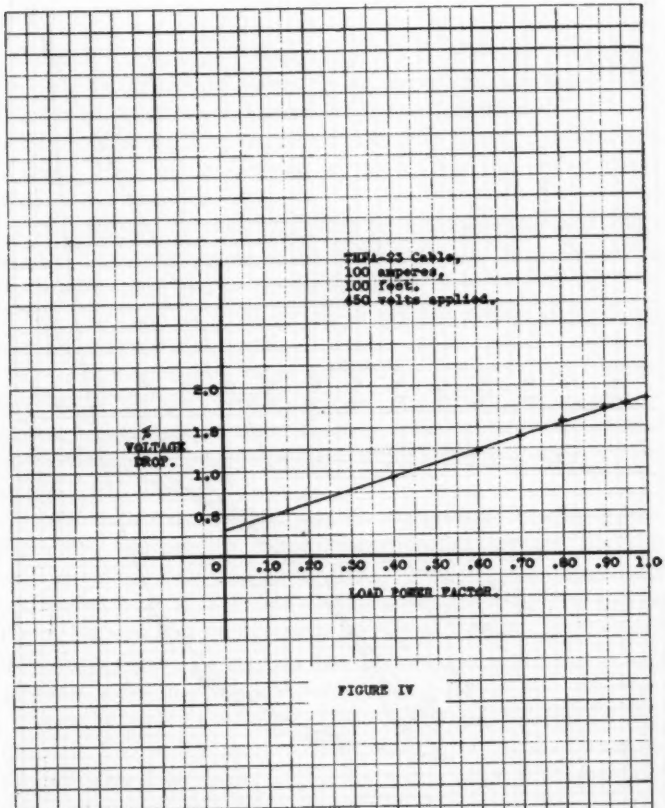
THWA-23 Cable,
100 amperes,
100 feet.
450 volts applied.
% VOLTAGE DROP.
2.0
1.5
1.0
0.5
0
.10
.20
.30
.40
.50
.60
.70
.80
.90
1.0
LOAD POWER FACTOR.

FIGURE IV

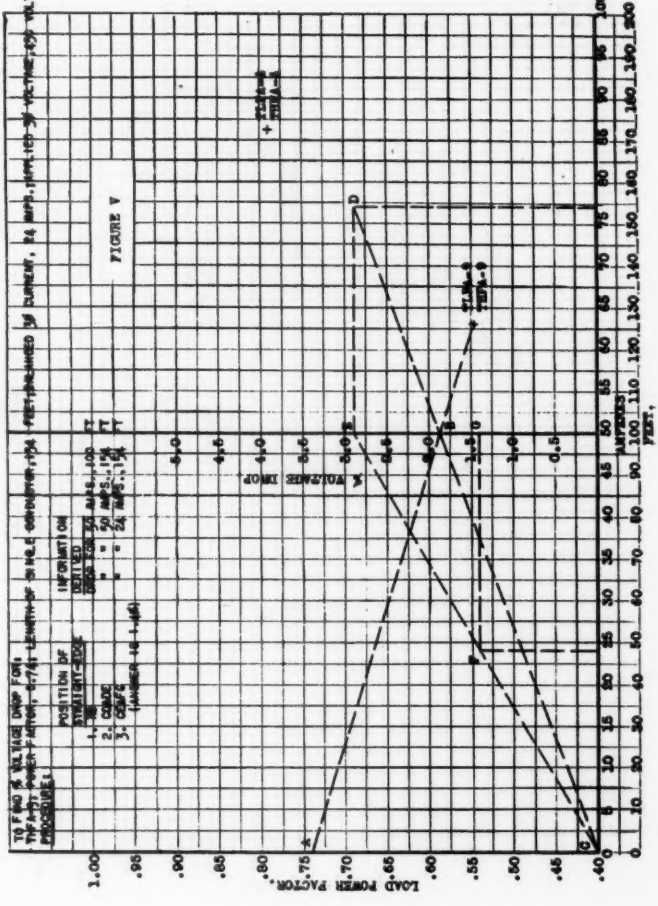
FIGURE V
% VOLTAGE DROP
LOAD POWER FACTOR.
AMPERES PER.

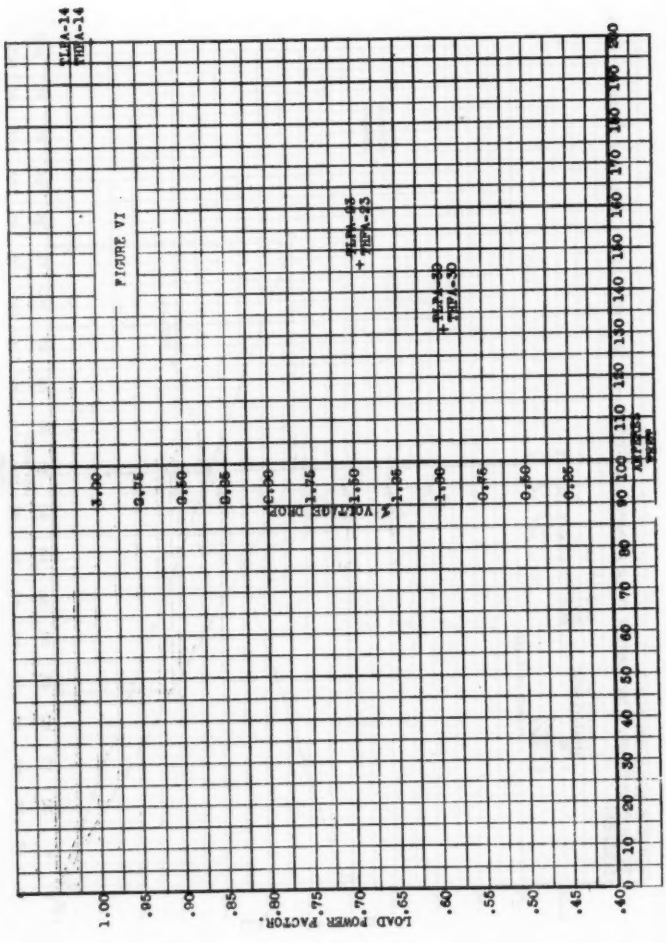
FIGURE VI
LOAD POWER FACTOR.
VOLTAGE DROP
AMPERES PER PHASE
1.00
.95
.90
.85
.80
.75
.70
.65
.60
.55
.50
.45
.40
3.00
2.75
2.50
2.25
2.00
1.75
1.50
1.25
1.00
0.75
0.50
0.25
0.00
10 20 30 40 50 60 70 80 90 100 110 120 130 140 150 160 170 180 190 200

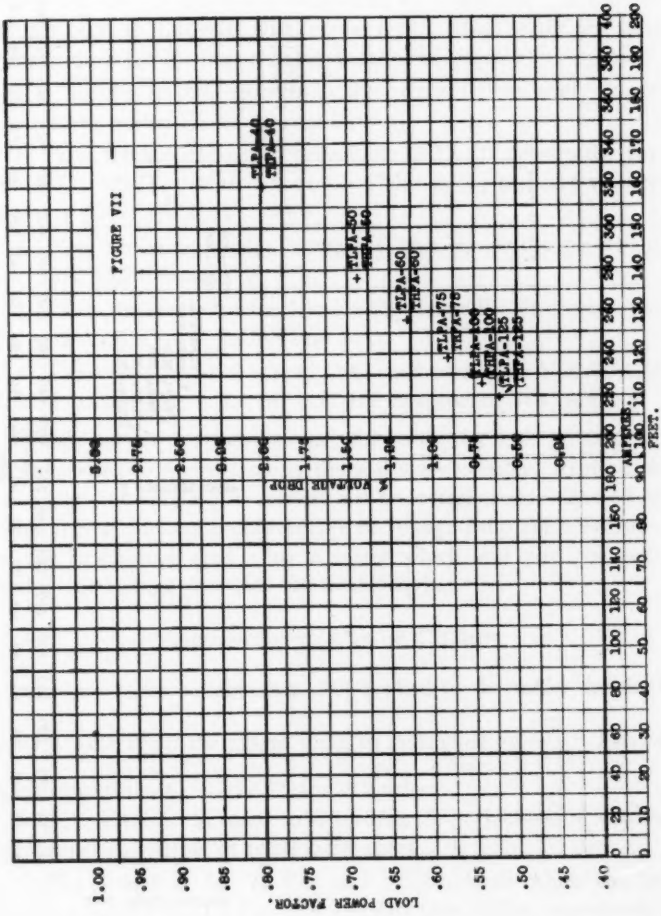
FIGURE VII
LOAD POWER FACTOR.
VOLTAGE DROP
AMPERES.
FEET.
TLFA-40
THFA-40
TLFA-250
THFA-250
TLFA-60
THFA-60
TLFA-75
THFA-75
TLFA-100
THFA-100
TLFA-125
THFA-125

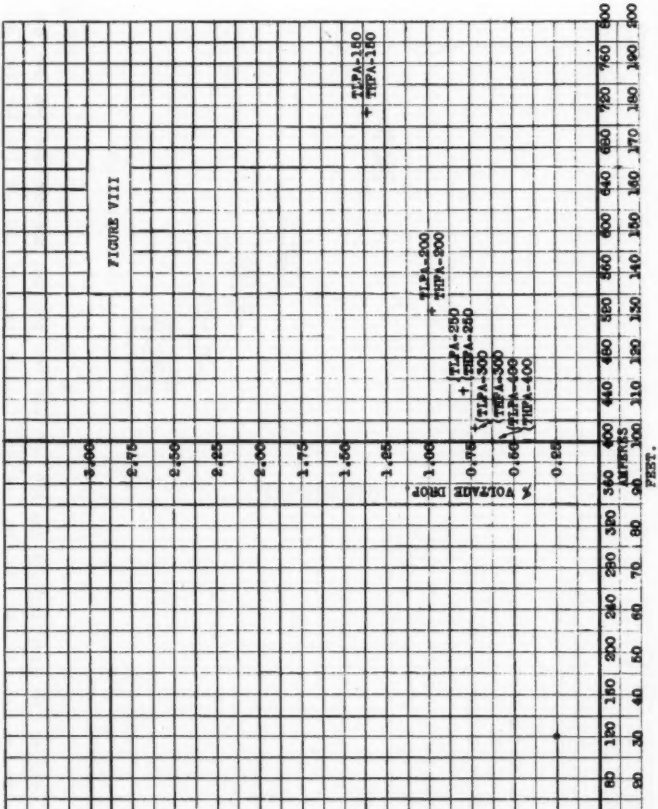
FIGURE VIII
TLFA-150
THFA-150
TLFA-200
THFA-200
TLFA-250
THFA-250
TLFA-300
THFA-300
TLFA-500
THFA-500
TLFA-600
THFA-600
% VOLTAGE DROP.
LOAD POWER FACTOR.
AMPERES
PRIMARY

Procedure:

1. Place a straight-edge from 0.74 (A) on the LOAD POWER FACTOR line to the mark designated by THFA-9. It crosses the per cent VOLTAGE DROP line at B. (This is the per cent voltage drop for 50 amperes, 100 feet.)

2. Place the straight-edge from the origin (c) through B. It crosses 154 on the FEET scale at D.

3. Place the straight-edge horizontally at D. It crosses the per cent VOLTAGE DROP line at E. (This is the per cent voltage drop for 50 amperes, 154 feet.)

4. Place the straight-edge between C and E. It crosses 24 on the AMPERES scale at F.

5. Place the straight-edge horizontally from F. It crosses the per cent VOLTAGE DROP line at G.

6. The answer desired is read at G on the per cent VOLTAGE DROP scale. This is 1.4 per cent for 24 amperes, 154 feet.

Should longer lengths than are shown on the scale be used, at least two methods of extending the scales are possible. If desired, the scales for length and current can be interchanged. The other way involves finding the percentage of voltage drop for a fraction of the length and then using a factor which will give the percentage of voltage drop for the total length.

Extensions to Use of Charts.

For any other voltage than 450 applied to the cable, the final values taken from the charts must be multiplied by $\frac{450.}{V}$ This is 1.955 for 230 volts, and 3.91 for 115 volts.

Figure III can be used to determine drop factors of double conductors as well as of triple conductors.

Tables I and II for TLPA- and THFA- type cables can be repeated exactly for DLPA- and DHFA- type cables, respectively.

To use equation (9) for single-phase circuits, the circuit length, which was $\sqrt{3}L$ for three-phase, becomes 2L for single-phase, or equation (9) becomes:

$$\text{P.D.} = \frac{4.79\ I_{\phi} L}{A} \times \text{D.F., per cent} \qquad (11)$$

for 450 volts applied.

Figures V, VI, VII, and VIII can be used for single phase calculations of double-conductor cable. If, for example, DHFA-14 is to be used, the percentage of voltage drop is determined for THFA-14. This is multiplied by the factor $\frac{2}{\sqrt{3}} = 1.15$ to give the correct answer. Other values of triple conductor drops can be converted to double conductor drops by using the same factor. Commercial cable drop charts can be made up by following the foregoing procedure using commercial sizes and strandings of cables.

TABLE III

Cable	Current, Amperes	Power Factor	Length, Feet	Calculated % Voltage Drop	Chart % Drop	Error in %
THFA—4	50	0.8	240	9.58	9.48	−1.043
			120	4.73	4.74	+0.211
			60	2.34	2.37	+1.28
			24	0.942	0.948	+0.638
THFA—23	100	0.8	600	9.83	9.76	−0.712
			300	4.87	4.88	+0.205
			150	2.42	2.44	+0.828
			60	0.965	0.976	+1.14
THFA—75	200	0.8	900	9.78	9.68	−1.021
			450	4.85	4.84	−0.206
			225	2.42	2.42	0.00
			90	0.97	0.968	−0.206
THFA—400	400	0.8	1640	10.25	10.25	0.00
			820	5.12	5.12	0.00
			410	2.55	2.56	+0.392
			164	1.027	1.025	−0.293

As has been stated above, Figures V, VI, VII, and VIII were made from a drop factor chart which is correct only at 5 per cent voltage drop. In many cases the voltage drops are less than this, and the values taken from the charts may be in error. To evaluate this error, Table III has been compiled showing the computed values and chart values of percentage voltage drop for various lengths of cable. If the lengths were held constant, and the current varied in the same proportion, the drops would be the same.

It will be noted that the error caused by using the 5 per cent charts at other percentage voltage drops is not appreciable.

III. Mathematical Determination of Cable Voltage Drops.

Equation (1) may be changed to provide an expression for the potential drop:

$$V_G - V_L = +V_e \cos(\phi_1 - \phi_2) \mp \sqrt{V^2_G - V^2_e \sin^2(\phi_1 - \phi_2)} + V_G$$

$$\frac{V_G - V_L}{V_G} = 1 + \frac{V_e}{V_G} \cos(\phi_1 - \phi_2) \mp \sqrt{1 - \left[\frac{V_e \sin(\phi_1 - \phi_2)}{V_G}\right]^2}$$

If the radical is expanded by the use of the binomial expansion formula, and only the first two terms are used, the error is less than 0.01 per cent of 450 volts if $V_e \sin(\phi_1 - \phi_2)$ is less than 76 volts. This is an error of 0.045 volts in the actual potential drop. The equation then becomes:

$$\text{P.D.} = \left[1 + \frac{V_e}{V_G} \cos(\phi_1 - \phi_2) \mp \left\{1 - 1/2 \frac{V^2_e \sin^2(\phi_1 - \phi_2)}{V^2_G}\right\}\right] \times 100 \text{ per cent.}$$

The negative sign before the parenthesis is the correct sign; using this,

$$\text{P.D.} = 1 + \frac{V_e}{V_G} \cos(\phi_1 - \phi_2) - 1 + 1/2 \left\{\frac{V_e \sin(\phi_1 - \phi_2)}{V_G}\right\}^2$$

$$\text{P.D.} = \left[+ \frac{V_c}{V_G} \cos (\phi_1 - \phi_2) + 1/2 \left\{ \frac{V_c \sin (\phi_1 - \phi_2)}{V_G} \right\}^2 \right] \times 100 \text{ per cent.}$$

$$\text{P.D.} = \frac{V_c}{V_G} \left[+ \cos (\phi_1 - \phi_2) + 1/2 \frac{V_c}{V_G} \sin^2 (\phi_1 - \phi_2) \right] \times 100 \text{ per cent.} \qquad (12)$$

If per cent voltage drop charts are to be made up, a value for P.D. is assumed. For example, if the charts are to be made up for 5 per cent, equation 12 is solved for V_c with 5 substituted for "P.D.":

$$V_c = \frac{V_G \cos (\phi_1 - \phi_2)}{\sin^2 (\phi_1 - \phi_2)} \left[1 - \sqrt{1 + .1 \frac{\sin^2 (\phi_1 - \phi_2)}{\cos^2 (\phi_1 - \phi_2)}} \right]$$

Again expanding the radical by means of the binomial expansion formula, this time using three terms to maintain the desired accuracy, and using $V_G = 450$ volts:

$$V_c = + \frac{22.5}{\cos} (\phi_1 - \phi_2) - .5625 \frac{\sin^2 (\phi_1 - \phi_2)}{\cos^3 (\phi_1 - \phi_2)} \qquad (13)$$

V_c can be evaluated for different cables at various power factors. Dividing V_c by the cable impedance per foot will result in the product of the current and length required to produce the 5 per cent voltage drop in this size of cable at the load power factor that was specified. Dividing the product of current and length by the current at the central vertical line of a set of coordinates such as are used in Figures V, VI, VII, and VIII will give the length required. With several sets of these values of current, length, and power factor at 5 per cent drop, a point corresponding to the cable size can be located. It will be found that this will not be a well-defined point for the larger sizes of cables since the variation of voltage drop with power factor is not exactly a straight line for these sizes, as it was in figure for THFA-23 cable. This brings up the question of accuracy obtainable by using the charts.

Table III shows that at 0.8 power factor the error in determining up to 10 per cent voltage drop is within about 1 per cent of this value for the various size ranges. This is much better than would be practicably obtainable, since the measurements of installed cable lengths and load currents are not usually known so closely.

At power factors other than 0.8, the error increases to about 2 per cent. While this will usually be permissible, for closer determinations the vector equations must be used. At unity power factor, voltage drops given by the charts are as much as 10 per cent in error for the larger cable sizes. This is because the charts were not originally intended to extend higher than 0.9 power factor, since the current versus power factor curve bends from a straight line above 0.9 power factor.

THE SALVAGE OF THE U.S.S. *LAFAYETTE.*

BY

CAPTAIN B. E. MANSEAU, U.S.N.

AND

LIEUTENANT C. M. HART, CC-V(S), U.S.N.R.

NOTE: *The opinions contained herein are those of the co-authors and are not to be construed as official or reflecting the views of the Navy Department.*

THE U.S.S. *Lafayette* CAPSIZES.*

Launched at Le Havre, France, on October 29, 1932, by the Compagnie Generale Transatlantique (French Line), the S.S. *Normandie* plied the North Atlantic sea lanes for almost a decade—the pride of the French merchant marine—before disaster overcame it.

Built to provide luxurious accommodations for 2000 passengers, and to attain a speed which would reduce the transatlantic crossing time by one day, the *Normandie* was one of the largest and fastest liners ever built. Its general characteristics were: length overall, 1029 feet; beam, 119½ feet; gross tonnage, 79,280; and displacement, approximately 65,000 tons. Any one of its three funnels was large enough in diameter to hold both tubes of the Holland Tunnel. Designed to have sufficient reserve speed to insure consistent and safe running at twenty-eight knots, its top speed was slightly in excess of thirty knots. The ship's main propulsion plant was turbo-electric drive with three-phase AC motors delivering approximately 160,000 horsepower through four screws. Twenty-nine boilers furnished the steam for the turbines.

The *Normandie* was requisitioned by the United States Government on December 16, 1941. She was transferred to the Navy

* Information concerning the fire, capsizing and preliminary investigation was obtained from newspapers, magazines and personal interviews which were considered reasonably reliable.

Department by the Maritime Commission on December 24, 1941, and renamed the U.S.S. *Lafayette*. Work was commenced at once to convert it to a troop transport. The items involved in the conversion included provision for berthing and messing over 10,000 men, installation of anti-aircraft guns, magazines, additional fresh water distilling plants, etc. The work was undertaken with the ship berthed on the north side of Pier 88, the French Line pier, North (Hudson) River, New York City.

Just prior to completion of the conversion work, at about 1430 on February 9, 1942, a fire broke out in the Grand Lounge where 1100 bales of life preservers had been placed for stowage and stenciling before distribution throughout the vessel. Investigations indicated that the fire started when a workman's torch ignited a bale of life preservers. In a very few minutes, the fire had spread throughout the Grand Lounge, destroying furniture, rolls of carpet, decorative trim and other combustible material. The fire, fanned by a strong northwest wind, swept forward over both sides of the promenade deck, until by 1530 it appeared that the entire deck was aflame. Shortly thereafter, the fire spread to the quarters of the boat and sun decks and the bridge, so that the three upper decks, in practically all spaces except the theater, were enveloped in flames or smoke.

The New York City Fire Department took charge of the fire fighting activities, battling the flames from the shore as well as from fireboats. Their operations were pointed chiefly towards keeping the fire from spreading to the lower decks and protecting the pier on the leeward side of the vessel. Scuppers and drains became clogged with debris, causing the water to pocket along the upper decks. By 1530, the vessel had taken a list to port which gradually increased to about 40° at 2330 on February 9th. At 0245 on February 10th, the vessel completely capsized, coming to rest on the port side at an angle of a little less than 80°. See Figures 2, 3, 4, 5, and 6.

The slip in which the ship lay between Piers 88 and 90, is 400 feet wide, the piers each being 1100 feet long. The range of tide is nearly five feet. As the ship rested in its capsized position, the forward end of the keel was about 180 feet north of Pier 88. At the stern, the rudder cut under the pier by about five feet, having

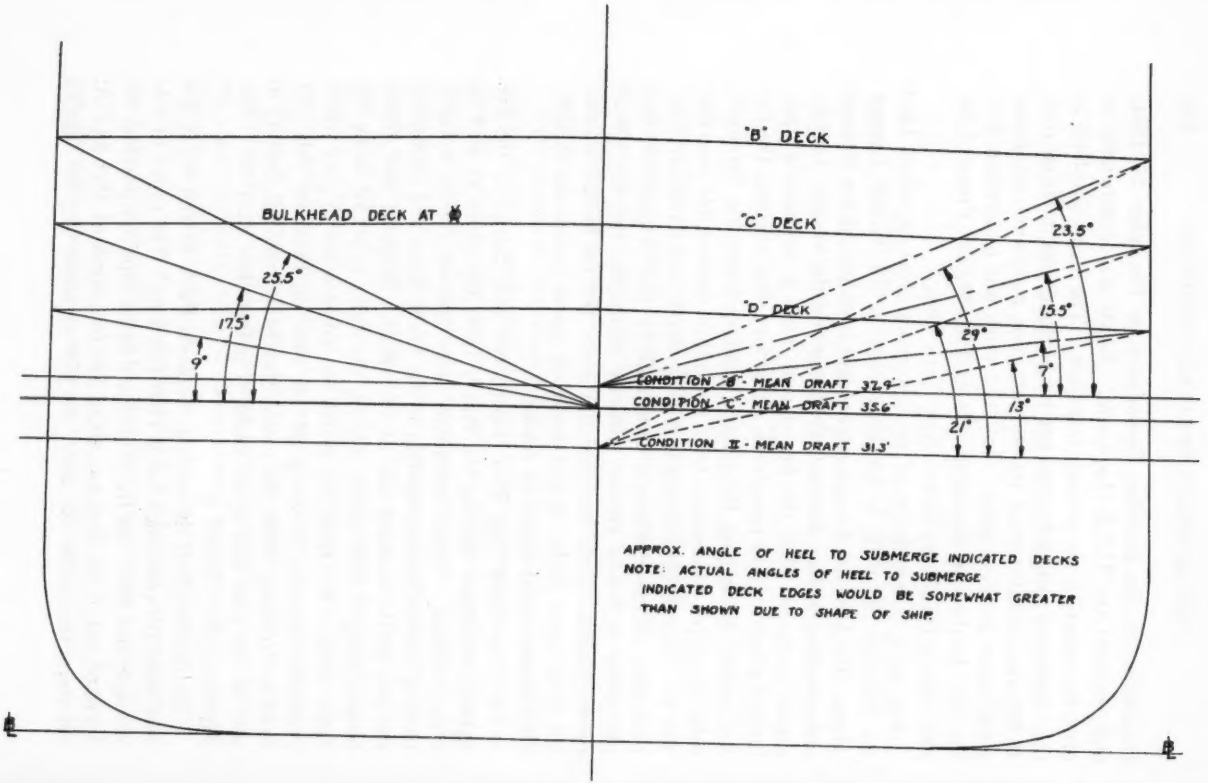
"B" DECK
BULKHEAD DECK AT
"C" DECK
23.5°
25.5°
"D" DECK
15.5°
17.5°
29°
9°
7°
CONDITION "B" - MEAN DRAFT 32.9'
CONDITION "C" - MEAN DRAFT 35.6'
13°
21°
CONDITION II - MEAN DRAFT 31.3'
APPROX. ANGLE OF HEEL TO SUBMERGE INDICATED DECKS
NOTE: ACTUAL ANGLES OF HEEL TO SUBMERGE
INDICATED DECK EDGES WOULD BE SOMEWHAT GREATER
THAN SHOWN DUE TO SHAPE OF SHIP.

FIGURE 7.

broken five piles at the time of capsizing. The forefoot was about five feet below mean low water, while the keel at the stern was about 13 feet below. The ship was completely flooded fore and aft and up to the outside waterline. Figure 9A shows the position of the ship relative to Pier 88, and Figure 9B the mean low water plane, and the bottom of the slip. At a point about one-third the length of the vessel from the bow, the rock profile of Manhattan Island, which had been cut away to forty feet, slopes off steeply into the river bed. A considerable portion of the vessel's weight rested on this edge of the rock shelf. The after two-thirds of the length of the ship were supported and surrounded by mud and soil of various densities.

The capsizing was the result of a combination of circumstances. First, the ship's initial metacentric height was reduced to a negative value. This took place soon after the streams of water which were directed on the fire had collected on the upper decks. Second, her effective freeboard was actually reduced to a height just above the level of the water due to open air and cargo ports. As the vessel listed beyond 13°, the first of these open ports became submerged. See Figure 7. The third, and final, factor was a further loss of stability and consequent increase in heel, due to the turn of the port bilge forward grounding on the rock ledge on the falling tide. While the rock ledge apparently prevented the ship from capsizing completely at low tide, her list had reached a point which hastened the inflow of water through ports as the tide rose. Figures 4 and 5 are photographs taken of the ship during the capsizing and clearly illustrate reduction of the vessel's effective freeboard because of open ports. In Figure 4 the forward cargo port is open just above the water. In Figure 5 this open port is nearly submerged. It was apparently about the time that the picture in Figure 5 was taken that the turn of the bilge grounded hard on the rock ledge almost directly below the forward stack.

FIGURE 7.

It is interesting to note that the initial metacentric height, GM, of the *Lafayette* just prior to the fire, was estimated as about .9 foot and her metacentric radius, BM, was approximately 28 feet. If the reduction of the vessel's metacentric height is considered a result only of the reduction of the metacentric radius, (*i.e.* neglecting change in cg), we find from the formula:

$$BM = \frac{I - i}{V}$$ Where: I = Inertia W. P.
i = Moment Inertia Freewater
V = Underwater volume

that to reduce the initial *GM* to zero required free water surface only sufficient to reduce the moment of inertia of the intact water plane by 1/28. While *BM* increases linearly with increase in size of ships, generally little, if any, of this increase results in an increase in *GM*. This is due to the constant attempt to include in a ship's design desirable items which raise the *cg* to the allowable limit. Therefore, impairment of the intact water plane by a fixed percentage ordinarily results in greater reduction of stability in large ships than in small ones.

Authority to Attempt Salvage.

Prior to the outbreak of war, the Office of the Supervisor of Salvage, U.S.N., was established in the Navy Department under the Chief of the Bureau of Ships to supervise the operation of Navy contract NObs-36 with the Ship Salvage Division of Merritt-Chapman & Scott Corporation. Under this contract, all facilities, including vessels, equipment and personnel, of the largest marine salvage concern in the world are operated by the Supervisor of Salvage, U.S.N. Commodore W. A. Sullivan, U.S.N. (then Commander Sullivan), had been designated as Supervisor of Salvage, U.S.N. He continued in this duty until November, 1942, when he was sent to Africa to direct Allied ship salvage activities in that theater of war. Commodore Sullivan was relieved as Supervisor of Salvage by Captain B. E. Manseau, U.S.N., who retained his other duties as head of the Ship Salvage Branch in the Maintenance Division of the Bureau of Ships.

On February 24, 1942, following the fire, jurisdiction over the *Lafayette* was assumed by the Chief of the Bureau of Ships. It was placed under the immediate cognizance of the Supervisor of Salvage, who promptly took steps to investigate the feasibility of salvage. Mr. John I. Tooker, one of Merritt-Chapman & Scott Corporation's leading salvage masters, was assigned as Salvage Officer. In view of his many years' experience as a diver, and particularly because of his long experience in the salvage of capsized vessels, Captain Tooker was well-suited for the *Lafayette* job.

Because of the location of the wreck in New York City, the investment it represented in labor and material, and the publicity the ship had received both as a liner and its possible use in the war, the disaster was constantly in the public eye and aroused considerable comment from the press and general public. It was necessary to exercise the greatest of caution and the best of judgment in determining what disposition to make of the wreck. Another important factor was that the wreck rendered useless two of the longest berths in New York Harbor. Consequently, in April 1942, the Secretary of the Navy appointed a special committee to make recommendations with respect to salvage and/or other disposition of the *Lafayette*. This committee consisted of:

Mr. J. Barstow Smull, J. H. Winchester & Co., Inc., New York, N. Y.—Chairman;

Mr. W. F. Gibbs, Gibbs and Cox, New York, N. Y.;

Rear Admiral H. S. Howard, U.S.N., Bureau of Ships, Navy Department;

Mr. H. G. Smith, President, National Council of American Shipbuilders;

Mr. H. D. Lapham, Chairman of the Board, American-Hawaiian Steamship Co.;

Rear Admiral H. L. Vickery, U.S.N., U. S. Maritime Commission;

Rear Admiral George H. Rock (CC), U.S.N., Ret'd., Administrator, Webb Institute of Naval Architecture;

Professor H. L. Seward, Yale University;

Commander W. A. Sullivan, U.S.N., Bureau of Ships, Navy Department, Secretary of the Committee and Supervisor of Salvage, U.S.N.

For guidance of the special committee, the Navy Department requested recommendations on the following:

(a) "Should this vessel be raised or should it be disposed of as scrap in her present condition, and, if the latter, what method is considered the most practical?"

(b) "If it is determined to raise the vessel, when she is afloat should she be scrapped or should the consideration of her disposition after raising be left for study until she is afloat?"

It was impossible for the committee to consider all of the thousands of suggestions which the Navy Department received concerning how the vessel should be raised. All letters and suggestions were read and studied by competent engineers. Many ideas submitted were good, but the writers, in general, did not know the particulars of the physical problem involved and the peculiar character of the bottom on which the ship lay, nor did they appreciate the immense size of the vessel. Most suggestions recommended the complicated application of certain principles of physics or methods of construction, with little or no regard as to whether actual conditions permitted their application. Almost invariably, it was assumed that all conflicting physical laws could be automatically waived to allow the suggested plan to work.

Many specialists in salvage, construction, and related matters, were consulted by the committee in an endeavor to explore all possibilities and arrive at the most practical and sound solution.

The idea of cutting up the hulk where it lay was abandoned early in the deliberations because of the prohibitive cost involved, and also because the uncertainty as to the ship's future use precluded leaving a large portion of the wreck embedded in the mud. Likewise, methods of salvage involving the construction of cofferdams around the ship or the application of external force through mechanical devices or both, were discarded, since the surrounding physical conditions would not permit their use at a reasonable cost in time and money. Even if these methods were successful, they offered only a partial solution, as in either case the vessel still had to be cut up or floated upright. Figure 9B shows the approximate bearing condition of the capsized ship, indicating that bearing was one of the controlling considerations, not only in choosing the method of salvage, but in permitting its accomplishment.

It was finally decided that the vessel could be raised, and that the cheapest, fastest, and most certain method of accomplishment was to right and refloat the ship in one operation by pumping. This required, first, making the underwater hull tight, and subdividing the interior into watertight compartments, so as to permit control of the vessel's movement and stability at all times during pumping.

Detailed estimates of time and cost indicated that salvage of the

Lafayette by this method could be completed in less than two years at a cost of about $5,000,000.

On May 1, 1942, the committee reported as follows:

(a) "The vessel should be raised."

(b) "Considering the uncertain future needs of the war effort, the committee feels that a decision as to whether the ship should be reconditioned and for what purpose should not be made at this time. Such a decision should await the development of future war conditions and needs as the salvage of the ship draws nearer. Since there is a possibility that the war emergency may make the reconditioning of the ship desirable, every reasonable effort should be made to expedite the salvage".

Development of Salvage Plan.

As a result of the recommendation of the special committee, the Supervisor of Salvage was ordered to proceed with salvage of the *Lafayette*. This was by far the largest, but none the less, just one of a great number of salvage operations conducted during 1942-43 by the Navy Salvage Service. However, in view of the enormity of this operation, it was necessary to deviate from the usual practice of utilizing the personnel and organization of the Ship Salvage Division of Merritt-Chapman & Scott. A more or less independent organization was set up for the project, using as little key personnel of Merritt-Chapman & Scott as possible, so as not to interfere with the extensive salvage work being conducted in coastal waters, resulting from marine and war casualties. Because of the great responsibility involved, it was necessary for the Supervisor of Salvage to take an active part in the management of the job.

Contrary to popular belief, no specific contract was let for the *Lafayette* project. It was carried out under the provisions of general salvage Contract NObs-36, by building an organization around the nucleus of key personnel and acquiring additional facilities as required.

From the time that the vessel capsized until the order was received to commence the actual salvage operations (May 17,

1942), work was restricted to removal of the superstructure, installation of scaffolding, removal of fire hazards within the ship, and the exploration of certain unknown conditions.

The possibility of salvage depended, first, on the bearing value of the soil in which the after portion of the ship rested. During the first six months, the after perpendicular settled three feet while the forward perpendicular rose two feet. Ultimately the ship developed enough bearing to resist the initial tendency to settle by the stern and settlement practically ceased when the after perpendicular had settled three and one-half feet.

Secondly, salvage depended on the possibility of removing mud in way of open cargo and air ports long enough to permit divers, working from the inside, to close the ports without undermining the soil bearing to the extent of causing failure and consequent settlement of the ship. The fluidity and depth of the mud, as well as the doubtful bearing value, made it impossible to close the ports by working from the outside. After four months of constant effort to remove the mud by use of air lifts—during the greater part of which time mud entered the ports as fast as it was pumped from the inside—the soil became firm enough to form an inverted dome under the ports long enough to permit them to be closed. *This was the most critical and decisive point in the entire operation.* Prior to this, the possibility of salvage was largely a hope—afterwards it was a matter of time and hard work in performing and checking the multitudinous details involved in closing and subdividing the structure.

It was also necessary to determine that the relationship between the center of gravity and the center of buoyancy was such, or could be so manipulated, as to permit righting as well as floating by pumping alone. As indicated in Figure 9B, with the superstructure and all decks above the promenade deck removed, the vessel was approximately one-half submerged and at an angle of a little more than 79°. Capsized, its total displacement was approximately 103,000 tons, ample to float the bare vessel, weighing about 50,000 tons, by pumping. Since the center of buoyancy was about two feet farther from the keel than was the center of gravity, it was calculated that pumping would right the vessel as it floated.

The pumping plan was developed in detail by Mr. A. C. W.

Siecke, consulting engineer for Merritt-Chapman & Scott, and Captain Tooker, under the direction of the Supervisor of Salvage, U.S.N. A preliminary plan was presented to the special committee for consideration prior to formulation of the final report. Development of the plan involved many modifications in the original because of practical considerations. For example, it was first planned to make the promenade deck and two intermediate decks tight throughout the length of the ship in order to safeguard stability and provide a wide range of manipulation of righting moment. It was later found impracticable and unnecessary to do this. The subdivision finally considered necessary and susceptible of working into the ship is shown in Figure 10. This Figure is an inboard profile of the *Lafayette,* in the capsized position, looking down on the surface of the water. It shows the watertight subdivision actually accomplished, prior to the start of dewatering.

Locating the Center of Gravity.

Vital to any salvage problem such as this is the location of the center of gravity. There was some doubt as to its actual location at the time of the fire, inasmuch as the ship had not been inclined for many years prior to the disaster. It was felt that the best value of *KG* was the one obtained from the District Materiel Office, Third Naval District, under whose cognizance conversion work was being conducted. In order to determine the movement of the center of gravity, resulting from removal of the superstructure, steel and wood from within the hull, and the installation of concrete and wood incident to salvage operations, considerable effort was made to keep detailed records of weight, added and removed. The table in Figure 11 indicates the movement of the center of gravity during the preparations for the floating and righting of the ship.

In order to determine the effect of pumping from the various compartments on the overall center of gravity (see Figure 10, sectional view of the *Lafayette*), it was necessary to calculate, in detail, centers of volume for each of the watertight subdivisions of the ship for various levels of water and various angles of inclination. The development of a final pumping schedule could only be determined by a series of trial and error studies of the vessel

APPROXIMATE WEIGHTS AND MOVEMENT OF THE CENTER OF GRAVITY

AS OF 1 JUNE, 1943

	Weight Long Tons	Component KG on Centerline Ft.	Moment	Component KG to Port Ft.	Moment	Abaft Mid-ships Section Ft.	Moment
Orig. Light Ship (Per D.N.O.)	56,200	50.3	2,826,860			24.6	1,382,520
Wt. Removed (31 Dec., 1942)	9,600	94.0	902,400			23.0	220,800
Add. Wt. Removed (to 1 June, 1943)	1,250	73.4	91,750			10.0	12,500
Est. Net - before adding Bulkheads and Misc.	45,350	40.4	1,832,710			25.4	1,149,220
Est. Wts. Added - Timber Bulkheads and Concrete (to 1 June, 1943)	1,900	74.0	140,600	29	55,100	46.7	88,730
Deck Bracing	200	61.8	12,360	24.9	4,980	135	27,000
Deck Patches	150	89.2	13,380	22.5	3,375	44.3	6,645
Ports and Doors	250	65.1	16,275	49.5	12,375	65	16,250
Wod and Misc.	500 =	50.0	25,000	50.0	25,000		
Total Hull	48,350	42.2	2,040,325	2.1	100,830	25.7	1,242,055
Add for Solid Tanks							
Port - D.B.	3,480	3.8	13,224	20.0	69,600	37.0	128,760
Port - Wings	4,480	22.0	96,560	46.2	206,976	8.0	35,840
No. 2 - Full	300	7.0	2,100			400	120,000
No. 41- Full	200	7.5	1,500			355	71,000
TOTAL	56,810	38.0	2,155,709	6.6	377,406	19.4	1,100,135

FIGURE 11.

at various assumed angles of list and loading. The shoring and stiffening plan in turn depended on the pumping schedule.

It had been proposed and considered that the *Lafayette* be subdivided and pumped in such a way that it would lift off the bottom under equilibrium conditions at approximately its capsized angle of list, 79°. It would then have been an easy matter to haul her stern clear of Pier 88, following which complete dewatering would right her. Calculations indicated, however, that the amount of transverse subdivision necessary to cut up the free water area enough to give the ship safe positive stability at 79° would be impractical, if not impossible, and would increase cost and time estimates enormously.

Compromises between the engineering theoretical desirables and practical limitations of underwater construction were made continuously throughout the salvage operations. An example of this was the final degree of subdivision decided upon. With the final subdivision as shown in Figure 10, the ship was calculated to be stable with a positive metacentric height of a little more than two feet when afloat at 60°. However, since the accuracy of the assumed location of the center of gravity was questionable, it was felt that the vessel should be rotated to 45° before floating, where it would then have better than a ten-foot metacentric height.

It should be noted that in the above discussion the metacentric heights referred to do not relate to the metacenter of the ship in the upright position, but to the vessel afloat at the stipulated inclination, with the compartments so dewatered that the vessel is in equilibrium at those inclinations. This required calculations for the moments of inertia of the entire waterplanes and the water-

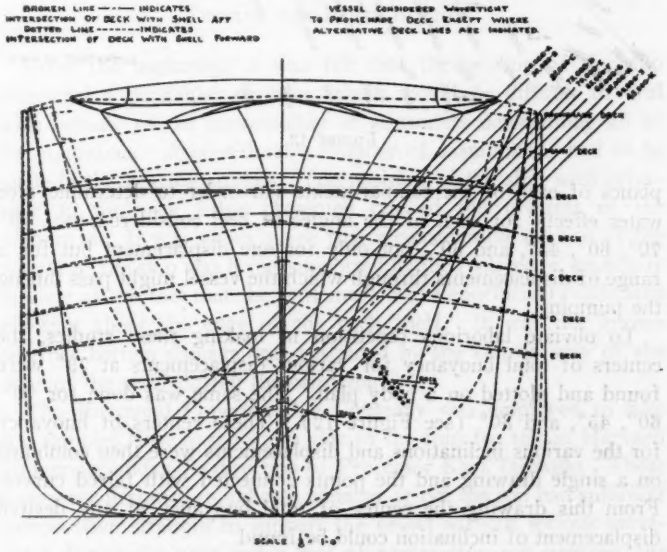

VOLUMES & CENTERS OF VOLUME
ANGLE OF INCLINATION 45°

FIGURE 12.

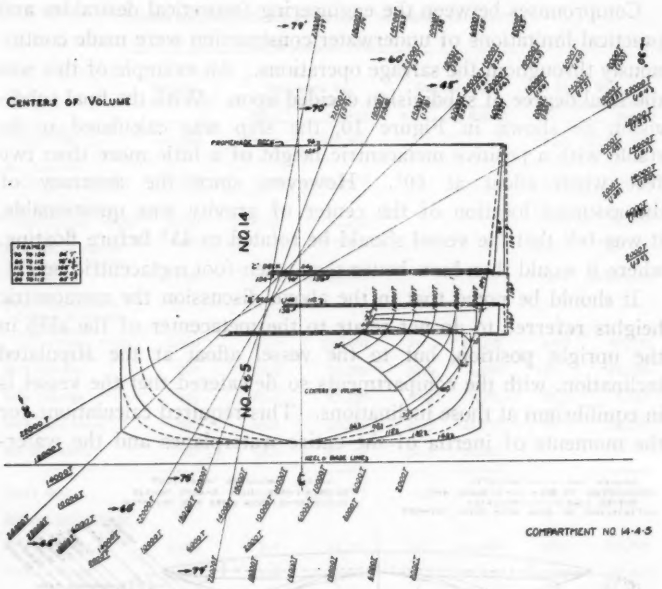

FIGURE 13.

planes of each of the compartments (in order to determine free water effect) for each of the angles of heel considered, *viz.*, 79° 70°, 60°, 45°, and 30°, not only for one displacement but for a range of displacements through which the vessel might pass during the pumping.

To obviate laborious repetition in making these studies, the centers of total buoyancy for various displacements at 79° were found and plotted on a body plan. The same was done for 70°, 60°, 45°, and 30° (see Figure 12). These centers of buoyancy for the various inclinations and displacements were then combined on a single drawing and the points connected with faired curves. From this drawing the center of total buoyancy at any desired displacement of inclination could be found.

The center of gravity (*i.e.*, center of gravity of ship and water inside) at any condition of dewatering of the compartments and

any angle of heel was required both for preliminary studies and for use during righting operations. Time consuming calculations for the movement of the center of gravity of the ship were avoided by determining and plotting the centers of volume for each of the watertight compartments at a series of decreasing volumes and at various angles of heel. Figure 13 is a drawing showing the centers of volume of Compartment 14-4-5. Also plotted and noted were the waterlines and tons of water in the compartment to each waterline. Drawings such as Figure 13 were made for each of the compartments. The position of the center of gravity of the ship, then, for any condition was obtained by selecting from the drawings the number of tons of water in each compartment and the location of the center of each of the volumes. In order that the trim of the ship could be controlled as well as the list, the fore and aft locations of the center of gravity and buoyancy also had to be plotted in a manner similar to the above.

Testing the River Bottom.

From the beginning, it was felt that the bearing of the ship presented a particular problem which would be difficult to deal with because of the impossibility of accurately determining all of the conditions. A considerable number of assumptions had to be made in the bearing studies. The position of the ship with reference to the rock ledge presented one of the greatest of the unknowns. It was strongly felt that a considerable portion of the weight of the ship was being supported by the rock ledge, especially in view of the fact that the settlement curve conclusively indicated pivoting about the edge of the rock shelf. It was not known whether bottom damage was sustained by the ship in way of the edge of the shelf during the capsizing.

The Raymond Concrete Pile Company was employed to take soil samples close to the south side of the ship for test at Harvard University under the direction of Professor Karl Terzaghi. These tests were designed to indicate whether or not the soil had sufficient compressive strength to support the vessel without serious movement during the year and a half of preparation for righting, the effect dredging would have on settlement of the ship, and the

probable effective soil bearing plane. Samples were obtained by means of a piston-type sampler using two-inch, twenty-gauge, seamless steel tubes, forty-eight inches long. These tubes were sharpened at the bottom and drawn in to provide an inside clearance of approximately two per cent. With the piston fixed at the bottom of the tube, the sampler was advanced from six to twelve inches below the bottom of a cased bore hole. The piston was then released and the sampler pushed down a distance of forty-two inches in a quick continuous motion.

Test results at Harvard indicated that the ship rested on soil consisting of three fairly well-defined strata. The top stratum, roughly twenty-five feet deep, consisted of a black, highly organic river mud whose water content (per cent of dry weight) decreased from about 150 per cent at the surface to about eighty per cent at its base. It had the consistency of a very thick liquid. Cylindrical samples with a diameter of two inches and a height of six inches, bulged and failed under the influence of their own weight.

The second stratum consisted of a gray, organic silt-clay whose thickness increased from zero at the rock ledge to about forty feet at a point 800 feet from the stringpiece of the slip. Its water content decreased from about eighty per cent at the upper boundary to about forty per cent at the base. The non-confined, compressive strength of this clay ranged between 0.3 to 0.6 tons per square foot. If a cut in the clay were made by dredging, the clay could stand at a vertical slope to a height ranging between twenty and forty feet.

The third stratum consisted of gray-fine sand which rested on the bed rock. (See Figure 9B).

From the soil studies, it was felt that the vessel rested on material of sufficient strength to preclude anything but minor settlement of the ship. This was borne out in the actual settlement. (See Figure 14). After weighing the possibilities, an effective bearing plane of minus forty-nine feet (*i.e.*, forty-nine feet below mean low water) was assumed for the bearing studies of the ship at rest and during the righting stages.

By locating the longitudinal centers of gravity of the ship and the bearing plane, and assuming the ship to be a beam supported at one point by the rock ledge and at another by the center of area of the bearing plane, the reaction at the rock was calculated

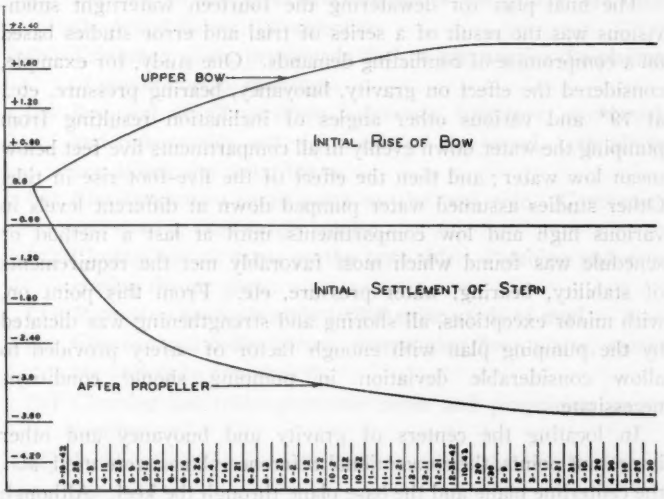

FIGURE 14.

to be approximately 5000 tons. As far as the assumed bearing plane itself was concerned, the eccentricity of loading resulted in a calculated intensity of pressure at the keel edge of about two tons per square foot and at the opposite edge about 0.8 tons per square foot.

THE DEWATERING PLAN.

The pumping schedule, or dewatering plan, was affected by many conflicting factors. It was considered that the intensity of pressure of the low edge of the bearing plane should not at any time exceed two tons per square foot; also, that the ship should be rotated with the bow light to minimize the danger of sustaining damage in way of the rock ledge. Then, there was the possibility of mud suction. Should such a resistance to initial movement develop, it was conceivable that the sudden breaking or release of the suction might cause the ship to lurch. In addition, the allowable heads of water between compartments and between the inside and outside of the ship had to be restricted lest they require extreme shoring and strengthening of decks and bulkheads.

The final plan for dewatering the fourteen watertight subdivisions was the result of a series of trial and error studies based on a compromise of conflicting demands. One study, for example, considered the effect on gravity, buoyancy, bearing pressure, etc., at 79° and various other angles of inclination resulting from pumping the water down evenly in all compartments five feet below mean low water; and then the effect of the five-foot rise in tide. Other studies assumed water pumped down at different levels in various high and low compartments until at last a method or schedule was found which most favorably met the requirements of stability, bearing, water pressure, etc. From this point on, with minor exceptions, all shoring and strengthening was dictated by the pumping plan with enough factor of safety provided to allow considerable deviation in pumping should conditions necessitate.

In locating the centers of gravity and buoyancy and other important points, the conventional reference planes were used, *viz.*, the centerline plane and the base plane through the keel. Although these reference planes were satisfactory at first, it was found later that to determine heads of water between compartments for different inclinations of the ship, reference planes parallel to and at right angles to the water plane were preferable. All measurements were taken perpendicular to the reference planes.

Under the plan to rotate the *Lafayette* to a 45° inclination before floating it clear of the bottom, rotational studies of various ship's sections were made. It was felt most likely that the ship would rotate about an axis near the bilge keel amidships, which meant that a portion of Pier 88 would have to be cut away in order to avoid contact with the ship. Figure 14A is a plan view showing the portion of the pier removed and the expected position of the ship at 45°. Pile clusters or dolphins were driven in such locations as to commence bearing as the ship reached the 45° position (see Figure 15, airview).

Preparations for Pumping.

The preparation of the vessel for righting and floating by pumping involved the following general operations:

(a) Removal of the superstructure above the promenade deck above and below the waterline.

(b) Trimming of the promenade deck to prepare for the placing of patches on all openings.

(c) Removal of all partition bulkheads, furniture, woodwork and inflammable material inside of the vessel, both above and below the waterline.

(d) Closing sixteen cargo ports on the port side. Concreting and bracing port cargo hatches.

(e) Closing 356 air ports on the port side. Patching and concreting the air ports.

(f) Removing approximately 10,000 cubic yards of mud.

(g) Cleaning out boiler rooms, rearranging floor plates, securing boilers to foundations.

(h) Cleaning out turbo-generator room and propulsion motor rooms.

(i) Patching all promenade deck openings below the waterline.

(j) Installing timber and concrete bulkheads.

(k) Shoring promenade and other decks as needed.

(l) Making intermediate deck tight; patching all openings.

(m) Checking pumping arrangements. Closing all pipe lines leading from one compartment to another.

(n) Checking all available plans of ship to determine strength of bulkheads and decks for dewatering operations.

(o) Installing and arranging forty-five ten-inch salvage pumps, twenty-eight six-inch salvage pumps, and twenty-five three-inch salvage pumps and piping for dewatering.

(p) Making detailed calculations of stability and strength for the righting operations.

(q) Removing portion of the pier and driving fender piles.

The task of preparing the interior satisfactorily for dewatering raised many problems, which were solved as the work progressed. Much of the luxurious trimmings, decorations, murals and furniture had been removed during the ship's conversion. Still aboard, however, were the majority of the ship's original fittings and lighting fixtures. In addition, berthing had been installed for over

10,000 men. The storerooms and holds had been loaded with cargo, and great quantities of perishable food had been stored in the refrigeration compartments. The galley was loaded with enough utensils to take care of all aboard. As the ship capsized, everything not secured was thrown in confused heaps to the port side.

Removal of the superstructure was accomplished by burning and hoisting out sections until nothing remained above the promenade deck to a depth of ten feet from the port side where the surrounding mud made further burning impossible. It was believed that the remaining superstructure would act as a dam against mud and silt entering the area next to the promenade deck where scuppers and holes had to be patched. See Figures 17 and 18.

Lack of accessibility was a major handicap in the above operations. At 79°, decks and bulkheads were interchanged in space so that bulkheads, a great many of which were not designed to carry weight, were the only means of support for workers. The companionways which averaged 3½ to 4½ feet in width gave only that amount of head room with the ship on its side, resulting in much work being performed in a stooped or crouched position. After all wooden compartments and debris had been removed, however, extensive staging and scaffolding made access considerably safer. See Figure 19.

Elevator shafts, now nearly horizontal, became companionways. Cargo hatches, originally extending from port to starboard, were used for hoisting debris and material both above and below the waterline. Numerous 1000 pound capacity air winches and fifty gallon barrels were employed for this work. See Figure 20.

Difficulties of access were keenly felt later on in the salvage operations when it was necessary to place the large salvage pumps. Forty-five ten-inch pumps, weighing 2760 pounds each, with approximate dimensions of 8′ × 5′ × 2′, and twenty-eight six-inch pumps, weighing 2000 pounds, with dimensions of 6′ × 2′ × 5′, had to be placed at various positions in the ship. It was, of course, necessary to rig suction and discharge piping to all of the pumps installed. The job of rigging pumps was very difficult and was accomplished only by the judicious use of chain hoists and rope falls.

As mentioned before, the entire salvage plan was based on extensive underwater bulkhead construction, shoring, and patching of openings in the hull by divers. At the beginning there was only a limited number of experienced divers available. Consequently, two diving schools were organized at Pier 88, one for civilians and one for Navy divers. Artificers were generally chosen as diving candidates. As the student divers gained proficiency in handling underwater tools, they engaged in underwater work of a limited nature on the *Lafayette*. Eventually, as many as seventy-three civilian divers were employed at one time, besides a considerable number of graduate Navy divers.

The divers' working conditions were hazardous and, in most cases, extremely undesirable. Before they could start work, submerged spaces had to be cleared of dunnage, debris, and miscellaneous stores and equipment with which they were filled. The submerged portion of the athwartship passageways between the cargo ports, through which much of the access to the spaces requiring attention by the divers was obtained, was completely blocked with debris. Footing through the honeycomb of compartments was unreliable and dangerous. Throughout the entire operations, divers were compelled to work beneath overheads which prevented their rising directly to the surface in case of trouble. This handicap was made even more hazardous when divers had to go through passages and doorways to reach their jobs. One of a diver's greatest fears is that of being fouled and not being able to reach the surface in an emergency. Because of the maze of piping, wiring, and compartmentation, divers were continually subject to fouling. See Figure 21. The water in the slip contained a dense colloidal suspension of mud and sewage, so that both inside and outside the ship divers were compelled to work in total darkness by their sense of touch alone. Underwater lights were tried but in most cases were found useless.

Three hundred and fifty-six air ports, submerged an average of sixty feet below the surface and in eight to ten feet of mud, had to be patched and braced with reinforced concrete in order to withstand the water pressure that was to be exerted on them when pumping commenced. See Figure 10. Almost all of the air ports

and cargo doors which required patching, were found to be covered with mud which had been squeezed into the ship. In many cases, divers found that the staging, hung on the port side prior to the fire, had been crushed under the side of the vessel with many large timbers protruding at sharp angles through open ports, making the patching of these ports extremely difficult. In some cases, both doors of cargo ports were open and mud to a depth of thirty feet had been squeezed in. It was necessary for divers to enter these compartments, sometimes sinking over their heads in mud, to clean out debris and direct mud discharge. The divers' lives were constantly in danger because of broken glass and ragged steel edges, which threatened to sever air and life lines.

Fire Protection.

After the fire and capsizing of the vessel, the embarrassment which might be caused by subsequent fires during salvage operations made it necessary to take extreme precautions. The fire hazard during the initial stages of the salvage operations was exceptionally great, and all preliminary work on the vessel was directed largely towards reducing this hazard. Although the strength members and companionways were constructed of steel, the interior subdivision and trim was largely of plywood. All compartments contained upholstered furniture, as well as canvas-covered berths, wood stanchions and wool blankets. A considerable oil fire hazard existed between Frames 148 and 237 due to leakage from fuel tanks. Smoking was not allowed inside the hull while the ship was being cleaned and cleared, nor during the final pumping operations when the possibility existed of gasoline fumes permeating the ship. A fire watch was posted whenever there was burning with an oxy-acetylene torch.

The fire watch was organized by Mr. John Keeley, former Battalion Chief of the New York Fire Department, and consisted of Mr. Keeley, as chief, three assistant chiefs, and twenty-one firemen, all ex-firemen with twenty or more years' experience. The watch was maintained twenty-four hours per day, three sections standing eight hours' duty each. In the original fire protection system which was maintained until shortly before righting

operations, an 8" waterline was led from the city water main to the third deck of the pier, then across the gangway to the ship. The line was split into two 4" lines, one leading forward and one leading aft on the starboard side of the ship. Outlets for 1½" hose were placed at intervals of seventy-five feet along the fire main with enough hose at each outlet to assure complete coverage of the ship. Fifty pounds pressure was maintained in the line at all times. As a standby, a 1000 gallon per minute auxiliary pump was installed which would increase the pressure to 150 pounds per square inch. A bank of twenty-four CO_2 bottles of 100 pounds capacity each, was located amidships on the starboard side. The CO_2 was piped forward and aft, through 1 inch lines with ¾ inch valve outlets to which two-hundred foot flexible hose with a CO_2 horn could be attached. In addition to the central system, portable CO_2 and pyrene extinguishers were distributed throughout the ship. A forty gallon portable soda-acid extinguisher was also available and ready for instant use, as were complete spares including nozzles, fire hooks, axes, etc.

Prior to the pumping operations it was necessary to rearrange the entire system so that it could function as the ship was dewatered and as it rotated. This was accomplished by transferring all equipment including fire mains and CO_2 banks to the promenade deck about eight feet above the working staging which ran parallel to and about ten feet above the waterline, and onto the barges alongside. Along the fire main on the promenade deck at intervals of every twenty frames, outlets for either 1½" or 2½" hose were installed. At intervals of 250' boxes containing 200' of 1½" hose with Navy Standard fog nozzles were kept. Any point in the ship could be reached with this equipment. See Figures 22 and 23. Before the beginning of righting operations the fire mains were disconnected from the city mains and hooked up to portable gasoline driven pumps. During pumping operations, two Coast Guard fire boats stood by at all times and firemen were stationed through the ship.

Combating Gas Hazards.

The hazard of poisonous, asphyxiating gases is a traditional one in ship salvage. The considerable organic material left inside the

vessel made the encountering of such gases extremely probable. In addition, city sanitary sewers empty into the slip and the river—one at the end of Pier 90, another at the head of the slip between Piers 88 and 90, and another one at the end of Pier 86, making the presence of gases during the salvage operations more than just a possibility.

Upon investigation, it was found that the flow of the city sanitary sewers could not be bypassed or diverted except at an enormous cost and would literally require the rebuilding of the sewer system in that area. It was found, further, that during dry weather periods, the sanitary flow was carried mainly by the sewer at Pier 90. The sanitary flow in these sewers was more or less constant during the period from 0600 to 0300. The city sewer engineers indicated that prior to the capsizing of the *Lafayette*, no chemical analysis had been made of the sanitary effluent of these sewers. The effluent carried the normal sewage waste which might be expected from a large area containing hotels, residences, manufacturing plants, garages, etc.

Soon after the order to salvage the *Lafayette* was received, the Supervisor of Salvage retained the chemical firm of Bull and Roberts to make a sanitary and bacteriological survey of the water in and around the hull of the ship. Eight different sampling locations were established and a series of samples taken at high and low tide, the sampling operations being repeated at weekly intervals for three weeks. It was hoped that the data so obtained would give a measure of the degree of pollution and its variation between sampling points at different stages of the tide. The tests finally established the existence of two general hazards. Because of the highly polluted water in the slip and in the hull, there was definite hazard of infection. It was also felt that an explosive and toxic gas hazard might develop in poorly ventilated compartments.

In view of the results of the tests and particularly of the experience with ship salvage at Pearl Harbor, gas analysis equipment was provided and a procedure instituted to cope with any gas hazard. The gas detection equipment consisted of one combination explosive meter and gas indicator, a carbon monoxide indicator, a hydrogen sulphide indicator, and two safety lamps for detection of oxygen deficiency. Routine gas surveys were made

in all compartments and care was taken to insure that adequate ventilation was provided wherever it was necessary for men to pass. Extension tubes on the gas testing equipment made it possible to test pockets in compartments without endangering the testing engineer. In general, the presence of explosive and toxic gases was tested before a miner's lamp was used to test oxygen content.

Possibly because all compartments were well ventilated by natural means or forced draft blowers, toxic gases were not encountered except in those compartments such as the refrigerating spaces where organic material underwater had decayed. In these compartments hydrogen sulphide was present in dangerous concentrations until divers and workmen cleaned out the entire space. As the dewatering phase of the salvage operations approached, the need for increased vigilance was realized. It was felt that as the water receded and was agitated, dissolved toxic gases would be given off. The foremen of all compartments were instructed to wash down their compartments with fire hose as the water receded. It was believed that this procedure would reduce the possibility of gas forming as well as cleaning the compartments and make access safe within them. In addition, a safety squad was organized, consisting of two Naval Officers in each of three watches who inspected all passages, compartments and access installation to see that no unsafe conditions or practices existed. They were also charged with the specific responsibility of insuring that no explosive or toxic gases developed in dangerous concentrations within the ship. All gas testing equipment was placed at their disposal.

Safety belts with lines attached and face masks with rubber hose connections to divers' airlines were maintained in each compartment. Two rescue breathing apparatus were kept in the engineering shack on the float along with an oxygen breathing mask and two tanks of oxygen. While it was felt that there would be few accidents, a medical watch consisting of a doctor and two corpsmen was maintained throughout the entire righting operations.

The precautions taken against gas hazards were extremely successful. Each time toxic gases were encountered, a forewarning had been received from the routine gas analysis before dangerous

concentrations had formed. Adequate forced draft ventilation plus active efforts towards reducing the hazard at its source solved the problem in each case.

Bulkhead Construction.

The method adopted for the salvage of the *Lafayette* has been called "Controlled Pumping" by newspaper men and others. During the righting operations it was obviously necessary to be able to control the relationship between the center of gravity of the ship, including contained water, and the center of buoyancy of the submerged hull, as well as their movements about the pivoting point in order to produce the required righting moment. It was also necessary to safeguard both transverse and longitudinal stability, control trim, limit the bearing pressure on the rock ledge, limit the amount the ship would right before floating, etc.

In order to accomplish this, the ship was subdivided into fourteen main watertight compartments, each of which could be pumped more or less independently of the others. The subdivision was chosen so that the development of a reasonable number of unforeseen leaks or local failures at any stage in the operation would not cause loss of control, even if operations had to be stopped while remedial measures were taken. Also, since the entire process depended on successful dewatering, it was considered that the ship as a whole should be almost absolutely watertight at the start of the operation. The underwater portion of the vessel was so large, with so many openings, plumbing drains, scuppers, sea chests, and potential sources of leakage of all sorts that it might easily have proved to be a hopeless task to locate and stop all leaks without first isolating compartments and testing the entire ship, portion by portion. See Figure 10.

The number, shape and location of the compartments were more or less indicated by the existing watertight subdivision of the vessel. Use was made of the vessel's watertight bulkheads for all athwartship boundaries of the lower compartments (Compartments 1-11); and the location and size of the upper compartments (Compartments 12-18) were generally indicated by them as well. The shell and appropriate decks were also used for some of the boundaries. The athwartship boundaries of upper Compartments

12 to 18, however, had to be constructed. This involved a tremendous job for the divers. Bulkheads had to be built between each pair of decks (Promenade, A, B, C, D, and E) from a few feet above the waterline down to the port side upon which the ship was resting about 60 feet below. In most cases, as in Compartment 15, for example, the upper compartment boundary consisted of four timber and concrete bulkheads, each spanning one between-deck space. In way of the main dining room, bulkheads had to span the equivalent of three and four between-deck spaces. The bulkheads had to be of sufficient strength to resist the hydrostatic head of thirty feet, and had to be watertight throughout, including the connections between the bulkhead and the ship's decks and side.

While the ship was generally symmetrical, port and starboard, in many cases it was found that there was enough difference in the locations of stanchions, deck houses, etc., that each tentative decision as to bulkhead location and details of construction based upon observations of the above-water half of the ship had to be followed by considerable exploration. Following the general cleaning out, all steel installations in way of the proposed bulkhead were cut with hydrogen cutting torches and removed. Cuts were made through steel compartments, ventilators, cables, and all material except the ship's structural members until a clean swath existed from the waterline down to the skin of the ship in way of each proposed bulkhead. All this work had to be done in total darkness because of the murky water.

Although the design of each particular bulkhead had to be modified slightly to conform to the peculiarity of deck frames and length of the span between decks, all the bulkheads were essentially similar. See Figure 24. One end of each 8×12 timber was secured to a beam and the other end bolted to a long angle bar which previously had been prepared and bolted vertically to the adjacent deck immediately opposite the deck beam. The angle or guide bars and deck beams were thus employed as temporary fasteners for the timber bulkheads. The latter were built from the top down by lowering weighted, grooved and splined timbers held in clamps, to the divers who floated and fitted the splined side into the timber installed above. The splines were 2″×4″ and were cut with a slight taper and generally toenailed in the top

groove of each timber, thus providing a guide to make placing by the diver easier. The clamps, or cradles, were rigged with slings so that each timber could be lowered to the divers. Once the timbers were in place, chain falls were lowered from the opposite sides of the bulkhead and connected to eyes in the cradles. By hauling on both sides with chain falls, the timbers were set up and held securely in place while divers bolted the ends to the guide bars and deck frame.

Construction of an 8×12 splined bulkhead in this manner presented no difficulty in obtaining water tightness between timbers;

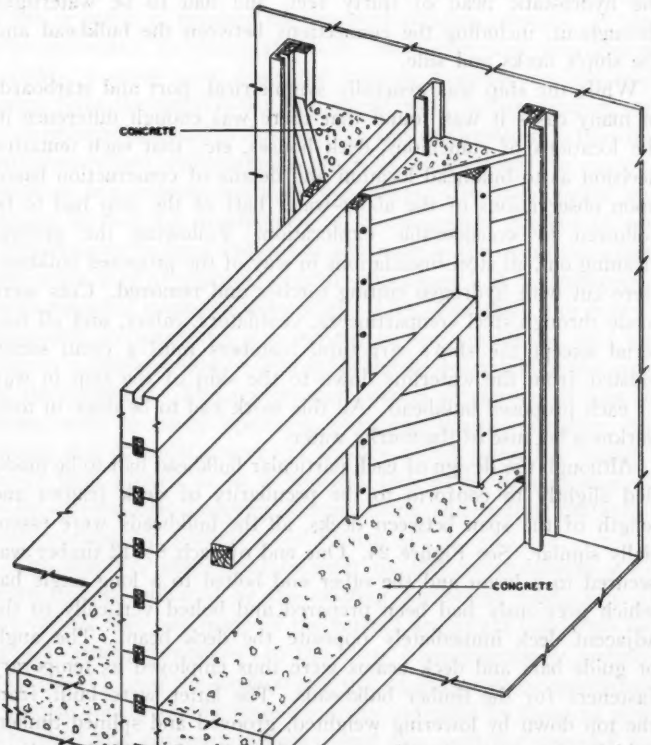

FIGURE 24.

however, the end connection to the decks and connections to the ship's side at the bottom still had to be made tight. The space between the lower timber and the ship's side was dammed by wooden forms and sandbags. Likewise, wooden triangular section forms, having the appearance of brackets, were set between adjacent deck beams and the timbers, so as to enclose the end connections. The entire boundary of the bulkhead—corresponding to the bounding bars of a steel bulkhead—was then embedded in concrete by pouring concrete into the forms by the Tremie process, working from the bottom up.

Figure 24 is a drawing which shows general deck-to-deck bulkhead construction. Figure 25 is a series of artist's drawings illustrating how bulkheads were built by divers. Figure 26 shows a model of the bulkhead at Frame 204, which was built to help the divers visualize the overall picture of the entire bulkhead construction at this point. The bulkhead is viewed from aft looking forward. The vertical members of the model correspond to the decks of the capsized vessel and the deck at the far left represents the promenade deck. The bulkhead between the promenade and main deck spanned about nine feet. However, between the main and C deck (frame 204 in way of the main dining room), the bulkhead had to span three deck spaces, as indicated in the model, from the waterline down to where A and B decks again appear to port of the dining room. From this point down, bulkheads spanned one between-deck space apiece. At this particular frame, C deck was stepped slightly, as is indicated by the model, so that the span of the large bulkhead was not quite three deck spaces.

Drawings in Figures 27, 28, and 29 show details of the bulkhead construction at frame 204. Figure 30 is a photograph of a completed bulkhead, showing the waterline, concrete poured at the ends of the bulkhead, and the kicker timbers designed to prevent the concrete form boards from moving out of place as the concrete was laid. Figure 31 is another picture taken of the same bulkhead after the water had been pumped out of the ship. At the top of the figure is clearly seen a gauge board used in measuring the depth of the water in the compartments. Kickers, spaced at four-foot intervals, are clearly shown as is the concrete poured at the bottom of the bulkhead which made the connection of the bulk-

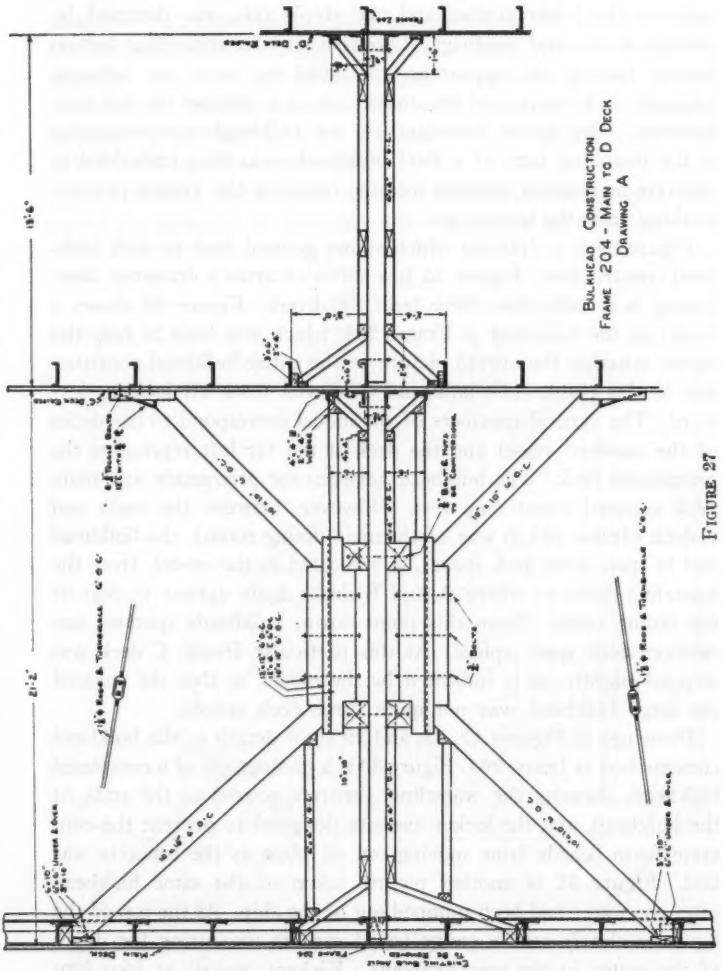

FIGURE 27

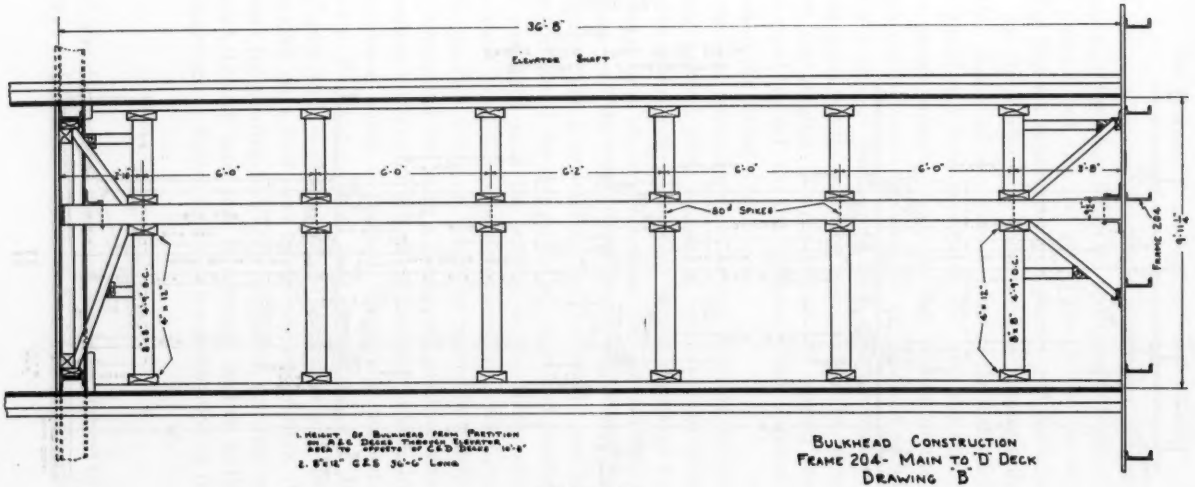
36'-8"
Elevator Shaft
6'-0"
6'-0"
6'-2"
6'-0"
6'-0"
3'-8"
80d Spikes
Frame 204
6"x12"
8"x8" 4'-7" O.C.
1. Height of Bulkhead from Partition on A & C Decks Through Elevator Area to Upside of C & D Decks 16'-8"
2. 8"x12" C.E.S. 36'-6" Long
Bulkhead Construction
Frame 204- Main to "D" Deck
Drawing "B"

FIGURE 28.

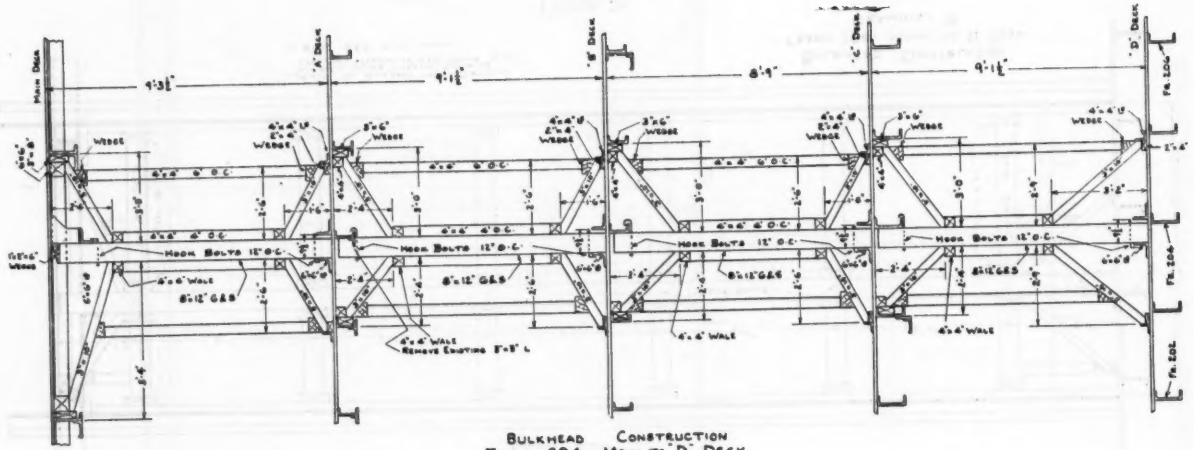

BULKHEAD CONSTRUCTION
FRAME 204 - MAIN TO 'D' DECK
DRAWING "C"

FIGURE 29.

head and the port side of the vessel watertight. Figure 32 is a picture taken of the large bulkhead at Frame 165 after the water had been pumped out. At the top of the picture can be seen the ends of the timbers bolted to the angle bar and embedded in the concrete. In the center the bulkhead knee brace stiffeners are clearly seen. Figure 33 is a picture taken in the main dining room after the vessel had been rotated to 25° and the water pumped out of the compartment. The entire left portion of the compartment in the picture was underwater in the capsized position. Next to the bright light is the staging upon which workmen prepared the compartment for the pumping operations. The waterline was just below this staging. To the left of the staging can be seen knee braces and beyond that the bulkhead which spanned the three deck spaces of the dining room.

The problems encountered in laying concrete underwater by the Tremie method were much the same as are generally encountered in other underwater jobs. It was necessary to complete a pour once it was started because of the impossibility of divers getting down into the retaining forms to wash away the laitance at the surface. The lower end of the Tremie pipe was kept below the rising surface of the concrete at all times and pouring in each case was continued until the surface of the fresh concrete rose to two or three feet above the high water line. As a considerable amount of concrete, 900 tons, was to be poured in widely scattered locations throughout the ship, a pumpcrete machine was installed in a convenient location for delivering the mix to the desired points. Although several mixes were used, the greater portion consisted of two parts Portland cement, three parts sand, and four parts gravel. Figure 34 is a photograph of the mixer and the concrete pump installed on a float next to the promenade deck. When the preparations for pouring had been completed, concrete was mixed and pumped through steel pipe to a trough leading to the Tremie pipe, as illustrated in Figure 35 which is a photograph of the Tremie pipe rig.

Port Patching

Once it was decided that the vessel would be righted by dewatering, surveys were immediately made to determine the number and

location of the many openings in the hull plating and in the promenade deck which was chosen to be the upper watertight boundary of the ship. Prior to the fire, many of the air ports were covered by steel plates. However, there were 356 open ports below the promenade deck which had to be patched to withstand the pressure to which they would be subjected during the pumping operations. Sixteen large cargo ports were also found open on the port side. With the superstructure above the promenade deck cut off the vessel, pipe openings, stairways, boiler uptakes, and machinery hatch openings had to be patched in order to make that deck watertight. Figure 10 shows, among other things, the locations of cargo ports and air ports on the port side of the vessel which were to be patched.

The mud handicap was encountered more in porthole patching than in any other of the diver's work. Once clearing away of rubbish and removal of mud in way of the air ports on the interior had been accomplished, divers working through the ports from the inside were able to excavate enough soil from the outside to permit folding air port patches to be slipped through the ports, opened and pulled up tight against rubber gaskets on the outside of the hull. Following this, the diver placed a length of channel across the inside and secured the patch to it. Concrete was then taken down in bags and laid over the patch to insure strength and watertightness. In this manner patches were placed on the outside of the vessel from the inside so that the water pressure would tend to tighten rather than break the seal. Figure 36 is a photograph of a diver descending into the interior of the ship with a porthole patch which he is about to place.

Pipe fittings were installed on a number of patches prior to being placed by divers. These pipe connections were later used in the jetting operations during the early stages of pumping. Figure 37 is a picture of the port side taken when the vessel was at an inclination of 25°. It shows two types of porthole patches. The rectangular one shown was not a folding patch, but the diver was able to fit it to the outside of the vessel by guiding it through the rectangular porthole with the narrow end first. Figure 38 is a photograph of two patches taken in the interior of the ship soon after they emerged from the water. The strongbacks are clearly

visible, as are the bolt connections from the patch. The concrete poured by divers is also clearly seen. The patch on the left is one of those which had a pipe fitting installed. The handle of the valve and the end connection of the pipe can be seen protruding from the concrete of the patch on the left.

Patching the large openings in the decks presented quite a different problem. The large hatch openings in the promenade deck required some of the largest patches ever used in the history of salvage. One of these patches weighed 52 tons. It was 54 feet long, 22 feet wide, and 3 feet deep. The patch was built of a heavy timber frame covered with tongued and grooved planking (4″×12″) and with steel I beams (21″×9″) as interior strength members. Figure 39 is a photograph taken of this patch as it was being completed. Figure 40 shows the deck patches coming out of the water during the righting operations. Patches were placed over all openings in the promenade deck. The installation of patches was preceded by the preparation of a rubber gasketed seat or a coaming to which the patches could be bolted. Existing structure was cleared away or utilized as necessary. The large patches were swung into place by means of a crane and seated through the guidance of divers.

When the patches were properly seated, the rods or bolts which previously had been secured at the inboard end to suitable ship structure by means of hinged shackles or levers were run through corresponding bolt holes in the patches and bolted by divers from the outside. See Figures 41 and 42. Large patches were equipped with gate valves through which water was permitted to flow to keep the water levels inside and outside equalized until ready to commence pumping. It was necessary to avoid any internal pressure which might unseat the bearing on the gaskets. Small patches were assembled at the site and where difficult to make tight or where additional strength was required, they were backed with concrete. Concrete was also extensively used to close numerous openings which could not conveniently be closed with wooden patches or plugs.

As mentioned above, sixteen cargo doors or ports had to be closed by the divers. Once this was done, tightness and strength were insured by placing reinforcing rods at right angles to the

strongbacks which secured the doors. With diver-built wooden forms around the ports, concrete was laid by the Tremie method.

Shoring and Final Preparations for Pumping.

In all salvage jobs where extensive pumping is to be done, the ability of decks and bulkheads to withstand the expected hydrostatic heads requires thorough consideration. In the salvage of the *Lafayette*, the great amount of shoring which had to be done is indicated in Figure 10. The strength of the decks and bulkheads was calculated and compared with the anticipated strength requirements of the salvage plan. In other words, all shoring in the *Lafayette* was based upon the anticipated pumping schedule plus a little extra in case deviations from the salvage plan were found to be necessary once the righting operations were started. Of course, the decks of the vessel were not originally designed to withstand the pressure heads to which they were to be subjected in the capsized position.

Because of the symmetry of the ship, it was possible to take most of the measurements for the individual pieces comprising the shoring at each location from the above water side of the vessel. In many cases, however, the diver had to make original measurements and, in all cases, had to check those taken above water. Measurements and checks were made by use of wooden battens. Where the deck plating rather than the deck girders and beams required stiffening the timber was placed between the deck beams and suitably shored to the opposite deck.

The heavy timber shores were weighted by sections of railroad iron so that the diver could more easily control them underwater. Once the timbers were set in place, the Manila lines were cut and the weights hoisted to the surface. The shores were tightly secured by means of double wedges and to prevent them from becoming dislodged by buoyancy, they were secured to the deck beams and decks by steel straps. Figure 43 is a photograph taken of the shoring placed by divers under C deck in way of Compartment 14A. When these photographs were taken, the vessel was at an angle of 25°. The view is looking forward. The wooden beams running parallel to steel deck beams are clearly discernible as are the shores, now nearly vertical. The stringers ran fore and aft along the tilted deck. Figure 44 shows one of the numerous

interesting and special problems encountered in strengthening and shoring decks in way of obstructions.

Placing the pumps inside the vessel just prior to the righting operations was a hazardous and difficult job, involving considerable ingenuity on the part of the riggers. It was necessary to locate a suitable number of ten-inch and six-inch pumps in each of the watertight subdivisions of the ship to adequately dewater the compartments in a short time, and at the same time provide a reserve to handle unexpected leakage. It was also necessary to have enough initial reserve capacity available to compensate for the expected reduction due to increasing heads as the vessel rotated, dropping the water level. In each case, suctions extended down to the port side of the ship, and where possible, close to the lower watertight boundary of each compartment. All discharges ran nearly horizontal through the promenade deck. In order that gasoline-driven pumps would not exhaust in the compartments, flexible steel exhaust lines were carried up to the starboard side and out air ports. The pumps were placed on platforms, hinged to the then vertical decks, and rigged in such a manner that, as the ship rotated, they could be kept in a horizontal position by slacking off on chain falls. It was hoped that giving the pumps an initial 15° inclination toward the promenade deck would permit righting the ship a total of at least 30° before it would be necessary to rotate the pumps. This idea was practicable since the salvage pumps are designed to operate satisfactorily at angles of inclination up to 15°. Figure 45 is a photograph of a six-inch pump completely rigged and ready for operation.

For the year and a half that the *Lafayette* lay on its port side, all of its interior, including the machinery spaces, was flooded up to the outside water-line, the water level following the five foot rise and fall of tide. In the motor room, the high water-line was slightly below the center line of the starboard inboard shaft. Consequently the water alternately flooded and uncovered the lower section of the starboard inboard main machinery installations. Both port installations were entirely submerged. In the fire rooms, as in the motor room, both high and low water marks were slightly above the center line of the ship.

Detailed plans and preparations were made before pumping operations to treat the machinery by washing down and spraying with Polar type rust preventive compound. The main machinery above the water was cleaned and treated with rust preventive compound as a measure of protection and also to give the preservation crew practice and experience. As the machinery emerged from the water, it was found that mud, asbestos and other waste material covered all of the below-water portion of the machinery and machinery spaces with layers varying in thickness from nothing in the upper open spaces to several feet in the low corners and pockets. All of the machinery spaces were thoroughly washed down with high pressure fresh water as the water receded. Access was at first extremely difficult, not only because of the oily slime which coated everything, but also because of the inclination of the ship and the fact that floor plates, etc., which had become dislodged, lay unsupported in all sorts of positions. Figure 47 is a photograph taken just after water was pumped down below the auxiliary turbine. It can be seen that the floor plate, adjacent to the auxiliary turbine, was missing and that the ten foot space between the floor grating and the tank tops was entirely full of the deposit which covered all of the machinery.

By the time washing down had progressed far enough to observe the condition of the machinery, it was found that corrosion had set in and that some deterioration had taken place during the eighteen months the ship lay in the polluted water. It was impossible to lift any of the casings due to the large angle of heel but such inspections and machinery treatment as could be made were carried on immediately following dewatering with the ship inclined at 26°. Figure 48 is a photograph showing two of the preservation crew with a high pressure hose treating machinery with rust preventive compound. The outboard unit can be seen half submerged in water.

As the water receded in the turbines, the blades were found to be covered with a film of reddish-brown material which could easily be scraped off. The motors, exciters, and other electrical equipment appeared to have deteriorated slightly more than the other units. Even though some deterioration of the machinery had apparently taken place before the righting operations were started,

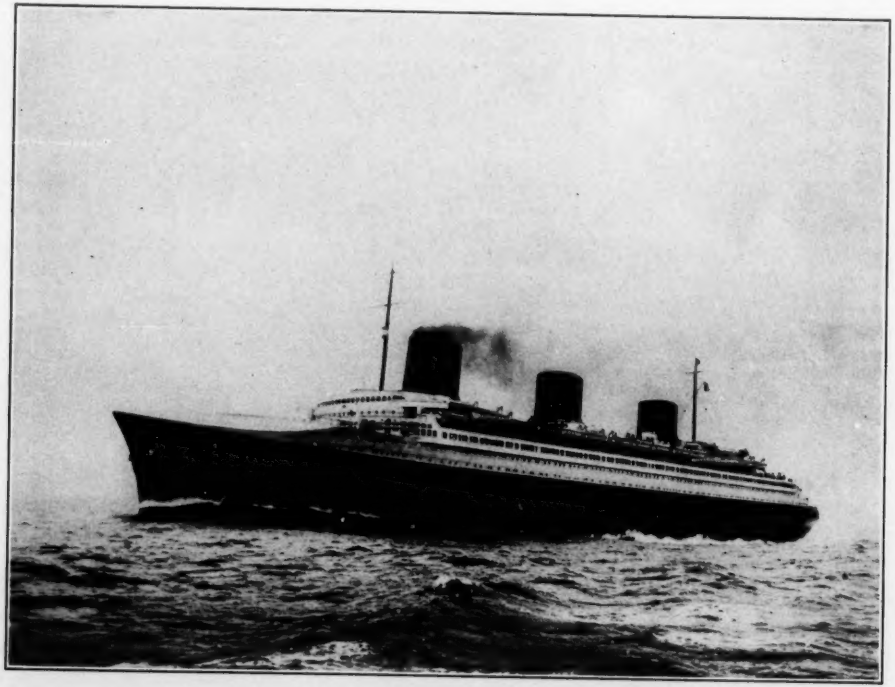

FIGURE 1.

FIGURE 2.

A strong northwest wind over the port quarter fanned the fire.

A strong northwest wind over the port quarter fanned the fire.

FIGURE 3.

The vessel has taken an initial list to port. Note the water streaming off the upper decks.

FIGURE 4.

Note the open cargo doors (*left*). Open air ports in the deck below near amidships have already been submerged.

FIGURE 4.

Note the open cargo doors (*left*). Open air ports in the deck below near amidships have already been submerged.

FIGURE 5.

With a list of 30°, the open cargo doors are half under water.

FIGURE 6.

Completely capsized, the ship rests at an angle of nearly 80°, almost half submerged.

Completely capsized, the ship rests at an angle of nearly 80°, almost half submerged.

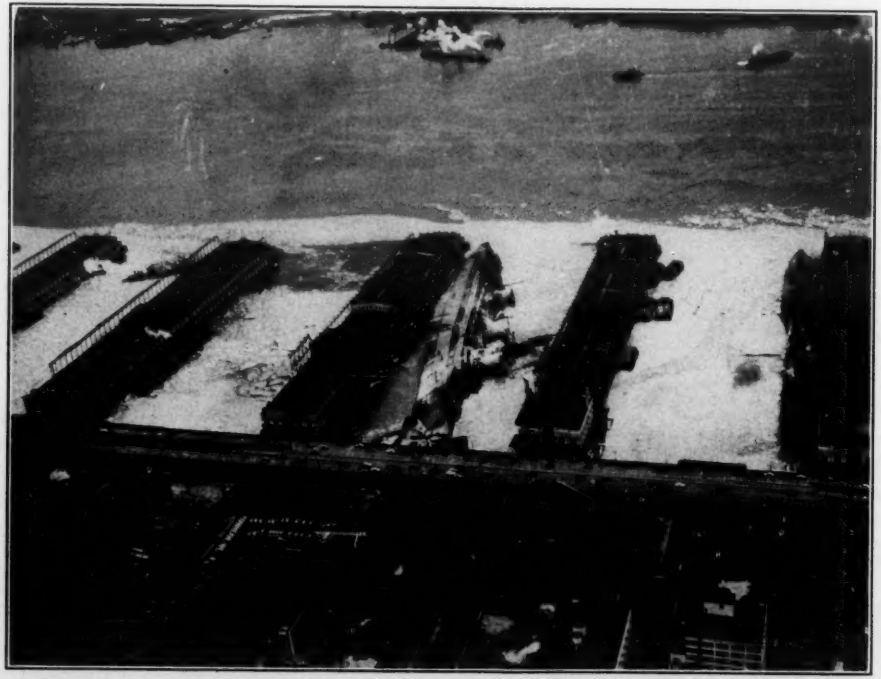

FIGURE 8.

When the ship capsized, its rudder structure wedged under Pier 88, breaking five piles.

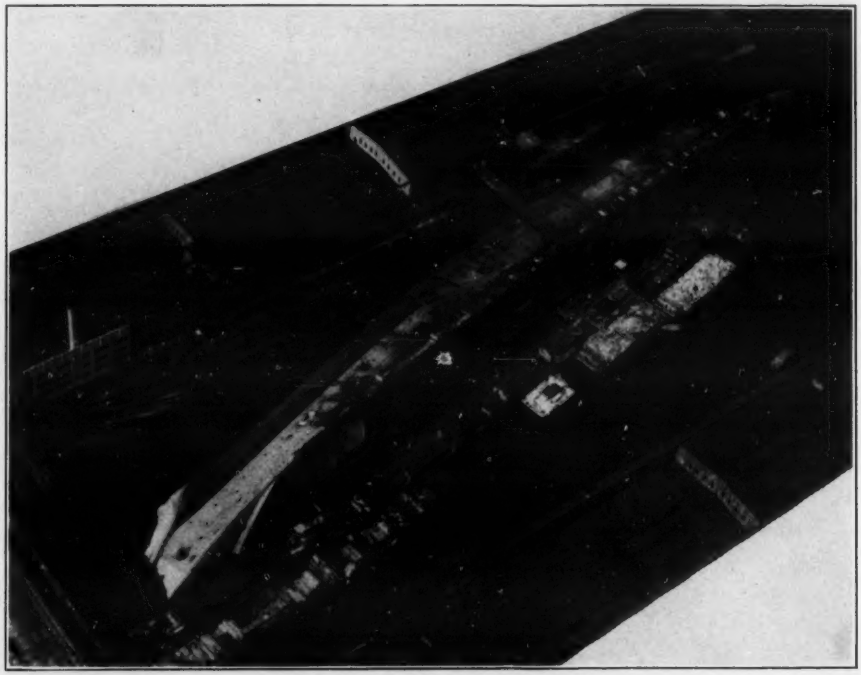

FIGURE 15.

Just prior to dewatering. Note the section of the pier cut away and the fender piles. Carpenter and machine shops, etc., are on car floats which were moved clear as the ship rotated.

Just prior to dewatering. Note the section of the pier cut away and the floating pontoon [illegible] machine shops, etc., are on car floats which were moved clear as the ship rotated.

FIG. 9b

U.S.S. LAFAYETTE
CAPSIZED POSITION

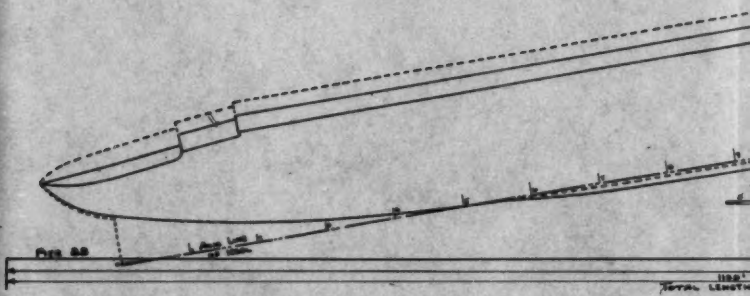

FIG. 8a

POSITION OF C

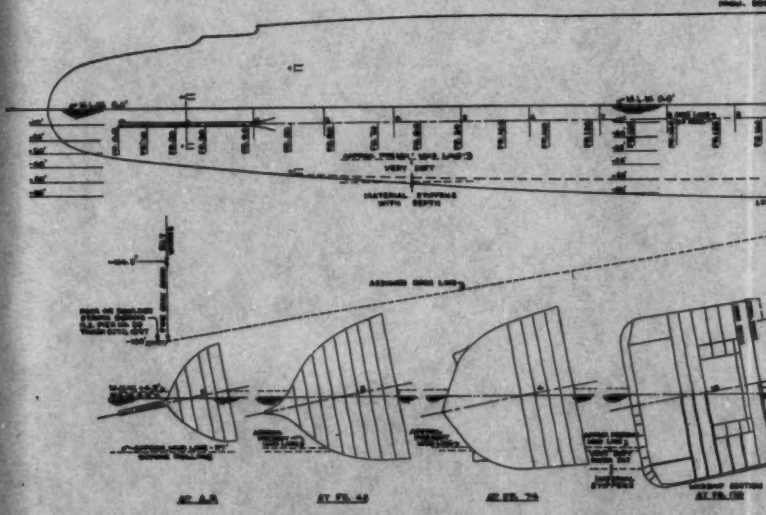

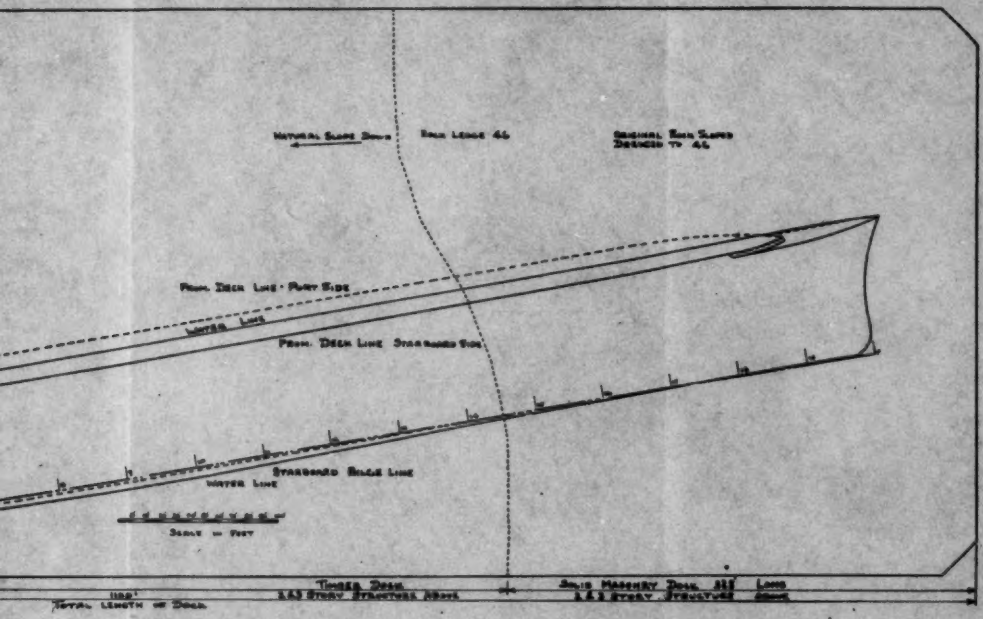

FIGURE 9A.

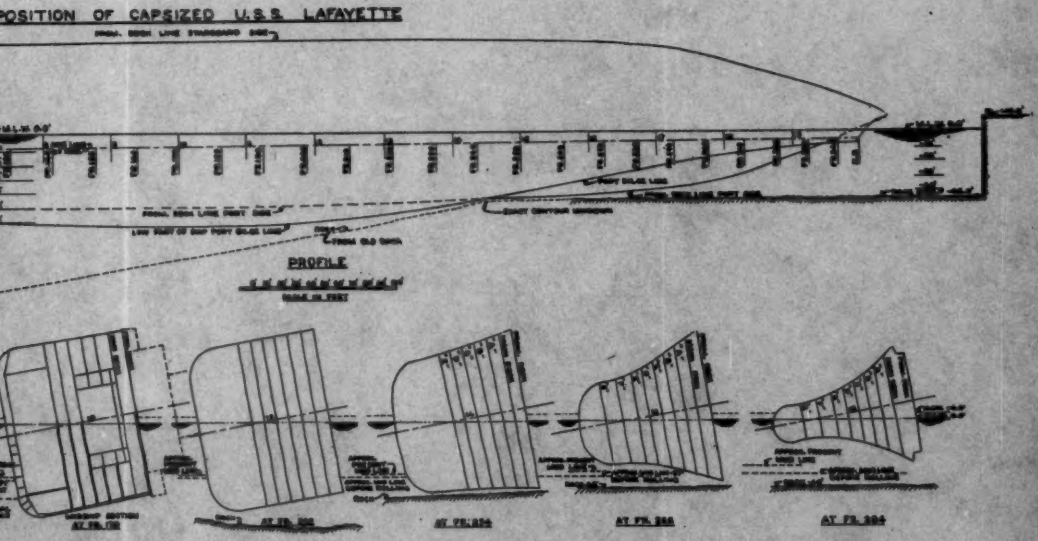

FIGURE 9B.

U.S.S. LAFAYETT

SECTIONAL VIEW

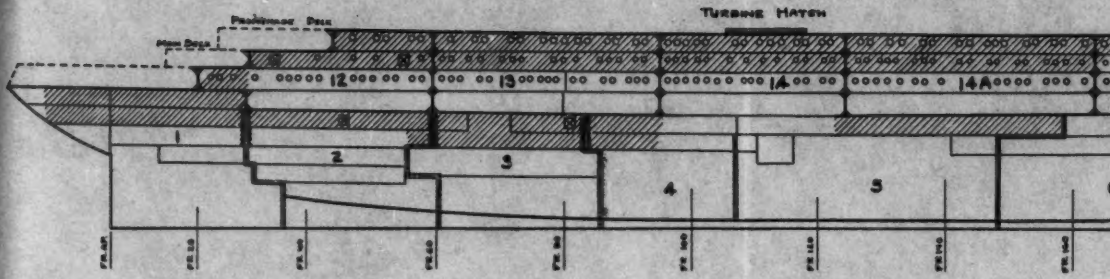

LEGEND

- NEW WATERTIGHT BULKHEADS
- ORIGINAL WATERTIGHT BULKHEADS
- DECK SHORING
- NEW TIMBER AND CONCRETE BULKHEADS
- ORIGINAL DECKS
- PORTHOLES (356) — CLOSED BY DIVERS - BRACED BY REINFORCED CONCRETE.
- CARGO PORTS (16) — CLOSED BY DIVERS - BRACED BY REINFORCED CONCRETE.
- BULKHEAD STIFFENING
- MOORING LINE PORTS

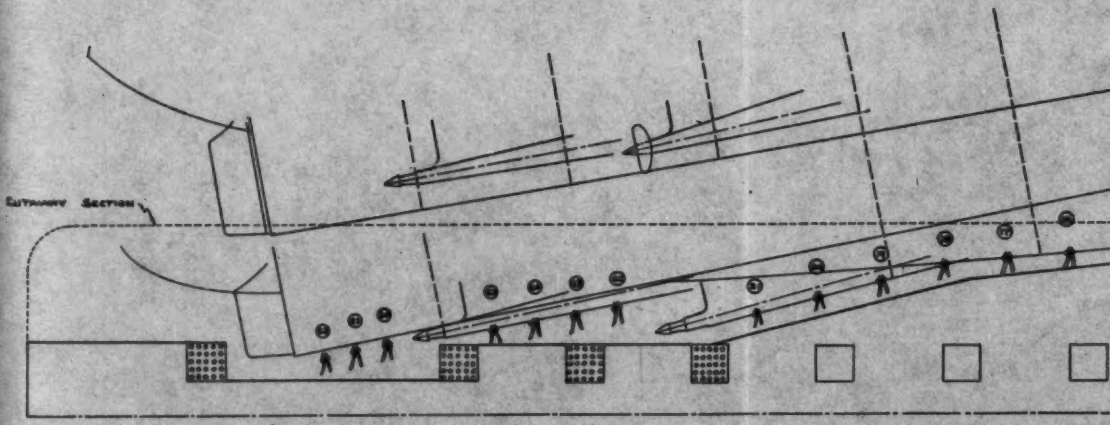

S. LAFAYETTE

TIONAL VIEW

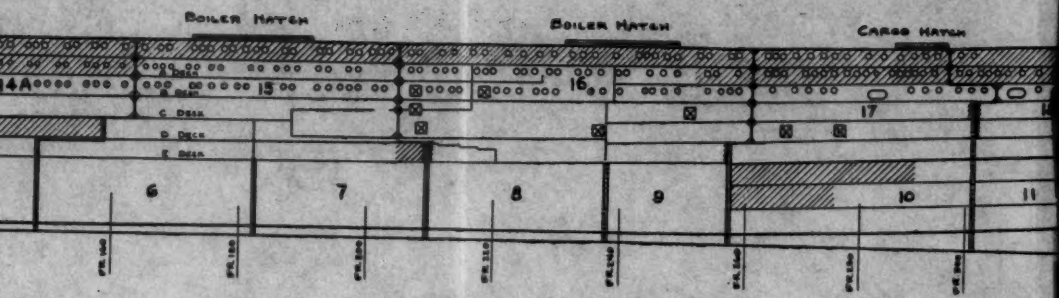

FIGURE 10.

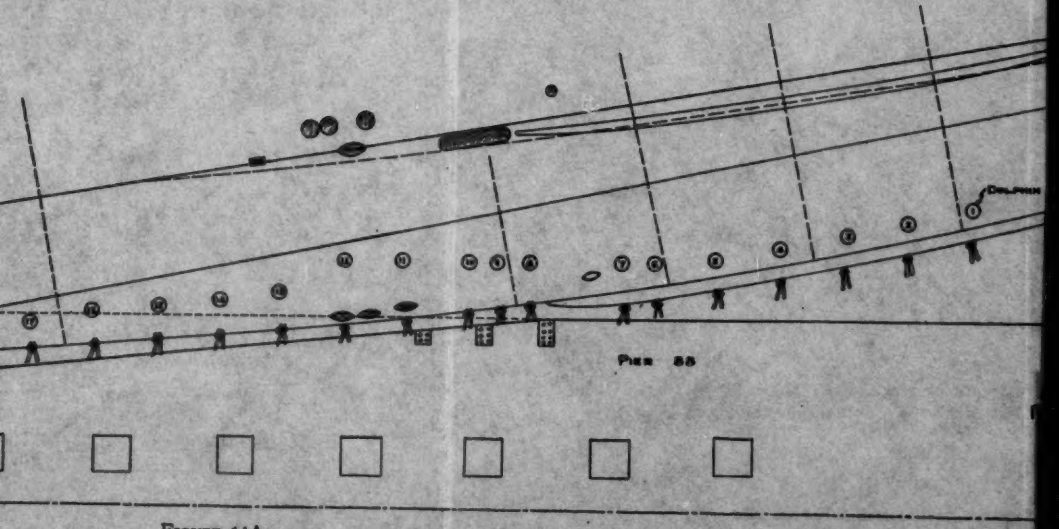

FIGURE 14A.

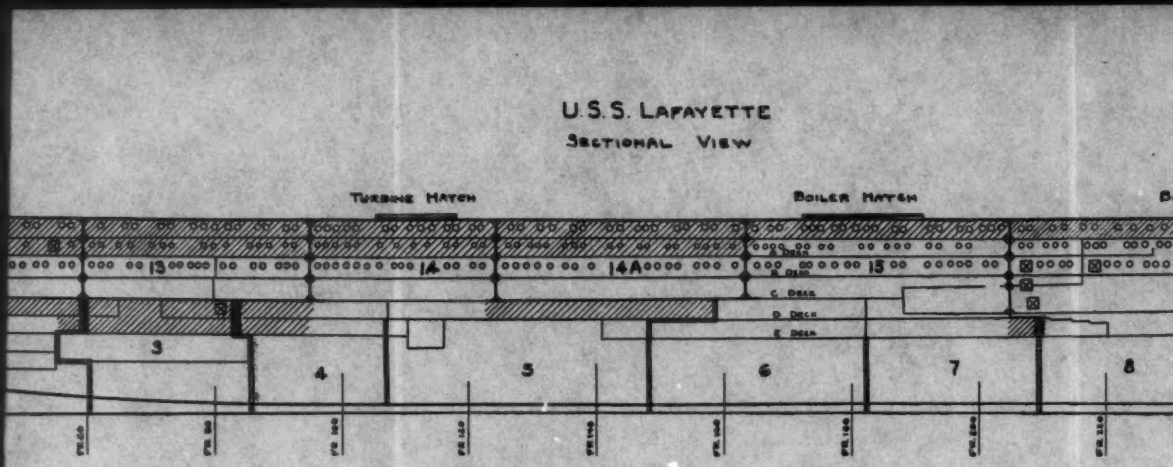

FIGURE 10.

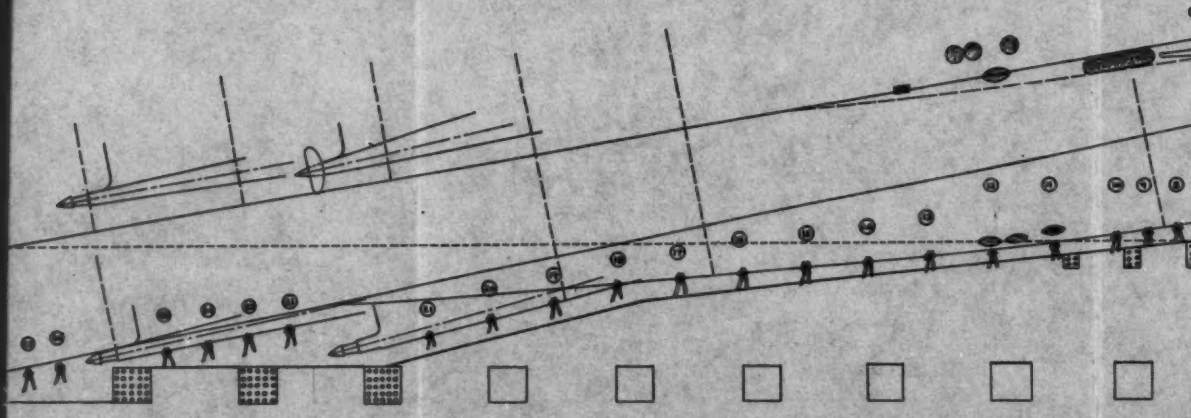

FIGURE 14A.

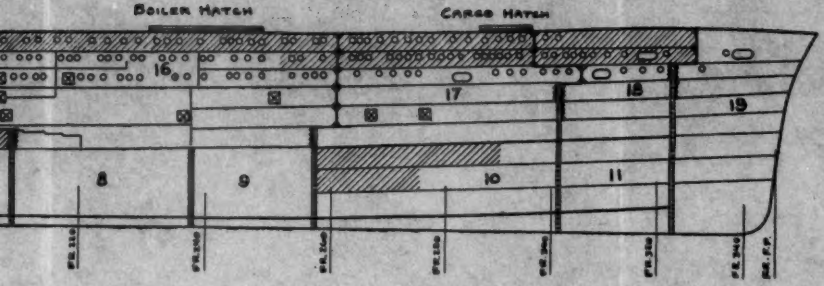

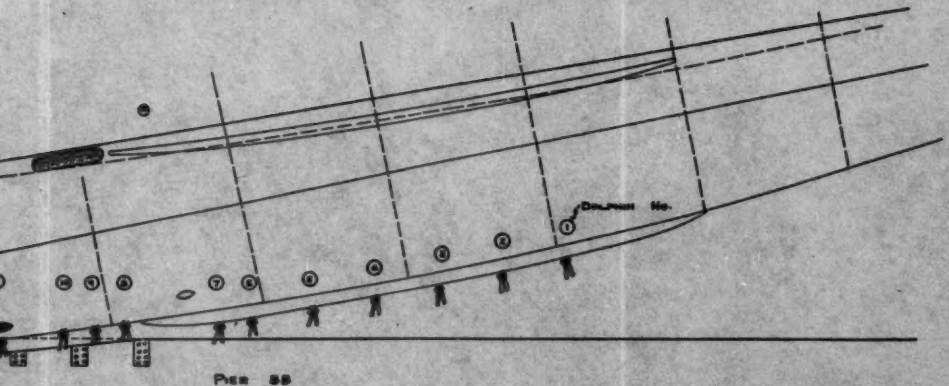

Study of Necessary Pier Work
For Rotation of Lafayette to 45°

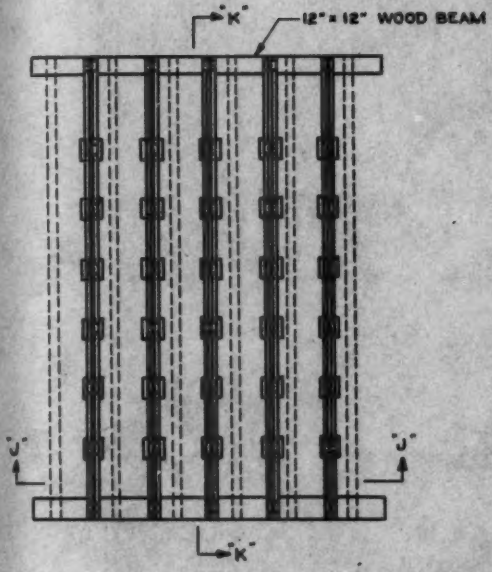

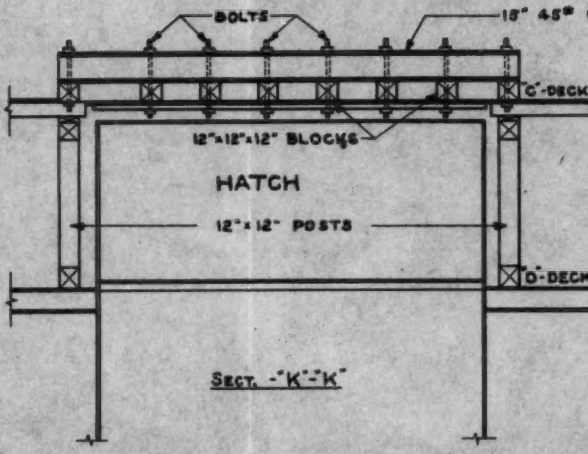

SHORING OVER BOILER HATCH

FIGURE 44.

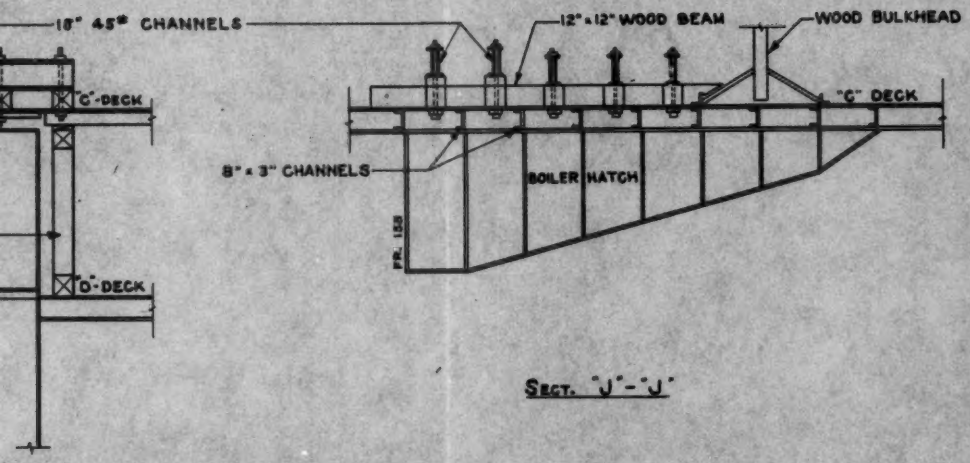

SECT. "J"-"J"

ATCH

IN ORDER TO STRENGTHEN THE "C" DECK IN WAY OF THE BOILER HATCH, THE ABOVE "BRIDGE" CONSTRUCTION WAS USED. THIS WAS NECESSARY IN AS MUCH AS THERE WAS NO STRENGTH STRUCTURE DIRECTLY BELOW THE "C" DECK AT THIS POINT. IN THIS CASE THE LOAD ON THE "C" DECK IN WAY OF THE BOILER HATCH WAS TRANSMITTED TO THE CHANNELS BRIDGING THE HATCH STRUCTURE AND THENCE TO THE 12"x12" POSTS TO THE "D" DECK.

E 44.

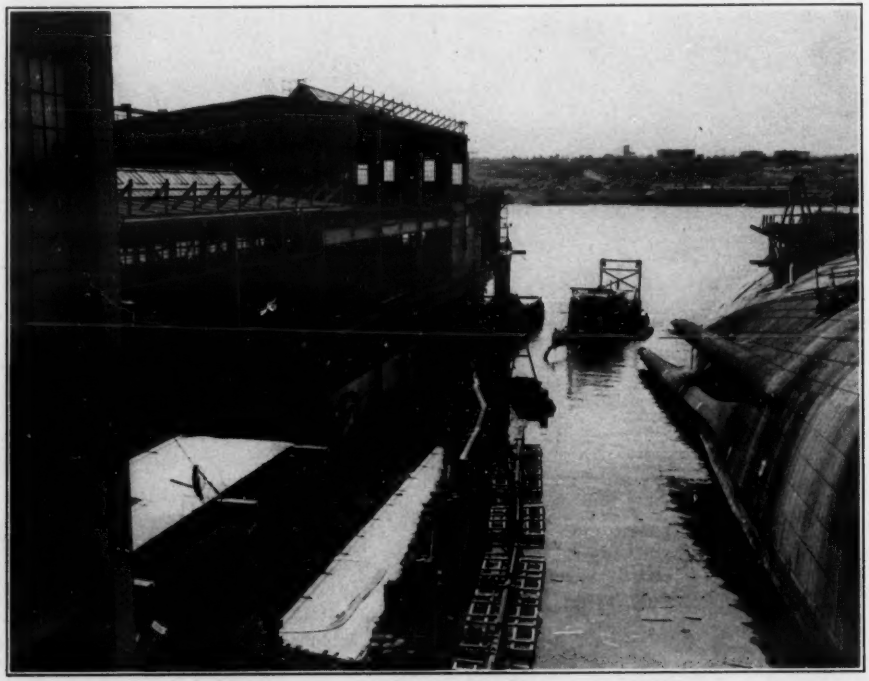

FIGURE 16.

A close-up of the cut-away portion of the pier and the fender pile clusters.

FIGURE 17.

Between February and May, 1942, the stacks and superstructure were removed, awaiting the order to proceed with salvage.

FIGURE 17.

Between February and May, 1942, the stacks and superstructure were removed, awaiting the order to proceed with salvage.

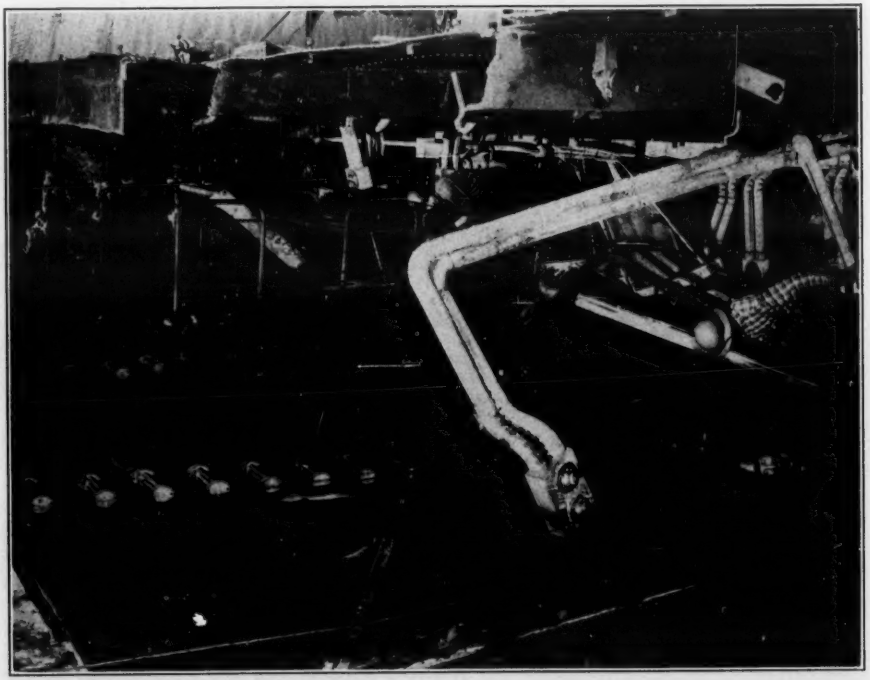

FIGURE 18.

Another preparatory step, removing debris from the ship's interior.

FIGURE 19.

Companionways provided only three and one-half to four feet headroom.

FIGURE 19.

Companionways provided only three and one-half to four feet headroom.

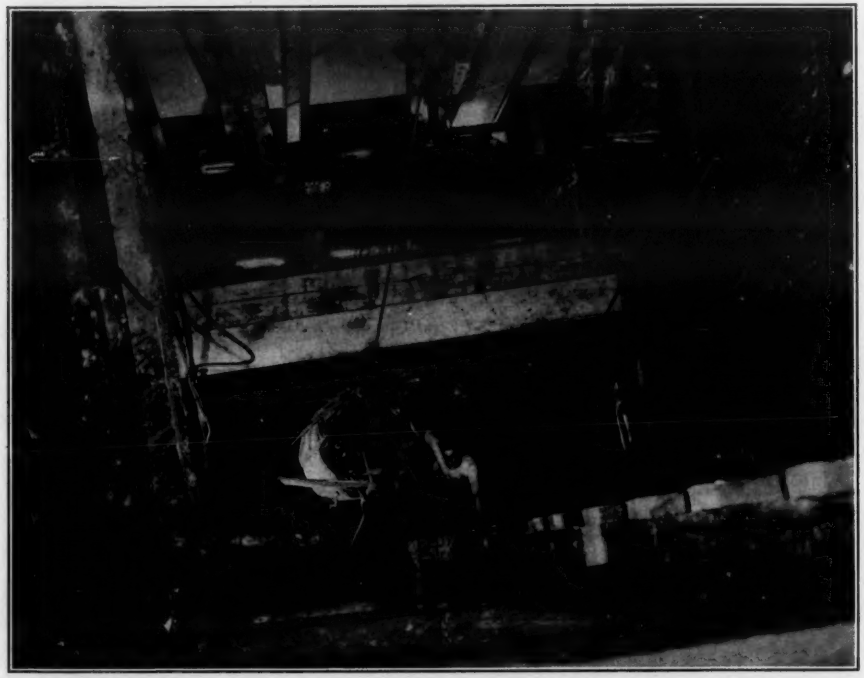

FIGURE 20.

Debris was removed by hoisting loads through cargo doors and other openings to the nearly horizontal starboard side of the ship.

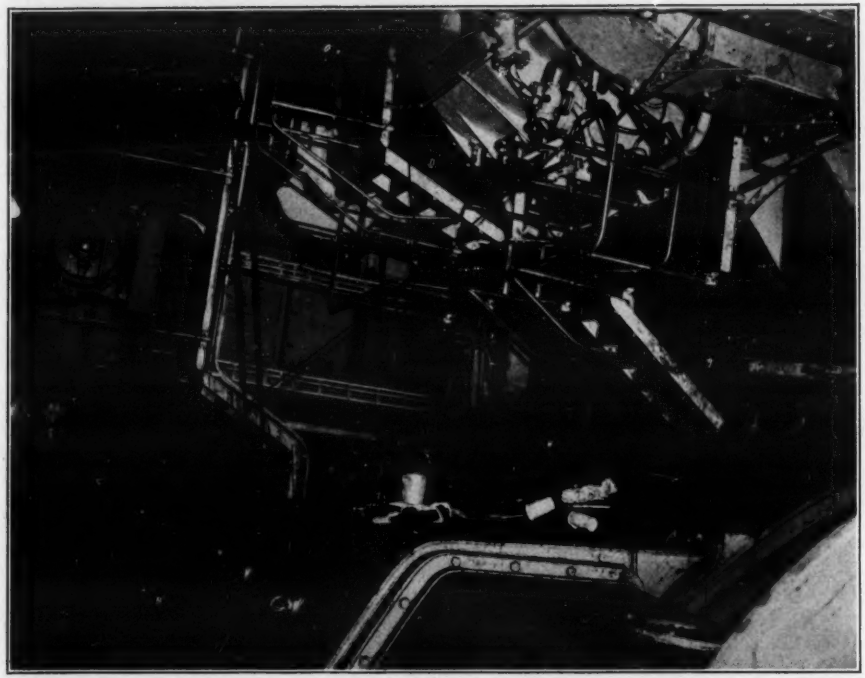

FIGURE 21.

Diving in the machinery spaces was extremely hazardous, due to the myriad pipes, railings, etc.

Diving in the machinery spaces was extremely hazardous, due to the myriad pipes, railings, etc.

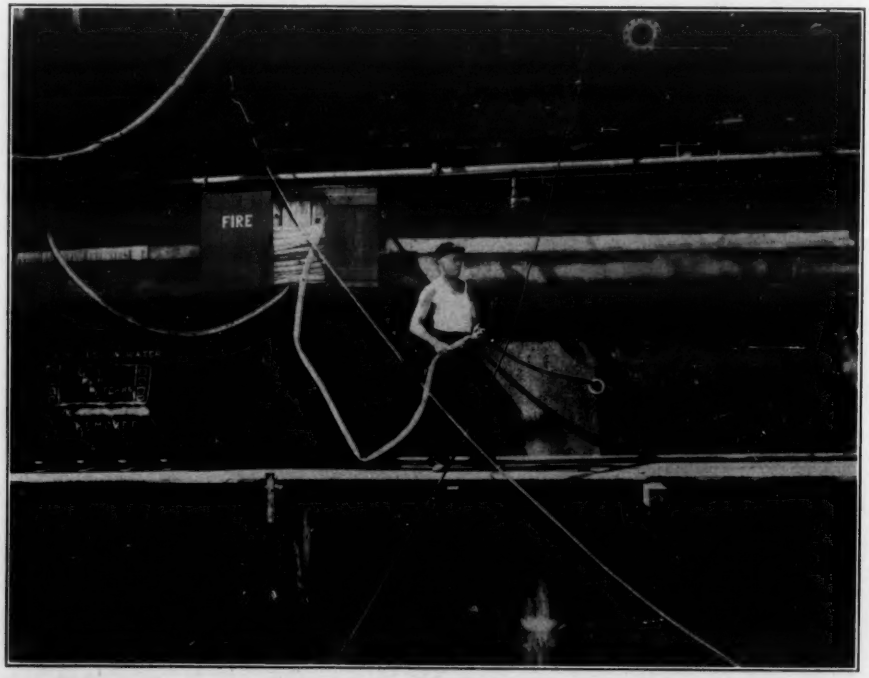

FIGURE 22.

A hose box on the promenade deck. They were placed at 100 foot intervals along the length of the fire main.

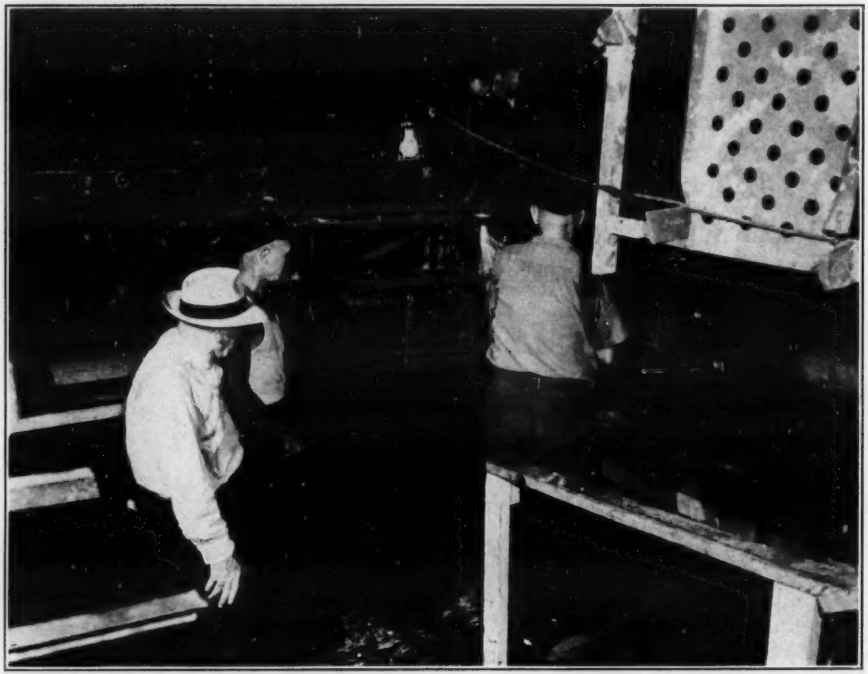

FIGURE 23.

No burning was done without inspection and approval of the fire watch who stood by with water buckets and fire extinguishers.

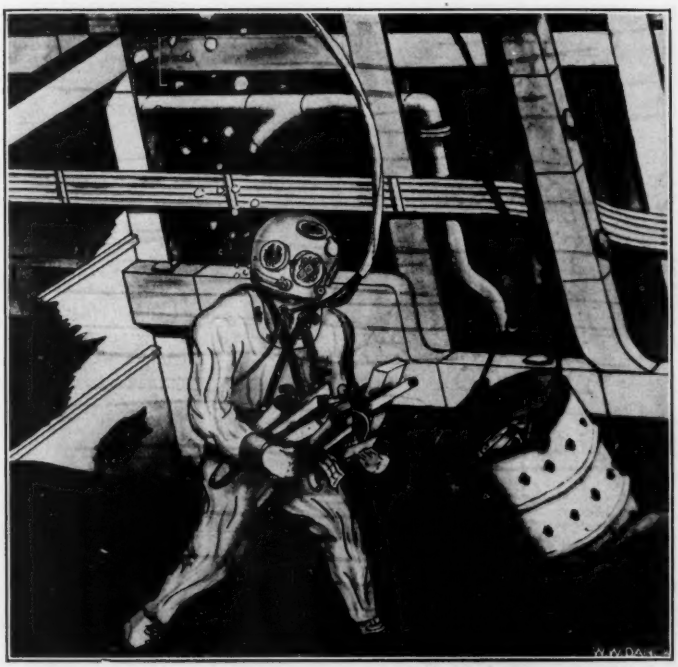

FIGURE 25.

1. In the capsized position, the *Lafayette's* decks were nearly vertical. In order to divide the vessel into watertight compartments for pumping control, timber bulkheads embedded in concrete were built under water between decks and down to the skin of the ship. The first step involved the cleaning out of all loose objects and material which had fallen to the port side. Large items such as chairs, beds, etc., were removed first and the removal of the smaller scrap material followed. In most of the compartments, ten to twenty feet of mud had to be removed as well.

FIGURE 23.

No burning was done without inspection and approval of the fire watch who stood by with water buckets and fire extinguishers.

FIGURE 25.

2. Following the general cleaning out, all of the material in way of the proposed bulkhead was cut out with hydrogen cutting torches. Cuts were made through steel compartments, ventilators, cables, and all material except the ship's structural members until a clear swath existed from the waterline down to the skin of the ship. Because of the nature of the silt in the water, all underwater operations were carried out in total darkness. Divers worked by sense of touch alone.

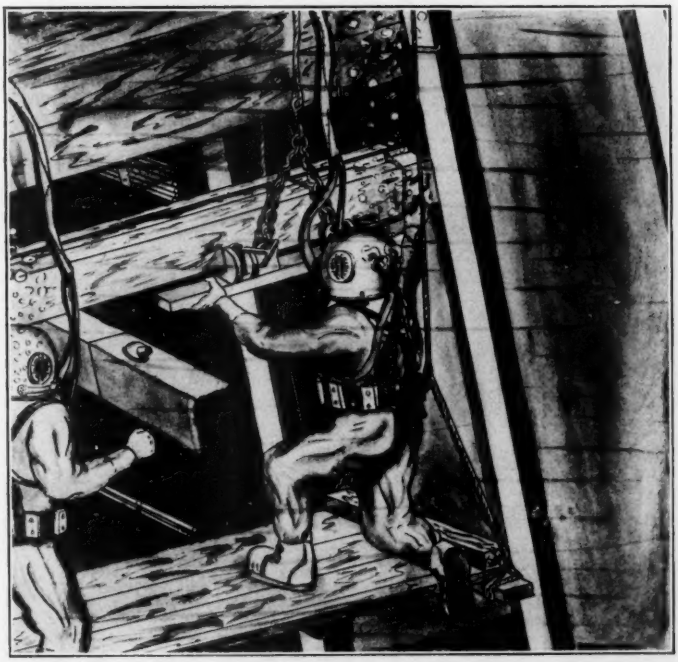

FIGURE 25.

3. One end of each 12 x 12 timber was bolted to deck frames (on what previously was the under side of the deck), as shown below. The other end was bolted to a long vertical angle bar which had been fastened to the adjacent deck and which extended from the waterline down to the skin of the ship. Bulkheads were built from the top down by lowering the timbers, weighted in clamps and slings as shown below, to the divers who fitted each splined timber into the partial bulkhead. Timbers were fitted tight by hauling on the clamps from topside. Divers then bolted timber ends to frames or angle bars.

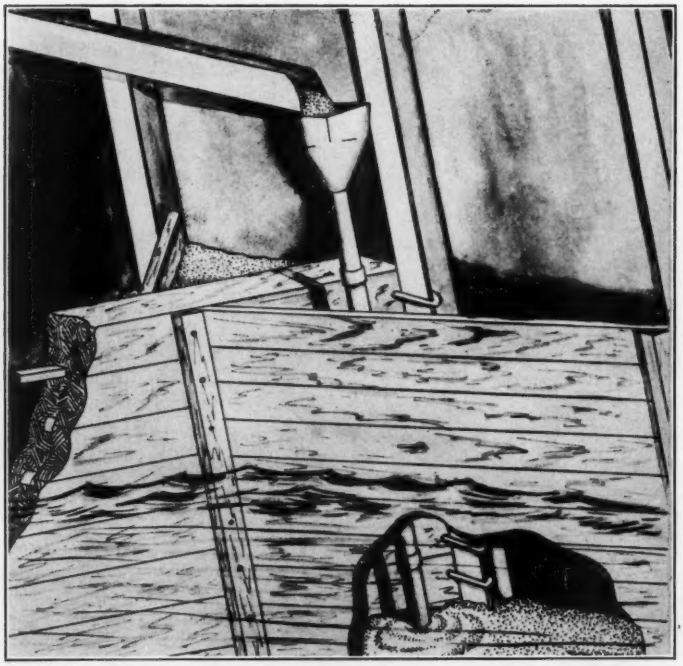

FIGURE 25.

4. In order to embed the timber ends in cement, divers constructed retaining forms from the waterline to the skin of the ship. Concrete was then piped from the mixer into the ship and thence to the vertical sectioned pipe. This rig enabled the salvors to pour concrete in the forms without its falling through water. The mouth of the pipe was at all times kept below the rising surface of the poured concrete.

FIGURE 26

This model of the bulkhead barrier at Frame 204 was built to train the divers for constructing it underwater.

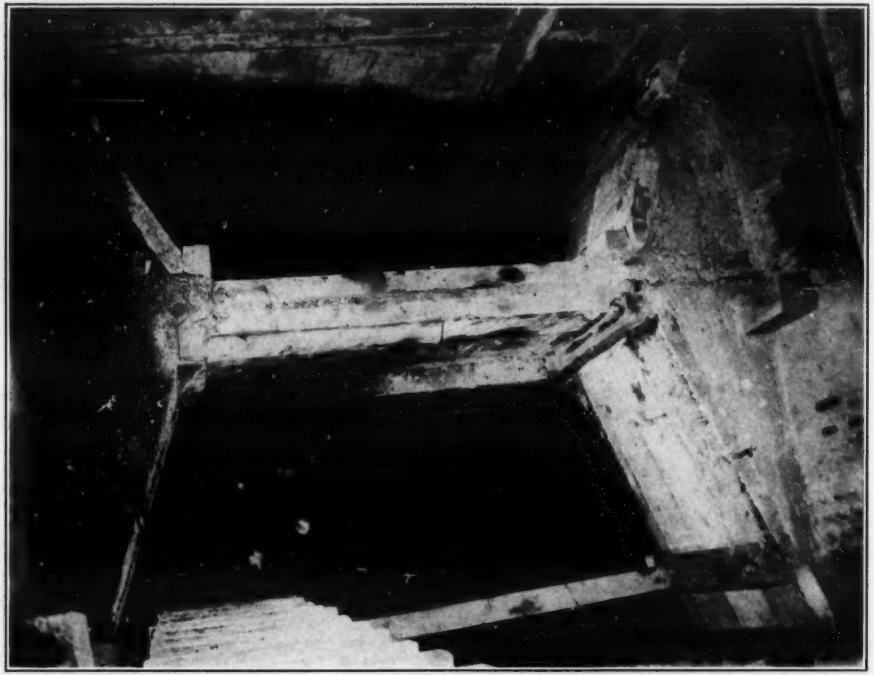

FIGURE 30.

A completed bulkhead spanning one 'tween-deck space. The waterline is evidenced by the debris floating on the surface at the foot of the ladder.

FIGURE 30.

A completed bulkhead spanning one 'tween-deck space. The waterline is evidenced by the debris floating on the surface at the foot of the ladder.

FIGURE 31.

The same bulkhead as in Figure 30, after dewatering of that part of the ship. Note the gauge board extending down to what once was the bottom of the compartment.

FIGURE 32.

Timber bulkheads span three deck spaces. Note concrete-filled form at the upper end. Because of the great span, it was necessary to brace this bulkhead against the differential in heads of water between adjacent compartments.

FIGURE 32.

Timber bulkheads span three deck spaces. Note concrete-filled form at the upper end. Because of the great span, it was necessary to brace this bulkhead against the differential in heads of water between adjacent compartments.

FIGURE 33.

The interior of the dining salon after the ship had been righted to 25°. Everything shown above was originally below the waterline except the area in the upper right-hand corner.

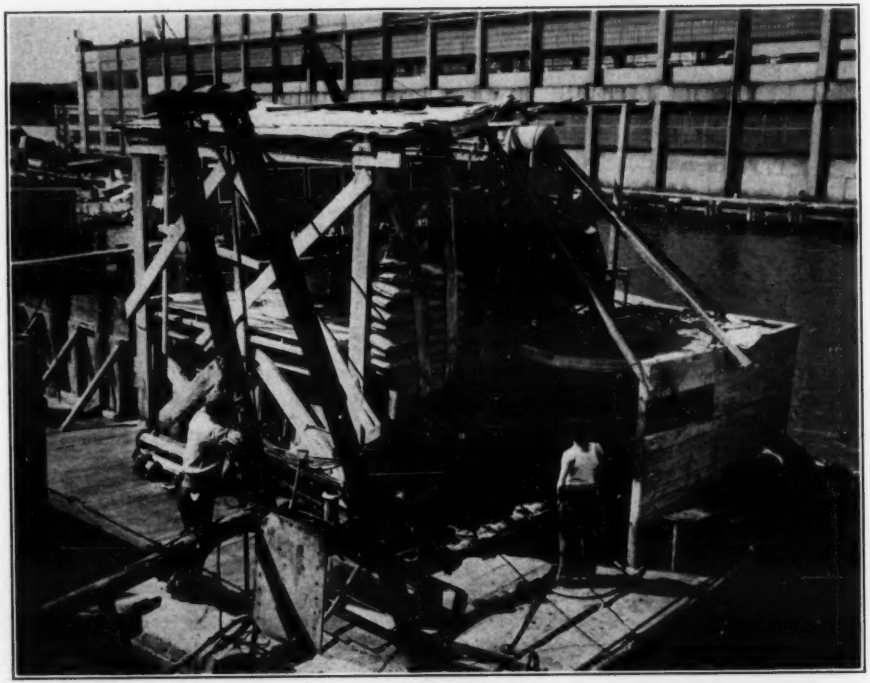

FIGURE 34.

So much concrete had to be laid, a mixer was used in conjunction with a pumpcrete machine.

FIGURE 34.

So much concrete had to be laid, a mixer was used in conjunction with a pumpcrete machine.

FIGURE 35.

Workmen laying concrete underwater through the Tremie pipe, the end of which had to be kept below the surface of the pour at all times to keep the concrete from "washing".

FIGURE 36.

A diver going down to place a "Tooker" patch.

FIGURE 36.

A diver going down to place a "Tooker" patch.

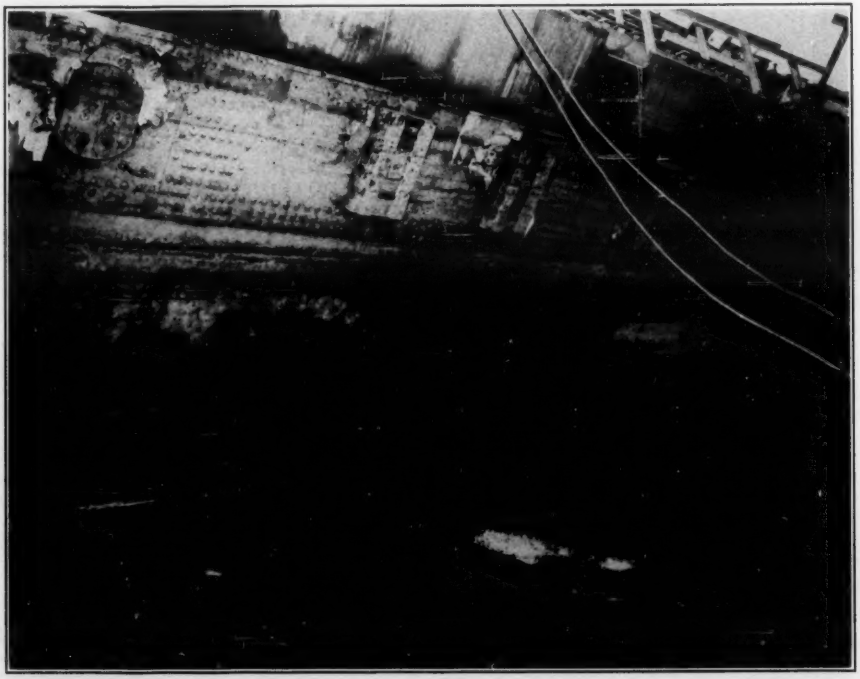

FIGURE 37.

Some of the 356 porthole patches placed from the inside by divers are visible. Note hole in patch (*lower left*) through which air or water was blown during initial pumping to break mud suction.

FIGURE 38.

In the port side of the main deck, after the ship had been righted to 25°. Note concrete backing for porthole patches laid between and over strongbacks.

FIGURE 38.

In the port side of the main deck, after the ship had been righted to 25°. Note concrete backing for porthole patches laid between and over strongbacks.

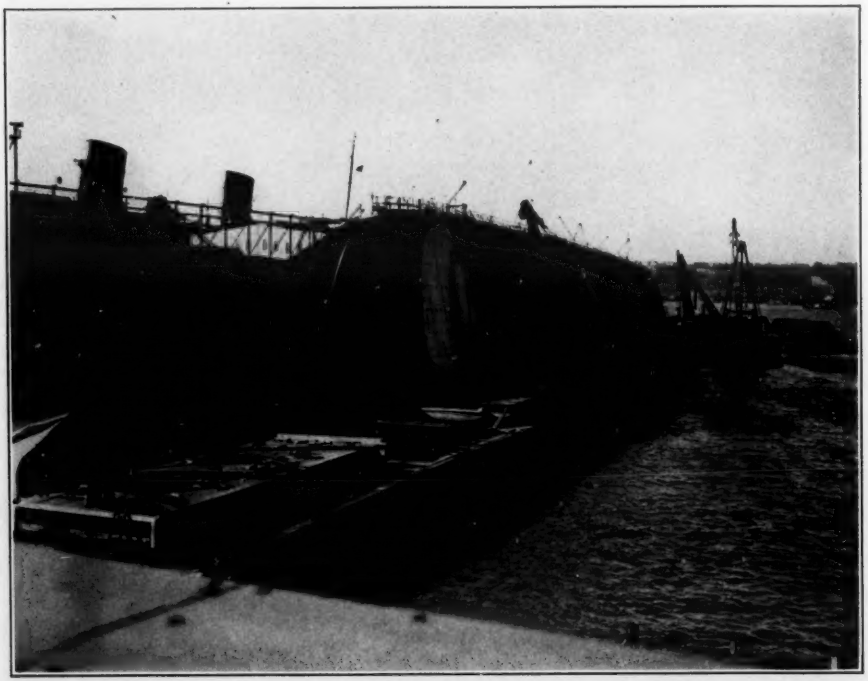

FIGURE 39.

A completed uptake patch. Note size of the corresponding opening in the promenade deck over which this patch was placed.

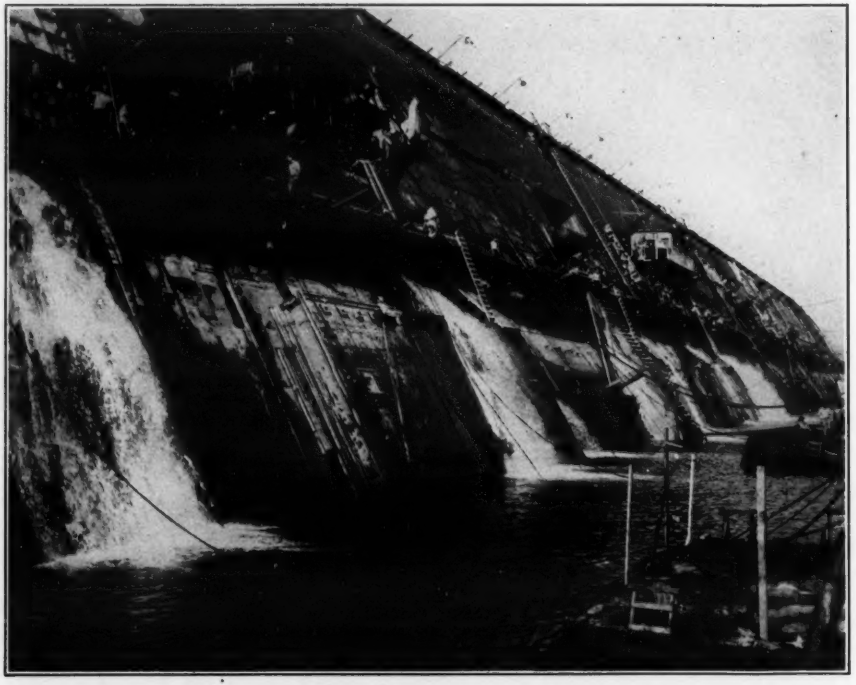

FIGURE 40.

The control tower was hinged in such a way that it could be maintained level at all times. The catwalk was originally a few feet above the waterline.

FIGURE 40.

The control tower was hinged in such a way that it could be maintained level at all times. The catwalk was originally a few feet above the waterline.

FIGURE 41.

The large patches over the uptakes in the promenade deck are shown secured by tie rods.

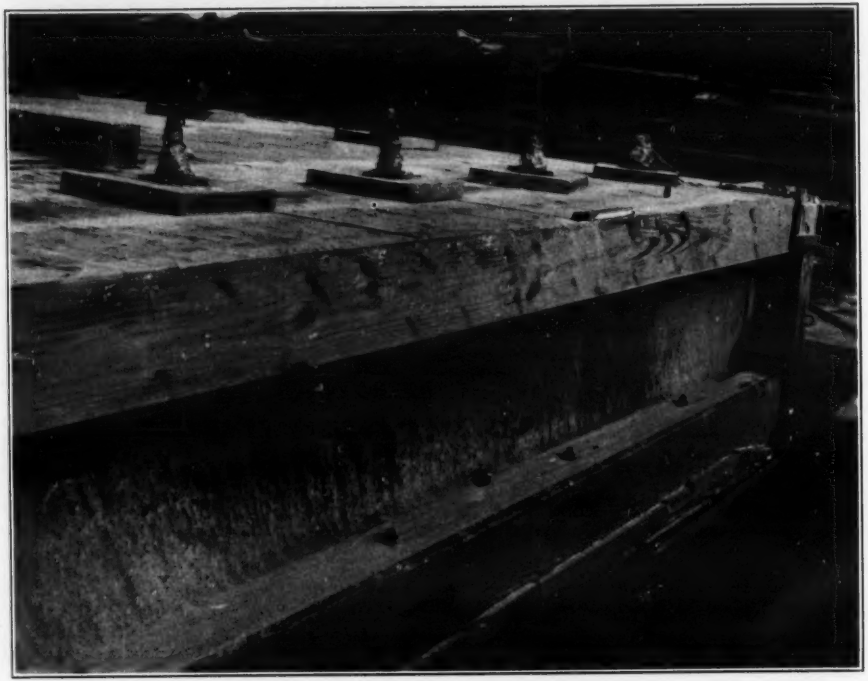

FIGURE 42.

A close-up of one of the large promenade deck patches.

FIGURE 42.

A close-up of one of the large promenade deck patches.

FIGURE 43.

The deck under Compartment 14A had to be shored in order to withstand water pressure to which it would be subjected during pumping.

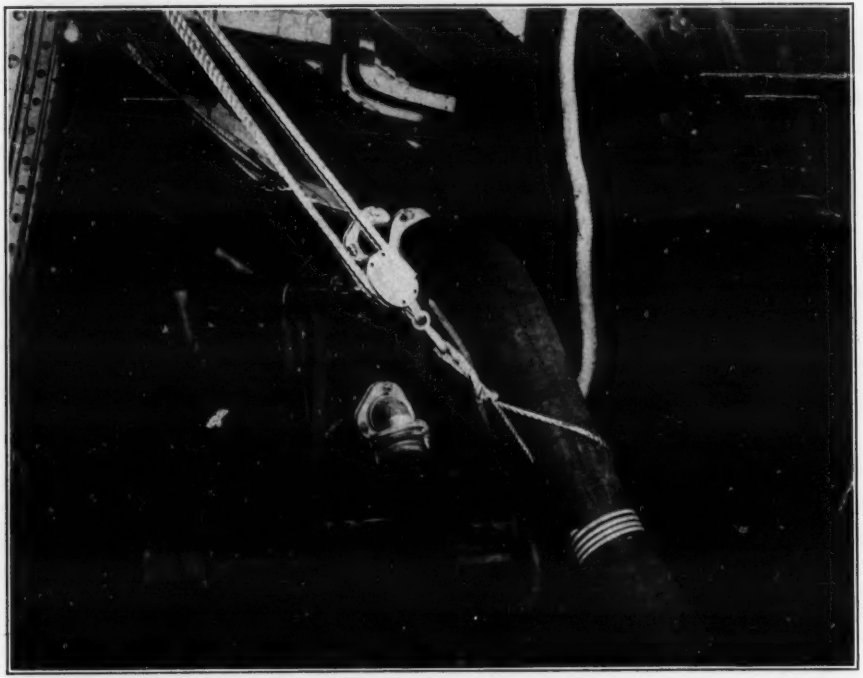

FIGURE 45.

Pumps were placed on hinged platforms and secured by chain falls so that as the ship rotated they could be maintained in horizontal position by slacking off the falls.

FIGURE 45.

Pumps were placed on hinged platforms and secured by chain falls so that as the ship rotated they could be maintained in horizontal position by slacking off the falls.

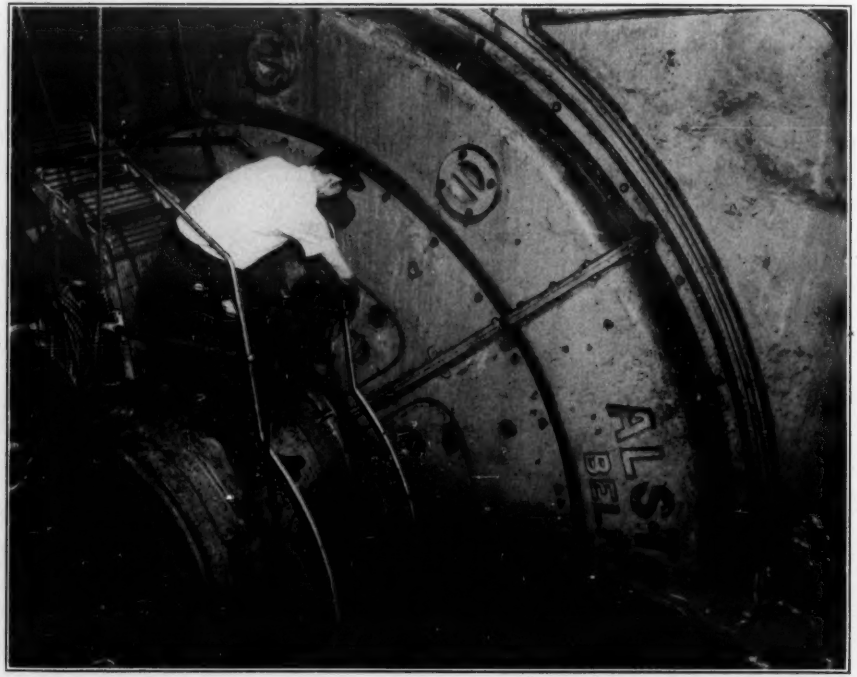

FIGURE 46.

The starboard inboard motor, showing the high water mark. Oil visible on the surface of the water is rust preventive which was sprayed inside the motor.

FIGURE 47.

The machinery has just emerged from the water. Note the mud and waste material almost up to the floor plates.

FIGURE 47.

The machinery has just emerged from the water. Note the mud and waste material almost up to the floor plates.

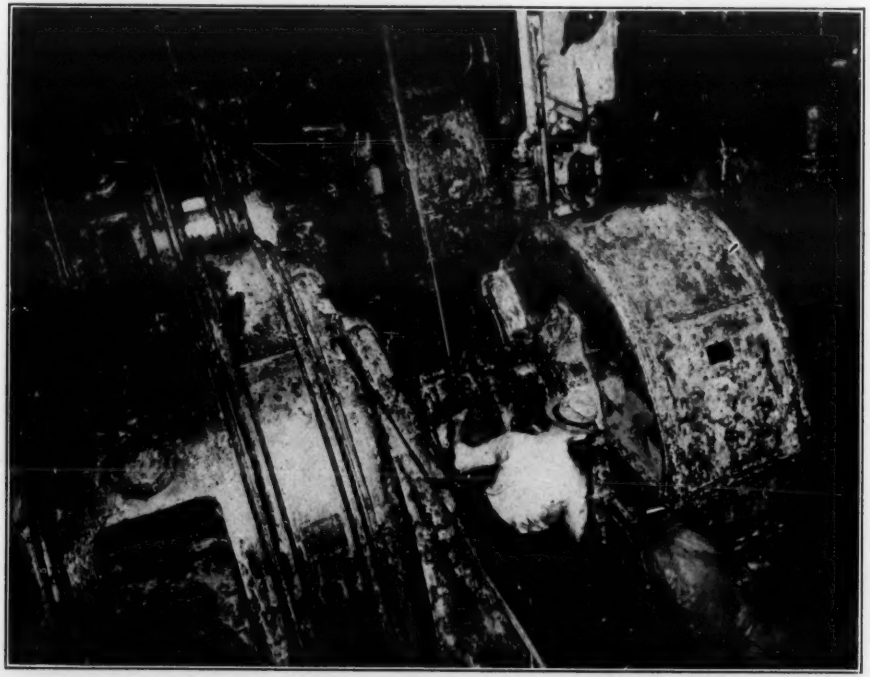

FIGURE 48.

After washing down the machinery, crews with hose and spray guns attempted to cover all surfaces with rust preventive.

FIGURE 50.

This photograph was taken just prior to the start of righting operations. Note the mooring cables leading to right and left, and the exhaust manifolds protruding from open ports on the starboard side.

FIGURE 50.

This photograph was taken just prior to the start of righting operations. Note the mooring cables leading to right and left, and the exhaust manifolds protruding from open ports on the starboard side.

FIGURE 51.

Early in the morning on August 4th, the over-all pump testing merged into the start of actual pumping and righting operations. Floodlights permitted the salvage crew to work continuously in two twelve-hours shifts.

FIGURE 52.

In the early morning of August 6th, the angle clinometer had registered a very slight rotation of the ship. Transit readings at the bow marked vertical movement.

FIGURE 52.

In the early morning of August 6th, the angle clinometer had registered a very slight rotation of the ship. Transit readings at the bow marked vertical movement.

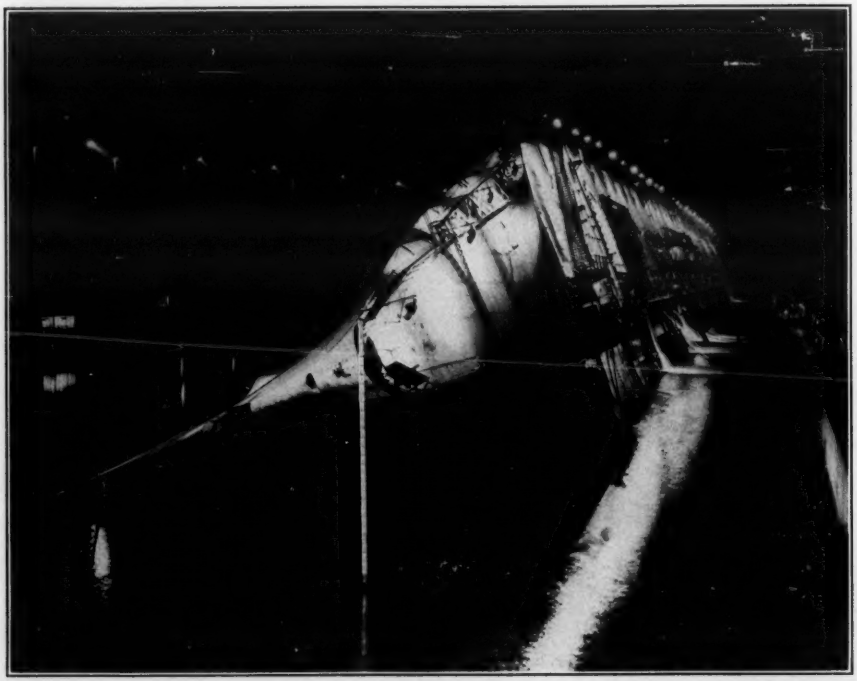

FIGURE 53.

By the evening of August 7th, the ship had rotated to about 70°. This photograph was taken at that time. Note the large patch over the forward uptake emerging from the water.

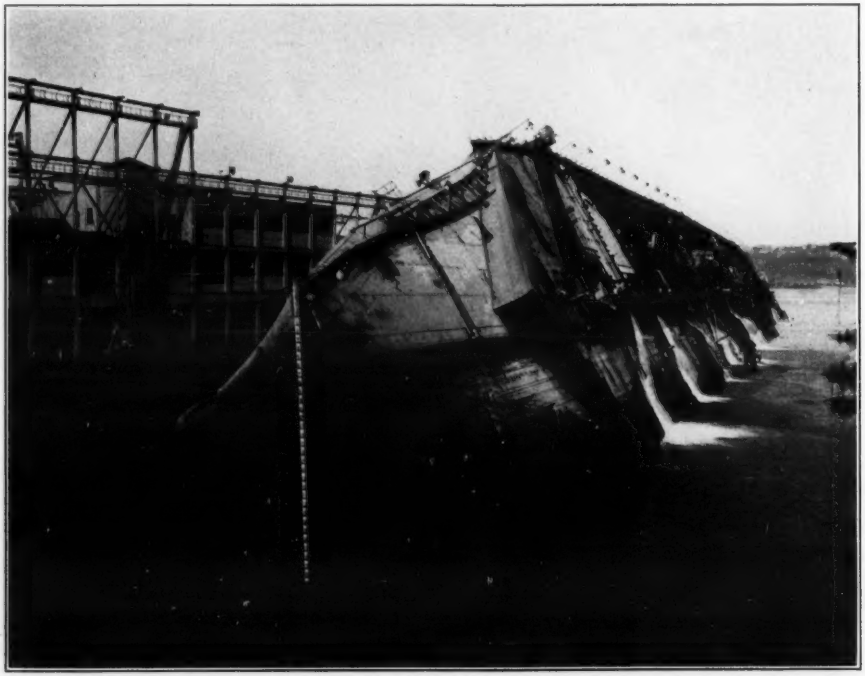

FIGURE 54.

On the morning of August 8th, all patches on the promenade deck came clear of the water. It was here that leakage in Compartment 16 went beyond control, delaying completion of salvage for several weeks.

FIGURE 54.

On the morning of August 8th, all patches on the promenade deck came clear of the water. It was here that leakage in Compartment 16 went beyond control, delaying completion of salvage for several weeks.

FIGURE 55.

It was necessary to tie the superstructure to the above-water side of the promenade soon after pumping operations started.

FIGURE 56.

On August 11th, the removal of 500 tons of superstructure began. Large sections were cut with burning torches and removed by derricks.

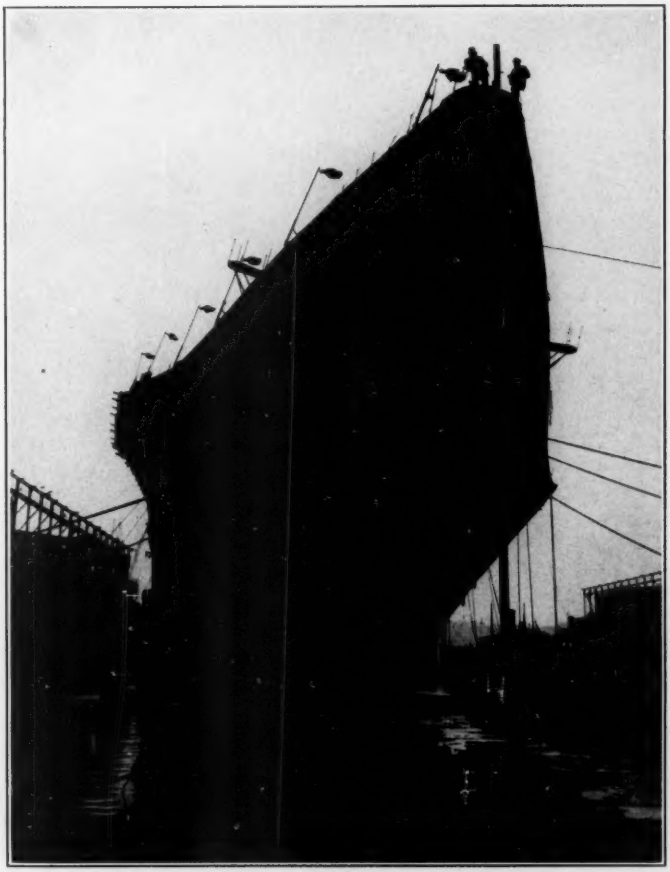

FIGURE 57.

By September 30th, the *Lafayette* was held at a 10° list to facilitate cleaning out the bulkheads and shoring. Note the successive waterline marks on the hull.

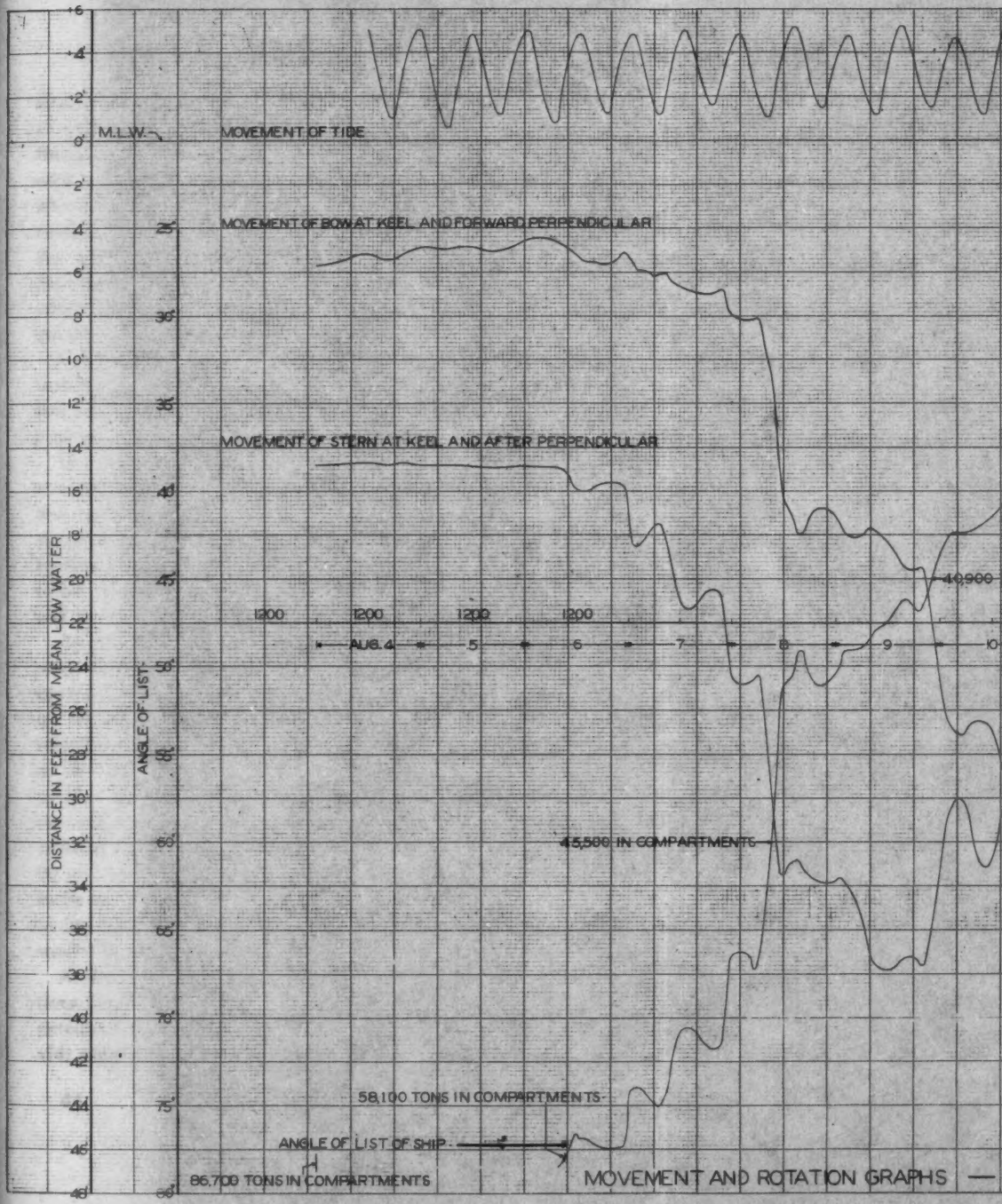
+6
+4
+2
M.L.W.
0'
2'
4'
6'
8'
10'
12'
14'
16'
18'
20'
22'
24'
26'
28'
30'
32'
34'
36'
38'
40'
42'
44'
46'
48'
DISTANCE IN FEET FROM MEAN LOW WATER
25'
30'
35'
40'
45'
50'
55'
60'
65'
70'
75'
80'
ANGLE OF LIST
MOVEMENT OF TIDE
MOVEMENT OF BOW AT KEEL AND FORWARD PERPENDICULAR
MOVEMENT OF STERN AT KEEL AND AFTER PERPENDICULAR
40,900
1200
1200
1200
1200
AUG. 4
5
6
7
8
9
10
45,500 IN COMPARTMENTS
58,100 TONS IN COMPARTMENTS
ANGLE OF LIST OF SHIP
86,700 TONS IN COMPARTMENTS
MOVEMENT AND ROTATION GRAPHS

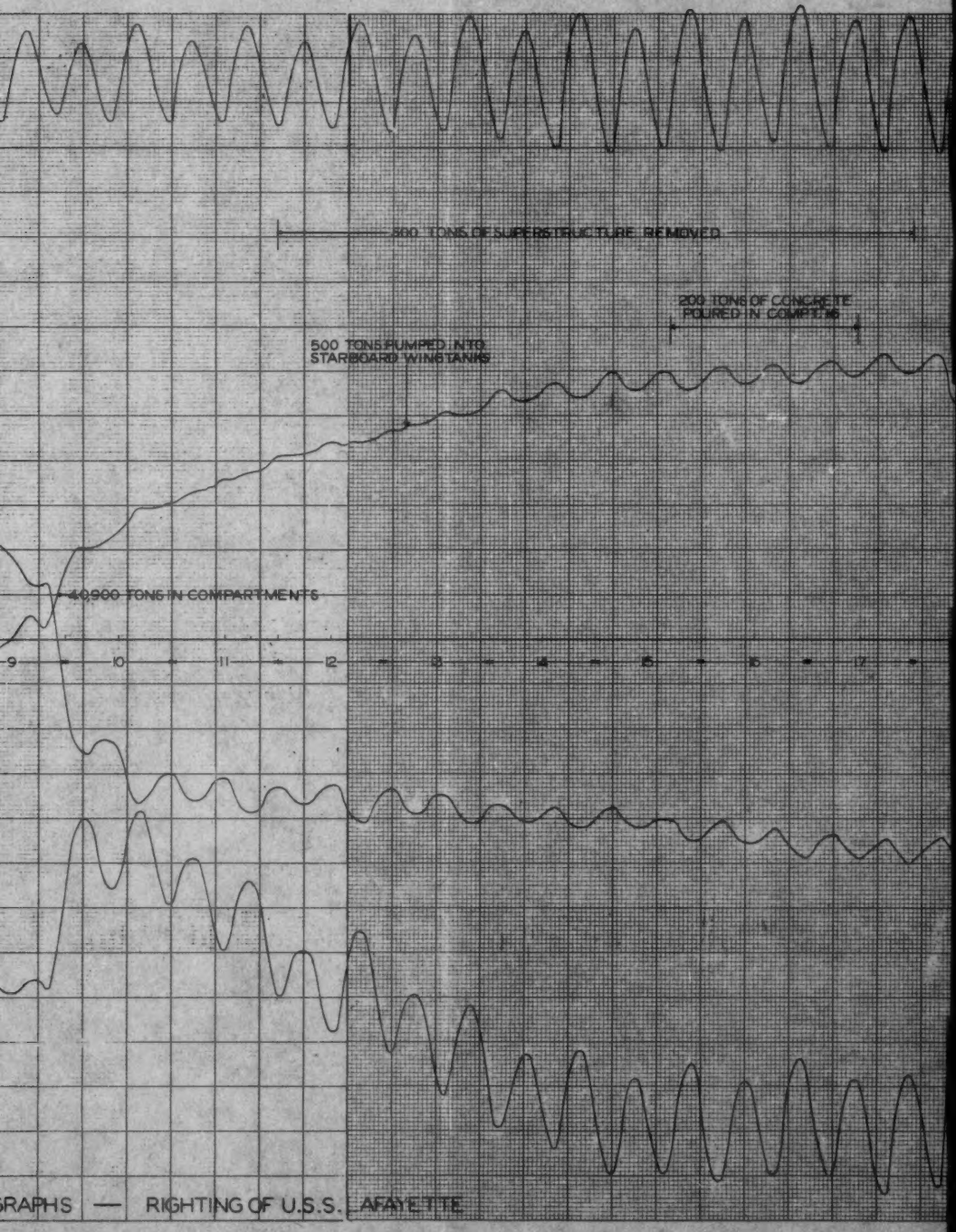

GRAPHS — RIGHTING OF U.S.S. LAFAYETTE

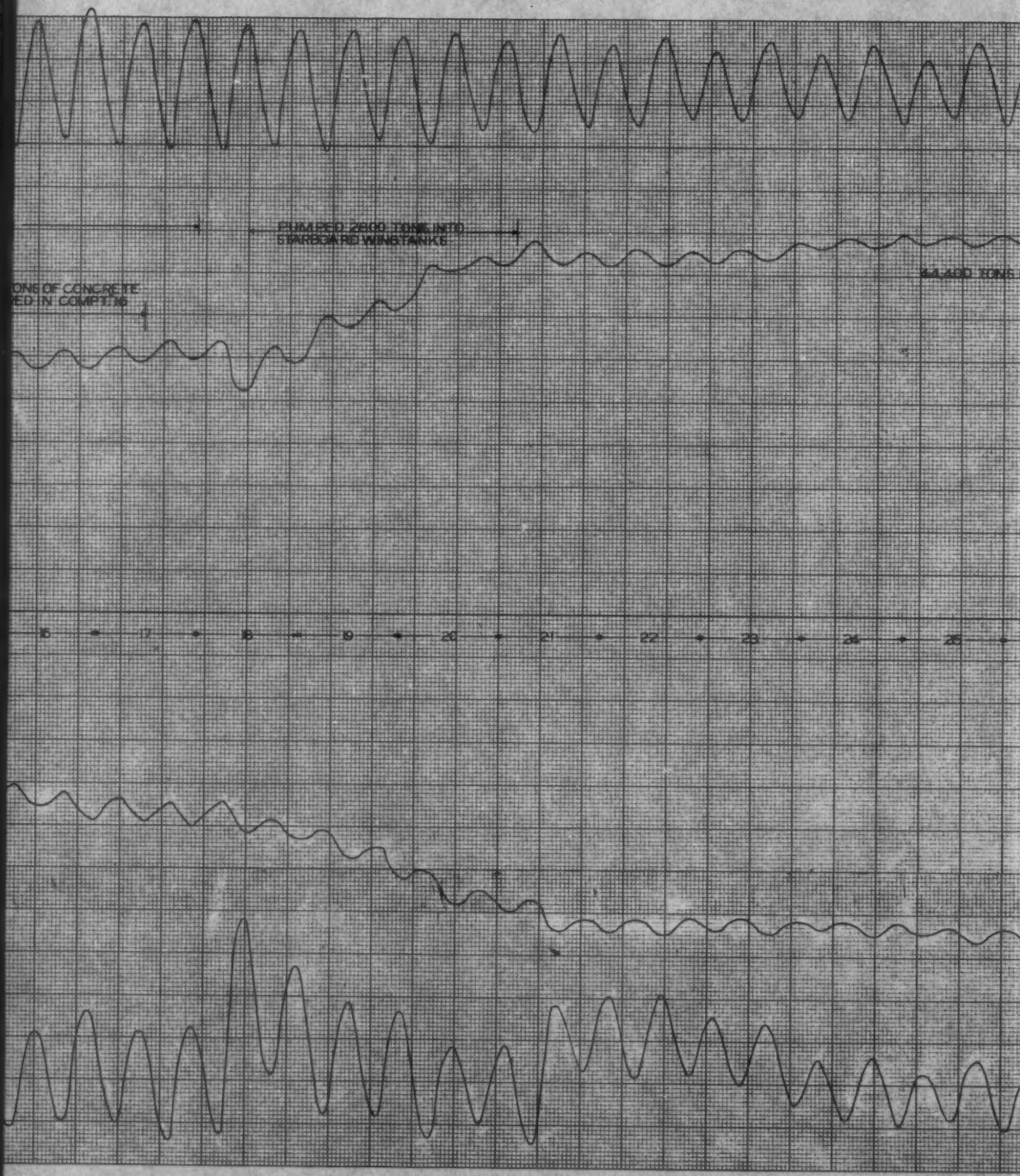
PUMPED 2600 TONS INTO
STARBOARD WING TANKS
44,400 TONS
ONS OF CONCRETE
ED IN COMPT. 16
16
17
18
19
20
21
22
23
24
25

Fig

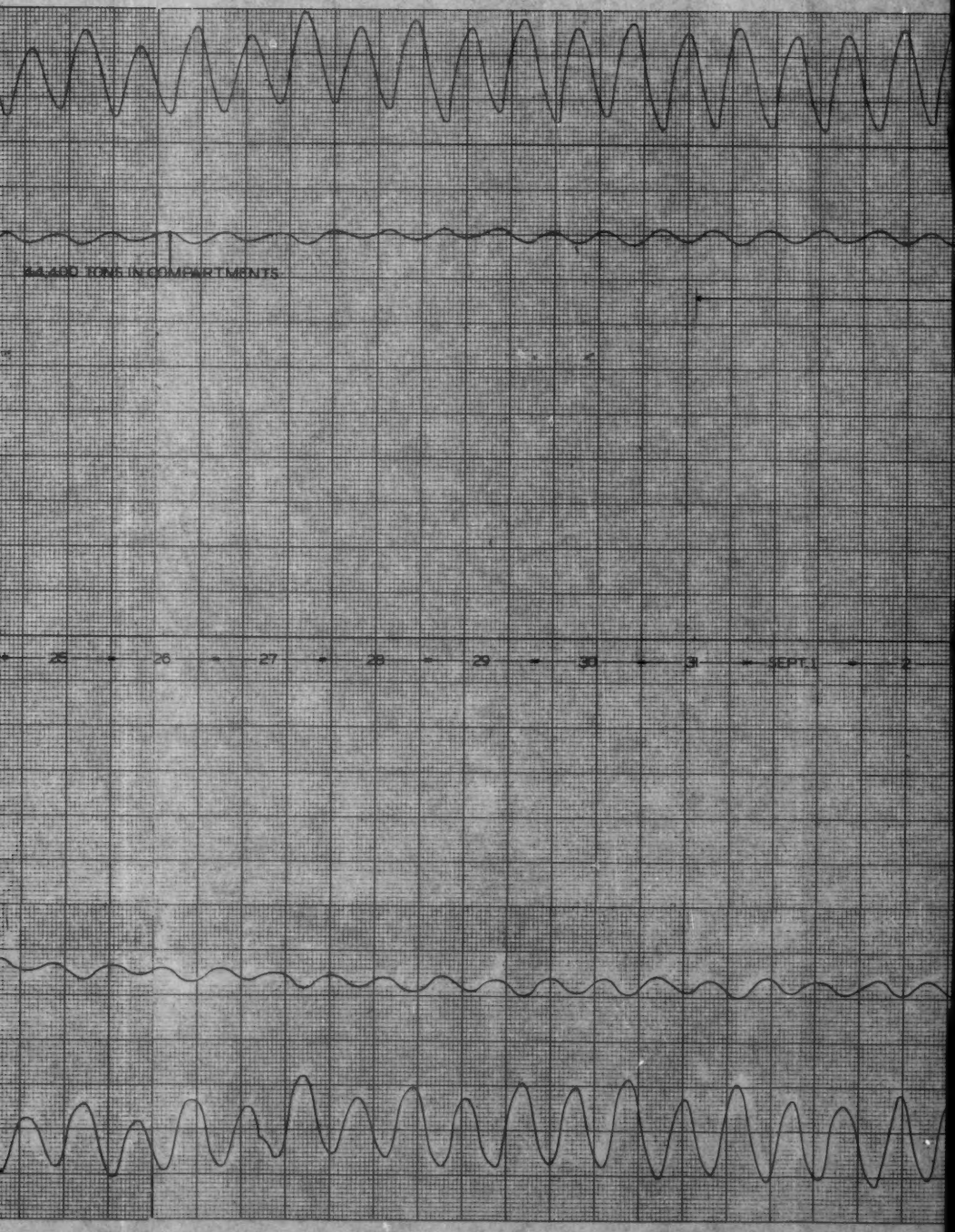

Figure 58

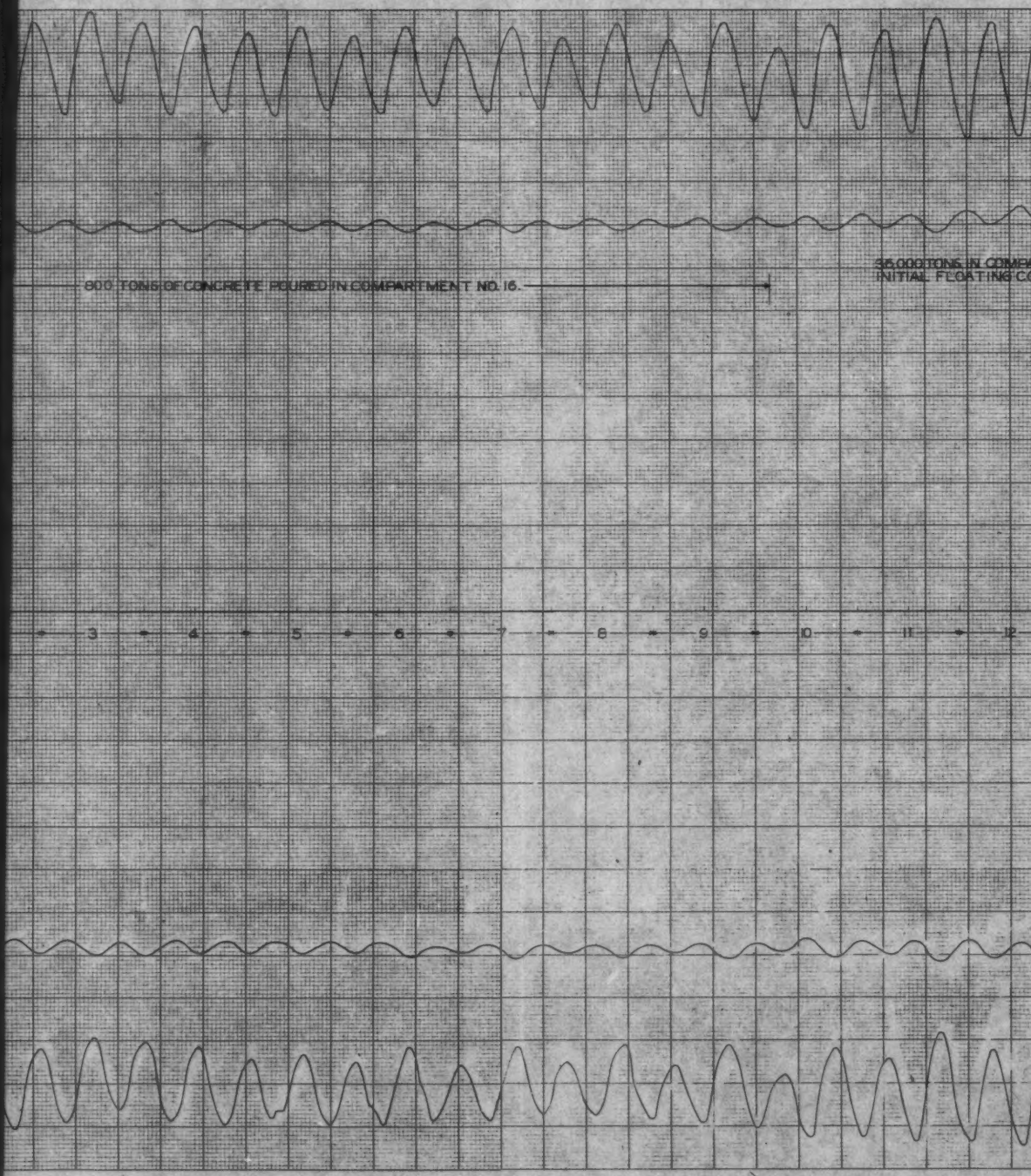
800 TONS OF CONCRETE POURED IN COMPARTMENT NO. 16.
35,000 TONS IN COMPA
INITIAL FLOATING CO
3
4
5
6
7
8
9
10
11
12

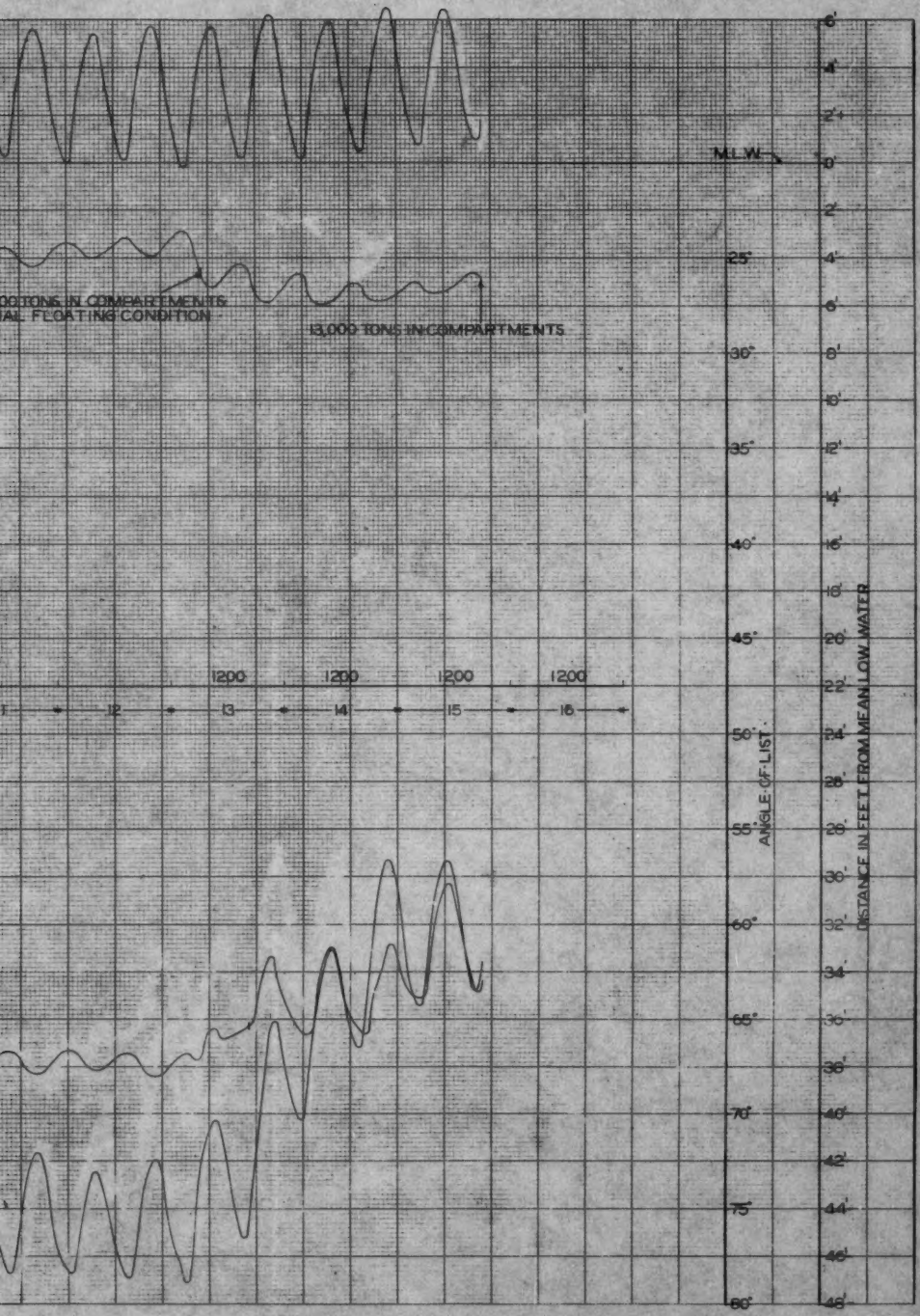
M.L.W.
13,000 TONS IN COMPARTMENTS
1200
1200
1200
1200
12
13
14
15
16
ANGLE OF LIST
DISTANCE IN FEET FROM MEAN LOW WATER

treatment was continued in an effort to check corrosion. A film of rust preventive was sprayed on all areas that could be reached through inspection plates, lubricating oil lines and all other accessible openings. Navy Standard Grade III rust-preventive oil was applied throughout except for a small amount of non-volatile rust preventive oil used prior to pumping on the machinery above the waterline. It was felt that the high volatility of the Navy Standard Grade III oil might result in an explosive atmosphere, which would provide a real danger since all the salvage pumps were gas-driven.

Final technical preparations prior to dewatering included the installation of gauge boards, clinometers and other movement measuring devices, so that the control room would know the exact position of the ship at any given moment.

In order to secure absolute control of the vessel's fore and aft movement in the slip, special mooring arrangements were designed and installed, as shown in Figure 49. Five ton, two drum winches supplied the hauling power for each set of mooring lines. The hauling part of the standard nine-part beach gear tackle was led to the drum of the winches. By this arrangement, a forty ton line pull on the mooring wires was available.

At no time during the actual righting operations were the mooring lines used to rotate the ship. As the stern came afloat during the early stages of pumping, a steady pull was maintained on the cables leading around the ship to Pier 90, so that by the time the vessel approached its 45° position, the stern was well clear of the safety fender pile clusters along the outboard north side of Pier 88. Following the partial success of choking with concrete the major leak which developed in Compartment 16 during the righting operations, the bow was hauled 10 to 15 feet towards Pier 90 in a successful attempt to bring the rupture in the hull over a cache of rag and sawdust bags which divers had previously buried in the mud as close to the hull as possible in the hope that some would be sucked into the openings.

As final preparations for righting as well as the righting operations themselves required working twenty-four hours per day, extensive floodlighting arrangements were made in order to provide approximately two foot candles of light on the hull side of the

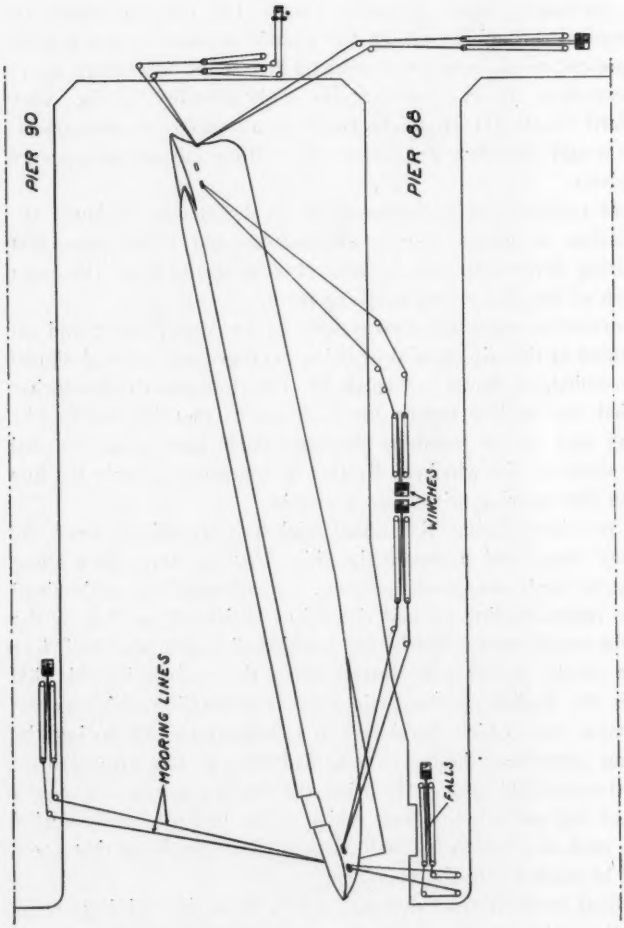

MOORING DIAGRAM

FIGURE 49

ship and five to ten foot candles of light on the promenade deck, or working side of the ship. Figures 51, 52 and 53 are photographs taken at night showing their effectiveness.

Pumping Operations.

While the actual pumping of the ship was the definite and final stage of the salvage effort, there was no sharp division between the preparations for pumping and the commencement of final dewatering operations. The last stages of making the compartments watertight and testing them for leaks merged into the final pumping operations.

As the construction work in each compartment was completed, the water was lowered inside the compartment to levels of ten to fifteen feet in order to determine the extent and location of leaks and to correct them. With the *Lafayette,* an equivalent of fourteen separate ships had to be made tight. Despite the fact that plans were studied in minute detail and despite the emphasis placed on leakage prevention throughout the year or more of preparatory work, in almost every compartment the initial pump test resulted in long hours of search and plugging of leaks by divers. In some instances, open ports, not shown on the ship's drawings, were found; in others, leakage through unblanked pipelines and ventilating ducts had to be located and made tight. Most of the troublesome leakage developed through scupper and plumbing drains. When a compartment had been tightened until one ten-inch pump, working at half speed, could hold a ten-foot head, it was considered satisfactory, although work was continued until the last minute to secure absolute tightness, if possible. Due attention was given throughout the tests to the amount of buoyancy gained in compartments from the pumping. During this phase there was never enough water removed from the ship to result in any change in physical position. Likewise, compartment testing and search for leaks were restricted to a certain extent by the allowable heads of water on the bulkheads of the compartment under test.

Compartment testing continued throughout the latter half of July, 1943. By August 2nd, an over-all pump test was made. The water in the high or promenade deck compartments (Nos. 1, 12, 13, 14A, 16, 17, and 18) was lowered one foot, and in the

lower or keel side compartments two feet, so as to place a head on the pressure side of each patch. See Figure 10. This test was maintained for about forty-eight hours during which time divers applied sawdust to all patches, seams, etc., where minor leakage might exist. Sawdusting, along with the tightness gained by setting up on the patches, resulted in the ship overall being close to bottle tight. It was estimated that two six-inch pumps could control all leakage during the rise of tide. The importance of securing as much preliminary tightness as possible cannot be overemphasized, because of the great probability of leakage increasing during pumping due to increased heads, working of the structure and local failures to an extent which might otherwise not be within the control of the pumps.

At 0430 on August 4th, the water was lowered to seven feet in the high compartments and eight feet in the low with reference to mean low water. At high tide, a small vertical movement of a bench mark on the bow was perceptible but this movement was attributed to change in trim or strain rather than rotation. It is well to note here that the entire pumping plan was designed to lighten the bow as much as possible to relieve the pressure that was believed to exist at the rock ledge in way of Compartment 16.

Because there was no particular reason for speed and because it was extremely important that no forces be allowed to build up or leakage develop which could not be controlled, pumping continued cautiously and each rising tide was utilized to supply the additional buoyancy necessary to move the ship. At 1730 on August 4th, just prior to flood tide, the water in the high and low compartments was lowered to minus nine and minus nine and one-half feet, respectively, so that the five-foot rise in tide would give a fourteen and fourteen and one-half foot negative head inside. Air and water jets installed in various patches in the port side and along the port edge of the promenade deck were started and maintained continuously in order to relieve any mud suction which might exist. The midship movement-measuring devices indicated a horizontal movement of the promenade deck of a little less than one inch during the rise in tide. It was felt that this movement in the right direction was a definite sign that the tendency for righting existed and that all was well.

During the morning of August 5th, water in the compartments was maintained at fourteen feet as the tide fell. At low tide, the ship was pumped to about minus fifteen feet. Between 0440 and 2250 on August 5th, compartments were pumped and flooded to hold the above negative heads. As the tide fell and rose no appreciable movement was noted. During the day fifteen wire rope cable stays were rigged from the uncut portion of the superstructure buried in the mud to the above-water side of the promenade deck, to strengthen the superstructure which in righting would have to plow through many feet of thick mud.

It was evident that additional buoyancy would be required before the vessel would commence righting. Consequently greater heads would have to be imposed on the promenade deck. An inspection was made of the deck and shoring. As there was absolutely no evidence of undue loads on the exposed shores or of leakage through seams and rivets, such as might be expected from overloaded deck plating, it was decided to pump down, at 0800 on August 6th, to about sixteen feet negative head and allow this head and buoyancy to increase with the rise in tide. It had been calculated that the moments of buoyancy and of gravity about the bilge keel would be approximately equal at that point. By 0915, at about half flood tide, the vessel started to roll slowly and steadily. This is the first movement indicated on the curve in Figure 58 and constituted the first critical point in the movement of the ship.

At 1200, following the parting of some of the superstructure stays, rotation (totalling about 1½°) was stopped by flooding all compartments two feet. Pumping was halted while all hands turned to installing additional one-inch cable stays with turnbuckles. Such action was necessary lest the inadequately supported cantilever load overstrain the connection of the superstructure in the promenade deck with the result that serious ruptures might occur.

The tying of the vessel's superstructure to the promenade deck was completed about 2200 on August 6th. The pumps were again started and the ship once more responded quickly. After fifteen minutes of steady movement, amounting to about 4°, the compartments were again partially flooded to stop the ship's rotation in

order to inspect the superstructure stays and relieve the strain on the superstructure incident to the rapid motion. At this point, one fact was definitely ascertained. There was no appreciable mud suction resisting the movement of the ship. This became apparent when it was observed that each time the water in the ship was lowered relative to the outside water level, the ship started to rotate, and the instant pumping stopped the ship's movement ceased. It was felt that absolute control of the vessel's every movement had been obtained.

During both tides on August 7th, pumping continued slowly and the ship rotated to about 67°. On the morning of August 8th, it was decided to move the ship from its 67° inclination directly to 45° by removing more than 11,000 tons of water chiefly from compartments 14, 15 and 16. The steep rise in the rotation curve (Figure 58) illustrates the results of this pumping.

By the time the ship reached 49° inclination, pumping was stopped in order to shift a considerable number of pumps so that more favorable suction heads could be had. Early in the morning of August 9th, pumps in Compartment 16 were unable to lower the water beyond the existing level and by 0800 the head in that compartment was reduced to an alarming degree in spite of the operation of all pumps at full capacity. Shortly thereafter, as many as nine pumps could not maintain anything more than a two-foot head in Compartment 16. A leak of an extremely serious nature had developed in way of the rock ledge.

While efforts were being made to locate the leak it was decided to attempt to dewater the compartment by sheer pumping volume. During the night and early next morning, activities were centered around shifting reserve pumps from other compartments into Compartment 16, where by this time the inside waterline was at the same level as the water outside the ship. It was considered unwise to further lower the water in other compartments appreciably because of the resultant great differential in head between adjacent compartments and Compartment 16. However, such pumping as could be done brought the ship over to about 42° by August 10th.

It was still impossible to gain more than a foot or two head in the leaking compartment with nine 10" pumps operating full

capacity. From the out-of-phase movement of the bow and stern, it was evident that the stern was afloat and the ship was pivoting about the rock ledge with the rise and fall of the tide. See Figure 58. At this angle of inclination, most of the uncut portion of the superstructure, including boat davits, had emerged from the water. While divers searched for ruptures inside and outside of Compartment 16, some 500 tons of the superstructure were removed. See Figure 56. Early in the morning of August 11th, the first of a series of ruptures in the double bottom and wing tanks forward of the first row of boilers in No. 2 fire room was found. Divers were unable to get down through the mud and rock to locate the rupture from the outside at this time. By the morning of August 14th, it was felt that all the ruptures in the tanks in Compartment 16 had been located and it was decided to attempt to fill most of the wing tanks No. 3 and 4, double bottom tank No. 13, and the corner between the wing tanks and double bottoms with some 100 cubic yards of concrete. The concrete pour was to be made by the Tremie method and was bound forward by No. 4 watertight bulkhead and aft by a dike which divers built of bags of cement. During this period the ship righted about 6° as a result of adding ballast in two starboard tanks and the removal of the remaining superstructure.

By the morning of the 17th, pouring of the concrete had been completed. Twenty-four hours were allowed for the concrete to harden and pumping was once again resumed on the morning of the 18th. At first, Compartment 16 held tight, but suddenly, with a negative head of 10 feet, the water in the compartment commenced to rise rapidly with all pumps going. Within about half an hour the head was reduced to five feet. Subsequent inspection by the divers indicated that a rupture in the tanks had opened abaft the concrete dam which had been previously laid. These new ruptures were found to be in way of the boilers; and, because the clearance between the boilers and the sides of the wing tanks was so small, divers could not actually reach them.

Following the failure on the morning of the 18th to dewater Compartment 16, it was felt that if the vessel were righted to 20-25°, it would be safe to attempt floatation by pumping compartments adjacent to No. 16. At that angle, the greatest head

would be within the allowable limit. Consequently, on the afternoon of the 18th, water was pumped into the empty starboard wing tanks. By the morning of the 21st, a total of 2800 tons had been placed in the wing tanks. This resulted in righting the ship to about 25°. Additional water was then removed from Compartments 14 and 3. Meanwhile, divers were busy scouring and using an air lift in the general vicinity of the hull damage, in the hope that the new rotation would make the rupture in the hull accessible. Failing to get close enough to the rock pinnacle to actually locate the bottom damage, divers were instructed to place rag and sawdust bags near the outside ruptures with poles or any other means possible in the hope that some of them would be sucked into the ruptures and partially choke off the leakage. Explorations of the rock ledge finally revealed that the bearing was very jagged, so further righting by counterflooding was abandoned.

After considerable study and search between August 22nd and 30th, it was decided to again attempt to stop the leaks by filling all of the double bottoms and wing tanks in way of any of the ruptures with concrete. This involved considerable preparation, including burning and clearing out in the No. 2 fire room so that Tremie pipes could be fitted in place. Some 800 tons of concrete were poured into the tanks. This operation continued until the morning of September 10th, after which forty-eight hours were allowed for setting. Not much faith was placed in the probability of reducing the leakage by the use of concrete alone, but it was necessary to provide an obstruction of some sort in the bottom to prevent bags, mats, etc., which would ultimately be necessary to stop the leak, from being sucked clear through the openings.

Since it was necessary to float the ship clear of the rock in order to "feed" bags to the leaks, dependence had to be placed on something other than the ability to pump out Compartment 16. Inasmuch as only about 5000 tons had to be removed from adjacent compartments to float at high tide, the boundaries of Compartment 16 were inspected and reinforced by shoring. This permitted pumping out entirely compartments 10 and 17, just forward of Compartment 16 and gaining at least five feet more differential in head between Compartments 16, 15, 14, etc.

Compartment 16 was given a trial test by pumping down and holding three feet. This test seemed fairly successful, so at 2300 on the evening of September 12th, pumping was once again attempted. By the morning of the 13th, it was realized that the latest attempt at choking the leak by pouring concrete was only partially successful. Thirteen 10" pumps, delivering approximately 9000 tons per hour, were required to hold a 5-7 foot head in Compartment 16. Pumping several thousand tons of water out of Compartments 10, 15, and 14 at this time, however, had definitely brought the vessel afloat at high water on September 13th. At the same time, a heavy strain was maintained on the bow mooring lines so that the ship was moved laterally about 16 feet. It was hoped that the rag and sawdust bags which had been planted close to the turn of the bilge would be sucked into the ruptures as a result of this movement. This operation was partially successful and resulted in gaining control of the leakage in Compartment 16, so that about a twelve foot head could be maintained. As shown in Figure 58, the ship floated clear both at high and low tides by the morning of September 15th.

Thereafter, pumping in all compartments was prosecuted as rapidly as possible. However, access for shifting pumps, as they lost suction, became very difficult, it being necessary to cut openings through doors, bulkheads, etc., to move the pumps and run suctions to the numerous low pockets. Insofar as compartment 16 was concerned—the bottom being well clear of the rock ledge—it was just a matter of time and labor for divers to choke off the leakage until it could be controlled and pumped all the way down with one 10" pump in each of the two firerooms comprising that compartment. Some 3000 bags of rags were ultimately fed into the ruptured hull to fill the voids between the plating and the concrete before the leakage was finally reduced to a negligible amount.

Because of the large off-center weights and the flooded condition of the ship, it floated in equilibrium at about 26°. Since September 16th work has been directed toward removing the tremendous amount of timber and concrete construction from the port side of the ship, cleaning out cork and oil, ballasting the starboard wing and bottom tanks, removing the remaining water and large quan-

tities of mud and debris from the ship, preparatory to turning it over to the Commandant of the Third Naval District for rebuilding.

Analysis.

Figure 58 is a curve of the rotation of the *Lafayette* from 79° to 26° during August and the first half of September. On the same graph are curves of vertical movement of the keel at the forward perpendicular and the keel at the after perpendicular. All of the critical points in the righting operations can be noted and interpreted from these curves.

The plan of salvage of the *Lafayette,* like the plan in most ship salvage jobs, was subject to certain unknown and indeterminate factors which vitally influenced the success or failure of the final salvage effort. The salvor, after making every attempt to determine as closely as possible these unknown factors, must incorporate in his plan of action enough elasticity so that it can easily be modified, depending upon the accurate determination of the unknowns as they become apparent once the operations have commenced.

A good example of the above occurred during the floating of the *Lafayette.* It was impossible to know exactly how the ship was supported by the soil and the rock ledge. Efforts to determine the consistency of the soil on which the ship was resting were only partially successful. Consequently an assumption or best guess had to be made concerning where the axis of initial rotation of the ship would be. One extreme considered the ship being supported by fluid mud to the extent that the axis of rotation would very nearly be an axis through the center of area of the bearing plane. Such a condition would obviously require very little righting moment to start the vessel's rotation. The other extreme considered the ship resting on soil of such hard surface that rotation would take place about the extreme outboard edge of the bearing plane. An assumption had to be made as to just where, between these two extremes, the axis of actual rotation would exist.

Therefore, an axis location based upon extensive study and investigation was assumed. The righting moment which would be required for rotation about the assumed axis was then determined by calculations which, in turn, determined the net buoyancy

required and the shoring needed to stiffen decks and bulkheads against the negative heads. Additional shoring was installed, beyond that calculated as necessary for the promenade deck, as a factor of safety against possible errors in axis assumption and also against the possibility of mud suction which would require additional buoyancy.

It was believed that by the initial pumping, an average of seven and one-half feet throughout would give the ship enough buoyancy and righting moment to start the rotational movement. The ship did not move, however, until the water had been pumped down nearly sixteen feet at low water. Once movement was started, the ship moved or stopped immediately following minor pumping or flooding. This response of fine variations in pumping conclusively proved that mud suction, if it ever existed, was broken by air and water jets or by time, long before enough net buoyancy to move the ship was obtained. It was strongly felt, however, that no mud suction resisting the movement of the ship ever existed.

Discounting mud suction, then, it is concluded that the ship did not move until nearly twice as much water as originally estimated was removed because the axis of rotation was much further outboard than was initially assumed. Section rotational studies indicate that the ship actually rotated the first several degrees about the turn of its bilge. The above is consistent with the later known fact that the turn of the bilge in vicinity of Frame 237 was in contact with the rock ledge. Certainly the combination of the rock and soil bearing constituted a rigid bearing plane. After the initial move, however, the ship moved away from the pier and rotated within the basin it had been resting. This movement was possible in view of the fact that the net buoyancy which was required to rotate the ship was almost enough to float her and a considerable mud bank had built up under its bottom.

Figure 58 indicates that as early as August 7th, the stern was more or less afloat and that from then on the ship was, practically speaking, only aground at the rock ledge. This is evidenced by the fact that on August 7th and 8th the movement of the stern came directly into phase with the movement of the tide, and the movement of the bow came directly out of phase with the tide. From August 10th until the ship came afloat on September 13th, the

amplitude of the bow curve was approximately one-half of the amplitude of the stern curve, and continued its out-of-phase movement.

On August 9th, the five week fight to overcome the leakage in Compartment 16 began. This leakage was the result of the damage to the ship's hull in way of the ledge itself. The damage may have been partially incurred when the ship capsized. It is felt, however, that most of it occurred as the ship was righting to 49° inclination, in spite of the attempt to rotate the ship with the bow light. Until the vessel reached the 49° inclination, Compartment 16 was apparently "riding on her bottom and wing tank tops." At about 49°, the combination of stress on the inside tank plating due to the rock reaction and the large negative head resulted in a series of tank top ruptures.

The first concrete pour, August 15-17, was successful as far as initial leakage was concerned, but the subsequent working of the ship over the rock ledge resulted in the opening of new ruptures. The second concrete pour of some 800 tons in all the ruptured bottom and side tanks was again only partially successful. However, it was successful in that it provided a dam against which bags of sawdust and rags fed to the leaks were stopped, which resulted in eventual reduction of leakage to an inconsequential amount.

It is important to note that the ship could have been floated at the beginning with Compartment 16 completely flooded to the outside waterline by pumping a sufficient amount of water from the adjacent compartments, had the boundaries of Compartment 16 been adequate to support the resultant hydrostatic pressure heads. As it developed, the bulkheads between Compartments 16, 15 and 10 were eventually strengthened beyond the original designed limit sufficiently to permit flotation with Compartment 16 filled.

Except for the failure and consequent leakage in Compartment 16, where at the start there was no indication of leakage, and where bearing on the rock precluded inspection, absolutely no leaks developed, nor were there any signs of failure in any of the construction work, practically all of which was done underwater and not susceptible of thorough inspection. Examination after dewatering

revealed workmanship of as high a quality as is usually encountered in work done on the surface. As a result, there was little anxiety on the part of those in charge during the long period required to conquer Compartment 16, because the leakage into the remainder of the ship was so small as to require very little attention and it was a simple matter to hold any gains made.

On the whole the entire salvage operation, from the initial development of the plan through the preparations and the final floating and cleaning of the ship, was considered extremely successful. Credit is primarily due to the supervisors, the divers, and other workmen who were responsible for devising means for and the actual accomplishment of the many details of the construction and other preparatory work on which success of the plan depended.

Discussion of the Paper

DETERMINATION OF TOTAL SOLIDS IN BOILER WATER FROM ALKALINITY AND CHLORINITY BY RAYMOND E. KAUFMAN.

By Robert C. Adams.*

The accuracy of the equation for calculation of total solids in boiler water, developed by the author from a series of unwieldy stoichiometric calculations in which ionic equilibria and pH have been disregarded, either must be fortuitous or be based upon the assumption that no reaction occurs between treating chemicals and potentially scale-forming salts. Such an assumption is invalid. Any calcium, magnesium, iron or similar ions in the feedwater must react in a properly treated boiler-water to precipitate the corresponding carbonate, phosphate or hydroxide with consequent reduction of alkalinity. Since the equilibrium between dissolved and precipitated salts cannot be calculated without the complete and accurate analysis of water which the author's method is intended to obviate, it would appear more reasonable to recognize the empirical and approximate nature of the result of calculation and substitute a simpler method of calculation whose limitations are defined.

If it be assumed that all salts dissolved in the boiler feedwater and all treating chemicals added to the boiler water remain in solution, an assumption not seriously in error during the first hundred hours of steaming with good feedwater, an equation of the form proposed by the author can be used. The inaccuracy of the premise should be recognized so that after long steaming the formula will not be expected to give reliable results. However, the formula for Naval boilers whose water is treated with Navy Boiler Compound 1941 is easily derived.

* Assistant Head, Chemical Laboratory, Naval Engineering Experiment Station.

It may be assumed, without significant error, that all titrated alkalinity is supplied by the sodium carbonate in the boiler compound, since at the phenolphthalein end-point approximately ninety-five per cent of the phosphate is present as $H\ PO_4^-$. The equivalent weight of Navy Boiler Compound 1941, therefore, is the quotient of the equivalent weight of sodium carbonate divided by the proportion of sodium carbonate therein: $53/0.39 = 136$. Since multiplication of *per cent normal* by 10 converts it to *equivalents per million,* and epm. $\times$ equivalent weight equals parts per million; multiplication of the regularly determined alkalinity by 1360 yields ppm. of dissolved solids introduced as boiler compound.

All saline contamination of boiler feedwater on Naval vessels is derived from sea water whether the flow path be entrainment from evaporators, weeping seams in storage bottoms or condenser-tube leakage. Although the concentration of sea water varies among the oceans, the ratio of the salts therein is constant with chloride (Cl^-) constituting approximately 55 per cent of the total. Thus by dividing the factor for conversion of *grains per gallon* to *parts per million* by the foregoing ratio: $17.1/0.55$; the coefficient 31 is obtained for the second term of the equation.

The complete equation is: $S = 1360A + 31C$.

The symbols have the following significance:

S = Dissolved salts, ppm.

A = Boiler-water alkalinity, % N

C = Chloride concentration, gr/gal.

Using this equation, the maximum permissible concentration of boiler water anticipated by current instructions to Naval vessels may be estimated. For the usual boiler with small water tubes the equation yields:

$$S = 1360 \times 0.35 + 31 \times 30$$
$$= 1406 \text{ ppm.}$$

That this is a conservative limit, intended to be well below the concentrations at which foaming becomes troublesome, is indicated

by the fact that a common, empirical limit used for blowdown calculations for shore plants is 4000 ppm. The Navy limits for fire-tube boilers barely exceed the latter figure.

The correlation between the foregoing equation and that proposed by the author could not be tested because the conversion of *per cent normal* to *phenolphthalein alkalinity in parts per million,* to which the author assigns the symbol *B,* could not be deciphered. In this connection it should be noted that alkalinity per se cannot be measured in *parts per million,* because the latter is a weight-per-weight unit and alkalinity is not a weighable entity. The device of reporting alkalinity as *ppm. of calcium carbonate* or of some other alkaline salt, although ponderous, is commonly used. For brevity, part of the expression frequently is omitted, but such elision should not occur in a publication.

COMMENT ON MR. R. C. ADAMS' DISCUSSION OF THE PAPER "DETERMINATION OF TOTAL SOLIDS IN BOILER WATER FROM ALKALINITY AND CHLORINITY"—BY RAYMOND E. KAUFMAN.

By Raymond E. Kaufman.

The primary premise made in the above paper was that any reactions between the treating chemicals and the scale forming salts are relatively unimportant as far as making a field check on boiler solids is concerned. This premise is something more than an assumption. The scale forming solids are only 15-20 per cent of the total sea salt weight and have approximately that degree of importance in forming both salts that are precipitated and salts that are not taken care of in the alkalinity and chlorinity determinations. This percentage is not cumulative because a boiler in the normal course of events will be dumped when the chlorinity gets too high, 30-50 grs./gal. chl. for small and large tube water tube boilers.

Whether or not the stoichimetric calculations are unwieldy as Mr. Adams suggests, the validity of this method as a field operation is not affected. Ionic equilibria and PH while not indicated were not disregarded.

Conventionally, quantitative reactions are generally written as if the reactants were molecules since the only interest is in the principal products at the endpoint or in the residue upon evaporation.

The amount of dissolved $Mg(OH)_2$ and $Ca_3(PO_4)_2$ in boiler water for most purposes may be safely ignored and it is not inaccurate for practical purposes to say that they are 100 per cent precipitated.

The NaOH that goes into the formation of Na_3PO_4 from Na_2HPO_4 is almost completely titrated to the phenolpthalein end point and the amount of Na_3PO_4 recovered by an evaporation is

directly proportional to the NaOH titrated. The reaction therefore may be represented by an equation in the molecular form, even though there are several forms of PO_4 ions in solution at the same time.

There is evidence from several sources [1, 2] indicating that dilute Na_2Co_3 solutions at boiler water temperatures do decompose within a few minutes after being injected into the boiler. This decomposition is of the order of 85-95 per cent. The reaction goes essentially to completion since the CO_2 is driven off reducing much of its reversibility.

In the opinion of the writer, the original premise is valid even after a long steaming period. It is suggested, however, that further discussion of this be held in abeyance until a few analyses of long steamed boiler water are in.

This method is not intended to obviate accurate chemical tests made on boiler water for technical study. It is instead an approximate field test to guide an engineering officer in treating boiler water.

The correlation between the equation suggested by Mr. Adams and a converted form of the equation listed in the article is reasonably close.

From article $S = 1145A + 31C$ $S =$ ppm dissolved salts
$A =$ % N alkalinity

Mr. Adams' $S = 1360A + 31C$ $C =$ grs/gal. chlorinity

Mr. Adams' coefficient of A will be higher since his coefficient is based on the undecomposed compound added; the writer's equation in the article is based on the solids recovered by evaporation, assuming CO_2 evolution.

---

(1) U. of I. Eng. Exp. Station Bulletin No. 261, F. G. Straub.
(2) The Inside Story of Boiler Water Conditioning, Elgin Softener Corp

NOTES.

INDEX TO NOTES.

RUDDER CONTROL AND THE MANEUVERABILITY OF SHIPS.
—The Shipbuilder and Marine Engine-Builder, July, 1943.

A NEW PRIME MOVER.
—The British Motor Ship, June, 1943.

THE BLACKBODY.
—General Electric Review, July and August, 1943.

IMPORTANCE OF GOVERNING ARRANGEMENTS FOR MARINE INSTALLATIONS.
—Transactions, Institute of Marine Engineers, July, 1943.

TAPERED AND STEPPED COLUMNS.
—Product Engineering, August, 1943.

MISCELLANEA OF INTEREST TO NAVAL ENGINEERS.

Under-Water Arc Welding.
—Welding Journal, August, 1943.

Producer-Gas Tests of a Converted Gasoline Engine.
—Engineering (London), June 11, 1943.

The Amplidyne.
—The Nautical Gazette, June, 1943.

Radius of Action.
—The Marine Engineer, August, 1943.

Dry Ice Kills Coal Pile Fires.
—Journal of the Franklin Institute, July, 1943.

RUDDER CONTROL AND THE MANEUVERABILITY OF SHIPS.

R. A. Collacott, author of this paper, considers rudder effect made up of two components; namely, the reaction of the propeller race and the projecting surface aspect. His paper was published in the July, 1943, issue of The Shipbuilder and Marine Engine-Builder.

Rudder design has in the past relied very largely upon trial-and-error methods; and, in the absence of detailed information, it may be that the only satisfactory method of arriving at the best rudder for a given vessel is to try different rudder forms and to choose the best. The lack of useful information relating to the design of rudders must be considered a serious matter, for a rudder is an expensive item; while, if several vessels of the same type are under construction, it is most undesirable that their completion should be delayed by lengthy trials on the prototype to determine the ideal form of the rudder. Some notes on certain aspects of the problem may therefore be useful as a guide to designers and engineers alike.

Rudder Design—General Considerations.

The effect of a rudder is derived from two sources, viz.:

(*a*) The reaction of the propeller race; and

(*b*) The obstruction to motion arising from the impact of fluid on a surface projecting from an immersed body.

In less general terms, these mean, first, that the rudder may deflect the jet of water forced away by the propeller, and, second, that its action is to divert the general motion of the fluid through which it is passing.

(*a*) Propeller Reaction.

Considering, first, the influence of propeller-race reaction, the turning effect is derived from the reaction of the race as it impinges against, or, rather, diffuses into, the undisturbed liquid, the force transmitted through the jet giving rise to a reaction on the rudder surface. The force on the rudder therefore depends upon the following:

(1) The rate at which fluid is ejected by the propeller;
(2) The momentum of this fluid;
(3) The angle at which this fluid strikes the rudder surface; and
(4) The effective rate of diffusion into the surrounding fluid.

The quantity of fluid upon which the propeller acts cannot be readily determined; in fact, until the position is clarified by research, none of the factors involved in this argument can be easily assessed. In general, however, it may be assumed that the "slip" velocity will allow for the difference in speed between the issuing jet and the speed of the vessel, although this term itself is subject to modification once the vessel has commenced to turn and transverse velocity components are introduced.

If, however, the discussion be limited to the simplified version, it is obvious that propeller factors such as blade width, form and thickness will, together with the state of the "approach flow," seriously influence the effective velocity. These factors will also control the mean effective axial-velocity distribution in the issuing stream; for, if the discharge from a propeller be examined, it will be found to vary across the diameter, as shown in Figure 1. In general, the effective quantity of fluid in cubic feet per minute may be written:

$$Q = \left[h_1 (\pi ND) \right] \times k_2 \frac{\pi}{4} D^2$$

$$= \left[\frac{\pi^2}{4} k_1 k_2 \right] ND^3$$

$$= KND^3 \qquad (1)$$

where $N =$ Rpm., $D =$ diameter of propeller in feet, and K is a constant whose value (assuming $k_1 = 0.10$, $k_2 = 0.70$) will be approximately 0.16. The true value must, however, remain a matter for further investigation.

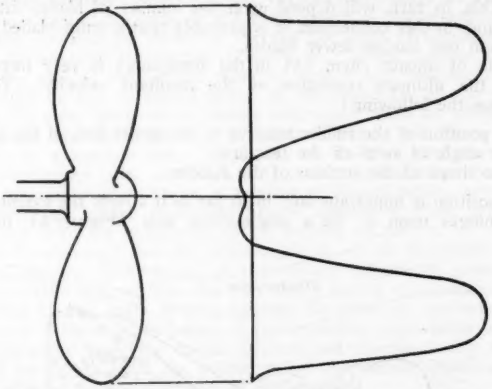

Fig. 1.—Axial Velocity Distribution in the Propeller Race.

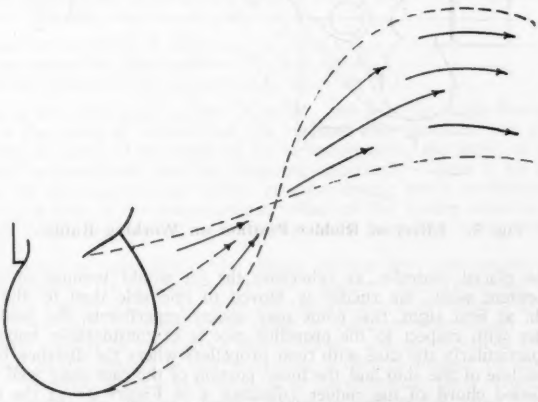

Fig. 2.—Screw Vortex behind a Propeller Blade.

Although reference is here made to the axial or thrust component of velocity, the discharge from a propeller is in reality a complex vortex sheet, as shown in Figure 2, with a three-dimensional velocity distribution. The effect of this is not very important so far as the axial component of velocity is concerned, although a careful examination of the circumstances reveals that a velocity fluctuation will occur at each point of the wake according to the position of the propeller blades and their pitch. As a result of the swirl or vortex, the momentum of the stream will not be entirely in a direction at right angles to the plane of the screw, so that some force will be lost so far as maneuverability is concerned. The amount of control lost in this way is, however, partly dependent upon the number of vortices which are formed. This, in turn, will depend upon the number of blades fitted to the propeller, and, in this connection, it is probable that a multi-bladed propeller is better than one having fewer blades.

The angle of impact (item (3) in the foregoing) is very important in regard to the ultimate resolution of the resultant velocity. This angle depends upon the following:

(*i*) The position of the rudder relative to the center-line of the jet;
(*ii*) The angle of swirl of the jet; and
(*iii*) The shape of the surface of the rudder.

Rudder position is important only in so far as it affects the extent to which the jet impinges upon it. In a single-screw ship (Figure 3), the rudder

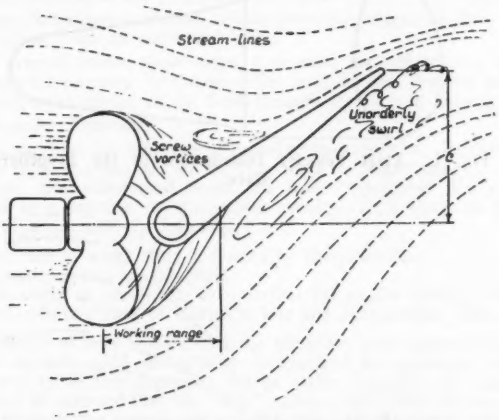

Fig. 3. Effect of Rudder Position on Working Range.

should be placed centrally, as otherwise the jet would impinge on it to a greater extent when the rudder is moved to one side than to the other. Although, at first sight, this point may appear superfluous, the position of the rudder with respect to the propeller race is of considerable importance. This is particularly the case with twin propellers where the distance between the center-line of the ship and the inner portion of the race may well exceed the projected chord of the rudder (distance c in Figure 3) at the smaller rudder angles. In such circumstances, the rudder of a twin-screw vessel

will operate, for the earlier part of its movement, without coming under the influence of the propeller race; while, for the extreme part of its movement, it will come within the propeller race. Again, the fore-and-aft length of the rudder, with either a single screw or twin screws, should be such that the area of its projection on a transverse plane at the maximum angle includes as much of the race as possible. Thus, for the best possible condition, the minimum rudder length for a single-screw installation is given by:

$$L = \tfrac{1}{2}D \operatorname{cosec} \theta \quad \ldots\ldots (2)$$

where θ is the maximum rudder angle.

The angle of swirl of the jet, i.e., the vortex angle, may, for all practical purposes, be taken to be equal to the pitch angle of the propeller. When, however, this swirling jet strikes a surface, the point of impingement will vary with the angle of the surface (Figure 4). If the surface is at right angles to the axis of the jet, the point of impact will describe a circle at the same rate as the rotational speed of the propeller; if the surface is inclined to the axis, the point of impact will move round an ellipse; while, if the surface is edge-on to the axis, the point of impact will move vertically, to and fro, in a straight line. It should be observed that the foregoing applies to the vortex from one blade only, and a similar effect results from the joint action of multiple blades, a number of impact-points, corresponding to the number of blades, traversing figures similar to those in Figure 4, in accordance with the inclination of the surface to the jet.

It should be observed that the phase-angle ϕ_1—ϕ_2 is dependent upon the blade pitch and the distance, x, of the surface behind the propeller disc. This may be easily derived from the elementary theory of sinusoidal motions. The variation of this angle, besides causing the point of application of the forces to vary with each revolution of the propeller, also causes a variation in the forces acting upon the rudder surface, and thereby doubly affects the moment of the forces upon the rudder about the rudder stock—a moment which is balanced by the operation of the controls.

It will be seen by reference to Figure 5 that the force, F, due to the momentum of one swirl, i.e., the vortex from one blade tip, will have the following components on striking a surface whose plane is at right-angles to the line of thrust:

$$\text{Normal component} = F \cos \alpha \quad \ldots\ldots (3)$$
$$\text{Vertical tangential component} = F \sin \alpha \sin \phi \quad \ldots\ldots (4)$$
$$\text{Horizontal tangential component} = F \sin \alpha \cos \phi \quad \ldots\ldots (5)$$

where α is the pitch angle of the propeller, and ϕ is the angle between the radius to the point of impact and the vertical. If, however, the plane of the surface is placed at an angle to the reference axis, the angle of inclination must be introduced into the foregoing equations. There is no need to examine the above-mentioned factors in great detail; but it is obvious from the foregoing that, if the instantaneous values of the rudder moment due to the swirl could be obtained, a variation with propeller angle would be observed.

The influence of curvature of the rudder surface does not require considerable discussion. It is equivalent to the "bucket" effect observed when a jet strikes a curved plate. As, however, the surface of a rudder is generally plane, the jet will probably slide along it without rebounding. To the author, this appears to represent a loss of effort, and, as explained later, the ideal shape of the surface is one possessing a certain amount of curvature, giving a "bucket" effect which imparts to the departing jet a velocity component normal to the surface. Such a device is used by fish when "changing

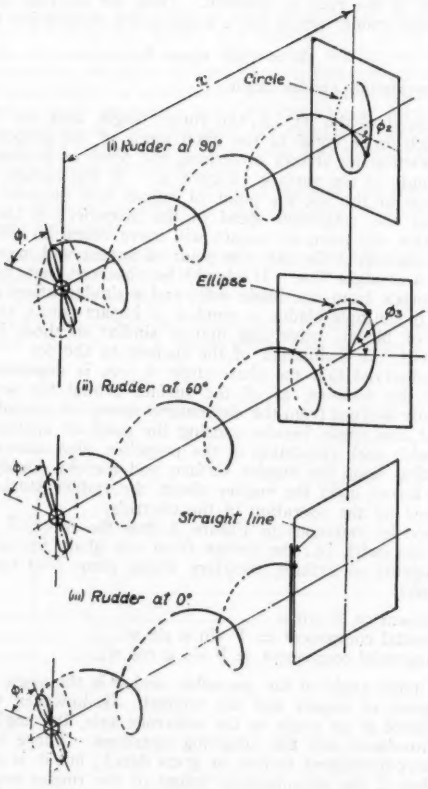

Fig. 4.—Vortex Reaction on a Plate.

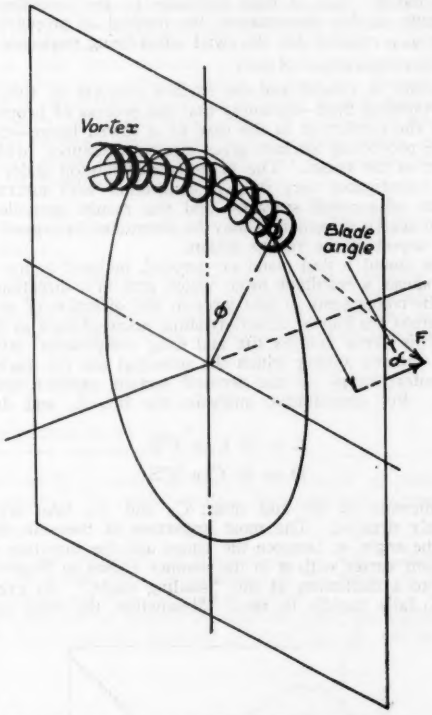

Fig. 5.—Forces on an Inclined Plate due to an Impinging Vortex.

course" suddenly, and might possibly be applied to high-speed launch construction in the form of a rudder jointed in the center in such a way that the after part might move through a larger angle than the forward part. This would provide a small "bucket" effect which would be particularly useful at extreme rudder angles when rapid change of course is called for.

Although the author does not think that the rate of diffusion of the jet into the surrounding water is especially important, it is an aspect of the rudder problem which should be carefully studied. The value which such a study might have would be to determine the "jet length" before diffusion is complete—a factor which may have a practical bearing upon the time lag between the movement of the rudder and the ship's response to rudder action. There is no need to enter fully into this subject; but if a length of jet, l_1, say, is required for the full development of thrust, the turning effort on the ship will not attain an effective value until this length of jet has been reached. The response is, therefore, a function of the rate of turbu-

lence diffusion and the rate of fluid discharge by the propeller. For simplicity, in a study of this phenomenon, the method of propulsion might be regarded purely as a reaction jet, the swirl effect being neglected.

(*b*) *The Projecting-surface Aspect.*

When the rudder is rotated and the surface projects so that it is forced against the surrounding fluid—assuming that the process of propulsion exerts no influence on the rudder, as in the case of a towed barge—the impact of the fluid on the projecting surface gives rise to pressures, which induce a turning moment on the vessel. The pressure distribution under such conditions has been investigated very fully in connection with aircraft design in the development of aerofoil surfaces, and the results provide a splendid storehouse from which information may be abstracted in regard to the projecting-surface aspect of the rudder action.

The fluid flow round a thin plane or aerofoil, inclined to the direction of the stream, produces a resultant force which acts in a direction inclined to the stream. The components of this force in the direction of motion and at right-angles thereto are known in aerodynamic nomenclature as drag and lift respectively. This force and its lift and drag components vary according to a number of factors, among which the principal are the angle of inclination of the aerofoil, shape of the aerofoil section, surface roughness and speed of flow. For quantitative analysis, the lift, L, and drag, D, are given by:

$$L = \tfrac{1}{2}\, C_L \rho\, V^2 S \qquad (6)$$

$$D = \tfrac{1}{2}\, C_D \rho\, V^2 S \qquad (7)$$

where the coefficients of lift and drag, C_L and C_D take account of the factors previously detailed. The most important of these in the operation of a rudder is the angle, α, between the chord and the direction of the flow. The lift coefficient varies with α in the manner shown in Figure 6, increasing from zero to a maximum at the "stalling angle." At greater angles, the value of C_L falls rapidly to zero. Meanwhile, the drag coefficient C_D

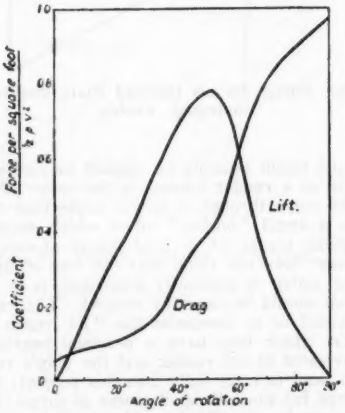

Fig. 6.—Effect of Rudder Angle on C_L and C_D.

increases steadily over the whole range of movement. The reasons for such behavior are to be found in the fact that, up to the critical angle, fluid passes over the surface without breaking away, and resumes its original orientation at some little distance in the rear of the surface; while, at angles greater than the stalling angle, vortices are formed in the wake. During the first stage, the pressure distribution is progressively modified on each side, so that C_L gradually increases up to a maximum until eddies form, and suction on the down-stream side of the surface rapidly decreases. This causes C_L to diminish rapidly, while the rate of increase of C_D also falls. Aerofoil design, therefore, aims at:

(1) Increasing the value of C_L up to the stalling angle,
(2) Increasing the angle at which stalling takes place, and
(3) Reducing C_D.

These are achieved by studying the flow round the aerofoil, and it will be seen from a study of the forces upon a rudder that, although conditions are somewhat different, the lines of development are much the same.

Considering the moments of the lift and drag forces about the rudder axis, we have:

$$\text{Moment due to lift} = xL\cos\theta = xc\,C_L\cos\theta \quad \ldots\ldots (8)$$

$$\text{Moment due to drag} = xD\sin\theta = xc\,C_D\sin\theta \quad \ldots\ldots (9)$$

where $c = \frac{1}{2}\rho V^2 S$, x is the distance of the center of pressure abaft the rudder axis, and θ is the rudder angle. Thus the total moment will be

$$M = cx\,[C_L\cos\theta + C_D\sin\theta] \quad \ldots\ldots (10)$$

All the parts of this equation are determinate, C_L and C_D being obtained by experiment on aerofoils, etc. The position of the center of pressure varies somewhat, although not to a very large extent.

From calibration curves applied to equation (10), the variation of rudder moment with angle may be obtained (Figure 7). It will be seen that M

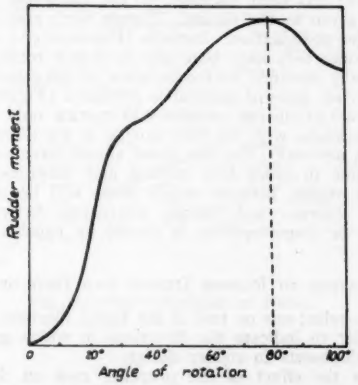

Fig. 7.—Variation of Rudder Moment with Angle of Rotation.

increases rapidly at first, and then less rapidly, until, at an angle of 80 degrees, the rudder moment attains its maximum value. These variations of M with angle have two effects, viz., (1) on the steering gear, and (2) on the rate of turn of the ship.

In practice, it is almost impossible to define the character of variation of rudder moment owing to the importance of other factors, such as wave velocity and size, rate of roll and forward speed, factors which have considerable influence. If, however, in the search for a basis of rudder design, we compare ships operating in calm water, a fine-lined vessel will, other things being equal, give a better response to the rudder than will a vessel having fuller lines aft.

The effect of the rudder forces on the remainder of the turn and on the process of turning will now receive attention.

A Theory of Steering and Maneuverability.

When a vessel which is proceeding on a steady course is suddenly subjected to a turning moment, the immediate reaction is for the vessel to yaw rather than to alter course, as in Figure 8(d). This causes the propeller thrust to be applied in an off-course direction and the vessel is therefore encouraged to travel along this course. The turning forces, however, oppose motion in this direction, so that the rate of turn is reduced by the rudder itself. When this occurs, the angle (θ) between the center-line of the vessel and the direction of motion of the C.G. of the ship will vary according to the combination of rudder moment and thrust. Although the author has no concrete information upon which to base a determination, a more detailed study of this phenomena suggests that it is reasonable to assume that θ varies with the distance moved, so that the vessel turns in a wide curve.

Calculations of the actual yaw would have to take into account the "aerofoil shape" of the ship-rudder combination. To explain this statement more fully, when the rudder is put over, its relation to the hull produces an "aerofoil" effect, and the forces engendered may be regarded from two points of view, viz., (1) impact forces on the rudder, and (2) the "aerofoil equivalent" of the ship-rudder combination when the vessel has begun to turn.

The former aspect has been discussed in the foregoing, and some attention will now be given to the second. Figure 8(c) and (d) represent an idealized ship-rudder combination. Initially [Figure 8(c)], only lift and drag forces exist; but, once they have been able to induce rotation, the forces on the rudder are rapidly modified by the presence of the vessel in the approach stream, so that a crude form of aerofoil is produced (Figure 8(d)).

In effect, the forces producing rotation will operate only while the rudder is at a fairly large angle, with the hull moving in the direction of its longitudinal axis. It is necessary that the vessel should have some slight motion in the new direction, in order that turning may continue. Turning must therefore occur in stages, between which there will be sections of (relatively) straighter course; and though alternation between turning and straightening may be imperceptible, it should be capable of experimental determination.

Application to Rudder Design and Development.

It is proposed to select one or two of the topics discussed in the previous paragraphs, in order to indicate the directions in which greater knowledge might lead to developments in rudder design.

Considering first the effect of the propeller race on the rudder forces, experiments are required to determine the additional force derived from this source. The results of such experiments with twin rudders—in conjunction,

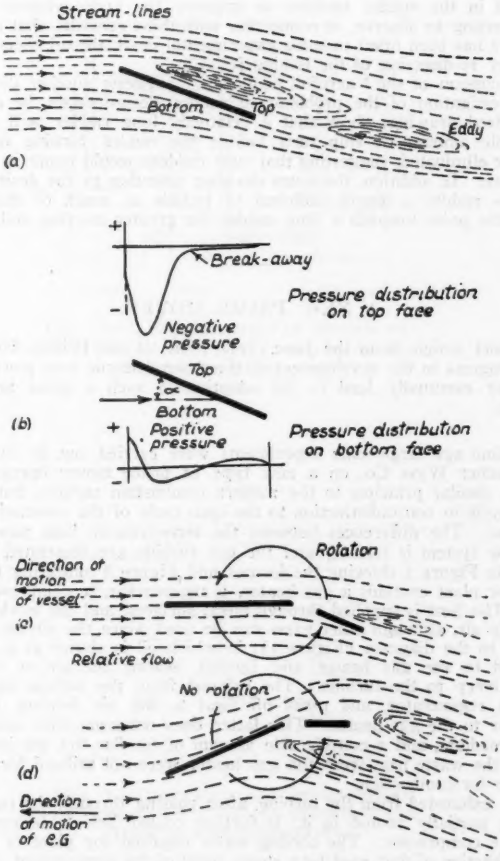

Fig. 8.—Characteristics of Flow.

perhaps, with a Kort nozzle, might afford scope for improvement in maneuverability. Besides making possible increased rudder area, twin rudders might be arranged to form a contracting channel, producing a jet which again would increase maneuverability. Additional concavity might be incorporated in the rudder surfaces to improve the hydrodynamic reaction. It is interesting to observe, in connection with these remarks, that an adjustable nozzle has been fitted in some experimental craft abroad, steering being obtained by re-direction of the issuing jet.

The discussion of the "aerofoil equivalent" suggests another direction in which investigation of the problems of rudder design might be developed. The idealized drawings show that a relatively long rudder will permit a considerable amount of ship turn before the rudder turning forces are reduced or eliminated, suggesting that such rudders would result in increased rate of turn. In addition, the notes drawing attention to the desirability of giving the rudder a length sufficient to include as much of the race as possible also point towards a long rudder for greater steering ability.

A NEW PRIME MOVER.

This short article from the June, 1943, issue of the British Motor Ship reports progress in the development of the "aerodynamic heat power plant" which may eventually lead to the adoption of such a plant for marine propulsion.

Some time ago large-scale experiments were carried out in Switzerland by the Escher Wyss Co. on a new type of prime mover operating on a somewhat similar principle to the modern combustion turbine, but utilizing a closed cycle in contradistinction to the open cycle of the constant pressure gas turbine. The differences between the aero-dynamic heat power plant, as the new system is termed, and the gas turbine are illustrated diagrammatically in Figure 1 showing the former and Figure 2 indicating the latter.

The new plant contains a gas heater, a regenerator, a compressor and a turbine. The heat is supplied through metal surfaces, and the working agent is normally air, although other gases can be used, since the circuit is closed. Referring to the diagram (Figure 1), in which oil is shown as a fuel, this is supplied to the gas heater and ignited, heating the air or other gas before delivery to the turbine. The exhaust from the turbine takes place through a regenerator, and gives off heat to the air flowing from the compressor to the gas heater. This latter does not come into contact with any cold medium, and a considerable amount of the flue fire gas heat would be lost if the waste heat from the gas heater were not utilized for preheating the air for combustion.

The air exhausted from the turbine, after passing through the regenerator and being partially cooled in it, is further cooled before delivery to the inlet of the compressor. The cooling water required for plant of this kind is only a fraction of that used by a steam plant of the same output, especially as the temperature of the water can be raised considerably without causing any harm. As the water does not come into contact with any delicate parts it is not required to be particularly pure, and all difficulties of supply associated with a high-pressure steam plant cease to exist.

The entropy diagram for the system is shown in Figure 3. Expansion of the air in the turbine takes place along AB and regeneration occurs along the lines BC or DE. The air is compressed isothermally from C to D, and

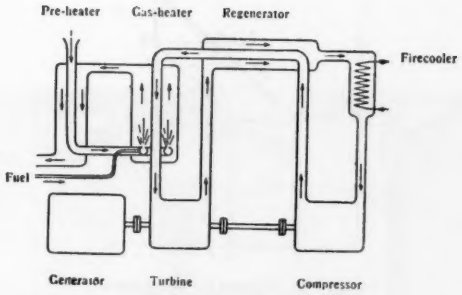

Fig. 1.—Diagrammatic sketch of closed-cycle aero-dynamic heat power plant.

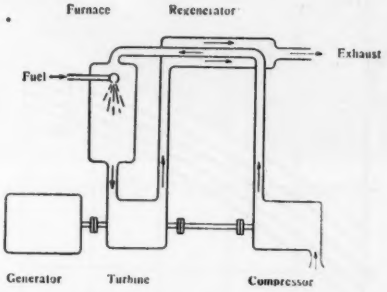

Fig. 2.—Diagrammatic arrangement of open-cycle constant-pressure gas turbine with regenerator.

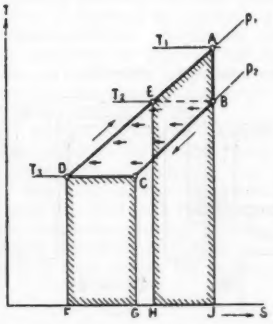

Fig. 3.—Entropy diagram of the ideal process of aerodynamic heat power plant with perfect regeneration.

$$\eta_c = \frac{T_1 - T_3}{T_1} = \text{Efficiency of the Carnot cycle}$$

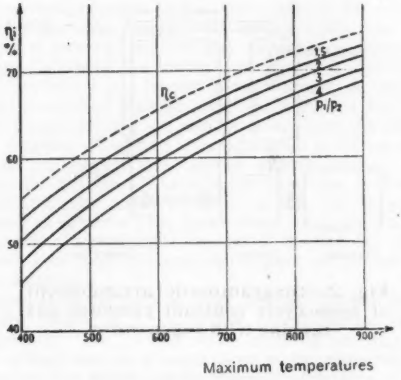

Fig. 4.—Thermal efficiency of the ideal process according to Fig. 1. (T_3 = 300 deg. abs.)

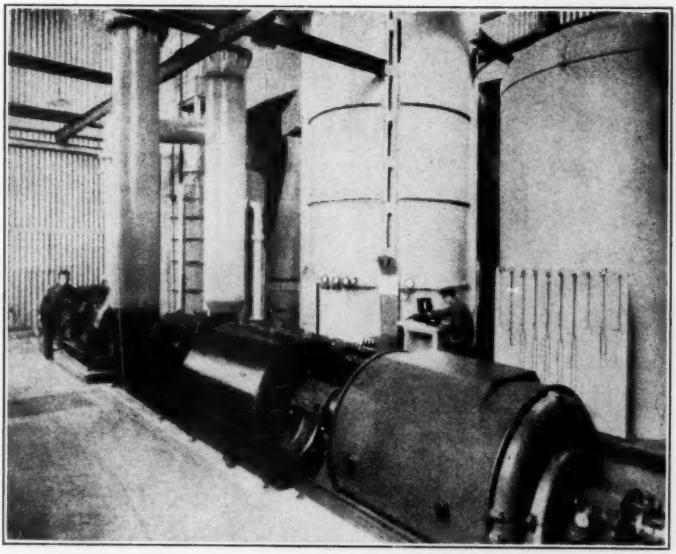

FIGURE 5.—AN EXPERIMENTAL AERO-DYNAMIC HEAT POWER PLANT.

this is carried out in several stages with intercooling. The external heat is supplied to the working medium in the air heater along the lines EA. The area ABCD represents the work done, this being the difference between the work effected by the turbine and that absorbed by the compressor. Referring to the diagram, the work carried out by the turbine is equivalent to the heat supplied externally, EAJH, while the work absorbed by the compressor is equal to the heat given up by the cooling water of the compressor DCGF.

The thermal efficiency of the ideal cycle with an ideal gas, omitting turbine, compressor, gas heater and heat exchanger losses and with complete regeneration, is shown in Figure 4 and is given by the equation

$$\eta_1 = \frac{C_p\,(T_1 - T_2) - AR\,T_3 \lg \frac{p_1}{p_2}}{C_p(T_1 - T_2)} =$$

$$1 - \frac{AR\,T_3 \lg \frac{p_1}{p_2}}{C_p\,T_1\left[1 - \frac{1}{\left(\frac{p_1}{p_2}\right)^{\frac{k-1}{k}}}\right]}$$

If the maximum and minimum temperatures T_1 and T_3 are fixed, the thermal efficiency of an ideal cycle depends only upon the ratio of the pressures and not upon the absolute magnitude of the pressures between which the cycle operates. The smaller the ratio of the pressures, the higher the efficiency. This is a great advantage compared with the usual process employing steam for the working agent, since the available heat cannot be used to the utmost efficiency unless the steam is at high temperature and pressure.

There is a large amount of heat in the gas after it has performed its work in the turbine, and further use must be made of this, since the waste heat in free discharge, as in gas turbine plants, would reduce the efficiency below that of a moderately economical steam plant. By keeping the fire out of the closed circuit system and operating the entire circuit under pressure, the cross-sectional areas of the heat exchangers and piping can be of moderate dimensions, also the surfaces, and an efficient system can be arranged in this manner. Another advantage of the pressure circuit is that the coefficient of heat transmission on the gas side of the gas heater is better, so that the mean temperature of the wall is lower and moves considerably to the cold gas side, more than would be the case with low pressure. Moreover, both turbine and compressor can be made of much smaller dimensions. If, for instance, the initial pressure on the inlet side of the compressor is 9 atmos. instead of atmospheric, with the open cycle gas turbine process, the diameters both of the turbine and compressor can be reduced to one-third, temperatures and speeds remaining unaltered. The saving in cost is thus considerable.

Such a plant has to be started up by external means, but this can be rendered much easier by lowering the pressure of the closed circuit. If the inlet pressure to the compressor be reduced to 1 atmos. instead of 9 atmos. the output is reduced to one-tenth and the ease of starting correspondingly increased.

A plant operating on this principle has already been constructed, and an illustration is seen in Figure 5. From left to right are the compressor, the two-stage turbine and the generator. Immediately behind, from right to left, are the regenerator, air heater and, in the background, the inter-cooler

for the compressor and the air preheater. There are two vertical insulated pipes for the supply of hot air to the turbine, and the other pipes are arranged under the floor. No regulating valves are needed, since control is effected by variation in pressure.

It is believed that many possibilities are opened out to this class of machinery for the propulsion of ships requiring fairly high power, and although it is clear that coal-firing could be utilized if necessary, the employment of oil fuel is naturally much more advantageous and would probably alone be considered in the case of marine propulsion. The efficiency of the plant has not been recorded, as no results of the test have been made public. But it is understood that efficiencies equal to those of the combustion turbine have been obtained, and it is understood that further development work is in progress, which may lead to the adoption of the plant for marine propulsion after the war.

THE BLACKBODY.

Mr. Frank Benford of the General Electric Research Laboratory points out that blackness and brightness are but phases of the same thing and are as natural partners as ham and eggs. Because of the very strangeness of blackness being necessary for brightness, he considers "Blackbody" a most appropriate name for this article since it brings out emphatically the one idea that must be caught before the subject can be understood. Mr. Benford's article is reprinted from General Electric Review, July and August, 1943.

The eternal pursuit of knowledge is, after all, merely a striving for higher accuracy. What we know in a scientific way we first put into words, then into an equation, and finally the equation is reduced to a numerical value and checked with experiment. The physical and chemical divisions of science are so intimately connected that there is usually a number of different ways, both physical and chemical, of experimentally arriving at the value of the physical constants. All methods should yield identical values, but actually each method will yield a sightly different figure; it is then the self-imposed task of someone to estimate the relative worth of the various results and thus arrive at a weighted mean.

Dr. Raymond T. Birge has, on several occasions, made a complete survey of the more important physical and chemical constants and in his latest publication[1] he says, "Among the new discrepancies the greatest, on a percentage basis, involve the radiation constants c_2 and σ." With the newer and more consistent data now available, it is an appropriate time to make a survey of Blackbody data and to add a few items that are of particular interest to the engineer.

Constants and Symbols.

The constants as revised by Birge are:

Velocity of light	$c = 2.99776 \times 10^{10}$ cm sec^{-1}
Planck constant	$h = 6.6242 \times 10^{-27}$ erg sec
Boltzmann constant	$k = 1.38047 \times 10^{-16}$ erg deg^{-1}

[1] "A New Table of Values of the General Physical Constants," by Raymond T. Birge, *Reviews of Modern Physics, 13,* 233, (1941).

With these three constants all the radiation constants can be computed, but before doing this certain changes can be made to advantage in the system of units. Since the micron ($\mu = 10^{-6}$ meter) is a much more usual and convenient unit for indicating wavelengths it will be used in place of the centimeter. Also, the microwatt is a more convenient unit in many applications than the erg per second; therefore, energy per second will be expressed as power, in microwatts. As a matter of further convenience, the spectrum will be considered as made up of zones differing in wavelength by 0.01μ. On this new basis the radiation constants are:

First radiation constant, total power radiated from 1 cm^2 of Blackbody.

$c_1 = 2\pi hc^2 = 3.7403 \times 10^8$ microwatts per cm^2 per 0.01μ zone of spectrum.

First radiation constant, intensity of radiation along normal to surface

$c_1\ 2hc^2 = 1.1906 \times 10^8$ microwatts per cm^2 per steradian per 0.01μ zone of spectrum.

First radiation constant, power in 1 cm^3 of volume within a radiating enclosure

$c_1 = 8\pi hc = 4.9907 \times 10^{-2}$ microwatts per cm^3 per 0.01μ zone of spectrum

Radiation density constant

$a = 8\pi^5k^4/15c^3k^3 = 7.5694 \times 10^{-16}$ microwatts per cm^3.

Second radiation constant

$c_2 = hc/k = 14{,}384.8$ micron deg.

Stefan-Boltzmann radiation constant

$\sigma = 2\pi^5k^4/15c^2h^3 = 5.6728 \times 10^{-6}$ microwatts per cm^2.

Stefan-Boltzmann photon constant

$\sigma' = 4\pi k^3\ [1 + (1/2)^3 + (1/3)^3 + \ldots\ldots]\ /c^2h^3$
$= 1.52138 \times 10^{11}$ photons per cm^2 per sec.

First radiation constant for photons

$c'\lambda = 2\pi c$
$= 1.883548 \times 10^{11}$ photons per cm^2 per sec per 0.01 μ zone of spectrum.

The following symbols are used in the equations of radiation and photons:

μ = micron, or 10^{-6} meter
λ = wavelength, measured in microns
T = temperature on the absolute scale (°C + 273)
J = microwatts per square centimeter
Jλ = microwatts per square centimeter at wavelength λ
Ψ = microwatts per cubic centimeter
$\Psi\lambda$ = microwatts per cubic centimeter at wavelength λ
P = pressure per square centimeter, in dynes
Pλ = pressure per square centimeter, in dynes, at wavelength λ
ω = solid angle, in steradians.

Physical Theory.

The theory of the Blackbody assumes the existence of a perfect radiating surface. Although there are certain theoretical reasons for believing that such a surface is a physical impossibility, there is, fortunately, a rather sim-

ple method of constructing a "reasonable facsimile thereof." In order to understand better the substitute for the ideal surface, let us first consider the action of a radiating surface. Any surface that is emitting radiation (and all surfaces are doing so at all temperatures) can be thought of as possessing two sides, an inside and an outside. Those surfaces, such as glass, that permit observations of radiation incident on the outside and also on the inner side of the surface, always show equal transmissions in the two directions. Thus if a glass surface permits the entry of 95 per cent of the energy incident at a certain angle, the transmission along the same path but in the opposite direction is also 95 per cent. The two sides of the surface, therefore, are identical in their total transmissions, all angles being considered. Also, they are equal in reflectances since no energy is lost and the sum of reflectance and transmittance must be equal to unity. *A perfect emitting surface, being one that offers no resistance to the outward flow of energy, is therefore perfect in permitting the inward flow of energy and hence is perfectly black.* By "blackness" is meant the absorption not only of visible radiation but also of all radiation of whatever wavelength.

No known surface is perfect either as an absorber or as an emitter. Thus soot, which to the eye seems perfectly black is fairly "white" to certain wavelengths in the infrared. All substances seem to show wavelength selectivity in some manner or other. But while *no* substance is a perfect emitter *any* opaque substance may be used to build an experimental substitute for the ideal surface, as will now be described.

Select some solid and opaque material in which a cavity can be formed and leave a comparatively small opening into the cavity so that some of the inner surface can be seen. Assume that we are interested in the light emitting properties of the surface and that the emissivity of the surface is e, where e is less than 1 because the surface is not a perfect emitter. Since the absorptivity a of the surface is equal to the emissivity a, we have

$$e = a$$

in all cases. Also, the sum of the reflectance r and absorptance a is unity, or

$$r + a = 1$$

If the temperature of the material is raised until incandescence is reached, the outer surface will have a brightness

$$b = B_o\, e$$

where B_o is the brightness of an ideal surface at the same temperature. The initial brightness of the inner surface will also be b, but the radiation will be reflected back and forth between the walls of the cavity and at each reflection reduced by the fraction r. Writing the infinite mathematical series for the infinite series of reflections, we have for the brightness B of the inner surface:

$$B = B_0 e + B_0 er + B_0 er^2 + \ldots\ldots$$
$$= \frac{B_0 e}{1 - r} \qquad (1)$$

But

$$1 - r = e$$

therefore

$$B = B_o$$

and the walls of the cavity have a brightness equal to that of an ideal Blackbody at the same temperature.

Since e and r vanish from the equation, it follows that the walls of the cavity may be made of any material, or of any combination of materials, and the observed brightness will depend only on the temperature of the walls, which must be uniform throughout.

This has been tested in the following manner: Three cylinders about 3 inches in diameter and 6 inches long were made respectively of graphite, soapstone, and magnesium carbonate. For the visible part of the spectrum, these substances have reflectances of about 0.04, 0.50, and 0.98 and hence their emissivities are 0.96, 0.50, and 0.02.

A hole one inch in diameter and five inches deep was drilled lengthwise of each cylinder, then the hole was capped with a disk having a quarter-inch hole in the center through which the bottom of the cavity could be viewed.

These cylinders were placed side by side in a furnace and observed as they came up to the furnace temperature. At the beginning all three cavities were black, but the graphite, probably due to its higher thermal conductivity, showed light before the others. After sufficient time had elapsed, all three cavities came to substantially the same brightness as measured by an optical pyrometer. Since graphite is 48 times $\left(=\frac{0.96}{0.02}\right)$ as good an emitter as magnesium carbonate, it is evident that the internal reflections in the carbonate cavity were 48 times as strong as the reflections in the graphite cavity. Thus the two widely dissimilar substances came to the same ideal condition.

TABLE I.

ALLOWABLE SIZE OF APERTURE α TO GIVE 99 PER CENT ACCURATE VALUES OF BRIGHTNESS.

Emissivity	Completeness S	Aperture a
0.01	0.9999	0.0001
0.10	0.9989	0.0011
0.20	0.9975	0.0025
0.30	0.9957	0.0043
0.40	0.9933	0.0067
0.50	0.9899	0.0101
0.60	0.9848	0.0152
0.70	0.9764	0.0236
0.80	0.9596	0.0404
0.90	0.9091	0.0909
0.96	0.7576	0.2424
0.98	0.5050	0.4950
0.99	0.0000	1.0000

In the preceding infinite series that represented the internal reflections it was assumed that the walls of the cavity were complete over 4π steradians, but this cannot be the case where there is an opening for observation. Let

the degree of completeness of the wall be represented by the fraction S, then the infinite series has a factor Sr between terms, and the observed brightness is

$$B' = B_0\,e + B_0\,e\,Sr + B_0\,e\,S^2\,r^2 + \ldots . \qquad (2)$$

$$= \frac{B_0\,e}{1 - Sr}$$

In Table I the data under S gives the proportion of a complete sphere that must be present if the difference between B′ and B_0 is not to exceed 1 per cent. It will be seen that if the emissivity is high, the aperture can be a large fraction of the angular area of the sphere walls; but if the emissivity is low, as in the case with magnesium carbonate, the opening must be relatively small. The errors in brightness are related to the effective wavelength (0.665μ) of the optical pyrometer, and the accompanying errors in temperature determination require further computation.

Blackbody Distribution Curve.

Prior to 1900 the best representation in equation form of the distribution of power in the spectrum of a Blackbody was given by Wien's equation.

$$J\lambda = \frac{c_1\,\lambda^{-5}}{e^{\frac{c_2}{\lambda T}}} \quad \ldots . \qquad (3)$$

It was from this equation that Wien derived his displacement law, that will be dealt with in some detail later in this article. About 1900 Max Planck began a series of observations, speculations, and mathematical researches that overthrew many of the classical theories of physics and chemistry, and established in their places some of the present-day theories.

Planck reversed the normal order of procedure. He started with numerical values computed by means of Wein's equation and found that they did not agree with experiment at long wavelengths. He changed Wein's equation by attaching —1 to the denominator purely as an arbitrary means of getting agreement. The later mathematical work of justifying this from a theoretical standpoint led to the idea that energy is emitted from a surface, not as a steady stream, but in small discreet bundles that he named quanta. Another name used is photon, and this designates bundles of radiation even when outside of the visible spectrum.

Let us assume that by some ideal optical arrangement all the radiation from 1 sq cm of surface is collected and then spread out into a spectrum of infinite length corresponding to the range of wavelength from zero to infinity. Planck's distribution equation tells how the power from the 1 sq cm is distributed in this spectrum and how the distribution changes with the temperature. The spectrum is considered to be divided into zones differing in wavelength by 0.01μ. This width of zone divides the visible region, 0.40μ to 0.70μ, into 30 parts, which is a convenient number for many computations.

$$J\lambda = \frac{3.7403 \times 10^3\,\lambda^{-5}}{e^{\frac{14384.8}{\lambda T}} - 1} \text{ microwatts per cm}^2 \text{ per } 0.01\mu \text{ zone of spectrum} \qquad (4)$$

This equation is plotted in Figure 1 for a temperature of 1000 K. The radiating surface is, of course, a perfect radiator and a perfect distributor,

that is, the distribution in space follows the cosine law. The analog in illumination would be lumens per sq cm from a surface that has equal brightness in all directions.

The intensity of radiation in a direction normal to the surface is

$$\frac{dJ\lambda}{d\omega} = \frac{1.1906 \times 10^{8}\,\lambda^{-5}}{e^{\frac{14384.8}{\lambda T}} - 1} \quad \begin{matrix}\text{microwatts per cm}^2\text{ per}\\ \text{steradian per 0.01}\mu\text{ zone}\\ \text{of spectrum}\end{matrix} \qquad (5)$$

This unit corresponds to the candle in illumination, and is found by dividing Equation (4) by π. The intensity at an angle θ varies as the cosine of θ, and the rules for computing irradiation from Equation (5) are identical to those for computing illumination.

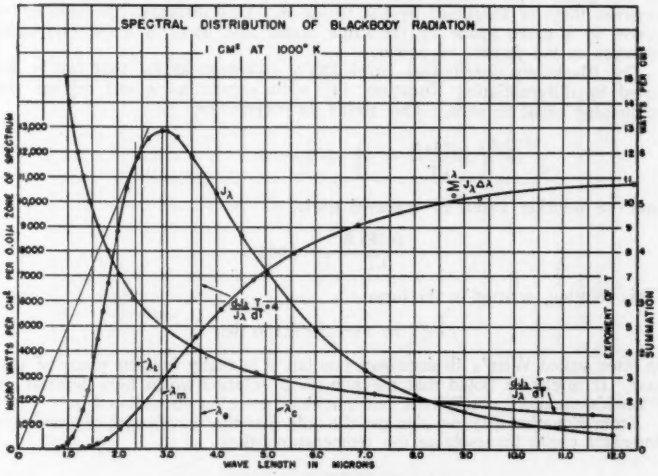

Fig. 1. Spectral distribution of Blackbody radiation

The $J\lambda$ curve shows the distribution of power in the spectrum for one square centimeter of perfect radiating surface at a temperature of 1000 K. The summation curve gives the total spectral power beginning at short wavelengths and summing up to the wavelengths given at the bottom of the graph. The $\frac{dJ_\lambda}{J_\lambda}\frac{T}{dT}$ curve shows how the power changes with small changes of temperature at each wavelength. The ordinates λ_s, λ_m, λ_e, and λ_c are explained in the text.

In a complete cavity of uniform temperature there is radiation passing through a given point in all possible directions; all points being alike since all are enclosed by the same radiating walls. In illumination a disk radiating I candles along the normal to one face gives πI lumens, while a sphere of equal diameter and brightness gives 4πI lumens, or 4 times as much. If the sphere is hollow and the radiation is inward there is the same amplifying factor of 4. Since the radiant power is passing across the cavity with the speed of light, the power within a cubic centimeter at any moment is the total power divided by 2.99776×10^{10}, the conversion factor in changing

from a flat surface to a hollow sphere therefore being 4/c. From Equation (4) we get the power within a cubic centimeter

$$\Psi\lambda = \frac{4.9907 \times 10^{-2}\,\lambda^{-5}}{e^{\frac{14384.8}{\lambda T}} - 1} \begin{array}{l}\text{microwatts per cm}^3 \text{ per} \\ 0.01\mu \text{ zone of spectrum}\end{array} \qquad (6)$$

If the enclosure is incomplete, the power in a cubic centimeter is proportional to the solid angle of the enclosing wall measured from the center of the space in question.

A piece of nonabsorbing material (such as glass for certain wavelengths) having a refractive index n when placed in this enclosure will have a power density at interior points of $n\Psi\lambda$. This concentration of power can be best illustrated by considering what happens when plane waves fall on the surface of flat glass. The waves that enter are reduced in speed and the distance between them is shortened by the factor n. This increases the number of waves in a given space by the same factor and there is a corresponding increase in the density of power.

The Blackbody distribution curve has a maximum at λ_m that can be located by differentiating Equation (4) with respect to λ and setting the numerator equal to zero. This yields the expression

$$e^{\frac{14384.8}{\lambda T}}\left(\frac{14384.8}{\lambda T} - 5\right) + 5 = 0 \qquad (7)$$

and one solution, found by repeated trials, is

$$\frac{14384.8}{\lambda T} = 4.96511 \qquad (8)$$

This solution, written in the form

$$\lambda_m T = 2897.2 \text{ micron deg} \qquad (9)$$

is often called Wien's displacement law but it is really but one phase of that law. It might be noted that the numerical solution given here depends on Planck's equation, not Wien's, but that does not alter its authorship.

From Equation (9) we also get the rule that the wavelength of maximum intensity varies inversely as the temperature, thus

$$\lambda_m = 2897.2/T \text{ microns} \qquad (10)$$

Since λ_m and T have a fixed relation either of these factors in Equation (4) can be eliminated. Substituting T for λ_m we get

$$J\lambda_m = 1.2874 \times 10^{-11}\, T^5 \begin{array}{l}\text{microwatts per cm}^3 \text{ per} \\ 0.01\mu \text{ zone of spectrum}\end{array} \qquad (11)$$

or, the power at the peak of the curve varies as the fifth power of the temperature.

All Blackbody radiation curves have the same form, as can be demonstrated as follows: Select any wavelength λ_m and the temperature T that will satisfy Equation (9). We can then write the equation in the form

$$J_{\lambda_m} = \frac{c_1 \lambda_m^{-5}}{e^{4.96511} - 1} \qquad (12)$$

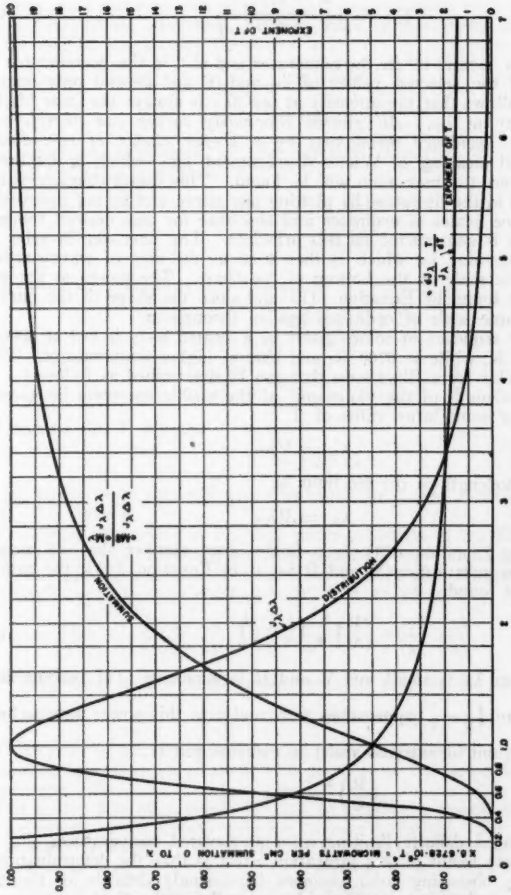

Fig. 2. Radiation characteristics of a Blackbody

This chart may be used to compute the distribution, summation, and rate of change of power at any temperature by using the factors given at the left of the chart. The wavelength scale is found by computing λ_m, from $\lambda_m = \frac{2897.2}{T}$ microns, for the desired temperature. The scale of exponents (on the right) does not change.

since the exponent of e is a constant. Keeping T constant, but selecting some other wavelength $\lambda = n\lambda_m$

then
$$J_{n\lambda} = \frac{n^{-5} c_1 \lambda_m^{-5}}{e^{1/n} e^{4.96511} - 1} \tag{13}$$

Here the new factors n^{-5} in the numerator and $e^{1/n}$ in the denominator are independent of the selected values of λ_m and T and depend only upon n. From this it follows that the intensity at say $3\lambda_m$ is always the same fraction of the intensity at λ_m. *All plotted Blackbody curves can therefore be brought into coincidence throughout by a proper choice of co-ordinates.* This is the full meaning of Wien's displacement law, which is not limited to showing where the maximum will be found. This useful characteristic is often employed in the literature by plotting one curve and giving instructions for changing the scales of ordinates and abscissae for any desired temperature. Figure 2 is constructed on this principle. The first step in using the curve is to determine λ_m which is then used as the unit of wavelength as described on the scale at the bottom of the chart. The power at the peak of the curve is found by Equation (11) and since the shape of the curve is constant the same scale of ordinates applies throughout.

The familiar sequence of colors given by a heated body is red at 1000 K, yellow at 1500 K, white at 6700 K, and blue at higher temperatures. There is a limiting color for a Blackbody that can be determined as follows:

Let the wavelength of the violet end of the visible spectrum be given in terms of λ_m for some large value of T

$$\lambda_V = V\lambda_m$$

and let the wavelength of the red limit be

$$\lambda_R = R\lambda_m$$

Since $e^{4.96511}$ in Equation (13) is a fairly large number the -1 may be dropped. Then substituting V and R for n in Equation (13), the ratio of violet to red is found.

$$\frac{J_V}{J_R} = \left(\frac{R}{V}\right)^5 e^{\left(\frac{1}{R} - \frac{1}{V}\right)} \tag{14}$$

When T is large λ_m is small, and V and R in Equation (14) become large. Toward the limit $\left(\frac{1}{R} - \frac{1}{V}\right)$ approaches zero, and e to this power approaches 1. Therefore the limit of extreme violet to extreme red is

$$\left(\frac{R}{V}\right)^5 = 16.4 \tag{15}$$

thus establishing a definite limiting color at elevated temperatures.

One immediate result of this saturation effect is that the determination of temperature by observing color becomes increasingly difficult as the temperature rises, and once a radiator becomes definitely blue in integrated color the accuracy of temperature determinations is inherently low.

In optical pyrometry it is occasionally desirable to calibrate a lamp at a temperature either higher or lower than the range of the standard lamp. A recent example was the request for a pyrometer calibration at 1073 K. The lowest calibration point on the primary standard used for this work was 1261 K. A rotating sectored disk with a ratio of 1/100 is available for

cases like this, and Wien's equations were used to compute an extension of the calibration of the primary standard.

An optical pyrometer usually is provided with a dense red glass in the eyepiece, thus confining the effective luminous radiation to a narrow zone at the red end of the spectrum, with a center of luminosity at about 0.665μ. At the desired temperature the power is

$$J_{0.665} = \frac{c_1\, 0.665^{-5}}{e^{\frac{14384.8}{0.665 \times 1073}}}$$

The matching brightness of the primary standard, which was viewed through the 1/100 disk, was

$$100 J_{0.665} = \frac{c_1\, 0.665^{-5}}{e^{\frac{14384.8}{0.665 T}}}$$

Dividing the second of these equations by the first

$$100 = e^{\frac{14384.8}{0.665}\left(\frac{1}{1073} - \frac{1}{T}\right)}$$

$$\frac{0.665}{14384.8} \log_e 100 = \frac{1}{1073} - \frac{1}{T}$$

and solving for T, we get

$$T = 1391 \text{ K}$$

as the temperature that will give 100 times the power at 0.665 that is given when T is 1073 K.

The center of gravity of the area under a section of the Blackbody curve as determined experimentally has been used by Foote (2) to compute the constant c_2. He showed that the center of gravity of a complete curve from wavelength zero to wavelength infinity is at wavelength

$$\lambda_c = \frac{c_2\, [1 + (1/2)^3 + (1/3)^3 + \ldots\ldots]\, \Gamma\ (3)}{T\, [1 + (1/2)^4 + (1/3)^4 + \ldots\ldots]\, \Gamma\ (4)} \qquad (16)$$

This expression used with the present value of c_2 gives the general relation

$$T\lambda_c = 5325.6 \text{ micron deg} \qquad (17)$$

This center of gravity is not the mid point in a summation of power, but is somewhat beyond it where about 67.5 per cent of the power lies to the short wavelength side.

The writer was once given the task of making a rough determination of the emissivity of the human skin for its own radiation. The body maintains an absolute temperature of about 310 K, and Equation (24), to be given later, tells us that 25 per cent of the radiation from a perfect radiator is of wavelength shorter than 9.3μ while Equation (17) shows that 67.5 per cent is in wavelengths shorter than 17μ. The skin, therefore, presumably does most of its radiation in the region from about 6 to 20 microns, which is difficult to explore, particularly when dealing with a low-temperature radiator. The solution to the problem, however, turned out to be rather ab-

2 "A New Relation Derived from Planck's Law," by Paul D. Foote, *Bull. Bur. Std.*, 12, 479 (1915-16).

surdly simple. A thermopile was placed in a box provided with numerous diaphragms so arranged that the only radiation from the outside that could reach the thermopile had to enter through a small hole in the end of the box. The palm of the hand was held over the hole so that the thermopile could "look" at the skin. Then the hand was so nearly closed as to leave only a small opening over the hole. The interior of the fist thus formed a crude cavity that served as a Blackbody. The ratio of the two galvanometer deflections was over 0.90 and from this we can conclude that for its own radiation the skin is nearly black.

Blackbody Summation Curves.

The total power emitted by 1 sq cm of perfect radiator can be found by integrating Equation (4) between wavelength limits 0 and ∞. It simplifies the integration to make the substitution

$$\frac{c_2}{\lambda T} = x$$

and then the integral becomes

$$J = \frac{c_1 T^4}{c_2^4} \int_{\infty}^{x} \frac{x^3 dx}{e^x - 1} \tag{18}$$

When integrated by parts this gives the infinite series

$$J = \frac{c_1 T^4}{c_2^4} \left[(x^3 + 3x^2 + 6x + 6)\ e^{-x} + 1/2 \left(x^3 + \frac{3}{2} x^2 + \frac{6}{4} x + \frac{6}{8} \right) e^{-2x} \right.$$

$$\left. + \cdots \frac{1}{n} \left(x^3 + \frac{3}{n} x^2 + \frac{6}{n^2} x + \frac{6}{n^3} \right) e^{-nx} + \cdots \right]_{\infty}^{x} \tag{19}$$

If the integration is carried from $x = \infty$ to $x = O$, the total radiation is found to be

$$J = \frac{c_1 T^4}{c_2^4} \left[1 + (1/2)^4 + (1/3)^4 + \cdots \right] \tag{20}$$

$$= \frac{c_1 T^4}{c_2^4} \cdot \frac{\pi^4}{90}$$

$$= 5.6728 \times 10^{-8}\ T^4 \text{ microwatts per cm}^2$$

where the coefficient is one form of the Stefan-Boltzmann constant σ.

Since all Blackbody radiation curves have the same form, it follows that an integration under all curves to find total power will lead to identical summation curves. Figure 2 gives a summation curve that may be used for any temperature by giving values to the abscissae and ordinates as indicated in the chart.

If a body at temperature T_2 is placed in surroundings that have a uniform temperature T_1 the net rate at which the body will absorb power is

$$J = \sigma\ (T_1^4 - T_2^4)\ e \text{ microwatts per cm}^2 \tag{21}$$

where e is the emissivity of the body. This equation assumes that the absorbing body has a smooth continuous surface, but if the surface is broken by cavities so that it is spongelike the emissivity rises toward unity and the

rate of exchange rises to that of two Blackbodies. The emissivity of the containing walls does not enter into the situation, for, as previously demonstrated. the wall radiation is independent of the nature of the walls.

In the literature of thermodynamics there is frequently encountered the statement that for small differences of temperature the rate of exchange between two flat surfaces at temperatures T_1 and T_2 is proportional to the difference $T_1 - T_2$. There is seldom or never a definition of what is meant by "small."

The correct expression for exchange of power is

$$J = \sigma (T_1^4 - T_2^4)\ e_1 e_2 = \sigma (T_1 - T_2)(T_1 + T_2)(T_1^2 + T_2^2)\ e_1 e_2 \quad (22)$$

in which the first factor is the simple difference of temperatures. The other factors, however, also change at a lower rate when either temperature is changed. When T_1 and T_2 are sufficiently different this rule of thumb can be in serious error. It might be pointed out that the first-power expression can also be used for any phenomena, provided the steps in variation are small enough, but no one ever seems to apply this rather crude method to anything except temperature difference.

Wien's displacement law permits the derivation of the T^4 law for the total radiation without having to resort to the calculus. Since the peak (and all other points) of the curve varies as T^5 and the wavelength scale varies as T^{-1}, the area under the curve varies as the product

$$T^5 \cdot T^{-1} = T^4 \quad (23)$$

just as has been found by the calculus.

When the integration of power is carried from $\lambda = 0$ to $\lambda = \lambda_m$ the result is

$$\int_0^{\lambda_m} J_\lambda\ d\lambda = 0.250056J \quad (24)$$

which is a convenient rule to remember when estimating the distribution of spectral power. *One quarter, very closely, is on the short wavelength side of the maximum, and three quarters on the long wavelength side.*

The rate of change of emitted power with change in temperature is of interest. The exponential rate is

$$\frac{dJ_\lambda}{J_\lambda} \cdot \frac{T}{dT} = \frac{\frac{c_2}{\lambda T} e^{\frac{c_2}{\lambda T}}}{e^{\frac{c_2}{\lambda T}} - 1} \quad (25)$$

When this is solved for the maximum point on the distribution curve at

$$\lambda_m T = 2897.2$$

the result is

$$\frac{dJ}{J} = 5\frac{dT}{T} \quad (26)$$

$$\int \frac{dJ}{J} = 5\int \frac{dT}{T}$$

$$J_m = kT^5$$

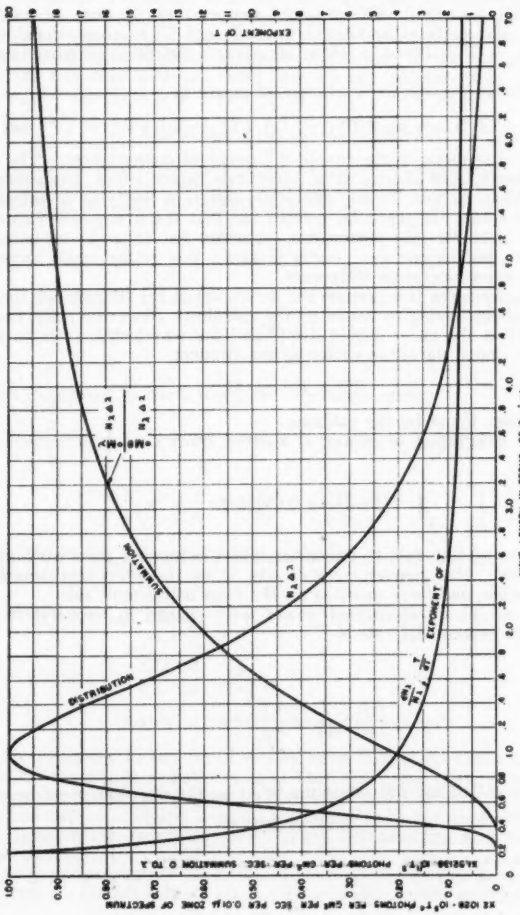
EXPONENT OF T
WAVE LENGTH IN TERMS OF $\lambda_m T = 1$
SUMMATION
DISTRIBUTION
EXPONENT OF T
$\frac{\lambda_1 \Phi \lambda_1}{\lambda_2 \Phi \lambda_2}$
$\lambda_2 \Phi \lambda_2$
$\lambda_1 \Phi \lambda_1$
$\frac{\lambda_1 \Phi \lambda_1}{\lambda_2 \Phi \lambda_2}

which agrees with Equation (20).

Worthing (3) has pointed out that when

$$\lambda T = 3668.9 \text{ micron deg} \qquad (27)$$

the rate of change is as T^4, that is, at this point the emission changes at the average rate for the entire spectrum.

The curve in Figure 2 shows that at wavelengths that are great as compared with λ_m the exponential rate approaches T^3 while at wavelengths small as compared with λ_m the exponential rate may be very high. These rates may have important effects in some experiments. For example, a pyrometer lamp operating at 2177 K will have λ_m at twice 0.665μ (the active wavelength) or 1.330μ. From Figure 2 the rate of change of brightness at 0.5 λ_m is approximately as T^{10}, hence a change of one per cent in temperature will make 10 per cent change in brightness. This requires an accurate control of current and therefore the ammeter must be both accurate and constant it the calibration is to be relied upon.

If a tangent is drawn on the short wavelength side of the maximum of the distribution curve in such a direction as to pass through the origin, the point of tangency will be found to give

$$J\lambda = kT^6$$

There are thus at least four unique points on the distribution curve that vary as an integral power of T. They are this tangency point (T^6), the maximum point (T^5), the maximum efficiency point (T^4), and the limiting tangent at infinite wavelength (T^3).

The power within 1 cm^3 of space in a radiating cavity can be found by integrating Equation (6) which gave the power for a single zone in the spectrum. This gives

$$\Psi = aT^4$$

where a is the radiation density constant previously mentioned, and its numerical value is

$$\Psi = 7.5694 \times 10^{-16} T^4 \text{ microwatts per cm}^3 \qquad (28)$$

in a cavity of temperature T and any emissivity.

Brightness and Color Temperatures.

The Blackbody is the standard of brightness in pyrometry and also the standard of color in photometry. A lamp is said to have a "Brightness temperature" of say 2700 K when it is as bright, in candles per sq cm, as an ideal radiator at that temperature. Tungsten at an actual temperature of 2700 K is as bright as a Blackbody at only 2437 K, a difference of 263 K. Its "Color temperature" is that of a Blackbody at 2770 K, a difference of 70 K in the opposite direction. This arises from the fact that the emissivity of tungsten is much less than unity at 0.665μ where the pyrometer measures and the brightness is therefore less. In color measurements the entire visible spectrum is used and the emissivity in the blue is higher than in the red. There is thus a higher ratio of blue to red and the color is that of a Blackbody at higher temperature. There is thus a spread of 333 K in the apparent temperatures as judged first by brightness and then by color, and this

3 "Radiation Laws Describing the Emission of Photons by Blackbodies," by A. G. Worthing, *Jour. Opt. Soc.* 29, 97 (1939).

spread increases as the true temperature rises until it amounts to about 450 K at the highest operating temperature of a long-life tungsten lamp.

Pressure of Radiation.

Drude, in his famous *Theoretical Optics* (1900), pointed out that, according to theory, radiation should exert pressure on a receiving surface; but, he unwisely added, "it is so small that it cannot be detected experimentally." His chastisement was prompt. Two experiments, one in the United States (4) and one in Europe showed in the following year that not only could it be detected but it could be measured with good accuracy in the laboratory.

Several centuries ago, it was observed and recorded that a comet's tail switches around so as to always point away from the sun, as if it were repelled by the sun's radiation. Later computation showed that this was indeed the correct explanation. Sometimes the tail splits into two or more parts making different angles with a radius from the sun. Since a small molecule has a greater area in proportion to its mass than a large one, it will be repelled more strongly and will move more nearly in line with the radius. A comparison of the angular deviations of the parts of the tail gives data that used in connection with the theory of the pressure of radiation permit an analysis of the tenuous gas in the tail of a comet.

The pressure of radiation when it falls in a parallel stream in a normal direction upon a perfectly black surface is numerically ten times the value of $\Psi\lambda$ as given by Equation (6).

$$P\lambda = \frac{4.9907 \times 10^{-1}\ \lambda^{-5}}{e^{\frac{14384.8}{\lambda T}} - 1} \text{ dynes per cm}^2 \text{ per } 0.01\mu \text{ zone of spectrum} \qquad (29)$$

and from the complete spectrum (from Equation (20))

$$P = 5.678 \times 10^{-5}\ T^4 \text{ dynes per cm}^2 \qquad (30)$$

There is occasionally seen in opticians' display windows a small turbine that spins when sunshine falls on it. When the turbine is still, it is seen that one side of each vane is bright metal while the opposite side is coated with soot. The radiation falling on the coated side is absorbed and exerts a pressure P, while that falling on the polished side is (theoretically) completely reflected and exerts a pressure 2P. This would cause the bright side to move away from the light, which is the observed direction of rotation when the vanes are in a high vacuum. But the required vacuum is unattainable in the optician's device. Therefore, he leaves an optimum amount of gas within the bulb. The black side of the vanes becomes warmer than the bright side by absorbing sunshine, and gas particles coming in contact with the soot are heated and repelled more than most of those touching the bright side. This repulsion drives the turbine so that the black side turns away from the light. The gas pressure is greater than the radiation pressure, and this explains why the experiment could not be done until good vacuum were attainable.

To find the pressure on the walls of a cavity containing Ψ microwatts per cm^3, let us assume that the cavity is in the form of a cube 1 cm on a side and having perfectly reflecting mirror walls. Divide the radiation into six equal parallel beams, each falling in a normal direction on one of the sides.

4 Nicols and Hull, *Science*, 1901.

With perfect reflectance the pressure on each side will be

$$P_d = 2\left(\frac{P}{6}\right) = \frac{P}{3}$$

Numerically we have for the average pressure

$$P_d = 1.8909 \times 10^{-8}\ T^4 \text{ dynes per cm}^2 \qquad (31)$$

and this constant is true for diffused radiation within any form of cavity.

Blackbody as a Quanta Generator.

According to Planck's quantum theory, radiation is emitted in bundles of definite sizes and not as a continuous stream. These bundles are often called photons (phot = light) even when they are in non-visible parts of the spectrum. The size of a photon varies inversely as the wavelength, hence a photon at 1μ has twice the energy of a photon at 2μ. The Blackbody photon distribution equation has the same denominator as the radiation equation but the numerator contains λ^{-4} in place of λ^{-5} and the numerical constant is different.

Following Worthing's notation

$$N\lambda = \frac{1.88355 \times 10^{21}\ \lambda^{-4}}{e^{\frac{14384.8}{\lambda T}} - 1} \text{ photons per cm}^2 \text{ per sec per } 0.01\mu \text{ zone of spectrum} \qquad (32)$$

The spectral distribution of photons is given in Figure 3 for a temperature of 1000 K. The resemblance to the radiation distribution is so great that the two can be distinguished only by an inspection of details. The scale of ordinates is vastly different (0.5×10^{13} to 1 at $\lambda = 1$), and the maximum is shifted toward longer wavelengths.

A solution for the maximum gives

$$e^{\frac{c_2}{\lambda T}}\left(\frac{c_2}{\lambda T} - 4\right) = -4 \qquad (33)$$

one solution of this being

$$\frac{c_2}{\lambda T} = 3.92069 \qquad (34)$$

from which we get the wavelength λ_m of maximum number of photons

$$\lambda_m' T = 3668.9 \text{ micron deg} \qquad (35)$$

The number of photons at the peak is

$$N\lambda_m' = 2.1028 \times 10^5\ T^4 \text{ photons per sec per cm}^2 \text{ per } 0.01\mu \text{ zone of spectrum} \qquad (36)$$

An integration under the emission distribution curve gives

$$\sigma' T^3 = -\frac{2\pi K^3}{c\,h^3}\left[(X^2 + 2X + 2)\,e^{-x} + 1/2\left(X^2 + \frac{2X}{2} + \frac{2}{4}\right)e^{-2X} + 1/3\left(X^2 + \frac{2X}{3} + \frac{2}{9}\right)e^{-3X} + \ldots 1/n\left(X^2 + \frac{2X}{n} + \frac{2}{n^2}\right)e^{-nX}\right]_{\infty}^{0} T^3 \qquad (37)$$

where $$X = \frac{c_2}{\lambda T}$$

A summation curve is given in Figure 3. When the integration is carried from 0 to ∞

$$N = \frac{4\pi K^3}{c^3 h^3} [1 + (1/2)^3 + (1/3)^3 + \dots] T^3 \qquad (38)$$

$$= 1.52138 \times 10^{11} T^3 \text{ photons per sec per cm}^2$$

This expression for total photons corresponds to the Stefan-Boltzmann equation for total radiation, but it is important to notice that the total emission of photons varies as T^3, not as T^4. The rate of change with respect to T at any wavelength is the same for radiation and photons since there is a constant ratio between the two at any λ.

The efficiency of production of photons, found by differentiating the quotient of Equation (32) divided by Equation (38) is a maximum when

$$\lambda_m' T = 3668.9 \text{ micron deg} \qquad (39)$$

that is, at the same wavelength at which the maximum production occurs.

The temperature exponent at various parts of the spectrum, as found from the solution of

$$\frac{dN}{N} \frac{T}{dT} = \frac{c_2}{\lambda T} e^{\frac{c_2}{\lambda T}} \left[e^{\frac{c_2}{\lambda T}} - 1 \right]^{-1} \qquad (40)$$

is identical with the rates found for radiation at the same wavelength, but there is a displacement between the two curves when referring to the maximum, which is now found to vary as T^4. The area under the curve varies as

$$T^4 \cdot T^{-1} = T^3 \qquad (41)$$

This change from T^4 is a result of the change of size of the photon with wavelength. As the temperature rises the center of gravity of the emission moves toward shorter wavelengths and there are fewer photons for the same amount of power.

Using Foot's formula, we find the center of gravity under the photon curve to be at wavelength.

$$\lambda_c = \frac{c_2 [1 + (1/2)^3 + (1/3)^3 + \dots] \Gamma(2)}{T [1 + (1/2)^3 + (1/3)^3 + \dots] \Gamma(3)}$$

$$= \frac{9842}{T} \text{ microns} \qquad (42)$$

Efficiency of Radiation.

In engineering design the efficiency of production is often "the essence of the contract," and even if it is not of prime importance it is seldom out of the thoughts of the designer. As a rule the physicist is not greatly concerned with efficiencies, and as a result the literature of physics seldom takes up the question of finding the conditions that will yield the greatest relative return. The equations that are to follow are based on the engineering point of view. Each equation touches some phase of the problem of getting the greatest return in radiation of some desired wavelength for a given input of wattage.

If the radiation in any zone of the spectrum is divided by the total radiation of the complete spectrum, the quotient is a measure of the efficiency of producing those particular wavelengths. This type of equation allows the determination of the temperature that will give the most efficient conditions and it also permits an easy engineering comparison of outputs at different temperatures. When the distribution curves are plotted in the usual way, showing the output from 1 cm², the total outputs change at such a high rate that curves for say 1000 K and 2000 K can hardly be visually compared. The peak on one is 32 times as high as on the other, and it is difficult to draw both curves to one scale and have both in readable form. When both are plotted so that they represent equal wattage then they can be plotted in legible form, since the maxima are now in the order of 1 to 2.

On the equal wattage basis we have

$$\frac{J\lambda}{J} = \frac{6.593 \times 10^{19}\ \lambda^{-5}}{\left(e^{\frac{14384.8}{\lambda T}} - 1\right) T^4} \quad \begin{matrix}\text{microwatts per } 0.01\mu \text{ zone} \\ \text{of spectrum per watt}\end{matrix} \qquad (43)$$

This distribution is plotted in Figure 4 for temperatures from 2000 K to 3400 K, this being about the range of tungsten-lamp temperatures. The area under all curves, when extended to infinite wavelength, would be found to be 10^6 microwatts, proper allowance being made for the selection of special zones 0.01μ wide. The curves read directly in efficiency $E\lambda$ of the standard zone when the ordinate is divided by 10^6, and for wider zones a summation can readily be made.

$$E_{\lambda_1-\lambda_2} = \sum_{\lambda_1}^{\lambda_2} J\lambda \cdot 10^{-6} \triangle\lambda \qquad (44)$$

Since the curves in Figure 4 are for equal wattages, the highest ordinate at any wavelength indicates the temperature that gives the best efficiency at that point. The curves overlap so thickly at the maximum point that they are not easily read, so arrows have been placed over the curves to indicate where each temperature has its maximum efficiency.

When Equation (43) is solved for a maximum we get

$$\lambda_m T = 3668.9 \text{ micron deg} \qquad (45)$$

This hyperbola forms the envelope—over the curves in Figure 4—that passes through the points of maximum efficiency. This is the fourth time that this identical constant, 3668.9, has been found and we might here summarize its different meanings.

When the product of λT is equal to 3668.9 micron degrees then

(1) The rate of change of power at λ with temperature is as T^4, that is, at the average rate for the complete spectrum.

(2) the production of photons at λ is a maximum for the given temperature.

(3) the efficiency of production of photons at λ is at a maximum for temperature T, and

(4) the efficiency of production of radiation at λ is at a maximum.

Equation (45) will probably be useful in a number of ways, as for example, when dealing with Blackbody radiation that has specific effects, such as producing light, activating chlorophyl, producing vitamin D, or heating by deep therapy. The peak of the luminosity curve is at 0.556μ, and if Wien's displacement equation is used to find the temperature that will give

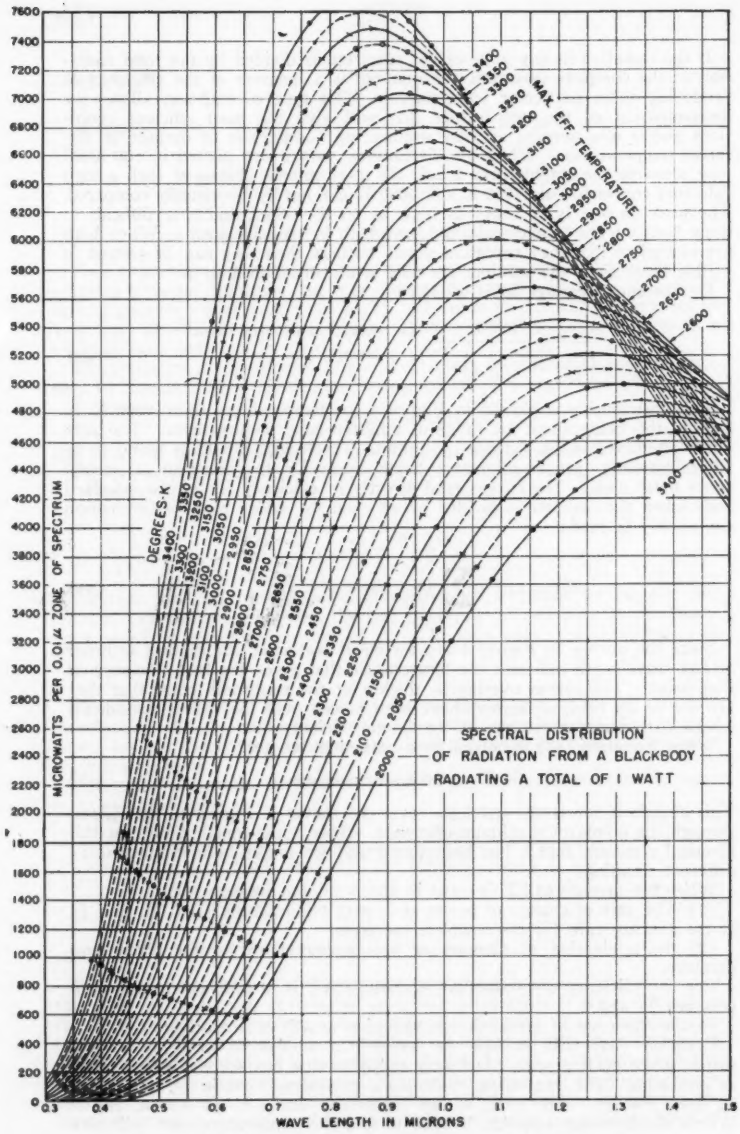
MICROWATTS PER 0.01 μ ZONE OF SPECTRUM
WAVE LENGTH IN MICRONS
DEGREES-K
MAX EFF TEMPERATURE
SPECTRAL DISTRIBUTION
OF RADIATION FROM A BLACKBODY
RADIATING A TOTAL OF 1 WATT

Fig. 4. Spectral distribution of radiation from a Blackbody radiating a total of one watt

These distribution curves are each for a radiator that is giving a total radiation of one watt. The curve that is highest at any ordinate, such as at 1.1 μ, gives the highest efficiency of production for that wavelength, and the optimum temperature is indicated by the scale near the top of the chart.

Fig. 5. Summation of radiation from a Blackbody radiating a total of one watt

These summation curves are derived from the curves in Fig. 4, and they may be used to find the fraction of the total power that is radiated in any zone of the spectrum.

a maximum at this wavelength the indicated temperature is 5210K. However, if we use the efficiency equation to determine the optimum temperature for the production of light we get T = 6630 K. Forsythe and Adams (5) have solved this problem by a summation over the visible spectrum and they get "about 6700 K." The efficiency equation therefore gives a better approximation.

Referring again to the family of curves, the peak of the 2500 K curve for example is near 1.15μ and has a value of 5670 microwatts. Equal wattage at 3100 K gives 6400 microwatts, an increase of over 11 per cent.

The temperature that gives maximum efficiency at λ_0 is

$$T = 3668.9/\lambda_0 \text{ deg} \qquad (46)$$

which is 26.6 per cent higher than that giving Wien's maximum at the same wavelength.

The power in a 0.01μ zone at wavelength λ_0 and temperature T is, for a total output of 1 watt,

$$J\lambda_0 = 2.000\ T \text{ microwatts} \qquad (47)$$

and the efficiency here varies directly as the temperature.

In Figure 5 the curves give the summation of power from $\lambda = 0$ to $\lambda = 3.8\mu$ for temperatures from 2000 K to 3400 K. The curves all reach unity height when extended to the limit of wavelength and the various ordinates therefore give the fraction of the total output up to the wavelength at the bottom of the chart. Multiplying these ordinates by the total emission, Equation (20), will give the total power up to the ordinates; and by computing at two ordinates, the power in the zone included between them can be found.

The zone width has been taken as 0.01μ in all the equations. If high temperatures, say about 1,000,000 K, are considered the bulk of the radiation will be confined within narrow wavelength limits, and the standard width of zone will be far too wide for accurate results. For example, at 1,000,000 K one quarter of the power will be at wavelengths less than 0.002897μ, and the application of Equation (47) to find the power at λ_0 leads to the absurd value

$$J\lambda_0 = 2{,}000{,}000 \text{ microwatts}$$

which is impossible since the total output is

$$J = 1{,}000{,}000 \text{ microwatts}$$

The difficulty here can be solved by taking spectrum zones that are narrow enough to permit a correct analysis of the spectrum. At 1,000,000 K, the zone width that has been used might be divided by 100, and the c_1 constants would accordingly be divided by the same number.

IMPORTANCE OF GOVERNING ARRANGEMENTS FOR MARINE INSTALLATIONS.

The investigation described in this paper by G. H. Forsyth illustrates the importance of additional torsional loading between the engine and the propeller under conditions of engine racing in rough weather. The effect of

5 "The Tungsten Filament Incandescent Lamp," by Forsythe and Adams, *Denison Univ. Bull., Journal of the Scientific Laboratories, 32,* 70 (1937).

fitting governors and the positioning of the major one-node criticals are discussed with reference to rough weather conditions. Mr. Forsyth's paper was published in the July, 1943, Transactions of The Institute of Marine Engineers.

The author's attention has been drawn on many occasions to cases of shaft failures resulting from torsional vibration both in the engine crankshaft and in the screwshaft. In the case of failure in the latter, fractures have generally exhibited the well-known characteristics of corrosion-fatigue. In other cases, however, failures, while indicating the presence of fatigue, have not shown corrosion-fatigue markings. On making investigations into the torsional vibration characteristics, it has in many instances been difficult to account for failures of the latter type. There have been sufficient numbers of failures in vessels, where the 1-node major critical was, say, 10-15 per cent above the normal running speed, to indicate that a margin of some 30 per cent was necessary to ensure freedom from shaft failure. The importance of this, however, was not fully realized until recent investigations were carried out under conditions of engine racing in rough weather.

Before proceeding further with the investigations to be described, the author considers it well to draw attention to a paper entitled *"The Relation of Fatigue to Modern Engine Design", of which the following is an extract. Figures 15 and 16 of that paper are included as Figures 1 and 2 of the present paper.

"Figures 15 and 16 are photographs of damage caused at the same time to a ship's crankshaft and its propeller-shaft. No fouling of the propeller is reported, but the combined quadruple-expansion and turbine engines raced violently under full head of steam. Figure 15 shows the crank-web having slid on its journal to an extent indicated by the dowel and dowel hole. The shrinkage was good as revealed by wholesale seizing between the journal and bore of the web. Enormous forces must have been applied, for a few beats of the propeller, as its blades entered the water in a heavy seaway. The tail-shaft exhibits a very unusual type of fracture in that it looks very like a fatigue fracture in texture, but it lacks (a) point of initiation, (b) splinters, (c) age-rings or (d) final granular ruptured area. The whole fracture is made up of many smaller ones located, and travelling, in a haphazard direction. It would seem that a few very heavy blows have brought about step-by-step impact cracking. On examination the material was found to be excellent:

Carbon	0.29 per cent
Tensile strength	29.6 tons
Elongation in 3 inches	35.0 per cent
Bends 1 inch × ¾ inch	180 degrees flat uncracked

This example is not a true case of fatigue cracking, but it is quite interesting in itself. The object of its inclusion is to illustrate by an extreme case the kind of conditions a marine engine has to face in service on occasion".

The type of brittle fracture discussed, which is not true fatigue cracking, is particularly interesting in view of the cause of failure to be described.

The torsional load necessary to create the failure shown in Figure 1 is very high indeed. In this connection it may be stated that the factor of safety of a shrink fit is in the neighborhood of four. Whether or not tor-

* Trans. N. E. C. Institution of Engineers and Shipbuilders, Vol. LI, 1935.

sional strength is added or subtracted by addition of a dowel is a debatable point, on which much has been written. It is clear, from Figure 1, however, that dowel shear area in itself does not produce the necessary strength, since in practice it is found that the shrink fails due to the web lifting clear of the journal, exposing corners at the journal and web where flow of metal takes place quite independent of shear of the dowel itself. Taking the probable factor of safety as four, the torsional load to produce such a failure would represent a stress in the intermediate shafting in the neighborhood of 20,000 pounds per square inch.

It is difficult to account for such high torques being developed, even taking into consideration the impact torque from the propeller upon being reimmersed after racing. * Investigations previously carried out using a stroboscopic torsion meter indicated that such impact torques would be in the neighborhood of twice the mean transmission torque.

The author's attention was recently drawn to the case of a vessel fitted with steam reciprocating triple-expansion engines, in which six crankshaft failures had occurred during the period April, 1938 to November, 1942. In each case the failure occurred at the L. P. crank, the after web of this crank moving on the journal in a similar fashion to that shown in Figure 1, which has been found upon enquiry to be that of a failure at the L. P. crank. These cranks were constructed by different well-known engine builders whose experience in crankshaft construction was beyond doubt. Various sizes of dowels were fitted from 1¾-inch diameter to 2½-inch diameter by about 4 inches long. It was at first considered that engine seatings might be the cause of the trouble, and since there was a complaint that movement did occur at the L. P. crank, very special care was taken, after the sixth crankshaft failure, to make the thrust seating integral with the engine seating, and to add longitudinal stiffness in way of the L. P. crank and extending forward of that crank-pit. Although such stiffening had been considered necessary in view of the movements which had been complained of, it was not thought that the real cause of failure, i.e., very high torques, had been ascertained. Furthermore, it was considered that lack of alignment would have set up fatigue bending of the crankshaft which would have resulted, if severe enough, in fatigue cracks rather than a torsional movement of the journal and the web.

In view of the foregoing, it was decided to investigate fully the torsional vibration characteristics of the engine and shafting system, and to take torsiograph records to confirm the calculations made.

Appendix I gives the torsional vibration calculations made before the trial and it will be noted that the natural 1-node frequency between the engine and propeller has been calculated at 324 Vpm.; with service Rpm. 65-70 it was necessary to calculate the stresses arising due to the 5th and 6th orders. The vibration stresses due to these orders amounted to 142 pounds per square inch and 1350 pounds per square inch respectively, these values being derived as shown in Appendix II. In spite of this low estimate of stress, it was still considered necessary to take Geiger records because of the number of L. P. crank failures which had occurred.

Trials at Sea.

It should be stated at this point that the vessel had the following particulars as given in Lloyd's Register, viz.:

* Ref. "Strength of Marine Engine Crank Shafts", by S. F. Dorey, D.Sc., Trans. N. E. C. Institution of Engineers and Shipbuilders, 1939.

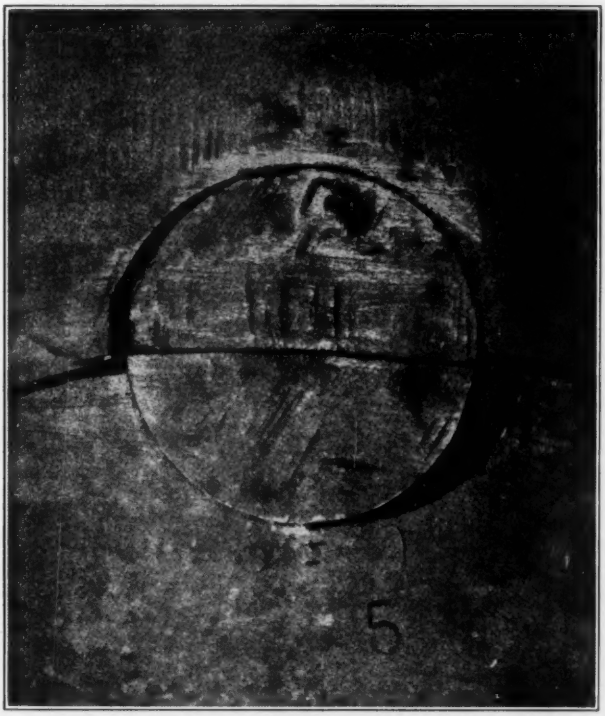

FIGURE 1.—SHIP'S CRANK-WEB MOVED ON JOURNAL BY IMPACT.

FIGURE 2.—TAIL SHAFT CONNECTED TO ABOVE CRANK BROKEN IN SERVICE BY FEW SEVERE BLOWS.

Length, feet	280.0
Breadth, feet	40.1
Depth mld., feet	21.33
Load draught, feet	18.5

The draughts forward and aft during the trials were 5 feet 11 inches and 12 feet 1 inch' respectively, the vessel being without cargo or bunkers, and the propeller blade being about 1 foot 6 inches out of water when at the top of the aperture. The weather during the trial could be described as "seas moderate to heavy".

Arrangements were made for taking Geiger torsiograph readings just aft of the thrust block. It had been hoped to take records over the speed range of 30-80 Rpm. at intervals of 5 Rpm., but owing to the state of the weather it was quite impossible to obtain or maintain any desired speed. In the circumstances there was no alternative but to take continuous records under conditions of engine racing. In spite of these apparently unsatisfactory conditions for taking records, very valuable results were in fact obtained. The records have yielded consistent results upon analysis and show that even with very rapid speed surges during engine racing, the various orders of torsional vibration all appear on the record as the corresponding critical speeds are passed through.

Discussion of Trials and Torsiograph Records.

Figure 3 shows the resonance curves obtained from the records, and it will be noted that the natural frequency is about 339 Vpm. This figure is somewhat higher than that calculated, and this can be accounted for to some extent by the fact that the calculations allowed 25 per cent for entrained water, whereas in fact the propeller was not fully immersed and under conditions at sea the amount of the immersion would vary very considerably. The stresses in Figure 3 are also higher than the calculated figures, as might be expected from considerations of propeller damping. This is an important point since propeller damping is very large under normal conditions, and prevents the development of enormous vibration stresses due to 1-node criticals. Lack of complete immersion of the propeller has the effect of reducing propeller damping, and this will be shown more fully in dealing with vibration stresses which occurred at 154 Rpm.

Figures 4 and 5 show resonant portions of the torsiograph readings corresponding to the 3rd, 4th, 5th and 6th orders. The revolutions per minute of the engines have been derived by the use of the fixed vibrator and by a make-and-break trace operating once per revolution. The values of revolutions so obtained have been indicated above the fixed vibrator trace, and it will be noted that violent changes in speed occur due to the propeller being alternately partially or completely out of the water and immersed. Under these conditions no steady resonant vibration was recorded, *but at the correct speeds for the various orders transient resonant vibrations appear, and the rapidity with which such resonance builds up is a remarkable feature of the records.*

In Figure 5 the speed surges were even greater than shown in Figure 4, and it will be seen that speeds of 154 Rpm. were attained. Moreover, the rise and fall of speed occurred in a very short space of time, namely, 2-2½ seconds respectively. In order to form some estimate of the torque loading in the straight shafting due to the speed surges, Figure 6 has been obtained from the records shown in Figure 5. The curves indicate the variation of velocity at the engine during two speed surges while racing. These curves have been differentiated to derive the maximum values of the angular acceleration during increase and decrease of engine speed. These calculations are

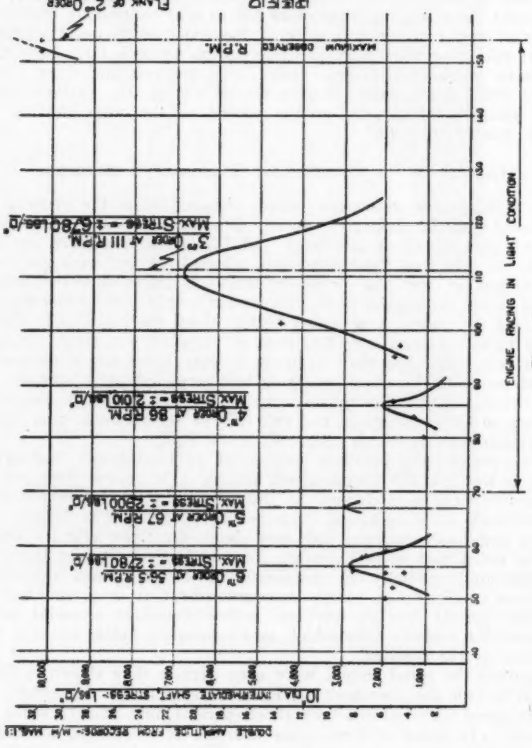
RESONANCE CURVES
Obtained From Tomahawk Records
Under Conditions of Rough Weather
With Propeller Valves R.P.M. and
Propeller Not Fully Governed.
MAXIMUM OBSERVED R.P.M.
ENGINE RACING IN LIGHT CONDITION
FLANK OF 2ND ORDER
STRESS = 10,250 + lbs./□"
3RD ORDER AT 111 R.P.M.
MAX. STRESS = ±6780 lbs./□"
4TH ORDER AT 86 R.P.M.
MAX. STRESS = ± 2100 lbs./□"
5TH ORDER AT 67 R.P.M.
MAX. STRESS = ± 2500 lbs./□"
6TH ORDER AT 55.5 R.P.M.
MAX. STRESS = ± 2780 lbs./□"
10 DIA. INTERMEDIATE SHAFT, STRESS- lbs./□"
DOUBLE AMPLITUDE FROM RECORDS- M/M

Fig. 3.

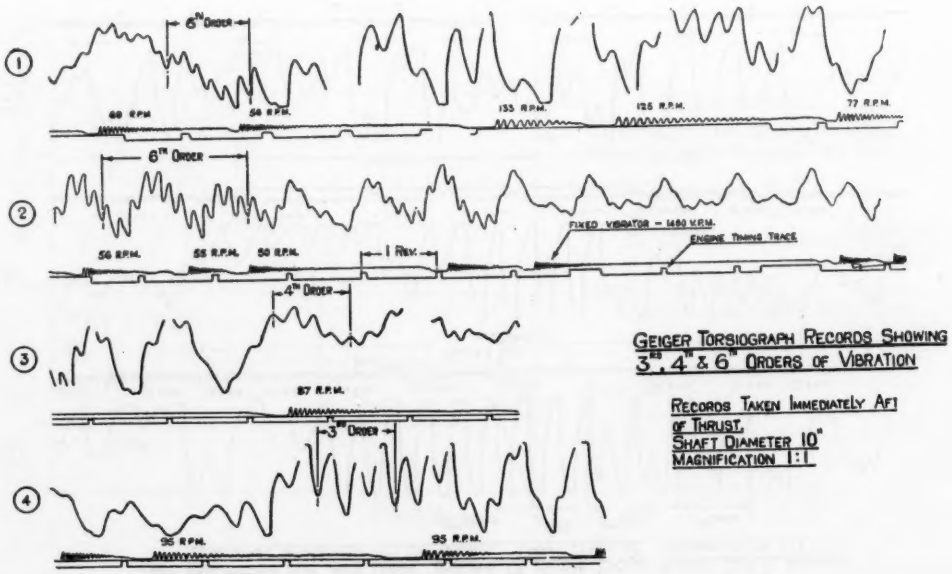

GEIGER TORSIOGRAPH RECORDS SHOWING 3RD, 4TH & 6TH ORDERS OF VIBRATION

RECORDS TAKEN IMMEDIATELY AFT OF THRUST.
SHAFT DIAMETER 10"
MAGNIFICATION 1:1

FIG. 4.

GEIGER TORSIOGRAPH RECORDS SHOWING 2ND, 3RD & 5TH ORDERS

N.B.– THESE RECORDS WERE TAKEN UNDER CONDITIONS OF SEVERE ENGINE RACING, DUE TO WEATHER CONDITIONS, IMMEDIATELY AFT OF THRUST. SHAFT DIAM. 10" MAGNIFICATION 1 : 1

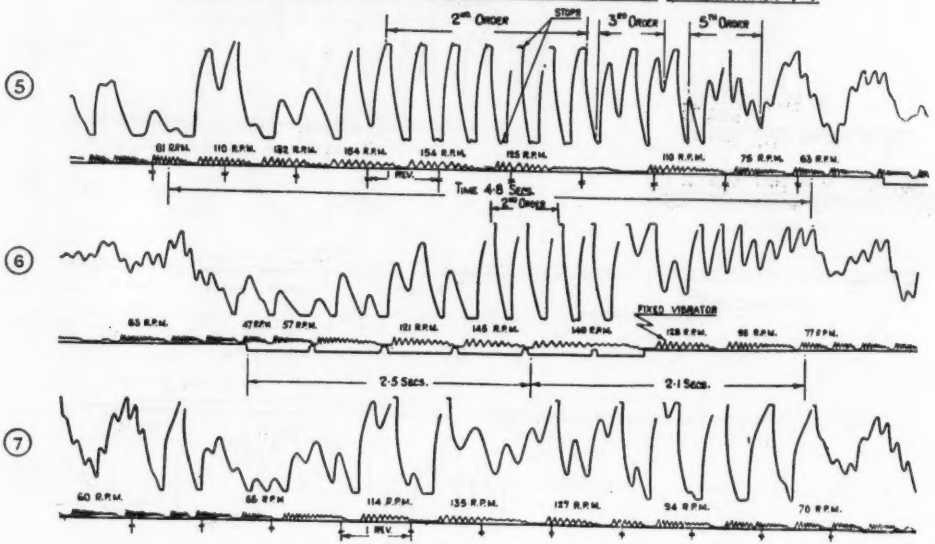

FIG. 5.

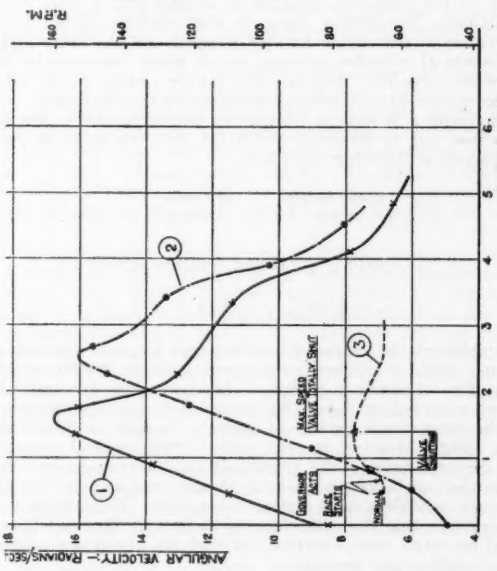
SPEED SURGES
DERIVED FROM TORSIOGRAPH RECORDS ⑤ & ⑥ Fig.
USING FIXED VIBRATION AND ENGINE TIMING TRACES.
CURVE ① FROM RECORD ⑤
ACCELERATION WITH PROPELLER LEAVING WATER = 2.5 RADS./SEC.²
MAX. DECELERATION WITH PROPELLER ENTERING WATER = 1.13 RADS./SEC.²
CURVE ② FROM RECORD ⑥
ACCELERATION WITH PROPELLER LEAVING WATER = 3.5 RADS./SEC.²
MAX. DECELERATION WITH PROPELLER ENTERING WATER = .70 RADS./SEC.²
CURVE ③
ESTIMATED SPEED SURGE IF GOVERNOR HAD BEEN FITTED
ANGULAR VELOCITY — RADIANS/SEC.
R.P.M.
TIME — SECONDS.
GOVERNOR ACTS
BACK BOUNCE
NORMAL
MAX. SPEED VALVE INITIALLY SHUT
VALVE OPENS

FIG. 6.

shown in Appendix III from which it will be noted that the maximum value of stress in the intermediate shaft resulting from these speed surges amounted to 3810 pounds per square inch. Such a value in itself could not have accounted for the type of failure shown in Figure 1. It should be mentioned, however, that apart from the records of racing shown in Figure 6, twice during the trial more serious speed surges occurred while adjustments were being made to the Geiger. The impression, however, from ordinary observation was of very severe conditions for the crankshaft.

Apart from the racing, another and more important fact emerges, namely, the very violent torsional vibration at 154 Rpm., where a distinct 2nd order occurs. It should be explained with reference to Figure 5 that the fixed vibrator trace is not in line with the vibration trace, the latter being 19 mm. to the left of the former. At 85 Rpm. and 113 Rpm. during racing, the 4th and 3rd orders respectively, also clearly appear in the records, resonance building up with amazing rapidity. When the speed reached 154 Rpm., although the instrument was hitting the stops hard, the 2nd order vibration frequency was maintained. With a double amplitude equal to that permitted by the stops, the stress would be equal to $\pm$ 10,000 pounds per square inch. By examination of the record and by the sound made by the instrument hitting the stops, all the indications were that the true amplitude was considerably greater than that which could be recorded. The conclusion to be drawn from this is that with the propeller out of water and a consequent surge of speed of 154 Rpm., the shafting is thrown into a state of violent torsional oscillation. The energy input to the vibration comes from the 2nd order harmonic of the engine turning moment and the large amplitude is due to the absence of propeller damping, which would otherwise be present with an immersed propeller. Further, the higher orders excite vibration during the speed surges at revolutions corresponding to resonance.

From the foregoing it is seen by addition of the torque due to the general speed surge to that due to torsional oscillation, that the resulting stress in the straight shafting at 154 Rpm. will be:

$$= \left\{ \begin{matrix} \text{speed surge} \\ \text{stress} \end{matrix} + \begin{matrix} \text{vibration} \\ \text{stress} \end{matrix} \right\}$$

$$= \left\{ 3810 + (> 10{,}000) \right\} \text{ lb. per sq. inch}$$

$$= > 13{,}810 \text{lb. per sq. inch.}$$

As already explained, the torsional load required to cause slippage at the crankshaft shrink would correspond to a stress of about 20,000 pounds per square inch in the intermediate shafting. In comparing this approximate stress with that recorded, it should be remembered that records were not taken during the most severe periods of racing. In spite of this, it will be noted that the margin of safety is very small. From general observations during racing, the conditions for the crankshaft seemed very severe. In consequence, before the conclusion of the trial, inquiry was made of the captain as to whether such conditions were typical or extreme. The inference drawn from this inquiry was that the conditions of loading of the vessel, namely, no bunkers and no cargo, were extreme, but that the racing was similar to that encountered during bad weather.

The engine was examined during the trial, particularly in way of the L. P. crank. All crankshaft bearings showed nothing more than a normal running heat with the exception of the after H. P. bearing (i.e., No. 2 bearing) which was slightly above normal running heat. No transverse movement was

noted at any of the crankshaft journals, and a vibrograph set up adjacent to the pocket of the after L. P. bearing showed no movement or pulsation whatever, excepting those due to the general movement of the hull in space.

At the conclusion of the trial the crankshaft was examined, and it was found that failure had again occurred at the after web of the L. P. crank. The type of failure was precisely as shown in Figure 1, the opening at the sides of the dowel being about 10/1000 inch and the lift of the web on the journal about 2/1000 inch. Torsiograph records had thus been obtained under severe conditions of racing, leading to the same type of failure as had formed the *raison d'être* for the investigation.

Conclusions From Torsiograph Records.

(1) Figure 3 indicates that under normal service conditions envisaging maximum revolutions of 70 per minute, the torsional vibration characteristics, even with propeller partially immersed, are entirely satisfactory.

(2) With weather and loading conditions during this trial, the torsional vibration characteristics are shown to be severe, due primarily to:

(*a*) Increases of speed to 154 Rpm. bringing in a 2nd order vibration.

(*b*) The absence of propeller damping, which is of great importance for reducing 1-node vibration torques. The records clearly show that at 154 Rpm. the vibratory torque on the L. P. crank was considerably in excess of that corresponding to a stress of $\pm$ 10,000 pounds per square inch in the intermediate shafting, the actual measurement being outside the range of the instrument.

(3) Apart from the vibratory torque mentioned in (2) above, there is an additional torque due to the general speed surge, which corresponds to a stress in the intermediate shafting of 3810 pounds per square inch. In this connection, it has already been remarked that twice during the trial, as far as could be judged from ordinary observation, more severe racing occurred than that recorded. If this was in fact the case, both the vibratory torque mentioned in (2) above and that due to the speed surge would be greater, the former because the 2nd order critical speed would in all probability be reached.

(4) It has been stated that a stress of 20,000 pounds per square inch in the intermediate shafting would produce a dangerous torque for the crankshaft shrink. While such a load was not recorded, a torque corresponding to a stress of at least 13,810 pounds per square inch in the intermediate shaft was actually measured, and all the indications are that the true maximum stress was actually considerably in excess of this figure. It is of interest to note that the failure under discussion in this paper invariably occurred in the *after* web of the L. P. crank. This is what might be expected from consideration of the cause of the failures as now ascertained. Both the vibration torque and that due to the general speed surge is reduced at the forward L. P. web by an amount corresponding to the torque required to accelerate and decelerate the heavy reciprocating L. P. masses including the pump gear driven from the crosshead. In view of this, it may be stated that for the machinery under investigation the after web of the L. P. crank has been stepped as shown in Figure 8, thus adding considerably to the strength of the shrink grip.

From the foregoing it is obvious that speed surges alone, with engines fitted amidships, do not produce unduly high torques; in other words, the propeller and long length of intermediate shafting are "kind" to the engine crankshaft during racing. The major cause of the excessive torsional loading during racing comes from violent torsional oscillation in the absence of

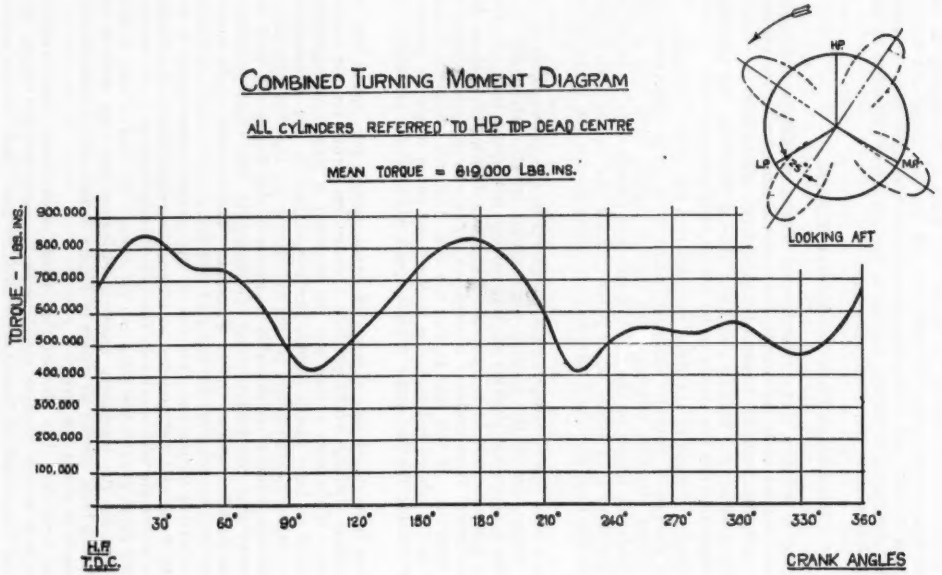
COMBINED TURNING MOMENT DIAGRAM
ALL CYLINDERS REFERRED TO H.P. TDP DEAD CENTRE
MEAN TORQUE = 619,000 LBS. INS.
TORQUE - LBS. INS.
900,000
800,000
700,000
600,000
500,000
400,000
300,000
200,000
100,000
30°
60°
90°
120°
150°
180°
210°
240°
270°
300°
330°
360°
H.P T.D.C.
CRANK ANGLES
HP
LP
MP
LOOKING AFT

FIG. 7.

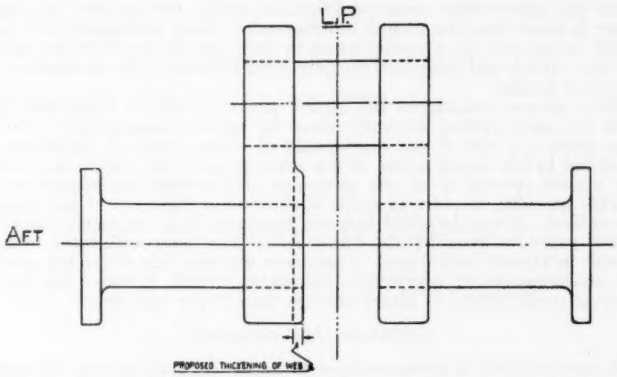

FIGURE 8.—METHOD OF INCREASING THE SHRINK IN THE AFTER WEB OF THE L. P. CRANK.

propeller damping. So far as steam reciprocating machinery is concerned, the aim should be to prevent speed surges taking the machinery into speed ranges corresponding to the 2nd and 3rd orders. Where this cannot be achieved, even by the fitting of a governor, care should always be taken to trim the ship by the stern to maintain, so far as possible, propeller immersion. For the case dealt with in this investigation, the frequency of 339 Vpm. is higher than usual for this type of installation; even so, the 2nd order vibration was excited during racing as shown in Figure 3. Had a governor been fitted to prevent speed surges in excess of, say, 100 Rpm. no damage would have occurred to the crankshaft. A more usual value of 1-node natural frequency for steam reciprocating machinery with engines amidships would be about 240 Vpm., giving 3rd and 2nd order criticals at 80 and 120 Rpm., respectively. In such cases, with normal running speeds of 70 to 80 Rpm. it would be difficult to avoid the 3rd order by the fitting of a governor, but a governor would prevent the higher torsional stresses due to the 2nd order, which would otherwise be fully excited at 120 Rpm. The results of this investigation indicate that the 3rd order torsional loading, while high, should not cause damage during racing, and it is likely that with proper attention to trimming the shift aft, the loading would be less than indicated in Figure 3.

With aft-end steam reciprocating machinery the 1-node frequency will be about 500 Vpm. Under these conditions only the higher orders of vibration would be excited and, since the magnitude of the resultant harmonic of the T. M. diagram for these orders is corresponding less, violent torsional oscillation would not develop during racing. On the other hand the torques resulting from the general speed surge would in all probability be higher, due to the reduction in resilience as compared with that present in the shafting of the amidships installation. This is a matter requiring further investigation. Regarding oil-engine installations with machinery fitted amidships, common values of 1-node frequency would be 200-350 Vpm., and the lowest order of major vibration would be the 3rd order with a normal running speed of 100-120 Rpm. Under these conditions it would not be possible always to

avoid the major order under conditions of racing, but provided the major order is lower than the normal running speed, which incidentally will generally be the case, the propeller would be immersed during transient passing of this critical, and propeller damping would prevent the development of excessive torques.

With aft-end installations the natural frequency will be about 500 Vpm. with the major critical generally above the normal running speed. In this case there is a risk of the development of violent torsional oscillations as described in this paper, unless care is taken to place the critical well above the normal running speed and governing arrangements are related to the margin provided, in order to avoid working on a high part of the flank of the critical. It may be added that this theorizing from the results described in this paper fits like a jig-saw into practical experience with many cases of trouble in aft-end installations. Experience indicates that where the governing arrangements are satisfactory, the major critical, if above the normal running speed, should be placed not less than 30 per cent above.

Governing Arrangements.

A common form of governor fitted to steam reciprocating and oil engines is of the ordinary inertia type fitted to pump or special governor levers. The nominal increase of speed for which these can be adjusted to act is 4–5 per cent above the speed at which the engines are required to run. These governors will, however, cut-out on any sudden acceleration, in spite of the fact that the average speed of 4–5 per cent above the running speed has not been reached. In addition, an emergency governor is fitted which comes into operation in the event of prolonged or excessive engine racing due to a fractured shaft or lost propeller. This emergency governor does not allow of the admission of power after such speed surges have ceased.

In the case of steam reciprocating engines running at nominal speeds up to 85 Rpm., the emergency governor locks up at twice the running speed, or even higher, this being necessary because of the sudden accelerations possible due to the low inertia of these engines. At higher speeds a slight reduction in the margin mentioned above is made, e.g., at 95 Rpm. (normal) the emergency speed might be fixed at 165 Rpm., and with 100 Rpm. (normal) at a speed of 180 Rpm. For oil engines the margin for the emergency governor may be closer, being usually 6–10 per cent above the speed specified for the engines.

However, the important point is the functioning of the main governor, which under conditions of rough weather should prevent excessive speed surges. It is claimed by one well-known firm of manufacturers of governors that had a governor been fitted to the engines on which this investigation was carried out, the speed rise would have been no greater than that shown in Figure 6, Curve (3). In these circumstances, reference to Figure 3 indicates clearly that no trouble would have been experienced with the shafting of this vessel.

The author believes that the importance of engine governing has not been fully realized in the case of the steam reciprocating engine, nor has that of the necessary margin between normal running speed and a major critical in the case of many oil-engined vessels.

Acknowledgments.

The author wishes to thank the Committee of Lloyd's Register of Shipping for permission, kindly given, to publish this paper, also to acknowledge help given, both on trials and in the preparation of the results for presentation, by his colleague, J. W. Burrill. B.Sc.

Appendix I.

Natural Frequency of Engine System.

The equivalent dynamic system is as follows:

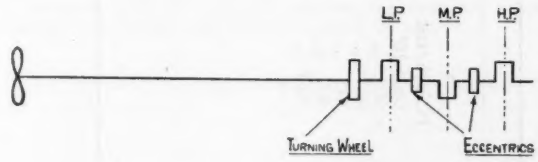

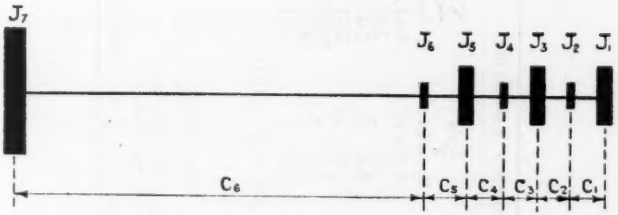

Where inertias and stiffnesses are:

Inertia.		Stiffness.	
J_1 =	2,890 lb. in. sec.^{2}	C_1 =	603×10^6 lb. in./radian
J_2 =	457 " " "	C_2 =	603×10^6 " " "
J_3 =	3,162 " " "	C_3 =	603×10^6 " " "
J_4 =	234 " " "	C_4 =	445×10^6 " " "
J_5 =	4,160 " " "	C_5 =	480×10^6 " " "
J_6 =	500 " " "	C_6 =	$10{\cdot}4\times10^6$ " " "
J_7 =	37,700 " " "		

N.B.—J_7 (propeller inertia) includes 25 per cent. for entrained water.

Giving for 1-node vibration:

2nd	order	occurs	at	162	r.p.m.
3rd	"	"	"	108	"
4th	"	"	"	81	"
5th	"	"	"	65	"
6th	"	"	"	54	"

$p^2 = 1{,}150$. 1-Node Frequency Tabulation.

No. of Mass.	$\frac{J}{g}$ lb.-inch-sec.^{2}	$\frac{J}{g}p^2$ lb.-inches.	θ Radians.	$\frac{J}{g}p^2\theta$ lb.-inches.	$\sum\frac{J}{G}p^2\theta$ lb.-inches.	C lb.-inch/rad.	*Twist* Radians.
1	2,890	$3{\cdot}33\times10^6$	1·0000	$3{\cdot}33\times10^6$	$3{\cdot}33\times10^6$	603×10^6	·0055
2	457	·526 „	·9945	·52 „	3·85 „	603 „	·0064
3	3,162	3·64 „	·9881	3·60 „	7·45 „	603 „	·0123
4	234	·27 „	·9758	·26 „	7·71 „	445 „	·0173
5	4,160	4·78 „	·9585	4·58 „	12·29 „	480 „	·0256
6	500	·575 „	·9329	·54 „	12·83 „	10·4 „	1·2315
7	37,700	43·40 „	−·2986	−12·94 „	−0·11 „	—	—

p^2 = (circular frequency in radians per sec.)^2 = 1,150.

$F = \frac{60}{2\pi}\sqrt{p^2} = 324$ vibrations per minute.

where $\frac{I}{G}$ = Mass moment of inertia in lb.-ins.-sec.^{2}

θ = Amplitude of swing at mass in radians.

C = Stiffness of shafts in lb.-ins. per radian.

N.B.—Without allowance for entrained water, $F = 332$ *vibrations per min.*.

Appendix II.

Estimated Stresses.

By Calculation.

In order to estimate the stresses set up in the shafting, the combined turning moment curve shown in Figure 7 was derived from actual indicator cards taken at 66 Rpm., the Ihp. being 652.

By harmonic analysis, using 24-ordinates, the combined harmonic torque co-efficients for various orders were obtained, as under:

T_n for 2nd order harmonic co-efficient $= 118{,}000 \sin. (2\theta + 65° 20')$ lb. in.
" " 3rd " " " $= 118{,}400 \sin. (3\theta + 307° 30')$ "
" " 4th " " " $= 26{,}800 \sin. (4\theta + 72° 48')$ "
" " 5th " " " $= 4{,}975 \sin. (5\theta + 21° 6')$ "
" " 6th " " " $= 39{,}400 \sin. (6\theta + 20°)$ "

Where θ = h.p. crank angle from t.d.c.

From * "Strength of Marine Engine Shafting".

Maximum value of actual vibration torque $= C \times \frac{\bar{L}}{L}$ lb.-ins.

Where $\frac{L}{\bar{L}} = \frac{N_1^2}{Q_1 \bar{E}^2 \times p \times 28{\cdot}6 \times H} \times \frac{T_n \times \bar{L}_m}{N}$

$N_1 = 66$ r.p.m.

Q_1 = propeller torque at 66 r.p.m. = mean torque × mech. effcy.
$= 557{,}000$ lb./ins.

$\bar{E}$ = propeller amplitude in frequency table = ·2986 radians for 1 rad. at No. 1 mass.

p = phase velocity $= \frac{324}{60} \times 2\pi = 33{\cdot}9$ radians/sec.

$H = 1 + 0{\cdot}2 \frac{(\bar{L}_m)^2}{(\bar{E})^2} = 3{\cdot}16.$

T_n = total harmonic co-efficient at critical considered.

$\bar{L}_m$ = mean engine amplitude from frequency table = ·9822 rads.

L = actual " "

$\bar{L}$ = one radian.

C = maximum torque given in frequency table with 1 radian at engine $= 12{\cdot}83 \times 10^6$ lb. ins.

N = r.p.m. at critical considered.

Then actual value of vibration torque $= C \times \frac{L}{\bar{L}}$

$$= \frac{12{\cdot}83 \times 10^6 \times (66)^2}{557{,}000 \times (·2986)^2 \times 33{\cdot}9 \times 28{\cdot}6 \times 3{\cdot}16} \times \frac{T_n \times ·9822}{N}$$

$$= 364 \times \frac{T_n}{N}$$

* Paper by S. F. Dorey, D.Sc., Trans. N. E. C. Institution of Engineers and Shipbuilders, 1939.

2nd Order (at 162 Rpm.).

$$\text{Max. torque} = \frac{364 \times 118{,}000}{162} = 265{,}000 \text{ lb./ins.}$$

$$\text{Stress in 10 in. diam. intermediate shaft} = \frac{265{,}000 \times 16}{\pi \times (10)^3} = \frac{265{,}000}{196.3}$$

Stress = 1,350 lb. per sq. in.

3rd Order (at 108 Rpm.).

Max. torque = 400,000 lb. ins.
Stress = 2,035 lb. per sq. in.

4th Order (at 81 Rpm.).

Max. torque = 120,500 lb. ins.
Stress = 614 lb. per sq. in.

5th Order (at 65 Rpm.).

Max. torque = 27,900 lb. ins.
Stress = 142 lb. per sq. in.

6th Order (at 54 Rpm.).

Max. torque = 265,000 lb. in.
Stress = 1,350 lb. per sq. in.

Estimation of Stresses From Torsiograph Records for 1-Node Vibration.

From Figs. 4 and 5.

Max.	double	amplitude	from	record	at	2nd	order	=32mm.	plus*
"	"	"	"	"	"	3rd	"	=21·2	"
"	"	"	"	"	"	4th	"	= 6·3	"
"	"	"	"	"	"	5th	"	= 9	"
"	"	"	"	"	"	6th	"	= 8·7	"

Diameter of shaft at forward station = 10 inches.

2 millimeters of double amplitude corresponds to $\pm$ 0.00788 radians at point of taking records, i.e., 5 feet aft of thrust block.

From frequency table when $\theta = 1$ radian at free end of system, single amplitude at point of taking records = .8074 radians.

Maximum torque for amplitude of 0.8074 radians from tables

$$= 12.83 \times 10^6 \text{ lb.-ins.}$$

Then torque for 1 radian at point of taking records

$$= \frac{12.83}{.8074} \times 10^6 = 15.9 \times 10^6 \text{ lb.-ins.}$$

Stresses in Intermediate Shaft for Amplitudes Listed Above.

2nd Order (at 169.5 Rpm.).

Maximum double amplitude recorded = 32 plus † millimeters with instrument on stops.

* It will be noted from Fig. 5 that the instrument was hitting the stops on this order, and the revolutions per minute were 154 instead of 166 for maximum resonance with the propeller out of water. In spite of the instrument hitting the stops, the 2nd order frequency was maintained, and the vibration torques and stresses have been calculated assuming resonant conditions as given by the frequency table in Appendix I.

$$\text{Torque at 154 Rpm.} = \frac{32}{2} \times .00788 \times 15.9 \times 10^6 \text{ lb.-in.}$$

Stress, 10 in. dia. shaft = 10,230 lb. per sq. inch
Similarly,

3rd Order (at 113 Rpm.).
Maximum torque = 1,330,000 lb. in.
Maximum stress = 6780 lb. per sq. in.

4th Order (at 84 Rpm.).
Maximum torque = 395,000 lb. inch.
Maximum stress = 2010 lb. per sq. inch.

5th Order (at 68 Rpm.).
Maximum torque = 565,000 lb. inch.
Maximum stress = 2900 lb. per sq. inch.

6th Order (at 56.5 Rpm.).
Maximum torque = 546,000 lb. inch.
Maximum stress = 2780 lb. per sq. inch.

Appendix III.

Torques Arising From Speed Surges During Racing.

Mean torque from turning moment diagram = 619,000 lb. in.

$$\text{Propeller moment of inertia} = \frac{J_p}{g} = 37{,}700 \text{ lb. in sec.}^2$$

$$\text{Total engine moment of inertia} = \frac{J_e}{g} = 11{,}400 \text{ lb. in. sec.}^2$$

Assume that T_m (the mean torque at 66 Rpm.) remains constant when the engine is racing, i.e., there is no wire-drawing of steam supply as engine speed increases, the engine settings and throttle valve openings being unaltered.

Let T_p be the torque in the intermediate shafting.

" α be the angular acceleration of engine.

Neglecting friction, losses, etc.

$$\text{Then } T_p = T_m - \frac{J_e}{g}\alpha \text{ during acceleration.}$$

$$\text{Also } T_p = T_m + \frac{J_e}{g}\alpha \text{ during deceleration.}$$

From speed surge diagrams Figure 6.

Acceleration during period of propeller *leaving* water

$$\alpha = *5.5 \text{ rads./sec.}^2$$

$$\text{Torque transmitted by shaft during acceleration} = T_m - \frac{J_e}{g}\alpha$$

$$= 556{,}000 \text{ lb. ins.}$$

$$\text{With 10 in. dia. shaft, Stress} = \frac{556{,}000 \times 16}{\pi \times (10)^3} = 2830 \text{ lb. per sq. in.}$$

Maximum acceleration during period of propeller *entering* water

$$\alpha = 11.3 \text{ rad./sec.}^2$$

$$\text{Torque transmitted by shaft during deceleration} = T_m + \frac{J_e \alpha}{g}$$

$$= 748{,}000 \text{ lb. in.}$$

With 10 in. dia. shaft, Stress = 3810 lb./sq. in.

*NOTE.—It is interesting to compare this figure of 5.5 rad./sec.^{2} with the acceleration which would result if the mean turning moment acted on a rigid system without any propeller resistance torque, then,

$$\alpha = \frac{T_m}{\frac{(J_e + J_p)}{g}} = \frac{619{,}000}{49{,}100} = 12.6 \text{ rad./sec.}^2$$

TAPERED AND STEPPED COLUMNS.

The inherent weight-saving possibilities of long columns with varying cross-sections are demonstrated by an analysis of stress distribution. Mr. A. H. Church, of New York University, compares hinged end columns with different types and proportions of taper. He also reports a method of designing and calculating the proportions of constant strength columns. This article is reprinted from Product Engineering, August, 1943.

In designing many structural members such as engine connecting rods, derrick booms, and aircraft struts to resist compression end loads, weight-saving considerations are important not only to reduce the power required to transport the structure, but also to obtain a minimum of inertia effects caused by sudden acceleration and deceleration.

Weight-saving designs usually take advantage of the fact that in long columns with hinged ends the flexural bending moment is a maximum at a cross-section equidistant from the ends. Also that the bending moment at intermediate cross-sections decreases as the cross-sections approach the ends of the column. Hence, the component of stress set up by flexure in columns of constant cross-section varies from a maximum at the middle of the column to a minimum at the ends. Therefore, it is possible to design a column having tapered ends or decreasing stepped cross-sectional areas that will weigh less than, but be equal in strength to, a column of constant cross-section.

A formula commonly used in working with short columns of constant section is that given by J. B. Johnson, in which

P_{cr} = Critical load on the column, pounds.
A = Cross-sectional area, square inches.
S = Yield point strength of material, pounds per square inch.
L = Length of column, inches.
k = Minimum radius of gyration, inches.
C = Constant dependent upon end conditions.
E = Modulus of elasticity of the material, pounds per square inch.

$$P_{cr} = A\,S\left[1 - \frac{S\,(L/k)^2}{4\,C\,\pi^2\,E}\right] \qquad (1)$$

The plot of Equation (1) is a parabola which is tangent to the plot of Euler's equation

$$P_{cr} = \frac{\pi^2\,C\,E\,A}{(L/k)^2} \qquad (2)$$

The value of L/k at which the two curves are tangent, found by equating the failure loads of Equations (1) and (2), is

$$\frac{L}{k} = \sqrt{\frac{2\,C\,\pi^2\,E}{S}} \qquad (3)$$

In design problems the Euler equation may be used when values of L/k are greater than that given by Equation (3), when values of L/k are less than that given by Equation (3) the J. B. Johnson expression may be used. When C equals 1 (hinged ends), E equals 30,000,000 and S equals 40,000 pounds per square inch, L/k is 122 at the point of tangency. With an alloy steel having a yield point of 120,000 pounds per square inch, and C equal to 1, the value of L/k drops to 70.5 at the point of tangency.

On this basis the Euler equation and the discussion which follows will apply to a greater range than is usually supposed when high yield point steels are used.

Euler's equation is based upon pure flexure caused by the deflection of the column centerline under the applied load. With

x = Distance measured from end of column
I_x = Moment of inertia of section at a distance x
y = Deflection of center line at distance x
P = Load on column

the moment at any point is Py (see Figure 1) and the differential equation of the deflection curve is

$$E\,I_x\,\frac{d^2y}{dx^2} + P\,y = 0 \qquad (4)$$

Since the deflection y at the ends of the column is zero, Equation (4) indicates that the ends are pointed, that is, have a zero moment of inertia. But, obviously, in practice the ends must have a bearing area based upon the compressive strength of the material used and the end load.

The solution of Equation (4) for stepped and tapered columns of various proportions and forms has been solved by Dr. A. N. Dinnik and reported by Mr. M. Maletz ("Design of Columns of Varying Cross-Sections,"

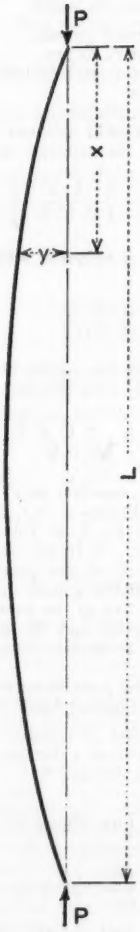

FIGURE 1.—DEFLECTION OF THE CENTER LINE OF A COLUMN HAVING HINGED ENDS UNDER APPLIED END LOAD.

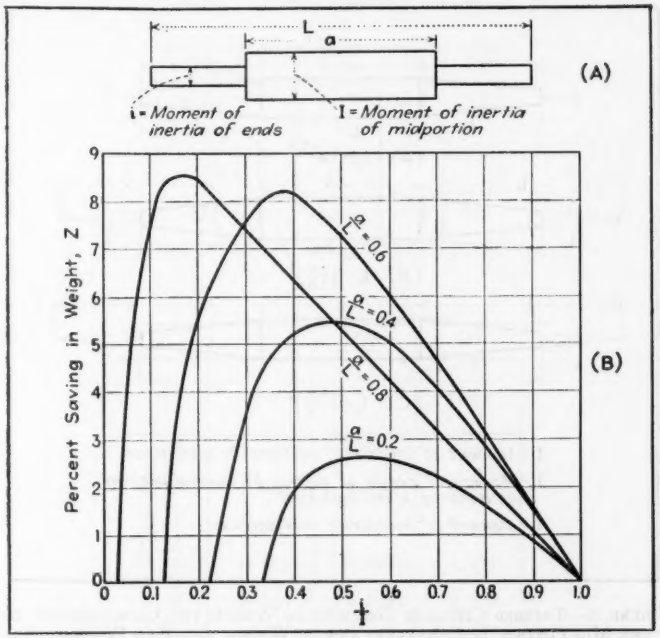

FIGURE 2.—(A) STEPPED COLUMN IN WHICH THE CROSS-SECTIONAL SHAPES OF THE CENTER AND END PORTIONS ARE OF SIMILAR PROPORTIONS. (B) PERCENTAGE OF WEIGHT SAVED, AS COMPARED TO COLUMNS OF CONSTANT CROSS-SECTION, BY USING A STEPPED COLUMN PLOTTED FOR VARIOUS LENGTHS OF MID-PORTION AND AREAS OF END-SECTIONS OR MOMENTS OF INERTIA OF ENDS.

A. S. M. E. Transactions APM 51-11, 1929 and APM 54-16, 1932). Dr. Dinnik uses a constant K the value of which depends upon the form and proportions of the taper or step. For a pin ended column of constant section K is π^2. I is the maximum moment of inertia. The critical load for each case is given by

$$P_{cr} = \frac{K E I}{L^2} \qquad (5)$$

To determine the lightest weight column to support a given load, the cases solved by Dr. Dinnik will be here investigated. The per cent saving in weight Z which results from using a tapered or stepped column instead of a similarly shaped, constant section column to carry the same load will also be found.

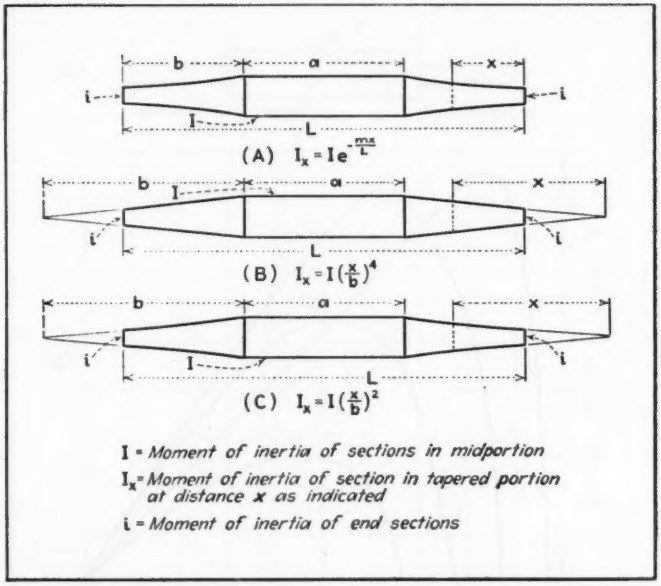
b
a
x
i
I
L
(A) $I_x = Ie^{-\frac{mx}{L}}$
(B) $I_x = I(\frac{x}{b})^4$
(C) $I_x = I(\frac{x}{b})^2$
I = Moment of inertia of sections in midportion
I_x = Moment of inertia of section in tapered portion at distance x as indicated
i = Moment of inertia of end sections

FIGURE 3.—TAPERED CIRCULAR COLUMNS IN WHICH THE CROSS-SECTION OF THE MID-PORTION IS CONSTANT, AND IN WHICH THE END PORTIONS ARE TAPERED IN ACCORDANCE WITH A MATHEMATICAL LAW. WEIGHT SAVED IS GREATER THAN IN TYPES HAVING ABRUPT SECTION STEPS.

The values of Z summarized in the following paragraphs for pin-ended columns do not include the required enlargements at the ends to resist the bearing loads, since the dimensions of the enlargements depend upon the physical properties of the material.

Stepped Columns may be made from pipe of different diameters riveted, welded or shrunk together, or may be constructed by attaching a stiffener to the mid-portion of a constant section column.

Values of Z for stepped columns, like that shown in Figure 2 (A) having cross-sectional shapes of similar proportions, are plotted in Figure 2 (B) in terms of i/I and a/L, in which i and I are the moments of inertia of the end and center sections respectively, a is the length of the mid-portion, and L is the overall length of column.

It can be noted from Figure 2 (B) that the greatest saving in weight, about 8.5 per cent, occurs with a/L approximately equal to 0.8 and i/I equal to 0.2 approximately.

Tapered Circular Columns. It is to be expected that if the ends of the column are tapered according to some mathematical law, as shown in Figure 3, greater savings in weight can be obtained than by an abrupt step in section. Dr. Dinnik has solved Equation (4) for several cases of tapering

TABLE I.—TAPERED CIRCULAR COLUMNS.

Type	$Z_{max.}$	a/L	i/I
$I_x = I e^{-mx/L}$	11.7	0.4	0.1
$I_x = I_c \left(\frac{x}{b}\right)^4$	12.0	0.4	0.1
$I_x = I \left(\frac{x}{b}\right)^2$	12.2	0.4	0.1

(1)	(2)	(3)	(4)
$\frac{x}{L}$	I_x	y	$y_o - y$
0.00	1.000	0.000	1.000
0.05			
0.10	0.990	0.009	0.991
0.15			
0.20	0.955	0.037	0.963
0.25			
0.30	0.885	0.083	0.917
0.35			
0.40	0.800	0.149	0.851
0.45			
0.50	0.695	0.235	0.765
0.55			
0.60	0.570	0.340	0.660
0.65			
0.70	0.430	0.470	0.530
0.75			
0.80	0.270	0.621	0.379
0.85			
0.90	0.118	0.800	0.200
0.95			
1.00	0.000	1.000	0.000

columns where I_x the moment of inertia at a section x inches from the end is a function of the maximum moment of inertia I at the mid-portion. From the equations developed by Dr. Dinnik, calculations can be made for the saving in weight for solid circular columns, or for hollow columns having a constant ratio of thickness to diameter, with tapered ends. Table I summarizes the results of such calculations for columns of the type shown in Figure 3, and gives the maximum Z and the corresponding values of a/L and i/I for each case.

Columns of Constant Strength. The greatest saving in weight will occur in a column in which the stress is constant over the entire length except, of course, at the ends where the stress must necessarily be zero. The mathematical solution of Equation (4) for this condition is difficult, but an approximate method developed by Prof. A. Morley (Engineering, Sept. 21, 1917, p. 295) based upon difference calculus or tabular integration can be used. The basic idea of this method of calculation was outlined in an article by the author ("Difference Calculus," Product Engineering, January, 1942, p. 13) as applied to beam deflections.

By Morley's method the critical load of a column can be found regardless of the variation in the cross-section along the length. Sections can be selected by trial which will give a constant stress along the column, and the saving in weight Z then determined.

Since the column is symmetrical about its midpoint, only one-half of the length need be considered. This portion is equivalent to a column fixed at one end with the load applied at the free end as shown in Figure 4. Equation (4) can then be written

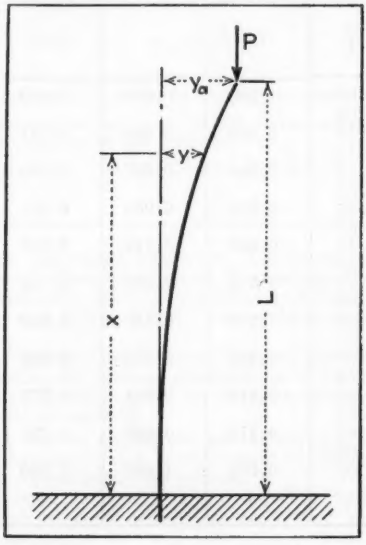

FIGURE 4.—DEFLECTION CURVE OF THE CENTER LINE OF A COLUMN FIXED AT ONE END AND WITH LOAD APPLIED AT THE FREE END.

$$M = E\,I_x \frac{d^2y}{dx^2} = P\,(y_a - y) \qquad (6)$$

By dividing the column into a number of equal increment lengths, for convenience each increment Δx is taken as 0.1 L, Equation (6) can be transformed to

TABLE II.—SOLUTION FOR A COLUMN OF CONSTANT STRENGTH.

(5)	(6)	(7)	(8)	(9)	(10)	(11)	(12)	(13)	(14)	(15)	(16)
(4)/(2)	f_1 0.1 (5)	Σf	$0.1\,\Sigma f$	$\Sigma\, 0.1\,\Sigma f$	y'	$y_0 - y'$	D_x	$\frac{(11)\times(12)}{(2)}$	S in percent	I_x	$0.1\sqrt{(15)}$
1.000		0.0000		0.0000	0.000	1.000	2.122	2.122	100.0		
	0.1000		0.0050							0.995	0.0998
1.001		0.1000		0.0050	0.009	0.991	2.120	2.122	100.0		
	0.1005		0.0150							0.972	0.0987
1.008		0.2005		0.0200	0.037	0.963	2.100	2.119	99.7		
	0.1022		0.0252							0.920	0.0960
1.037		0.3027		0.0452	0.084	0.916	2.060	2.133	100.2		
	0.1050		0.0355							0.843	0.0920
1.063		0.4077		0.0807	0.150	0.850	2.010	2.135	100.3		
	0.1082		0.0462							0.750	0.0866
1.100		0.5159		0.1269	0.236	0.764	1.938	2.126	100.1		
	0.1129		0.0572							0.633	0.0796
1.158		0.6288		0.1841	0.342	0.658	1.845	2.126	100.1		
	0.1195		0.0689							0.500	0.0707
1.232		0.7483		0.2530	0.470	0.530	1.720	2.120	99.8		
	0.1317		0.0814							0.350	0.0592
1.402		0.8800		0.3344	0.622	0.378	1.531	2.142	101.0		
	0.1518		0.0957							0.194	0.0441
1.694		1.0348		0.4301	0.800	0.200	1.245	2.108	99.4		
	0.0847		0.1077							0.059	0.0243
0.000		1.1195		0.5378	1.000	0.000	0.000	0.000	0.0		
										Total	0.7510

$$\frac{E}{P\,L^2}\,y = \sum_0^1 0.1 \sum_0^1 0.1 \left(\frac{y_a - y}{I_x}\right) \qquad (7)$$

which can be integrated in table form. Table II shows the procedure.

The column is divided into equal lengths of x/L equalling 0, 0.05, 0.10, and so on, as listed in Column (1) of Table II. The moments of inertia listed in Column (2) at the even tenth points are known or assumed. The deflections at these points are assumed and listed in Column (3); the maximum deflection y_a being taken as unity or 1 inch. The integration indicated by the right side of Equation (7) is then performed in Columns (4) to (9) inclusive.

As given by Equation (7) the values of Column (9) are a function of the derived deflection curve since E/PL^2 is a constant for a given case. If the maximum value 0.5378 is made equal to y_a and the other values changed proportionally a derived deflection curve Column 10 will result. To obtain a satisfactory solution this derived curve must agree with the original assump-

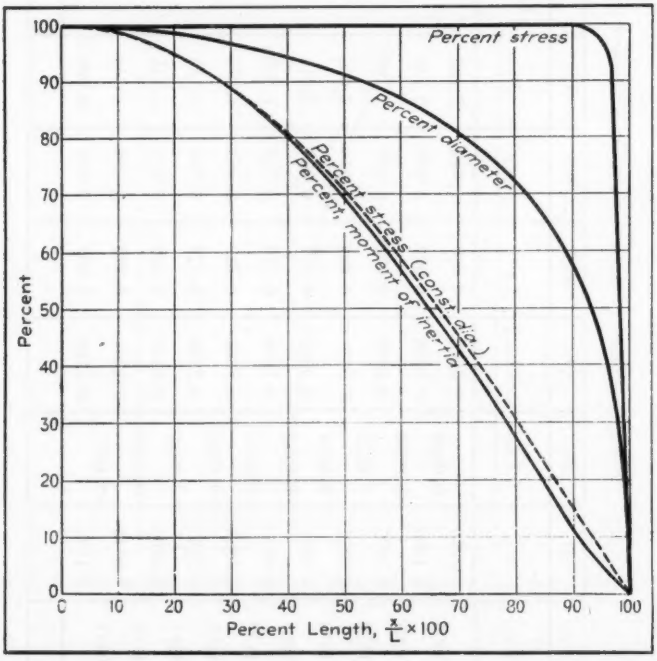

FIGURE 5.—STRESS, MOMENT OF INERTIA AND COLUMN DIAMETER PLOTTED ON A PERCENTAGE BASIS AGAINST PER CENT LENGTH FOR COLUMNS OF CONSTANT STRENGTH.

tion. If it does not, another curve must be assumed and the process repeated until agreement is reached. Usually the derived curve is used as the assumption for the next trial. It will then be found that the process is rapidly convergent, two or three trials being usually sufficient.

After agreement has been reached, the critical load can be found from Equation (7) by using the maximum values of y and

$$\sum_0^1 0.1 \sum_0^1 0.1 \left(\frac{y_a - y}{I_x} \right)$$

that is

$$P_{cr} = \frac{E' y_a}{L^2 \left[\sum_0^1 0.1 \sum_0^1 0.1 \left(\frac{y_a - y}{I_x} \right) \right]} \tag{8}$$

If the column calculated in Table II is made of steel having E equal to 30,000,000 and is 100 inches long, the critical load is

$$P_{cr} = \frac{30{,}000{,}000 \times 1}{100^2 \times 0.5378} = 5{,}580 \text{ lb.}$$

Stress S_x at points along the column is given by the flexure formula

$$S_x = \frac{M_x c_x}{I_x} = \frac{P(y_a - y') c_x}{I_x}$$

If the column has a circular section of diameter D_x, c_x equals $D_x/2$ and as P is constant

$$S_x = \frac{K' (y_a - y') D_x}{I_x}$$

The diameters corresponding to the moments of inertia listed in Column (2) are given in Column (12). The stress functions are calculated in Column (13). Since only relative values of stress are desired and the actual maximum deflection is unknown, the stress is found in Column (14) as a percentage of that existing at the base of the column. It will be noted that the percentage stress stays within plus or minus one per cent of the mid-point value for the values of I_x as assumed.

Stress, moment of inertia and column diameter are plotted in solid lines in Figure 5 on a percentage basis against per cent length. For comparison the percentage stress distribution for a constant section circular column is also plotted using a broken line. It is of interest to note that the relationship between I_x and x/L is approximated by the equation

$$I_x = I \left[1 - \frac{3}{2} \left(\frac{x}{L} \right)^2 + \frac{1}{2} \left(\frac{x}{L} \right)^3 \right]$$

The required moment of inertia of a column of constant section to carry the same load as the constant strength column can be found by equating Equations (2) and (8), remembering that I equals K^2A, y_a equals 1, and C equals ¼,

$$\frac{C\,\pi^2\,EA}{L^2/k^2} = \frac{\pi^2}{4}\,\frac{EI}{L^2}$$

$$= L^2\left[\sum_0^1 0.1 \sum_0^1 0.1\left(\frac{y_a - y}{I_x}\right)\right]$$

or

$$I = \frac{4}{\pi^2\left[\sum_0^1 0.1 \sum_0^1 0.1\left(\frac{y_a - y}{I_x}\right)\right]}$$

$$= \frac{4}{\pi^2\ (0.5378)} = 0.751 \text{ in.}^4$$

which corresponds to a diameter of 1.977 inches and a volume of 3.07 L cubic inches.

Since for a column with a circular section

$$\frac{I_x}{1} = \frac{D^4_x}{D^4}, \text{ and } \frac{A_x}{A} = \frac{D^2_x}{D^2}$$

the area at any section is A_x equals $A\ \sqrt{I_x/I}$ or, as I equals unity, A_x equals $A\ \sqrt{I_x}$ The volume is approximated by $A \sum \sqrt{I_x}(\Delta x/L)$ where the values of $\sqrt{I_x}$ are taken at the midpoints of the increment lengths. The values of $\sqrt{I_x}\ (\Delta x/L)$ or $0.1\ \sqrt{I_x}$, are listed in Column (16) and the summation is 0.751. The area A at the base is 3.543 square inches which corresponds to the moment of inertia of unity there. The approximate volume is 3.543 × 0.751 L, or 2.66 L. Hence, the percentage saving in weight Z by using a constant strength circular column rather than a constant section circular column which would carry the same load is 13.3 per cent. This is closely approached with end conditions of tapered columns solved by Dr. Dinnik.

As the curves of Figure 5 are plotted on a non-dimensional basis, the diameters can be used to specify a column of any length or material with a saving of weight as noted.

MISCELLANEA OF INTEREST TO NAVAL ENGINEERS.

UNDER-WATER ARC WELDING.—This article by A. J. Hipperson was first published in the Quarterly Transactions, The Institute of Welding, October, 1942. It was subsequently reprinted in the Engineering Foundation, supplement to the Journal of the American Welding Society, August, 1943. It is here reprinted from the latter publication.

The fact that under-water welding may be successfully carried out practically entirely with standard arc-welding equipment cannot be said to be very widely known. The process has many valuable applications such as under-water ship repair, lifting of sunken ships and the erection and repair of under-water structures, but it is believed that very little work of this

nature has yet been attempted. This article reviews the available literature on the subject of under-water arc welding and includes in an appendix details of a short series of tests recently carried out in this country.

It will be seen that under-water arc welding is no longer an experimental project, but rather a means of under-water construction and repair which is ready for immediate use.

It was first shown in 1802 by Sir Humphry Davy that the electric arc will continue to function when immersed in water. This principle was used at later dates in optical, calorimetric and chemical research, and notably for the preparation of colloidal solutions of metals and their oxides.

Early attempts at under-water arc welding were made with bare wire and thinly coated electrodes, but the efforts were futile and the results quickly suggested the need for some form of shielding of the arc so as to control and direct its action and to minimize its exposure to the surrounding agitated water.[2] More recent experiments such as those carried out by Schmidt [3] showed that this problem is practically solved by the use of covered electrodes, and that certain commercial electrodes met the requirements of under-water welding, since the coating burned evenly at a slightly slower rate than the core wire, forming thereby a protective covering around the arc. The main difficulty remains to be overcome—that of good visibility of the arc and the molten pool, which are practically concealed by local turbulence and the formation of black particles around the arc, the latter being rather troublesome except in flowing water.

The greatest depth at which arc welding has been carried out is 40 feet and successful results are reported.

Both organic coated electrodes and metallic oxide coated electrodes have been found to be satisfactory for welding under water—the former emitting rather more clouds than the latter, but deeper penetration is obtained.[3] In general it is desirable that the electrode be thickly coated and protected by a coating of varnish, particularly in the case where the electrodes are to be immersed for long periods in sea water before use. Varnishing the electrodes may easily be carried out by dipping into a spirit shellac varnish and drying. Not only does this render the electrode coating non-hygroscopic, but also provides an extra gaseous shield to the arc which gives added arc stability.

It has been suggested [4] that when an arc is struck under water, there is immediately formed a bubble or vapor pocket at the core of which is the arc; next would be found a mixture of incandescent gases emitted by the arc and highly superheated steam. Around this is an envelope of saturated steam in contact with the body of cool water in which the arc is immersed. The deposition of metal in an orderly fashion requires the maintenance of this very active bubble in a state of equilibrium and this is most easily attained by the use of a touch welding type of electrode with which the projecting end of the coating can be actually pressed on to the seam to be welded, providing the operator with added steadiness and minimizing the exposure of the arc itself to the surrounding water.

Both a.-c. and d.-c. commercial machines have been used with successful results for welding under water, but generally speaking, d. c. has been found to give better results than a. c., and normal polarity better than reversed polarity. From the point of view of arc stability, which is very important owing to bad visibility while welding, a rapid voltage recovery after short circuit is desirable. A choke inserted in the welding circuit is useful as a means of stabilizing conditions,[5] although this is not essential.

Due to current and heat losses through the water surrounding the arc and plates being welded, approximately 25 per cent higher current is required than that for similar work in air, and this should be kept in mind in deter-

mining the rating of the machine to be used. There is no record of any under-water welding having been successfully accomplished at a current below 150 amp.

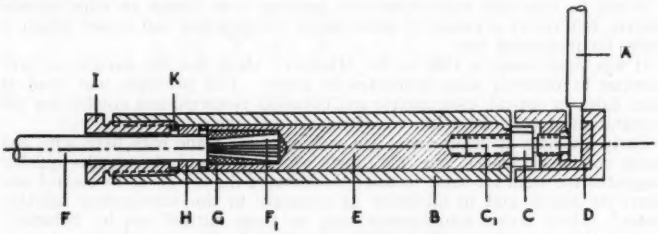

FIGURE 1.—INSULATED ELECTRIC HOLDER.

A, electrode; B, non-conductive material (ebonite); C, double-ended bolt; C_1 (left-hand thread); D, brass; E, brass; F, cable from welding machine; F_1, bared cable; G, tin solder; H, rubber; I, packing boxes (ebonite); K, packing rings.

TABLE I.—RESULTS FROM TENSILE SPECIMENS.

	Specimen Markings	Dimension of Cross Section of Specimen (inches)	Yield Point (lbs/sq. in.)	Ultimate Tensile Strength (lbs/sq. in.)	Description of Failure
In Water	BW1-2	1.80×0.211	40,420	55,900	Outside of weld.
	BW1-3	1.83×0.224	38,400	53,750	Outside of weld.
	BW1-4	1.38×0.226	38,000	53,700	Outside of weld.
	FW1-2	1.65×0.170	49,500	54,800	Outside of weld.
	FW1-3	1.65×0.159	—	54,400	Outside of weld.
	FW1-4	1.63×0.173	49,400	56,800	Outside of weld.
In Air	BA1-2	1.66×0.227	37,600	53,800	In weld.
	BA1-3	1.67×0.210	41,600	49,300	Progressive from edge.
	BA1-4	6.67×0.211	39,800	46,400	Progressive from floor.
	FA1-2	1.67×0.235	37,100	53,600	Outside of weld.
	FA1-3	1.67×0.221	38,600	54,700	Outside of weld.
	FA1-4	1.66×0.241	34,700	51,700	Outside of weld.

TABLE II.—RESULTS FROM FREE-BEND SPECIMENS.

	Specimen Markings	Dimension of Cross Section of Specimen (Inches)	Elongation on Half Inch Gauge Length %	Remarks.
In Water	BW5-2	1.7×0.35	16	Began cracking at edge.
	BW5-3	1.7×0.34	10	Began cracking at edge.
	BW5-4	1.7×0.30	12	Cracked in middle.
	EW3-2	1.7×0.34	18	Cracked simultaneously across section.
	FW3-3	1.7×0.34	17	Cracked at ¼ pt.
	FW3-4	1.7×0.26	7	Crack began at edge.
In Air	BA2-2	1.7×0.36	16	No fusion in middle third of section.
	BA2-3	1.7×0.34	14	No fusion in middle third of section.
	BA2-4	1.7×0.33	14	No fusion in middle third of section.
	Tested March 20, 1933.			
	BA3-2	1.65×0.35	22	Fractured from edge to centre.
	BA3-3	1.65×0.33	16	Fractured across weld simultaneously.
	BA3-4	1.63×0.33	16	Fractured from edge.
	FA3-2	1.65×0.33	24	Fractured in weld.
	FA3-3	1.63×0.36	14	No fracture—bent outside of weld.
	FA3-4	1.65×0.34	20	Small fractures throughout weld surface.

The electrode holder should be fully insulated to prevent electrolytic corrosion and current losses which might be quite substantial in sea water. Figure 1 shows a completely insulated electrode holder as used by Schmidt.[8] It is of the quick-action screw type and has obvious advantages inasmuch as speed of movement under water is necessarily greatly retarded by water resistance, and the time for changing electrodes is reduced to a minimum of about one minute by its use.[8]

The usual diving equipment may be used but it is desirable to insulate the external metallic parts of the suit such as the helmet, in order to avoid electrolytic corrosion and possible injurious effects to the diver should it be touched by the electrode. In the case of the diver's suit with air lines supplied with compressed air from a hand pump, only the copper helmet need be insulated, but in the tubeless type special care has to be taken of the air containers carried on the diver's back. It is considered that the former type of suit is more suitable for use with under-water welding. When weld-

ing at a depth of up to 18 inches a pair of rubber gauntlets is the only protection the welder need have.

Welding can be carried out under water in all positions, i.e., downhand, vertical and overhead, welding vertically downward having been found to give better results than vertically upward.[3] The electrode should not be longer than 14 inches, otherwise control of the arc becomes difficult. In general, less manipulation of the electrode is necessary in under-water welding. For downhand welding, the electrode should be held at an angle of 35 to 40 degrees to the direction of welding in order to avoid undercut.

Tensile tests on butt-welded specimens have shown that the strength of welds made in air can frequently be equalled by that of welds made under water.[1] In cases where under-water conditions are particularly difficult, lower strengths may be obtained due to bad fusion and slag traps. The rapid quenching of the weld by water can cause severe hardening in the higher tensile steels, but in the case of the German steel St42, the hardening was only from 150 Brinell in the metal to 180 Brinell in the zone adjacent to the weld. A much higher hardness was obtained in the tests reported at the end of this article.

Bend tests showed a lower ductility in the case of the under-water welds, and this has been put down to smaller grain size by Harvey, although Withrow argues that lowered ductility would probably be due mainly to a completely new welding condition, viz., welding in a stream of steam. Hibsham and Jensen's results on butt welds and free bend tests are reproduced in Tables I and II.

References.

1. Hibsham, N. S., Jensen, C. D., and Harvey, W. E., "Electric Arc Welding Under Water," Welding Journal (U. S. A.), 1933. October discussion, March, 1934.

2. Hrenoff, K., and Livishitz, M., "Electric Arc Welding Under Water," The Welding Journal (U. S. A.), 1934. April; discussion, June, 1934.

3. Schmidt, H., "Electrical Under-Water Welding and Cutting," V. D. I. Zeitschrift, January, 1941.

4. Tetzlaff, L., "The Most Commonly Used Under-Water Cutting and Welding Methods and Their Practical Application," Technisches Zentralblatt fur praktische Metallbearbeitung, 1941. January.

Appendix.

Report on Under-Water Tests.

This short series of tests was carried out in order to confirm in principle the facts given in the foregoing review of literature.

The first few welds were made in a tank of water 3 feet $\times$ 2 feet 6 inches $\times$ 1 foot 3 inches, welding at a depth of about 6 inches. The welding equipment used was the normal welding equipment available in the shop. The electrode holder was not insulated, since it was not intended to carry out any tests in salt water. Tests were carried out as follows:

1. Using a d.-c. machine at 85 v. open circuit a fillet weld was made in the downhand position using a touch-welding type of electrode. The electrode size was 8 s.w.g., negative polarity being used with the positive lead fixed to the plates by means of a G clamp. A weld 9 inches long was made at 210 amperes, the end of the electrode being pressed on to the seam being welded. Visibility was very poor due to surface reflection and the clouding

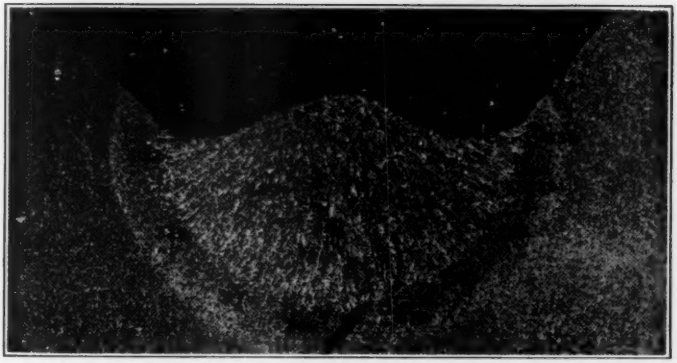

FIGURE 2.—MACROGRAPH OF A SECTION OF AN UNDER-WATER FILLET WELD SHOWING THE RESULTS OF A HARDNESS SURVEY. × 8.

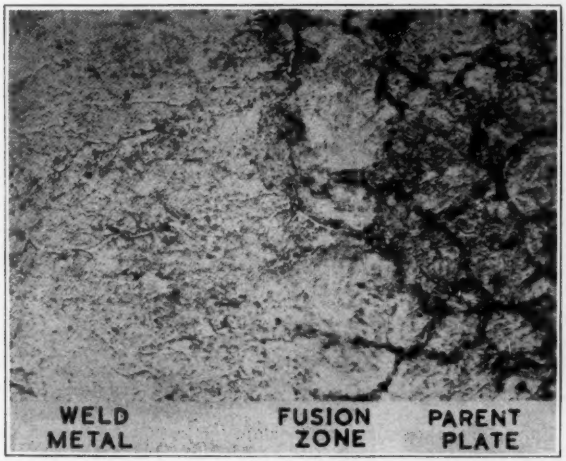

FIGURE 3.—MACROGRAPH OF THE WELD JUNCTION OF AN UNDER-WATER FILLET WELD SHOWING MARTENSITE AND TROOSTITE AT THE GRAIN BOUNDARIES OF THE HEAT-AFFECTED PARENT PLATE. × 80.

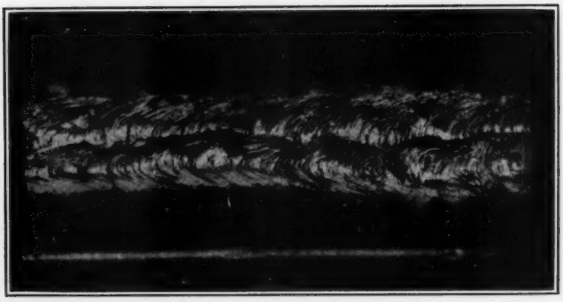

FIGURE 4.—MACROGRAPH OF THE SURFACE APPEARANCE OF A 3-RUN UNDER-WATER FILLET WELD. × 1¼.

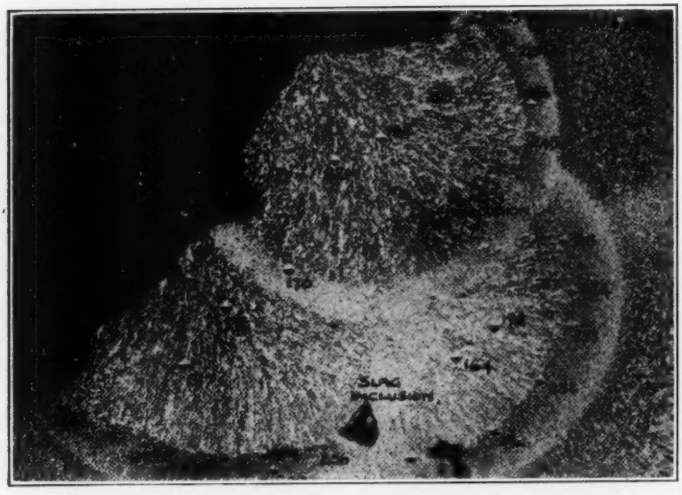

FIGURE 5.—MACROGRAPH OF A SECTION OF THE WELD SHOWN IN FIGURE 4. × 8.

of the water around the arc immediately the arc was struck. Intense turbulence was set up, the bubbles rising to the surface and occasionally igniting. The resultant weld was rather poor due to undercut although it was quite continuous. The touch-welding type of electrode was used in this instance because it was thought that the arc conditions would be better; that this was not the case is evident from the next test.

2. The test was repeated using a 6-s.w.g. electrode to B.S.S. 639 Class A, at 230 amperes and 85 v. open circuit. The end of the electrode was not pressed on the seam being welded, but the electrode was manipulated with a slight weave so that the edge of the coating lightly touched the plates at the end of each weave. This served as an excellent guide for welding. The weld produced was 9 inches long; it was easily de-slagged and had a good appearance. Figure 2 shows a photomacrograph of a section of the weld taken at random. The high hardness of the mild steel parent plate is of interest—its chemical analysis was C 0.20 per cent, Mn 0.62 per cent and the remarkable degree of hardening was due to the intense rate of cooling. Figure 3 shows a photomacrograph in the region of the fusion zone. The plate structure in the heat-affected zone has the appearance of martensite with troostite along the grain boundaries.

3. Figure 4 is a photograph of a 3-run fillet weld made in the H and V position. The electrode used and machine setting was the same as for Test 2. Figure 5 is a photomacrograph of a section of the weld taken at random. It will be noted that due to the fact that the molten pool cannot be watched as in air welding there are slag inclusions between runs.

Subsequent tests were carried out with the tank fitted with an inlet and outlet to provide running water, and an observation screen was used to improve visibility. The observation screen consisted of a tube about 5 inches diameter and 9 inches long, fitted with a plain glass at one end. This end was immersed in the water above the point where the welding was taking place, and served as a means of eliminating surface reflection. It is thought that the optical conditions obtaining with this device resembled fairly accurately the conditions of visibility in which a diver would work.

Visibility was increased to a marked extent and a light welding glass had to be used to reduce glare. The welding glass was not necessary in the previous experiments. A choke was introduced into the welding circuit and the open circuit voltage was stepped up to 100; it was found that these additions resulted in much smoother arc conditions. However, the quality of welds produced was not a great deal better than those shown in the photographs of the first attempts at under-water welding.

Under-water welds of a quality only slightly inferior to those made in air have been produced with standard equipment by a skilled welder who had had no previous experience in under-water welding. It is considered that the training of a diver in under-water welding could result in the production of completely sound welds.

PRODUCER-GAS TESTS OF A CONVERTED GASOLINE ENGINE.—This abstract of a report by Dr. E. Giffen and Mr. J. Spiers is reprinted from Engineering (London), June 11, 1943. Tests of six different fuels, namely, two kinds of anthracite, three kinds of coke and charcoal, are reported.

A comprehensive report of the Automobile Research Committee entitled "The Performance of a Converted Petrol Engine With Different Producer Fuels" is given in the Journal of the Institution of Automobile Engineers

for May, 1943. The report was presented by Dr. E. Giffen, M.I.Mech.E., and Mr. J. Spiers, M.Sc., A.M.I.Mech.E., and supplements two previous reports dealing with similar plant, one by Mr. Spiers, recorded in Volume 36 of the Proceedings of the Institution of Automobile Engineers, and one by Mr. Spiers and Dr. Giffen in Volume 37 of the Proceedings. The work recorded in the present report is interesting and important, but the space at our disposal will only permit us to give a brief summary of it. The plant tested comprised a 6-liter four-cylinder petrol engine and an 18-inch Government "Emergency" gas producer with a tuyère 1 inch in diameter and a two-stage sisal-packed gas filter connected by 2½ inch piping to the engine inlet manifold. The engine has a swept volume of 5893 c.c. (359.7 cubic inches) and throughout the tests the compression ratio was 4.7:1, which is the ratio normally used for petrol working. The gas/air ratio was controlled by separate butterfly throttles in the gas and air pipe lines, the mixture passing through 7 feet of pipe on its way to the inlet manifold. Gas and air flows were measured by means of orifice meters.

The plant as outlined above is generally similar to that employed for the tests described in the first two reports, but there was a modification to the producer in that an air and water preheater, designed by the Fuel Research Station of the Department of Scientific and Industrial Research, was fitted at the inlet to the tuyère, the object being to utilize the sensible heat of the producer gas. The preheater consisted virtually of an extension of the tuyère inlet, on the end of which was fitted a simple water carburetor while the extended inlet was a steel jacket through which the hot gases from the producer outlet passed on their way to the first gas coolers. The whole preheater was lagged with asbestos and the fitting was purely experimental. The Mark VI Government "Emergency" producer uses the two first gas coolers as the hot jacket of the preheater, an arrangement which is probably more efficient owing to the greater area of tuyère inlet exposed to the hot gases, but it is not expected that the behavior of the experimental and production types will differ markedly. Six different fuels were tested in the producer, namely, anthracite, delivered in bulk and stored in the open; anthracite activated by sodium carbonate delivered in canvas bags and stored under cover; low-temperature coke, similarly delivered and stored; high-temperature "Birmingham" coke, delivered in paper-lined canvas bags, this coke being tested in both the unactivated and in the activated forms; and charcoal, delivered in canvas bags.

Charcoal gave the best results in starting, the C.A.B. (critical air blast) value being 0.008 cubic foot per minute. The C.A.B. values represent the minimum rates of flow of air required to maintain combustion under standard conditions of test and thus indicate reactivity. Low-temperature coke came next with a C.A.B. value of 0.015 cubic foot per minute, and then activated anthracite and plain anthracite, the latter with a value of 0.032 cubic foot per minute. There was a considerable difference between unactivated and activated high-temperature coke, the C.A.B. value for the former being 0.038 cubic foot per minute and for the latter 0.051 cubic foot per minute, but it should be noted that the determination of the C.A.B. value was made in the unactivated condition. With all the fuel as supplied, the times for the gas to be available from lighting the fire to regular running were as follows: Charcoal, 1 minute to 1½ minutes; low-temperature coke, 1 minute to 2 minutes; activated anthracite, 2 minutes; unactivated anthracite, 1½ minutes to 6 minutes; unactivated high-temperature coke, 4 minutes to 8 minutes; and activated high-temperature coke, 10 minutes to 14 minutes. Charcoal and low-temperature coke show very short and consistent starting times, even when adulterated with as much as 50 per cent of fuel taken from a previous run. Anthracite, on the other hand, is not so easy to start and shows wide

variations in starting time. When mixed with 50 per cent of "used" fuel, starting times are appreciably longer, and when all the fuel is in the used condition, starting is very difficult.

Activated anthracite is more consistent in starting time than the untreated fuel. The latter requires constant attention to the air/gas ratio during the working-up period, whereas with the activated fuel, and with low-temperature coke and charcoal, the gas throttle can be opened wide almost immediately after regular firing has begun, and the time interval between regular firing and final full throttle operation is largely taken up in minor adjustments of gas/air ratio. Some improvement in starting quality was obtained with the activated high-temperature coke by using wet blast through the preheater almost immediately after lighting the fire. This change of technique caused the starting time with this fuel to be reduced from about 12 minutes to 5 minutes. In general, the C.A.B. value of the fuel gives a useful indication of the ease of starting the producer from cold.

The next section of the report deals with gas quality and engine power variations. The four widely-different fuels tested all show very similar variations in gas composition as regards CO and methane though anthracite gives lower percentages of CO and higher percentages of methane than the carbonized fuels. Variations in both calorific value and power output for any of the fuels, however, are mainly a result of the variations in hydrogen content. The importance of hydrogen contents as regards both the characteristics just mentioned was confirmed with all the fuels tested whether these were in the "as received" condition or mixed with "used" fuel. Under the steady running conditions of the tests, anthracite and low-temperature coke behaved in a very similar manner. Both fuels give gas rich in hydrogen and of high calorific value during the earlier period of the run, the gas quality then falling to a comparatively steady value, which is maintained until it falls off quickly at the end of the run due to exhaustion of the producer charge. Any admixture of "used" fuel results in a reduction in the hydrogen content and calorific value. Charcoal behaves differently, the gas produced throughout a run being of very uniform quality. It was found impracticable to test this fuel in the "used" condition. The maximum gross calorific values, dry, at N.T.P., in Btu. per cubic foot, were, anthracite, 170; activated anthracite, 172; low-temperature coke, 164; high-temperature unactivated coke (dry blast), 119, (wet blast), 135; high-temperature activated coke (wet blast), 138; and charcoal, 137. All these figures are for charges of new fuel and with dry blast, except where otherwise stated. The gross calorific values of the solid fuels are, in Btu. per pound, anthracite, 14,800; low-temperature coke, 13,930; unactivated high-temperature coke, 13,200; high-temperature activated coke, 13,400; and charcoal, 13,520. The gross calorific value of the petrol used for comparative tests is 18,720 Btu. per pound.

With optimum ignition timing, all the fuels tested show a straight line variation of brake mean effective pressure with the calculated calorific value of the gas produced. With a complete new charge, anthracite, whether activated or not, shows the greatest variation in gas calorific value and engine power over the producer run, low-temperature coke being similar in this respect, while charcoal and high-temperature cokes show only small variations under dry blast conditions with a complete new charge. The fuels can be rated in decreasing order of average power as follows: anthracite, activated or unactivated, low-temperature coke and charcoal (equal). The use of an air preheater and the addition of water to the producer tuyère brings the power output with high-temperature coke, either activated or unactivated, up to the level of that given by charcoal and low-temperature coke, while the average power from anthracite is not affected by this altera-

tion to the producer, though the range of variation is reduced. Admixture of "used" fuel results in an appreciable reduction in the power output from both anthracite and low-temperature coke while the high-temperature cokes are not affected. The use of wet blast with a complete charge of "used" anthracite gives an appreciable improvement in average power. In general, activation appears to have no appreciable effect on power output.

The tests for engine flexibility indicate that charcoal and low-temperature coke give the best power recovery after periods of partial shut-down. Anthracite is poor in this respect, but is somewhat improved by using air preheating and wet blast. The high-temperature cokes used with wet blast give results intermediate between anthracite and low-temperature coke. With the exception of the high-temperature activated coke, the fuels tested show increasing flexibility with decreasing C.A.B. value. It would appear that activation of a poor high-temperature coke brings its flexibility to the level of a good high-temperature coke. Other tests show that ignition timing for maximum power is largely determined by the hydrogen content of the gas, irrespective of the producer fuel used. The change in optimum timing is small over the engine speed range for constant hydrogen content and it is difficult in practice to choose an ignition setting for fuels like anthracite and low-temperature coke which show wide variations in hydrogen content. The mean hydrogen content, per cent, with the gas calorific values and conditions given above are, anthracite, 9.1; activated anthracite, 9.2; low-temperature coke, 6.2; high-temperature coke, unactivated, with dry blast, 1.7, and with wet blast, 6.4; high-temperature coke, activated, and with wet blast, 6.3. Charcoal which normally gives, and high-temperature coke which gives, with wet blast, uniform hydrogen content over the greater part of the producer run, may show to advantage under road conditions on this account.

With the exception of charcoal, all fuels tested showed a linear increase in consumption in pounds per hour with increasing engine speed, the actual figures being very similar to the petrol consumption figures at each speed. Charcoal shows higher consumption figures than the other fuels, but high-temperature coke with wet blast is comparable with it if the weight of the water used is taken into account. The fuel consumptions, in pounds per Bhp. per hour, and in increasing order of magnitude, are as follows: petrol; both forms of anthracite; high-temperature coke (neglecting water); low-temperature coke; high-temperature coke (including water); and charcoal. No other fuel compares with anthracite as regards the time of running on one fill of the producer, the nearest to anthracite in this respect being low-temperature coke, though the range per fill on this fuel is but little more than one-third that of anthracite. There was no trouble with clinker in any of the fuels tested, though charcoal and activated high-temperature coke were the most free from clinker. The sisal filters choked rapidly with the low-temperature coke, one or other of the two stages of the filter requiring cleaning after each run, and the high moisture content of the charcoal caused the sisal to become very wet, which made cleaning difficult. Anthracite rendered fairly frequent cleaning necessary, coming between low-temperature and high-temperature cokes in this respect. Cylinder and piston ring wear were not excessive throughout the period of testing with the engine used but the rate of wear appeared to be somewhat lower with the high-temperature cokes and charcoal.

THE AMPLIDYNE.—The versatile amplidyne, an externally driven DC generator, making an ingenious use of a short-circuit and compensating windings, is described by Mr. Fremont Felix of the Industrial Engineering Division of General Electric Company. Five schematic diagrams are in-

cluded showing the fundamental features of the amplidyne as compared to those of the conventional DC generator. The article is taken from The Nautical Gazette for June, 1943.

One of the most important electrical developments of recent years is the amplidyne, a product of G-E engineering which is being applied with numerous advantages to a growing list of duties.

Applications include mine hoists and power shovels, blast furnace skip hoists, electric furnaces, blooming plate, and cold strip mills, runout tables, flying shears, electrolytic tinplating lines, saw mill carriages, boring mills, and paper machines.

In these and in many other applications, the amplidyne is proving its versatility by performing a wide variety of functions, as follows:

1. It controls speed accurately over a wide range;
2. It limits loads to protect electrical and mechanical equipment;
3. It controls torque and tension to improve product uniformity in winding, drawing, and other similar operations;
4. It speeds up acceleration and deceleration to increase production of high-inertia machines;
5. It positions machine-tools, arc-furnace electrodes, simply and precisely;
6. It regulates current, voltage, power, speed;
7. It can be used with either a-c or d-c equipment;
8. It is a natural partner of electronic devices.

The amplidyne is an externally-driven d-c generator, outwardly similar to a conventional motor or generator. But its ingenious and unique use of a short-circuit and compensating winding creates such precise electrical balance that an electrical signal as small as half a watt will instantly release kilowatts of power capable of controlling the most powerful electrical machine. Figures 1 through 5 explain this unique principle of the amplidyne.

A conventional two-pole 10-Kw. d-c generator driven at constant speed may be shown schematically as in Figure 1. For the sake of simplicity, the armature is shown serving also as commutator and a single exciting field coil is shown on the north pole. The small circles with dots show conductors where the current is directed towards the reader and the small circles with arrow tails show conductors where the current is directed away from the reader.

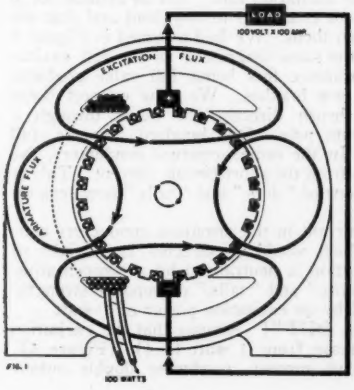

FIGURE 1.

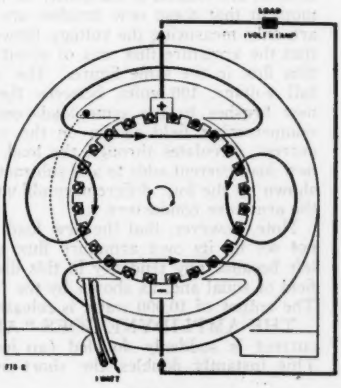

FIGURE 2.

About 100 watts of excitation power supplied to the field coil creates the excitation flux. This flux is producing a full-load voltage of 100 volts, which circulates 100 amperes full-load current through the load, taken as a resistance of 1 ohm.

The load current, in flowing through the rotating armature conductors, creates a stationary armature flux because the armature conductors on the left of the brush axis always carry current in the same direction and the armature conductors on the right of the brush axis always carry current in the opposite direction. The combined effect is the same as that of a stationary solenoid, producing flux as shown in the left and right flux loops. This armature flux is of about the same magnitude as the excitation flux but it is not doing any useful work.

Two questions arise: Can this idle armature flux be utilized? Can the excitation power, now too large for accurate control devices, be reduced to a point where small, fast response devices can be used, and yet release the same full output?

With a smaller field coil, and with excitation power reduced from 100 watts to 1 watt, the same conventional generator appears as in Figure 2. The new reduced excitation power creates only 1 per cent of the original excitation flux. Voltage at the brushes is reduced from 100 volts to 1 volt, and the load current, also reduced from 100 amperes to 1 ampere, produces only 1 per cent of the former armature flux.

Thus, one objective has been attained—excitation power has been reduced to a value where it can be readily supplied and handled by precise control devices.

How can we restore full-load working flux and yet retain this low excitation power? A SHORT CIRCUIT across the brushes, as in Figure 3, restores the armature current and consequently the armature flux to their full original values. This is because the internal resistance of the armature winding is assumed to be 1/100 of the load circuit resistance. The load has been disconnected. The excitation power and flux continue to be extremely small, but they now control the full-sized armature flux.

But the armature flux is still idle. Can we "harness" it, and put the armature back to work delivering full kilowatt output?

To put the short circuit to work, two new brushes are added, as in Figure 4, one in the center of each armature flux loop, just as the conventional brushes are located in the center of the excitation flux. Let us assume for a moment that these new brushes are not connected to any load and that we are only measuring the voltage between them. We had assumed in Figure 1 that the armature flux was of about the same magnitude as the full excitation flux in the same figure. The armature flux being full value produces full voltage, 100 volts, between the new brushes. We now connect these new brushes to the same load—one brush directly, the other through a compensating field shown on the south pole. One hundred amperes, full current, circulates through the load. In the same armature conductors, the new load current adds to and subtracts from the short-circuit current. This is shown by the four different combinations of "dots" and "tails" now seen on the armature conductors.

Note, however, that the new load current in the armature conductors cannot set up its own armature flux which would be directed from right to left because any tendency in this direction is neutralized by a compensating field of equal and, as shown by the "dots" and "tails," of opposite strength. The output of 10,000 watts is released by an excitation power of 1 watt.

THE AMPLIDYNE GOES "ALL OUT"! Assume that the excitation current is suddenly doubled (an increase from 1 watt to 4), (Figure 5). This instantly doubles the short-circuit current, producing double output

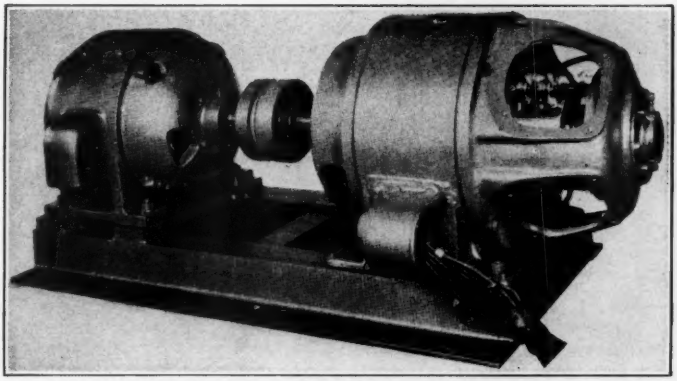

TYPICAL AMPLIDYNE MOTOR-GENERATOR SET, 3 KW., 1750 RPM.

voltage (200 volts) and forcing double current (200 amperes) through the load. Thus, by merely raising the control input by three watts, output is raised from 10 kilowatts to 40. To obtain comparable changes in output in response to minute changes of excitation with conventional generators

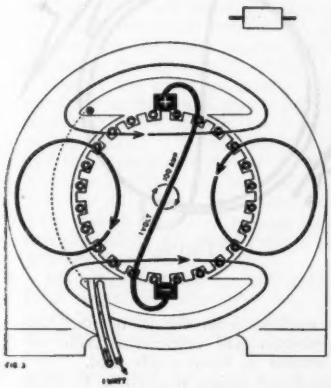

FIGURE 3.

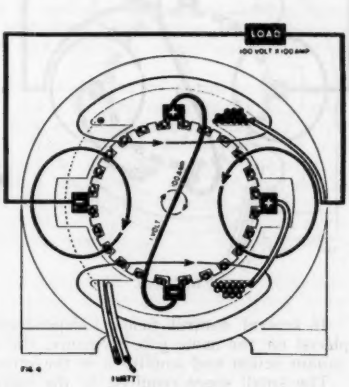

FIGURE 4.

would require two generators—a small control signal would excite the first one; the output of the first generator would excite the second. The output of this second generator would considerably amplify the small control signal to the first one but with a cumulated delay in response.

In the amplidyne, the equivalent of a full-size exciter (utilizing the same armature structure and conductors) is available to excite forcibly the output generator for fastest response. The speed of response of the amplidyne is further accelerated because the output flux is produced by the armature conductors from within the armature structure so that even the flux which leaks through the air produces useful voltage.

The symbol shown in Figure 6 graphically represents the amplidyne as two full-sized generators "compressed" into one. The minute control field and the short-circuited circle are identified with the first stage. The compensating field and the other circle connected to the load are identified with the second stage.

The amplidyne provides an entirely new combination of amplification and speed—two stages of amplification faster than any single stage could be.

Easy to work with, the amplidyne is in every outward aspect similar to a conventional exciter. All the user need concern himself with are the excitation input and working output. Because the amplidyne uses only the simplest laws of rotating electrical machines, and because there is practically nothing to wear out, it stays put. The bearings will last a lifetime, and the brushes which handle small currents will run a close second.

USE OF SEVERAL CONTROL FIELDS.

In Figure 6, we have shown the amplidyne as a two-stage amplifier responding to a single control field.

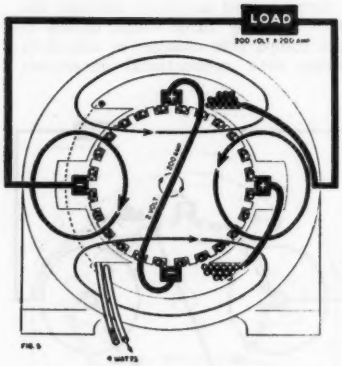

FIGURE 5.

FIGURE 6.

If several control fields, independently excited from signal devices, are placed on the same pole structure, the amplidyne will respond to their resultant action and amplify it in the same manner as for a single field.

The small space required by the individual coil makes it possible to have a normal complement of four fields permitting many independent functions to control the amplidyne output.

Each of these fields is easily adjusted by a small resistor or other means, and since their current requirements are so small, their action may be automatically blocked by small rectifiers as long as a certain operating condition or limit is not reached.

RADIUS OF ACTION.—The Marine Engineer, August, 1943, is the source of this article by Mr. Frank C. Bowen. Considerations which have controlled selection of warship radii of action during the past several decades are discussed.

It is certain that the increased power of destruction of modern weapons, and their greatly increased variety, will make the protection of warships one of the most difficult tasks of the post-war naval architect, but at the same time experience has shown the great importance of radius of action which must not be sacrificed to armor if there is any alternative. Modern men-of-war under all flags have to undertake colossal voyages; it is to the credit of the engineers that they are seldom curtailed by mechanical breakdown, but they cannot be undertaken without fuel and fuel demands weight.

In the old days of the wooden sailing warships their staying power was limited by their fresh water, just as it is by their fuel nowadays, and considering the enormous space occupied below deck by the hemp cables in Nelson's day their performance was remarkable. The introduction of chain cables greatly increased the time which the ships could spend at sea and in the early part of the nineteenth century the crack line-of-battleship in the fleet, H.M.S. *Queen*, of 116 guns, carried 500 tons of water at most, which, when the crew received their full allowance of a gallon a day, was used at

the rate of five tons a day. The lower tire of tanks was, however, only emptied in an emergency as the weight was needed for ballast and most ships would finish a three-year commission with this reserve of water still undisturbed, although the men might have been cut down to half rations. The frigate *Spartan* carried 60 tons, which was consumed at the rate of 1¼ tons per day, and her crew expected to be cut down right at the beginning of any cruise which promised to be protracted. Rain water was caught and drained into the tanks, and boats were sent ashore to collect water in barrels whenever the opportunity offered.

One of the great arguments for the introduction of steam power, as an auxiliary at first, was that the boilers could be used for distilling salt water into fresh in the fashion that had already been tried experimentally in purely sailing ships. The disadvantage was that this distillation demanded coal and their machinery was so extravagant that it always had to be eked out. The crack cruiser of the 'sixties, H.M.S. *Inconstant*, only had coal for 54 hours at full speed and many others were similarly cramped in that way. They did all their long passages under sail as a matter of course and many captains would fill their cold boilers with fresh water for drinking, which was not good for the boilers.

The frigates could at least sail reasonably well, but the early ironclads, fully rigged, literally sailed like haystacks. Their economical speed under steam was only 4¼ knots, which was insufficient to steam against a head wind and sea, especially with their heavy rig which offered so much resistance. But the Admiralty insisted that coal should be saved at every opportunity and issued standing orders that steam was not to be raised if the wind would permit the ship to make 4 knots on her course under sail.

Importance of Weight.

Lightening the steam machinery, and making it sufficiently reliable for the rig to be reduced to barque, barquentine, and finally schooner, with a great reduction in the resistance offered, therefore became the great aim of the naval engineers of the day and outstanding men like Napier, Penn, Maudslay and others made steady progress. Tubular boilers were the first improvement, followed by improved simple engines, and then, as the building of boilers progressed well enough to make a higher pressure safe, by the compound engine. As sail was abandoned a disproportionate amount of displacement had to be allotted to the bunkers of cruisers—up to between 20 and 25 per cent at one time—but to counter this the Admiralty, in 1870, introduced the dual system of recording bunker capacity. The introduction of compound engines had greatly reduced the coal consumption; big bunkers were still fitted in the newest ships to enable them to make a very long voyage, but for ordinary work they only carried what was known as the "normal" coal capacity which was reckoned to give, with the more economical engines, as great a steaming radius as that of the earlier ships with the simple engines. Actually, the full load was generally impracticable, for in many types it would submerge the top of their armor protection well below the waterline. The system also made the figures for the radius of action very misleading, for the maximum was worked out at full bunkers with the draught for normal stowage. In one famous case, the *Imperieuse* was claimed to have a radius of 2000 miles at 17 knots, but loaded down to full draught she could not contrive anything like that speed and when she was light enough to make it she could only steam about 1200 miles.

The increased number of dry docks available in overseas ports, the more frequent drydocking of ships and the sheathing and coppering of practically all ships designed for overseas service greatly improved economy, as did

the improved anti-fouling paints for those not coppered, and more scientifically designed propellers. But the greatest credit has to be given to the engineers in their development of better boilers and engines. The change from compound to triple-expansion engines brought the average coal consumption down from 2.2 to about 1.65 pounds per Ihp. per hour and the introduction of the water-tube boiler, although it caused many mishaps owing to inexpert handling, effected further economy in time as well as great saving in weight.

Economy at Cruising Powers.

The practically simultaneous introduction of turbine machinery and the oil-fired boiler meant a further reduction in weight, part of which was devoted to improving the fighting qualities of the ships—for instance, belt armor for light cruisers—and part to increasing the radius of action. But the introduction of the turbine brought serious problems of economy in cruising, for while the original turbine destroyer (H.M.S. *Viper*) was very economical at record speeds she was disappointing at cruising powers. When the turbine destroyer *Velox* was laid down in 1901 two triple-expansion engines of 150 Ihp. each were arranged for driving the low-pressure shafts when cruising below 13 knots, and when the *Eden* was built two years later she was given special cruising turbines, to which arrangement the *Velox* was converted in 1906. When the first turbine cruiser *Amethyst* came out in 1904 she went through a gruelling series of trials against her reciprocating-engined sisters which gave interesting results. At 14 knots the economy was about the same, at 18 knots the turbine ship had a superiority of about 20 per cent and at 20 knots nearly 30 per cent. But at 10 knots, which was then the normal cruising speed for men-of-war, the *Amethyst* only ran 7.42 miles per ton of coal while her sisters managed 9.75 miles with ease.

This elusive problem of cruising economy remained unsolved as long as the direct-drive turbine was fitted. The German battleships of the *Kaiser* class were given various types of cruising turbines as an experiment; the *Prinzregent Luitpold* had space left for Krupp Germania cruising diesels of 12,000 Bhp. on the center shaft, but it was not delivered by the outbreak of the last war and was never fitted. It was also proposed to give H.M. destroyer *Hardy* diesel engines for cruising at 12 knots, but they again were never installed and in the meantime geared turbines were making such good progress that they were fitted for cruising purposes in the battleships of the *Queen Elizabeth* type, which had direct-coupled turbines for full speed.

The progress of this war has shown the importance of steaming radius more and more, although published figures at economical speed can be misleading as every man-of-war must keep a reserve of bunkers in hand for a spurt at extreme speed at any time. The waste involved in maintaining steam for this is considerable, but it cannot be helped. At the beginning of the war a big radius was made even more important by the shortage of ships owing to ill-advised economy between the wars. In the old days the economical cruising speed was generally regarded as 10 knots, but nowadays it is 15 which can be a considerable disadvantage on occasions.

Although, of course, a great deal of their performance is regarded as confidential, the Admiralty has released bulletins and figures which show that our capital ships have been sent to the ends of the earth, where they must have had great use for the big bunkers with which they have been fitted and the economy which their designers have so skilfully worked into their machinery installations. The *Nelson*, and *Rodney*, for instance, burn only 2¼ tons of oil per hour at economical speed and stow 4000 tons. Capital ships

have been reported convoying in the North Atlantic, where their cruising speed economy would be useful. They have also put in an immense amount of time steaming in the Mediterranean, always ready to work up to full speed should the Italian Fleet appear, and ships of the *Queen Elizabeth* and *Royal Sovereign* classes have been officially reported in the Eastern Fleet.

Commerce Raiders' Radius.

In the work of destroying and protecting commerce both sides have great need for bunkers; the enemy in order to remain at sea for the longest period and the Allies in order to dash to any threatened point, which may be many miles away, without the least delay. In this game the odds are always in favor of the attacker, as was proved by the case of the *Emden*, which demanded nineteen Allied ships to run her down, and calls at neutral ports for bunkers, with the certainty of the ship's presence being reported by enemy agents, are always a disadvantage. Before and during the 1914 War German cruisers were given comparatively small bunkers and on active service they had to top them up wherever they could, taking coal from every tramp that they sank, while the British policy was to stow as much coal as possible, culminating in the *Hawkins* type, specially designed to run down and sink German surface raiders, which were given 1000 tons of coal plus 1500 tons of oil in their original state. They were later converted to carry 2600 tons of oil. All German cruisers since 1919 have been given big bunkers and the much-discussed "pocket battleships," which were really big raiding cruisers, had a radius of no less than 10,000 miles at 15 knots and, by their arrangement of eight diesels geared to two shafts, a tremendous radius at slow speed.

In their new 8-inch gun cruisers like the *Prinz Eugen*, the German designers have paid particular attention to cruising radius. They are like the post-Versailles ships in having three screws, with a diesel on the central one for cruising. The bunker capacity, radius of action, and the power of the cruising diesel plant have not been published, but the power of their turbine engines is 80,000 Shp., and it may be that a comparison can be made with the 60,000 Shp. *Nurnberg*, whose cruising diesels are of 12,000 Bhp. In H.M. cruiser-minelayer *Adventure*, launched in 1924, Parsons'-type geared turbines were installed for full speed and Vickers' turbo-electric machinery for cruising, although the experiment was not repeated, doubtless because of weight and undesirable complication in the engine rooms.

The policy of the British constructors for the protection of commerce is shown by a comparison of the 8-inch gun cruisers of the "Washington" type. The original *Kent* class stowed 3400 tons of oil; the improved *Devonshire* and *Dorsetshire* classes 3200 tons. The French cruisers of the same general type stowed from 1800 to 1900 tons. The Italians varied; some of them, designed for extreme speed, carried 3000 tons, largely at the expense of armor, and others 2200 tons. From all available information 2000 tons is the standard for the Japanese, but the Americans, who always believed in advanced bases, permanent or temporary, and a very large naval train to keep them supplied, only gave 1500 tons of oil to their first three classes and 1650 tons to the two later ones.

There is no doubt that the pre-1939 type of cruiser, remarkable as it is in many ways, has proved vulnerable and a high cruising radius is partly responsible for this. It is difficult to prophesy the trend of post-war design, but there would seem to be little doubt that additional protection to meet the varied forms of modern attack will have to be provided at a sacrifice of some steaming radius and/or speed. Which perhaps accounts for the present American anxiety in the matter of bases.

DRY ICE KILLS COAL PILE FIRES.—From the Current Topics section of the July, 1943, Journal of the Franklin Institute. This is an abstract of an article published in Volume 40, Number 4, of Heating and Ventilating.

A new and ingenious use for dry ice as an extinguisher of coal fires has been developed recently. An estimated 80,000,000 tons of bituminous coal is now in storage throughout the country, a figure double the usual season's reserve. This likewise doubles the risk of loss through spontaneous combustion, notwithstanding the protective effect of modern methods of storage. The dry ice is applied directly at the seat of the fire, through 15 feet, 3 inches, driven pipes fitted with perforated tips. Charges of 50 pounds of the solid CO_2 are placed in the pipes. Heat liberates the gas to blanket the hot zone and smother the smoldering coal, while the chilling action of the dry ice reduces the local temperature, this effectively eliminating the hot spot. To locate such danger points in the pile a hot spot indicator, consisting of an iron pipe containing a spring loaded signal, held back by a chain with fusible links at one foot intervals has been made available by the same manufacturer. Only the hot test link lets go, permitting the signal to rise, and this occurs only when temperature rises to 150 degrees F. Thus the location and depth of the danger point are advertised 72 hours before combustion can take place, at the normal rate of temperature rise for the average coal composition.

OBITUARY.

ALBION JAMES WADHAMS.

Albion James Wadhams of Dongan Hills, Staten Island, New York, a member of the American Society of Naval Engineers, died at his summer home in Elizabethtown, N. Y., on Sunday evening, August 22nd, of a heart attack.

Born at Annapolis, Md., April 21, 1875, son of the late Rear Admiral (U.S.N.) Albion V. and the late Caroline (Henderson) Wadhams, he was graduated from the Naval Academy in 1895. Mr. Wadhams served as an Ensign and later as a Lieutenant (j.g.) in the United States Navy from 1895 to 1901. He saw continuous sea service in North and South Atlantic and West Indies for six years, including the Spanish-American War during which he was attached to the U.S.S. *Mayflower*. During service in the United States Navy he received Spanish War Medal and Sampson Medal.

He had been with The International Nickel Company and its predecessor companies since 1901. Mr. Wadhams joined the Orford Copper Company at Bayonne, N. J., on March 1 of that year. He was transferred from there in 1904 to the American Nickel Works at Camden, N. J., acting as Superintendent until 1912. From 1912-1918 he was Assistant General Superintendent of Orford Works of International Nickel, becoming General Superintendent in 1918. Mr. Wadhams was named Manager of the Company's Development and Research Division in New York on April 1, 1922. In addition to this position, he had been a Vice President of The International Nickel Company, Inc., since October, 1935.

It was under his leadership and guidance that many of the wide applications of nickel and its alloys have been developed. He has written many papers on the history and uses of nickel.

Besides being a member of the American Society of Naval Engineers, Mr. Wadhams was a member of The Society of Naval

Architects and Marine Engineers; American Iron and Steel Institute; American Institute of Mining and Metallurgical Engineers; American Society for Metals; Mining and Metallurgical Society of America; Navy League of the United States; New York Electrical Society; Princeton Engineering Association; The Newcomen Society of England; United States Naval Institute, and American Association for Advancement of Science.

In 1902 Mr. Wadhams married Marcia Elizabeth Hand, of Elizabethtown, N. Y., who died on August 21, 1936. Surviving are two daughters and two sons: Mrs. Edward J. Carleton of Woodstock, Conn., and Miss Elizabeth H. Wadhams of Dongan Hills, S. I.; Richard H. Wadhams of Wilmington, Del., who is with the DuPont Company, and Albion James Wadhams, Jr., Captain, U. S. Army.

BOOK REVIEWS.

THE MARINE POWER PLANT, by Lawrence B. Chapman, Professor of Marine Transportation and Marine Engineering at the Massachusetts Institute of Technology. Published by McGraw Hill Book Company, Inc., New York, N. Y.

This is a completely rewritten second edition of the book which was originally copyrighted in 1922. The rewriting was done to permit covering the great improvements in economy and many changes that have taken place in Marine Engineering in the last twenty years.

The book is intended as a first book in marine engineering and makes no pretense of being an exhaustive treatise. Fundamental principles and the thermodynamic and economic features have been stressed. Descriptive matter and details have been held to a minimum to make clear the principles involved.

The point of view of the seagoing engineer and the shore operating staffs have been kept in mind throughout. The book also is designed for students of marine engineering, naval architecture and marine transportation.

OTHER BOOKS RECEIVED.

THE SKY IS MY WITNESS, by Captain Thomas Moon, Jr., U.S.M.C.R. Published by G. P. Putnam's Sons, 2 West 45th St., New York 19. $2.00.

OUT IN THE BOONDOCKS, by James P. Horan and Gerald Frank. Published by G. P. Putnam's Sons, 2 West 45th St., New York 19. $2.75.

THE FLEET IN THE FOREST, by Carl D. Lane. Published by Coward-McCann, Inc., 2 West 45th S., New York City. $2.75.

ASSOCIATION NOTES.

The Annal Meeting of the Society was held at Washington, D. C., on Tuesday, 5 October 1943, for the purpose of receiving nominations for offices for the calendar year 1944 and other business.

The following were nominated for offices for 1944:

For President:

Rear Admiral C. L. Brand, U.S.N.

For Secretary-Treasurer:

Captain James E. Hamilton, U.S.N.
Captain H. C. Sexton, U.S.N.

For Member of Council:

Captain E. E. Brady, U.S.N.
Captain R. W. Bruner, U.S.N.
Captain J. B. Dow, U.S.N.
Captain N. W. Goky, U.S.N.
Captain Paul F. Lee, U.S.N.
Captain B. P. Ward, U.S.N.
Commander R. B. Lank, U.S.C.G.
Commander S. J. Woyciehowsky, U.S.C.G.
Mr. Bryce W. Blair, General Electric Co., Washington, D. C.
Mr. T. H. Bossert, Vice-President, New York Shipbuilding Corp., Camden, N. J.
Mr. Robert E. Post, Fairbanks, Morse & Company, Washington, D. C.
Mr. C. S. Weber, Westinghouse Electric & Mfg. Co., Washington, D. C.
Mr. J. B. Woodward, Vice-President and General Manager, Newport News Shipbuilding & Dry Dock Co., Newport News, Va.

Ballots have been distributed. Polls close at 4:30 p. m., 27 December, 1943.

It was regretfully decided not to hold the usual banquet of the Society in 1944, except in the event that conditions change sufficiently to warrant resumption of the occasion.

ADDRESSES: Under present conditions, it is especially important that current addresses be available. Your cooperation is earnestly requested.

MEMBERSHIP.

The following have joined the Society since the publication of the August, 1943, number of the JOURNAL of the Society:

NAVAL.

Anthony, J. G., Lieut., U.S.N.R., 1427 Vernon Ave., Key West, Fla.

Borkowski, John V., Lieut., U.S.N.R.

Brooks, Raymond H., Electrician, U.S.N., 1560 N. W. Third St., Miami, Fla.

Brown, George, Lieut. Commander, U.S.N.R., 124 Maine St., Vallejo, Calif.

Campbell, Robert I., Lieut., U.S.N.R.

Cawley, James M., Ensign, U.S.N.R.

Craig, Charles Lee, Machinist, U.S.N.

Dorman, E. A., Lieutenant, U.S.N.

Dunn, Royal Charles, Lieut., U.S.N.R.

Fagan, John H., Jr., Lieut., U.S.N.R., Box 27, Submarine Base, New London, Conn.

Fox, Robert B., Lieut., U.S.N.R., 2510 Central Ave., Alameda, Calif.

Fitzpatrick, W. D., Lieut., U.S.N.R.

Garner, Wilfred James, Lieut. Commander, U.S.N.R., 163 Marten St., Ext., Holyoke, Mass.

Houtsma, Cornelius G., Lieut., U.S.C.G.

Jones, John P., Jr., Ensign, U.S.N.R., 117 East 15th St., Brooklyn, N. Y.

Johnson, Raymond L., Lieut., U.S.N.R.

Kelley, Morriss H., Ensign, U.S.N.R.

Markle, Edward L., Lieut., U.S.N.R., 405 Furman St., Schenectady, N. Y.

Marsters, Richard A., Lieut., U.S.N.R.

Meeker, Thomas Rusley, Lieut., U.S.N.R., Room IW 96, Bureau of Aeronautics, Navy Dept., Washington, D. C.

Mercer, James W., Ensign, U.S.N.R.

Pearce, John E., Lieut., U.S.N.R.

Pedersen, Rudolph F., Lieut. Commander, U.S.N.R.

Peters. Herbert Erskine, Lieut. Commander, U.S.N.R., 7057 19th Ave., N. E., Seattle, Wash.

Poindexter, Gale A., Commander, U.S.N., Ret., 3321 34th St., South, Seattle, Wash.

Porter, Albert W., Jr., Ensign, U.S.N.R.

Reed, John Shedd, Lieut., U.S.N.R.

Roth, W. J., Jr., Lieut., U.S.N.R., Asst. Supervisor of Shipbuilding, U.S.N., Charleston Shipbuilding & Dry Dock Company, Charleston, S. C.

Schweitzer, Paul H., Lieut. Commander, U.S.N.R., Professor of Engineering, Pennsylvania State College, State College, Pa.

Seyfarth, Francis, Ensign, U.S.N.R., Route 2, Princeton, N. J.

Sharp, George A., Ensign, U.S.N.R.

Smith, G. A., Lieut., U.S.N., Lieut., U.S.N.R.

Sommerhalter, O. W., Lieut., U.S.N.R.

Steele, Varian, Lieut., U.S.N.R., 1227 16th St., N. W., Washington, D. C.

Steinman, G. M., Lieut., U.S.N.R., 3232 Steinway St., Astoria, L.I., N. Y.

Vincent, Manuel, Lieut., U.S.N.R., Navy Yard, Mare Island, Calif.

Whillock, H. W., Lieut., U.S.N.R., 1111 North 7th St., Boise, Idaho.

CIVIL.

Kenlan, C. Clark, President, Kenlan Mfg. Co., 67 South Munn Ave., East Orange, N. J.

McCarthy, E. W., Vice-President & Naval Architect, Gulfport Boiler & Welding Works, Inc., P. O. Box 1179, Port Arthur, Texas.

Menendez, Ramon A., Electrical Engineer, Tampa Shipbuilding Co., Inc. Mail: P. O. Box 1627, Tampa, Fla.

ASSOCIATE.

Altenburg, Charles J., Marine Engineer, Gibbs & Cox, Inc., 21 West St., New York, N. Y. Mail: 170-14 84th Ave., Jamaica 3, N. Y.

Austin, Robert M., Engineer, Nordbert Mfg. Co., 912 Barr Building, Washington, D. C.

Bradley, J. L., Estimator, Hull Estimating and Designing Dept., Federal Shipbuilding and Dry Dock Co., 744 Broad St., Newark 2, N. J.

Butler, James Edward, First Cl. Engr. Steam & Diesel, British Merchant Marine, care Anglo Saxon Pet. Co., Ltd., St. Helen's Court, Ledenhall St., London, EC 3, England. Mail: 171 Ampere Parkway, Bloomfield, N. J.

Kempt, James Nelson, Owner, Royal Plating Co., Boston, Mass. Mail: Royal Plating Works, 75 Lamartine St., Boston, Mass.